Understanding Oligonucleotide Synthesis

By

James Lee Scotson

November 2016

A thesis submitted to the University of Huddersfield in partial fulfilment of the requirement for the degree of Doctor of Philosophy

**The Department of Chemical Sciences,
The University of Huddersfield,
Queensgate,
Huddersfield
HD1 3DH**

In collaboration with GlaxoSmithKline

Abstract

Oligonucleotides are synthesised almost exclusively via the solid-supported phosphoramidite method. However popular this method may be, the expensive reagents used in large excess during the synthesis as well as the large amounts of organic and aqueous solvents and purification steps makes the scale-up of oligonucleotide synthesis costly and possibly harmful to the environment. The therapeutic use of anti-sense oligonucleotides (ASOs) is hindered by their susceptibility to nuclease catalysed hydrolysis and to overcome this problem ASOs have been modified commonly by the introduction of a phosphorothioate backbone. This research aims to provide a better understanding of some of the more problematic stages of the synthesis cycle, the formation of the sulfurizing agent and sulfurisation of inter-nucleotide phosphite linkages, in order to make this method more sustainable and efficient.

The investigation of the activation, alcoholysis and hydrolysis of the phosphoramidites 2´-methoxy-5´-O-DMT-uridine 3´-CE phosphoramidite (UAm) and di-*tert*-butyl *N,N*-di-isopropyl phosphoramidite (DBAm) using several tetrazole activators found that complete conversion of the phosphoramidite UAm to products required an excess of activator and that this was due to the generation of di-isopropyl amine during coupling. Conductivity measurements show that the amine deprotonates the acidic activator and that the ammonium and tetrazolide ions that are subsequently formed strongly ion pair (K_{ip} = 6540 M^{-1}) removing free activator from solution. The tetrazole-catalysed reaction of phosphoramidites with oxygen nucleophiles was found to be first order with respect to phosphoramidite and activator and the nucleophilic displacement of the di-isopropyl amine group by the tetrazoyl group at phosphorus is rate-limiting.

Investigation into the 3-picoline-catalysed ageing of the sulfur transfer reagent phenylacetyl disulfide (PADS) has shown that the process is overall second order and is proportional to the concentration of PADS and 3-picoline. Deuterium exchange experiments show that ageing proceeds via abstraction of the methylene CH_2 protons of PADS via an E1cB-type decomposition of the PADS molecule generating a disulfide anion and a ketene by-product which was trapped using an intra-molecular [2+2]-cycloaddition reaction. Mass spectrometry data shows that disulfide anions act as nucleophiles with PADS molecules to generate polysulfides which are the active sulfur transfer reagents in aged PADS solutions. Using pyridines that are less basic than 3-picoline causes the rate of degradation of PADS to become slower, indicating the possibility that the rate-limiting step of this process is the generation of the disulfide anion.

The rate of sulfurisation of phosphites by both 'fresh' and 'aged' PADS in the presence of 3-picoline was found to be first order with respect to phosphite, PADS and 3-picoline at low concentrations of each. However, the rate of the reaction becomes independent of base when using aged PADS in the presence of high 3-picoline concentration. Brönsted correlations for the sulfurisation of alkyl phosphites using fresh PADS give a β_{nuc} value of 0.51, consistent with a mechanism involving nucleophilic attack by the phosphite on the disulfide bond of PADS to generate a phosphonium ion intermediate. This degrades to the phosphorothioate product via a base-catalysed mechanism which has been confirmed by removal of the methylene protons from the PADS molecule. Comparison of the β_{nuc} values seen when altering the pK_a of the pyridine catalyst used shows that the rate of the reaction of fresh PADS is much more sensitive to the pK_a of the pyridine than is aged PADS (β_{nuc} = 0.43 and 0.26 for fresh and aged PADS respectively). This suggests that in the case of aged PADS, the phosphite attacks the sulfur atom adjacent to the carboxylate group in the polysulfide chain. This generates a phosphonium intermediate which can be broken down via a much more facile S-S bond fission, as opposed to the C-S bond fission as seen in when using fresh PADS.

Acknowledgements

Firstly, I would like to thank my supervisors Professor Andrew P. Laws and Professor Michael I. Page for their relentless effort and endless patience. Their guidance over the years, academically, professionally and personally, has been invaluable and I am honoured to have been a student of theirs.

Secondly, this project would not have been possible without the contribution of GlaxoSmithKline. I would like to thank GlaxoSmithKline for their support throughout the process, in particular Dr. Benjamin I. Andrews for all of his help during my time at GSK and throughout the whole PhD process.

Thirdly, a special thanks to Dr. Neil McClay and Dr. Richard Hughes for all their help with NMR and HPLC and the team at IPOS for their help with just about every other technique used throughout this work. Thanks to Dr. Denisa Tarabová for her help with synthesis.

I would like to thank my partner Sophie who has been a pillar of support, particularly in the closing months of this work, and finally, my parents: all of them. They have given me every ounce of support possible over the years and for that I am eternally grateful. In particular, I'd like to thank my Mum Angela, whose kindness and selflessness have taught me more than any book ever could.

This thesis is dedicated to her.

Table of Contents

Word Count: 41,741

Table of Figures

Table of Tables

Table of Schemes

List of Abbreviations

PADS	Phenylacetyl disulfide
Me$_4$PADS	2,2,2´,2´-tetramethyl phenyl acetyldisulfide
Me$_2$PADS	2,2´-dimethylphenylacetyl disulfide
DBDS	Bis-benzoyl disulfide
TPP	Triphenylphosphate
TPPt	Triphenylphosphite
TPPnO	Triphenylphosphine oxide
BHT	Betahydroxy toluene
UAm	2´-methoxy-5´-O-DMT-uridine 3´-CE phosphoramidite
DBAm	Di-*tert*-butyl N,N-diisopropyl phosphoramidite
ETTH	Ethylthio tetrazole
DIA	Diisopropyl amine
ETTHDIA	Diisopropyl ammonium ethylthio tetrazolide
TetH	1-*H*-tetrazole
MTTH	Methylthio tetrazole
(4-F-Ph)TH	(4-fluorophenyl) Tetrazole
PhTH	Phenylthio tetrazole
DEA	Diethyl amine

1. Introduction

1.1 Introduction to Anti-Sense therapies

1.1.1 DNA

DNA (deoxyribonucleic acid) is a biopolymer contained within the nucleus of all eukaryotic cells (in prokaryotes the DNA is located in the cytoplasm and some viruses do not carry DNA) that holds the information necessary for the biosynthesis of proteins. The repeat units of the DNA polymer are known as nucleotides and consist of 3 main components; a nitrogen-containing base group, a sugar molecule (2′ deoxyribose) and a phosphate group. The phosphate group at the 5′ position of one nucleotide forms a phosphodiester linkage with the 3′ hydroxyl group of another nucleotide unit formed by an enzyme catalysed condensation reaction which creates the 'sugar-phosphate' backbone of the DNA polymer as follows (Fig. 1):

Nucleotide*

Purine Bases   Pyrimidine Bases

Adenine   Guanine   Thymine   Cytosine   Uracil
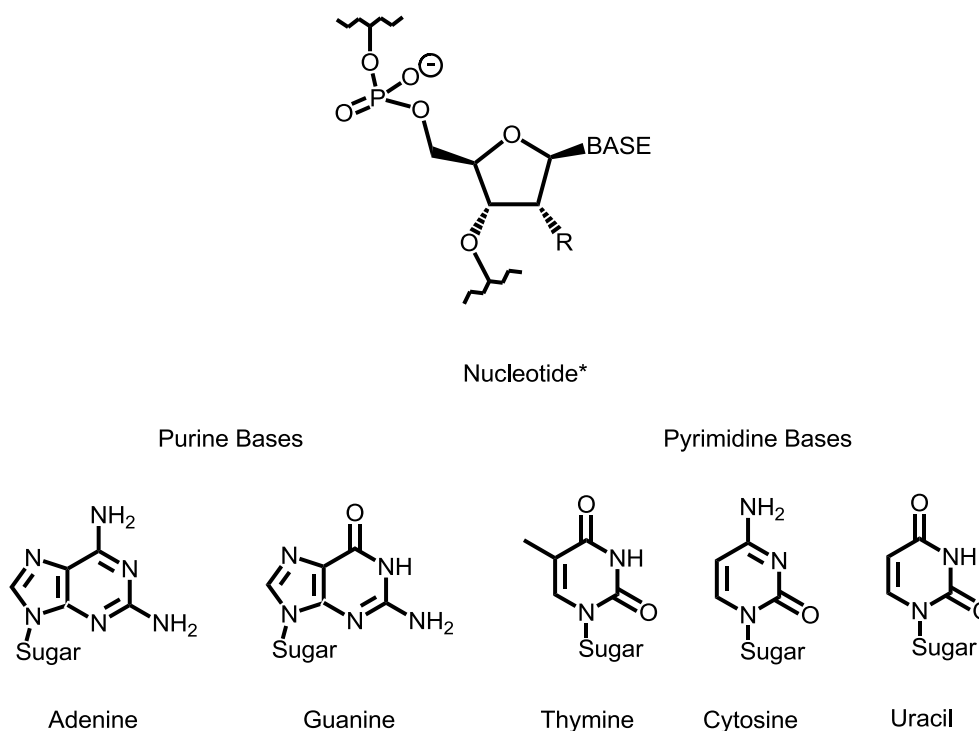
* DNA: R=H, BASE= Adenine, Guanine, Cytosine, Thymine. RNA: R=OH, BASE= Adenine, Guanine, Cytosine, Uracil

Figure 1 Basic structure of DNA and RNA nucleotides

In DNA there are 4 different nitrogen bases. The sequence of bases of DNA determines the amino acid sequence of the proteins for which the specific DNA segment codes. The nitrogen bases also have a structural role. The four nitrogen bases are split into complementary pairs; in DNA, cytosine and guanine are complementary bases and adenine and thymine are complementary. In RNA, thymine is replaced by uracil as the complementary base to adenine. Each base is able to hydrogen

bond specifically to its complementary base on another DNA strand. This interaction is the driving force behind the formation of the double helix macro structure of the DNA molecule. This double helix structure consists of 2 complementary DNA polymers bonded anti-parallel to each other i.e. one is read from 5′-3′ and one reads from 3′-5′. However, only one strand of the DNA molecule, the 'sense' strand codes for proteins. The other strand is a structural feature necessary for the mechanism of protein synthesis, and is known as the 'anti-sense' strand[1-5].

1.1.2 Protein Synthesis – Transcription and Translation

The function of DNA in biological systems is to code for proteins. This occurs via the processes of transcription and translation (Fig. 2).
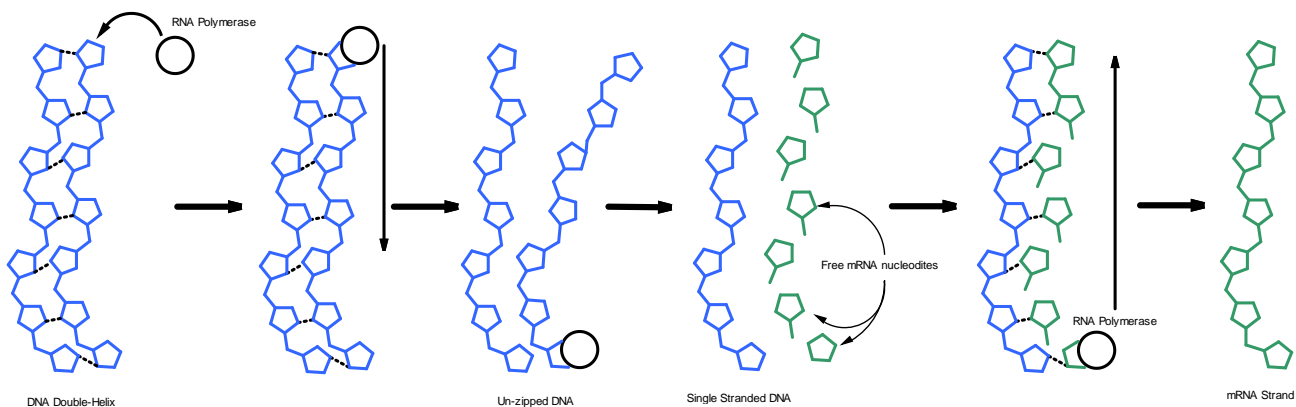
Figure 2: Simplified diagram showing mRNA synthesis via the transcription of DNA

Transcription is the process of translating DNA into a complementary RNA code. Transcription of the DNA into mRNA is necessary as a control mechanism in protein synthesis. For example synthesis of a particular protein may be amplified by transcription of the corresponding DNA sequence into multiple mRNA strands. Protein synthesis can therefore occur at several sites rather than just the one strand of DNA. Furthermore, the inclusion of the 2´-OH makes the mRNA strand more susceptible to hydrolysis[6]. This allows protein synthesis to be terminated upon hydrolysis of the RNA strand, leaving the DNA intact, inside the nucleus.

Transcription is initiated by the enzyme RNA polymerase. The RNA polymerase binds to the sense strand of the DNA at the point which indicates where the protein is to begin being synthesised from

and moves along the DNA double helix 'unzipping' it (breaking hydrogen bonds between strands) as it goes. This allows complementary mRNA nucleotides to bind to the DNA chain to create a RNA polynucleotide which has the same sequence as the original DNA sense strand i.e. RNA C nucleotides bind to DNA G nucleotides, RNA U nucleotides bind to DNA A nucleotides etc. The RNA polymerase catalyses the coupling of mRNA nucleotides to form the sugar-phosphate backbone of the mRNA chain. When the sequence has been fully transcribed the newly synthesised mRNA polymer dissociates. The RNA polymerase is able to rebind to the beginning of the sequence, initiating the synthesis again, meaning that multiple mRNA strands can be synthesised from the same DNA sequence[1-5]. Note that RNA fragments synthesised in this way are known as pre-RNA fragments as they contain non-coding regions known as 'introns'. Before translocation out of the nucleus these introns must be removed or 'spliced' out of the sequence. Translocation of the 'mature' mRNA then takes place as a single-stranded RNA unit.

Translation is the process by which polypeptides are synthesised from mRNA fragments. mRNA is translated three base-pairs at a time. These three-base-pair units are known as codons and there are 64 different codons in the universal genetic code. Each codon codes for one amino acid to be included in the polypeptide chain. Once mRNA is transported out of the nucleus a ribosomal unit is attached to the 5´ end of it which facilitates the addition of complementary tRNA to the mRNA strand. Each tRNA molecule contains one codon and the specific amino acid coded for by that codon. When the mRNA is completely translated into tRNA the polypeptide chain assembled alongside the chain is bonded together to form the completed polypeptide chain[1-5].
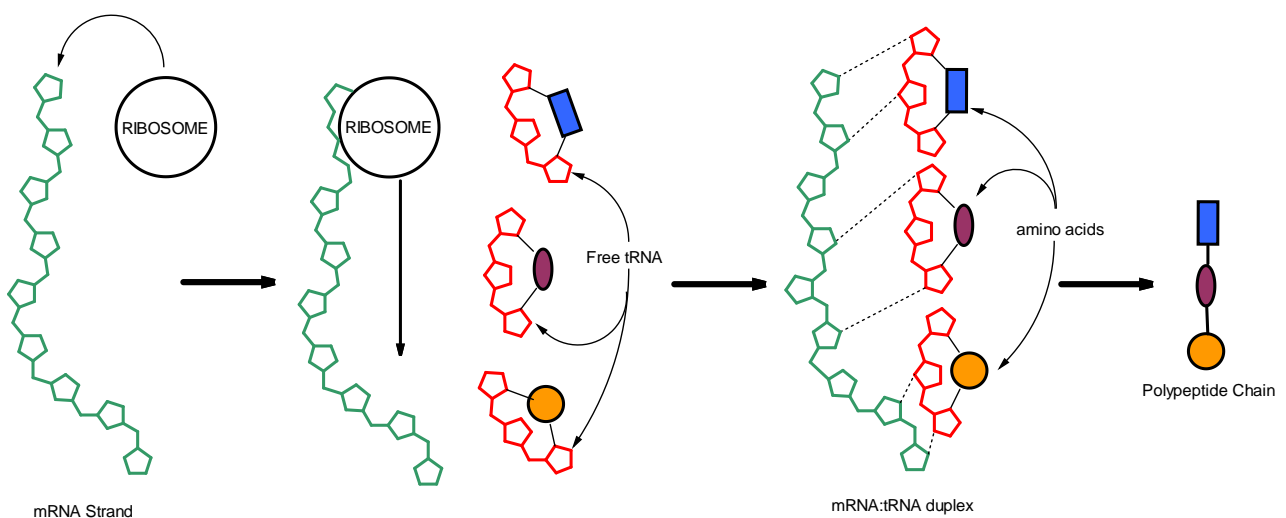
Figure 3: Simplified diagram showing polypeptide synthesis translation of mRNA

1.2 Anti-Sense Therapies

Many diseases are caused by the mis-expression of proteins i.e. under-expression or overexpression of a certain protein or proteins containing flaws such as the inclusion of extra or incorrect amino acids in the polypeptide chain. Therefore many conventional drugs focus on protein targets. However, developing these drugs can be time consuming and expensive and involve a lot of trial and error. The concept of anti-sense therapies is that small chains of modified or unmodified DNA or RNA can be synthesised that are complementary to specific sections of DNA or RNA genes that are involved in the biosynthesis of proteins causing pathology. Anti-sense therapies therefore focus on addressing the root cause of the protein mis-expression: the genes, rather than targeting the proteins themselves. The term 'anti-sense' is employed as the coding strand of the DNA double helix is known as the 'sense' strand and its complementary strand is known as the 'anti-sense' strand. Providing that an appropriate DNA sequence can be identified to affect the expression of the protein in question this method can be highly selective as any DNA sequence consisting of 17 nucleotides or above occurs only once in the entire genome.

This methodology was first proposed by Zamnecnik and Stephenson[7] in the 1970s. Since then many studies have looked at applying anti-sense techniques to provide therapeutic ageints for the treatment of a variety of diseases such as Alzheimer's disease[8], rheumatoid arthritis[9], viral infections[10] and Duchenne muscular dystrophy[11]. Therefore synthesising oligonucleotide sequences that are complementary to DNA/RNA targets allows simple Watson and Crick base pairing to occur bonding the oligonucleotide to its target. Though this may sound simple, since Watson and Crick base pairing has been established for decades, the use of synthetic oligonucleotides to alter protein synthesis is extremely complicated and therefore there are several mechanisms by which these therapies take effect.

1.2.1 Steric Blocking

Oligonucleotides acting through steric blocking use sequences that are complementary to the terminal end of a target strand of DNA or mRNA that is responsible for coding a particular protein. As the name suggests, these therapies work by forming a DNA:anti-sense or mRNA:anti-sense complex that is strongly bound and thus forms a steric barrier. The resulting complex prevents transcription (in the case of DNA:anti-sense complexes) or the downstream processes of translation or splicing (when the target is an mRNA strand)[3,5,7]. This mechanism of action is extremely versatile and can be employed to many targets to prevent genetic processing. There are no specific structural features necessary in the synthetic oligonucleotide for this mechanism to be employed, the molecules simply has to bind strongly to its target[5-7].
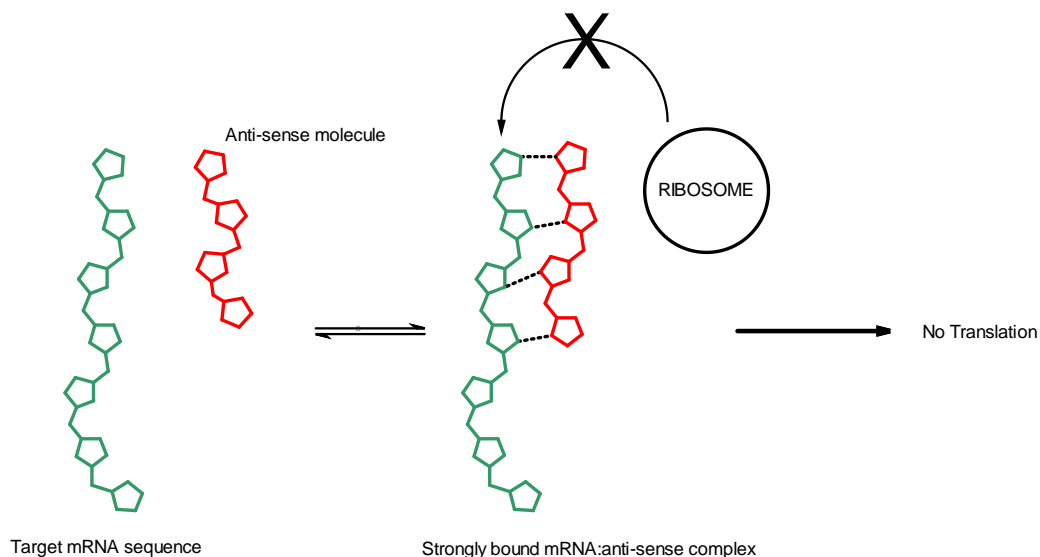
Figure 4: Simplified Diagram of a steric-blocking anti-sense therapy blocking translation of mRNA

As stated above, whilst the majority of therapies employing this strategy work at the transcription[12] or translation[13] level, some oligonucleotides have been reported to affect the splicing of pre-RNA to mature RNA[14] or to prevent translocation of mRNA across the nuclear membrane by forming an mRNA:anti-sense complex inside the nucleus[15].

Though this mechanism of action of oligonucleotide therapies is extremely versatile it is quite demanding in terms of the dose of oligonucleotide required as the effect is only observed whilst the oligonucleotide is bound to its target. Larger doses of these oligonucleotides are therefore required to be effective therapies[16].

1.2.2 Exon-Skipping Mechanism

Exon-skipping is a type of steric-blocking utilised by some anti-sense oligonucleotide therapies[17]. Exons are the sequences of mRNA that make up the final mature mRNA sequence. After DNA is transcribed into pre-mRNA, sections of nucleotides known as 'introns' are cut out and the resulting pieces (exons) are spliced together to make up the final mRNA sequence[1,2,4].

The exon skipping mechanism is similar to a steric blocking mechanism in that the oligonucleotide blocks the ribosome binding to the mRNA. However, in an exon skipping mechanism, the therapeutic oligonucleotide binds to a specific exon (the section of the mRNA responsible for the pathology of the disease) within the mRNA sequence rather than at the terminal end. This type of interaction does not prevent the ribosome from binding to the mRNA sequence but rather blocks the translation of the particular section to which it is bound. This allows some of the RNA to be translated into a polypeptide chain but skips misinformation thus synthesising an incomplete but functional protein[18,19]. This mechanism relies on the fact that the protein would still be functional without the inclusion of the small section coded for by the 'skipped' exon.
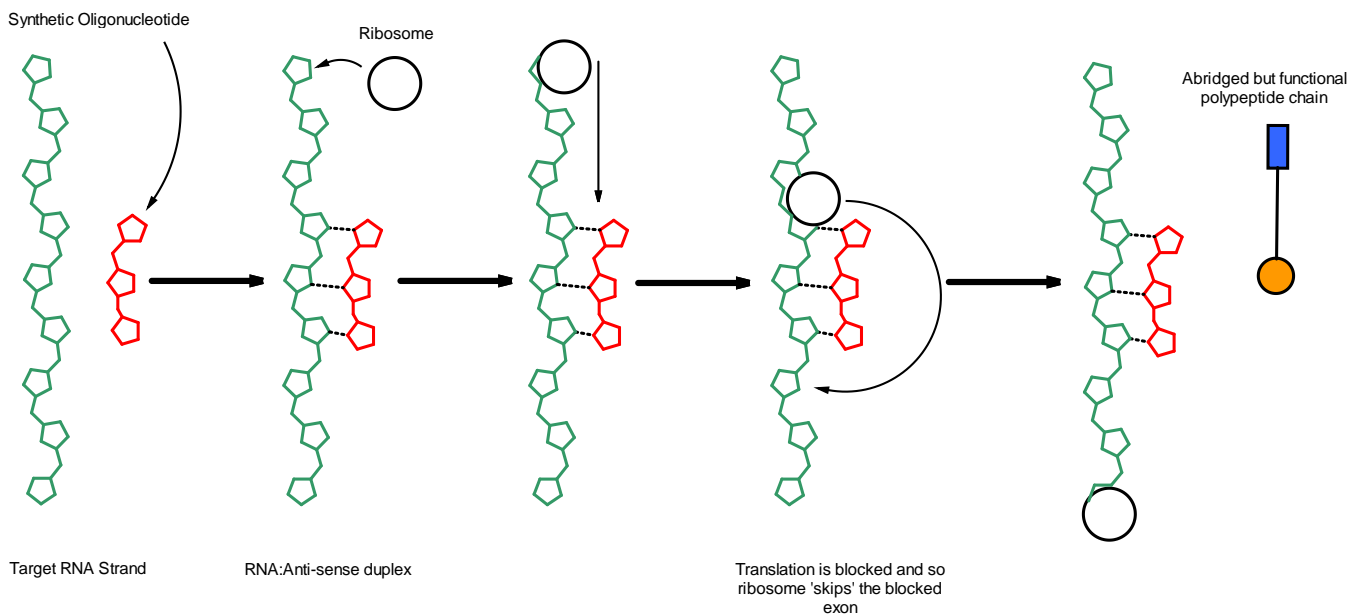
Figure 5: Simplified Diagram of an exon-skipping anti-sense therapy blocking translation of specific exons to generate abridged but functional proteins

In 2016 the exon-skipping drug 'Eteplirsen' from Sarepta Therapeutics was granted accelerated approval from the FDA as a treatment for Duchenne muscular dystrophy. This particular molecule contains 30 nucleotide units (a '30mer') and has a full morpholinodiphophoramidate backbone (see section 1.3)[20] however similar candidates have also been proposed containing full 2´OMe-phosphorothioate backbones[21].

Duchenne muscular dystrophy (DMD) has many manifestations from exon deletions, exon duplications or specific nucleotide mutations in the gene coding for the dystrophin protein; a key structural component in skeletal muscle[22]. The condition affects approximately 1 in every 3500 new-born boys and causes extreme muscle weakness, early loss of ambulation (pre-10 years old) and typically death between the ages of 20 and 35 years old. The gene contains 79 exons and over 3600 base pairs[23].

The exon-skipping anti-sense therapies used to treat the condition target exon 51 of the dystrophin gene. These compounds bind to exon 51 of the mRNA strand coding for the defective dystrophin protein prior to splicing and translocation out of the nucleus. This causes exons 50 and 51 to be omitted from the mature mRNA sequence which can then be translated into a polypeptide chain via the normal mechanism (Fig. 3)[21]. This causes the synthesis of a truncated but functional polypeptide chain. Though Eteplirsen was only found to afford patients 1% of the amount of functional dystrophin protein seen in the normal population, other candidates have shown levels of between 3-12% of the amount of the protein[21], a significant increase in patients whose natural, functional dystrophin production is negligible.

Due to the diversity of the manifestation of DMD, it is estimated that therapies targeting exon 51 of the dystrophin gene are able to treat around 16% of the patient population and the therapy must be administered for the rest of the patient's life[21]. This is nevertheless a promising example of the ability of anti-sense therapies to treat life threatening diseases that current medicines are only able to manage the symptoms of.

1.2.3 RNase-H Activation

RNase-H is a non-specific enzyme which hydrolyses the sugar-phosphate backbone of the mRNA strand in free DNA:mRNA complexes during DNA replication generating free DNA and short sections of the mRNA primer[3,5]. The function of RNase-H is to prevent translated newly synthesised mRNA from remaining bound to their template DNA for too long as this can prevent protein synthesis and reformation of the DNA double-helix structure. It must be stressed that RNase-H is only able to hydrolyse the mRNA strand and is inactive towards DNA polymers.

Oligonucleotides can activate RNase-H enzymes by forming mRNA:oligonucleotide complexes with the target mRNA. In order to activate this process, the RNase-H enzyme must recognise this oligonucleotide:RNA complex as a natural DNA:mRNA complex. The mRNA strand will then be cleaved in order to generate free oligonucleotide. Since most backbone modifications render oligonucleotides unrecognisable to RNase-H an essential inclusion in an anti-sense oligonucleotide employing this mode of action is an unmodified section of the backbone; i.e. a small section replicating wild-type DNA[24]. This of course increases the therapy's susceptibility to hydrolysis *in vivo* and may make it less likely that the sequence will be able to cross the phospholipid bi-layer of the cell due to the increased negative charge on the backbone[16].

Activating RNase-H is a desirable method of action of therapeutic, synthetic, anti-sense oligonucleotides since molecules acting in this way are able to bind to multiple targets, generating a catalyst-like effect.
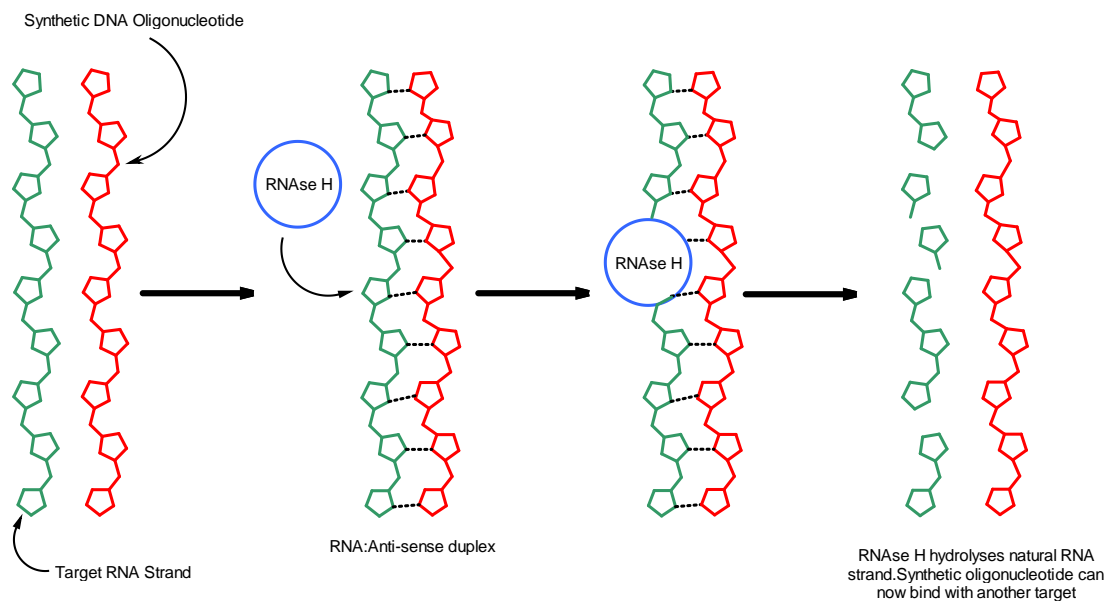
Figure 6: Simplified Diagram of RNase-H activation by synthetic oligonucleotides

1.3 Oligonucleotide Modifications

Though anti-sense therapies offer the possibility of an effective, selective and easily synthesised treatment for many diseases, oligonucleotides present several problems in terms of their physical properties[17]. Wild-type or natural oligonucleotides containing DNA or RNA units linked together via the sugar-phosphate backbone are very large molecules, with molecular weights in the order of 10^3 gmol^{-1}, and carry extremely large negative charges[17]. This poses problems in terms of cell uptake as such large, highly charged molecules have trouble crossing the hydrophobic phospholipid bi-layer of cells[25-27]. The second problem posed by these unmodified oligonucleotides is the fact that they are extremely susceptible to hydrolysis by nuclease enzymes. These difficulties can be largely overcome by modifying the synthetic oligonucleotide in one of several ways[26,27], each presenting their own advantages and disadvantages.

1.3.1 Backbone Modifications

Modifications can be made to the phosphate-backbone of the oligonucleotide in which one or more of the bridging or (more commonly) non-bridging oxygen atoms in the chain are exchanged with different groups. Some are shown below (Fig. 7).

W=O, X=O, Y=O, Z=O : Natural Phosphate

W=S, X=O, Y=O, Z=O : Phosphorothioate

W=CH$_3$, X=O, Y=O, Z=O : Methylphosphonate

W=NH$_2$, X=O, Y=O, Z=O : Phosphoramidate

W=BH$_3^-$, X=O, Y=O, Z=O : Boranophosphate

W=O, X=CH$_2$, Y=O, Z=O : Bridged Methylenephosphonate

W=O, X=NH, Y=O, Z=O : Bridged Phosphoramidate
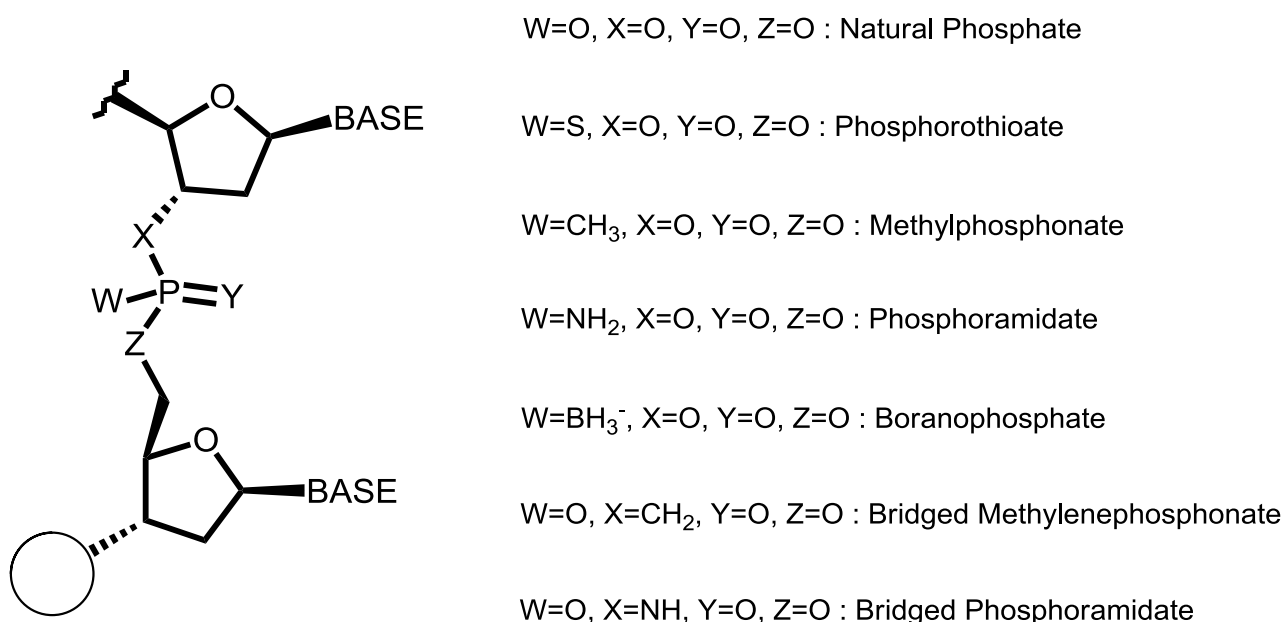
Figure 7: Examples of oligonucleotide backbone modifications

1.3.1.1 Phosphorthioates and Phosphorodithioates
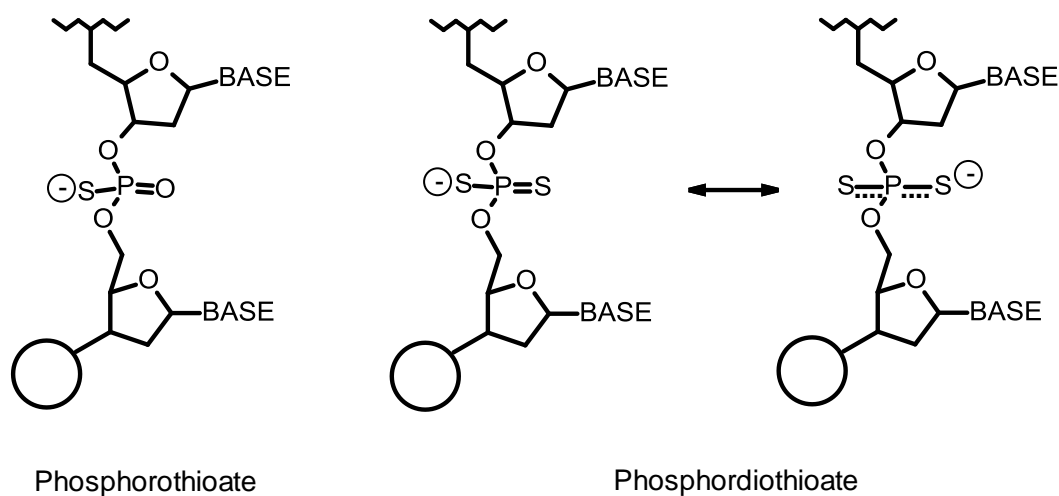
Figure 8: Phosphorothioate and phosphorodithioate linkages

The phosphorothioate linkage differs from the natural phosphodiester-type back bone in that it has one of the non-bridging oxygen atoms replaced by a sulfur atom. Naturally occurring phosphorothioate linkages have been found in the DNA of certain bacteria[28]. These types of derivatives have also been used to study enzyme stereochemistry[29] since the incorporation of sulfur into the phosphate backbone generates chirality at phosphorus. The resultant diasteroisomers show resistance and susceptibility to different enzymes, for example, snake venom phosphodiesterase (SVP) was found to hydrolyse the *R*p diastereosiomer, leaving the *S*p isomer in-tact whilst nuclease P1 cleaved the *S*p configured linkages and was inactive towards the *R*p[30].

These functional groups are now widely being employed as a non-bridging backbone modification in anti-sense therapies. The presence of the chiral phosphorus centres has been shown to decrease the overall binding efficiency of the oligonucleotide to its target as only the *R*p isomer binds more strongly since the orientation of the *S*p isomer is helix destabilising[31,32]. The chirality also has implications on nuclease resistance. Incorporation of sulfur into the phosphate backbone of the molecule increases nuclease resistance. However, it has been shown that whilst the *S*p diasteroisomer is entirely resistant to endo- and exonucleases, the *R*p diastereosiomer is sensitive to such enzymes, albeit only slightly[33].

Though attempts have been made to synthesise diastereomerically pure phosphorothioate linkages[32,34] these have often either shown low diastereomeric selectivity or incompatibility with current oligonucleotide synthesis techniques. An alternative to this is to replace both of the non-bridging oxygen atoms with sulfur, generating phosphorodithioate group which are non-chiral at phosphorus. As these molecules do not have chiral phosphorus centres they show increased duplex stability when compared to phosphorothioates and similar aqueous solubility to both phosphorothioates and phosphates. However, these molecules show a highly increased susceptibility towards nuclease hydrolysis compared to phosphorothioates[35,36].

The charge distribution of phosphorothioates is slightly different to that seen in the phosphate group. The wild-type phosphate groups are able to distribute their negative charge over both of the non-bridging oxygen atoms whereas NMR studies have shown that in phosphorothioates, the negative charge is largely on the sulfur atom. This gives the non-bridging oxygen a double bond to phosphorus[37]. The negative charge on sulfur greatly increases aqueous solubility. Suprisingly, due to the polarisability of the thioate anion, this functionality also facilitates cell uptake, meaning that phosphorothioates also have favourable cell absorption as compared with the wild-type[33,38]. Perhaps the most important aspect of the use of phosphorothioates is that they are able to activate RNAse H enzymes when complexed with the target DNA[5].

Synthesis of phosphorothioate containing oligonucleotides can be performed in many different ways, using many different reagents. The first instance of the synthesis of oligonucleotide phosphorothioates was described in 1970[39] and involved the oxidative sulfurisation of phosphite triesters using elemental sulfur in pyridine. Since then, many novel sulfur transfer reagents have been developed (detailed in section 1.6.2) that are compatible with most synthesis and coupling methodologies. Synthesis of phosphorodithioates is acheived in much the same way as that of phosphorothioates except that a protected phosphorothioamidite reagent must be generated in-situ prior to the coupling step. Also, whilst di-isopropyl phosphoramidites are the reagent of choice for phosphorothioate synthesis, the steric bulk of these compounds results in low coupling efficiency during phosphorodithioate synthesis[40].

1.3.1.2 Alkylphosphonates

Alkylphosphonates are oligonucleotides in which one of the non-bridging oxygen atoms in the natural phosphodiester groups along the backbone of the molecule is replaced with an alkyl group[14]. The major advantage of using this modification is that the resulting phosphorus species is neutral. This alters the mechanism of absorption in to cells, allowing passive diffusion across membranes rather than entering via endocytosis, as is the case with wild-type or other modified oligonucleotides[41,42].

These modifications also generate a chiral phosphorus centre. This has resulted in conflict in the literature as to whether this chirality is an advantage or disadvantage as it has both been shown that the stability of many duplexes of methylphosphonates is not influenced by the stereochemistry at phosphorus[35,43,44], and conversely, that duplex stability suffers when the methyl group is pointing into the major groove of the duplex due to steric repulsion[35]. Nevertheless, the elimination of electrostatic repulsion between the oligonucleotide and its target, caused by the lack of charge in this group, appears to have favourable results in terms of binding affinity. A further advantage of the inclusion of this modification into oligonucleotide chains is that they are resistant to hydrolysis by endo- and exonuclease enzymes[45]. However, this biological stability eliminates the ability of molecules of this type to activate RNAse H.

There are many reported methods of synthesis of these modifications. The most efficient methodologies, however, involve the use of either alkyl phosphonoamidites[46] as starting materials or the addition of alkyl groups via Arbuzov-type reactions[47] (scheme 1).
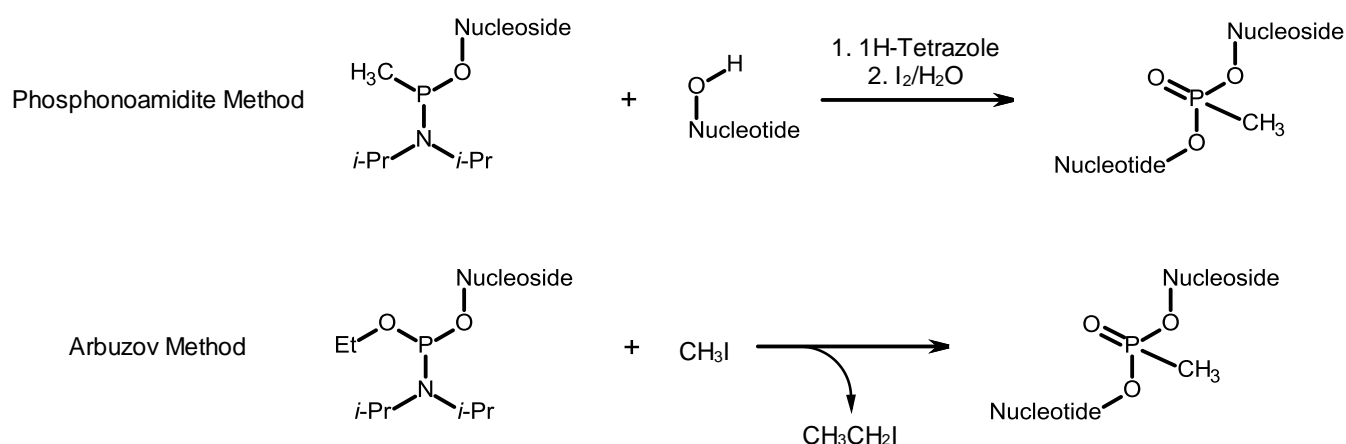
Scheme 1: Synthesis of methylphosphonates via the phosphonoamidite method (top) and the Arbuzov reaction (bottom)

13

1.3.1.3 Phosphoramidates

Phosphoramidates include the replacement of one of the non-bridging oxygen atoms with an amine group. These groups again generate chirality at phosphorus and so show decreased duplex stability. However, these groups have been shown to have increased binding efficiency at lower pH due to protonation of the amine group.

Modifying oligonucleotides in this way increases resistance to nuclease hydrolysis. However, oligonucleotides in which every phosphate group is replaced with a phosphoramidate group show decreased duplex stability due to distortions occurring in the molecule[35,48]. As with alkylphosphonates, phosphoramidates are unable to activate RNase-H enzymes and as such must act only in steric blocking pathways when used as anti-sense therapies.

Again, there have been many synthetic methods reported for these compounds. These, however, often involve the use of extreme conditions which are incompatible with modern solid-phase synthesis routes such as reflux or elongated reaction times[49]. The easiest method (and most widely compatible with solid phase techniques) involves the oxidation of phosphite triesters by iodine in the presence of alkylamines.This generates the desired phosphoramidite; however, yields can often vary between 50-90%[50].
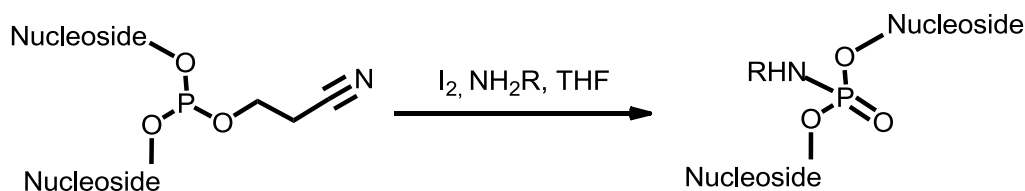
Scheme 2: Synthesis of phosphoramidates via oxidation of phosphite triesters in the presence of amine

14

1.3.1.4 Boranophosphates

Boranophosphates are chiral phosphate analogues in which a borane group has been introduced to replace one of the non-bridging oxygen atoms (Fig. 7). These can be considered a hybrid between the polar PO and PS linkages and the non-polar alkylphosphate linkages since the negatively charged borane group is isoelectronic with the chalcogen derivatives and isostructural with the alkyl analogue. Much like the wild-type phosphate linkage, the boranophosphate group has a permanent negative charge and therefore displays reduced binding affinity when compared with other analogues due to steric repulsion[45]. However, this functionality shows excellent nuclease stability and, unlike alkylphosphonates and phosphoramidates, this linkage is also stable to extreme reaction conditions and extreme pH[51].

Synthesis of these compounds can be performed easily and in a similar manner to that of modern oligonucleotide synthesis methods by using boronated phosphoramidites as the coupling substrate[51].

1.3.1.5 Exchange of the Bridging Oxygens and Dephospho Analogues

Exchange of the non-bridging oxygen atoms in the phosphate linkage provides possible solutions to problems with solubility, membrane translocation and binding affinity. Many of these modifications have also been shown to be applicable, in principle to the bridging oxygen atoms also, such as bridging phosphorothiolates[52], methylene bridged phosphonates[53] and bridging phosphoroamidates[54]. These groups all provide the desirable properties associated with removing the negative charge and eliminating chirality at phosphorus to improve overall binding efficiency and, in the case of the charge minimisation, improvement in transport across the cell membrane with minimal steric demand. However, changing the chemistry at the bridging oxygen atoms can have a much more drastic effect on the stability of the resultant complex than exchange of non-bridging oxygens. For example, exposing bridging phosphoramidates to acetic acid at room temperature causes cleavage of the strand[55] whereas treating a non-bridging phosphoramidate with acid can in fact cause increased duplex stability.

Similarly, it has proved possible to synthesise dephospho inter-nucleotide bridges which also meet these criteria such as replacement of the phosphate group with a siloxane[56], carbonate [57] or amide linkage to name but a few[58] (Fig. 9).

X = CH$_2$, S, NH   Carbonate Linkage   Amide Linkage   Siloxane Linkage
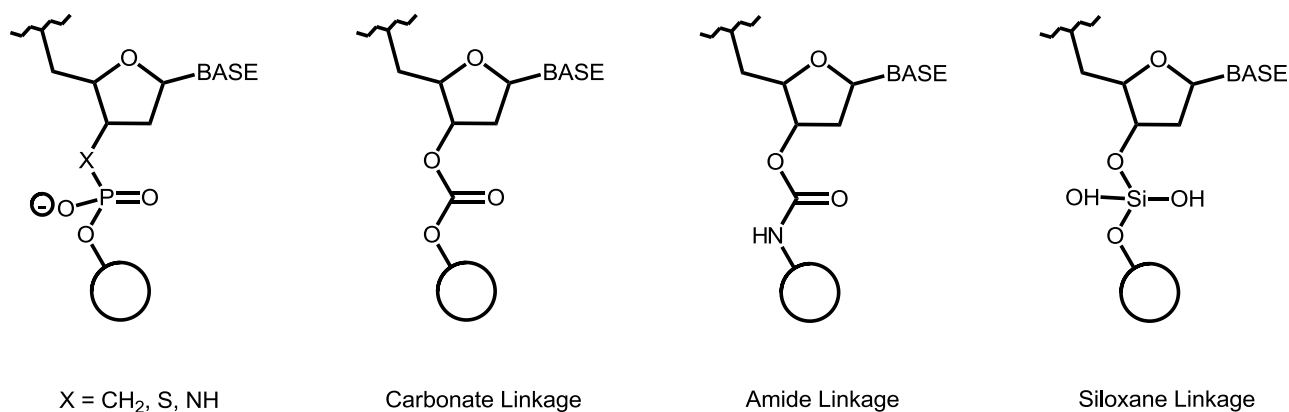
Figure 9: Various dephospho and bridge modified oligonucleotide linkages

The major issue with these functionalities is that they are generally incompatible with solid phase synthesis, requiring high temperatures or complex multi-step syntheses. Due to the difficulty in their manufacture few dephospho-oligonucleotides have ever been synthesised larger than trimers. One way to avoid this issue is to synthesise a dimer which can then be phosphitylated to form a phosphoramidite which can then be used as a coupling reagent in the phosphoramidite synthesis method. Whilst this may seem like a plausible solution, this greatly increases the cost and complexity of the synthesis and results in a backbone with mixed functionality.

The most promising dephospho-oligonucleotide analogue currently is the replacement of the phosphate group with a triazole linker using click chemistry as the coupling chemistry. This method has been used in tandem with modern solid-phase methodology and is able to produce oligonucleotides containing 100+ base units[59] (scheme 3).
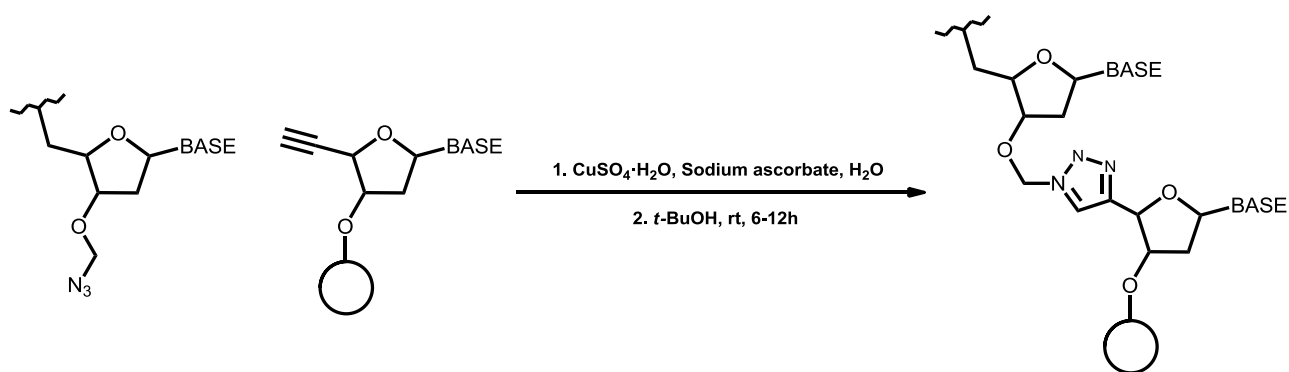
Scheme 3: Synthesis of dephospho-triazole-linked nucleotides using click chemistry

16

1.3.2 Sugar Modifications
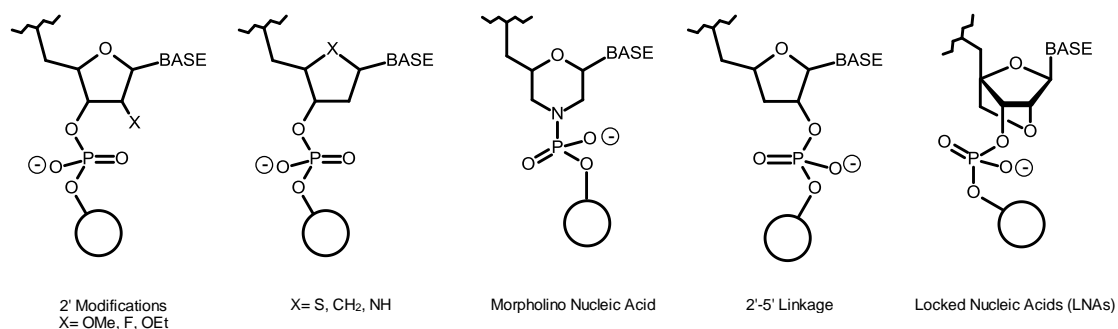
Figure 10: Examples of sugar modifications used in therapeutic oligonucleotides

Oligonucleotides have also been reported that feature modifications to the nucleotide sugar unit[35,60,61]. Altering nucleotides in this way has been proven to greatly increase nuclease resistance. For example, linkages comprised of nucleotides in which the furan oxygen is replaced with sulfur display hydrolysis rates of around nine times slower than the natural nucleotides[62], whilst replacing the furanose oxygen with a methylene group renders the linkage almost completely resistant to all tested nuclease enzymes[63]. Modifications of this type have little or no effect on duplex stability[64-66].

The most common sugar modifications used in therapeutic oligonucleotide are modifications at the 2′ position of the sugar. An electronegative group at this position, such as methoxy or fluoro groups, promote a favourable C_2-endo gauche conformation of the sugar (Fig. 11) The gauche relationship refers to the orientation of the nucleobase group relative to the O of the furanose ring. This increases the binding efficiency of the oligonucleotide:RNA duplex[67]. Large alkyl groups at the 2′-position decrease binding efficiency due to the steric bulk. Modifications of this type do increase resistance to most nuclease enzymes compared to the natural RNA or DNA-type oligomers. A disadvantage is that 2′-sugar modifications typically render the oligomer non-RNase-H active[61].
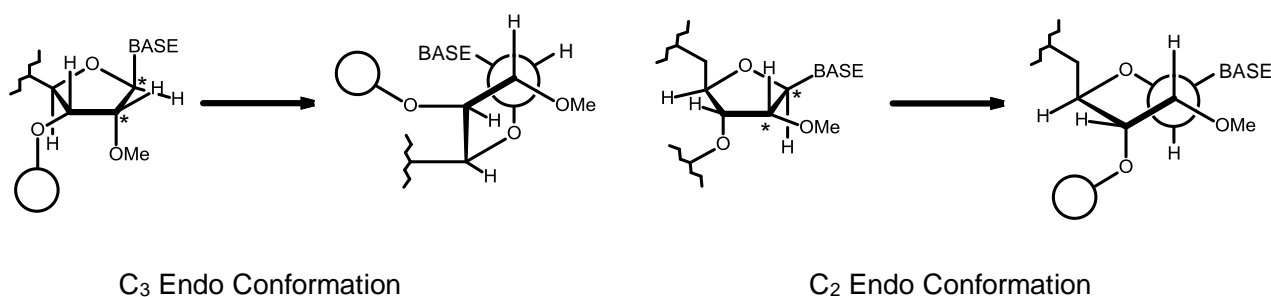
Figure 11: Diagram Showing C_3-Endo and C_2-Endo conformations of the ribose sugar ring and the resulting Newman projections along the $C_1{}^*$-$C_2{}^*$ bond.

17

1.4 Synthesis of Oligonucleotides

The first polynucleotide was synthesised, in solution, by Khorana and a team of researchers in 1960[68] using phosphate diester technology. At the time, there was no projected use for such compounds and this was seen purely as a synthetic challenge. Several other solution phase methodologies were later developed using phosphate triester of nucleic acids[69]. Caruthers introduced the idea of synthesising these molecules on a solid support in 1981[70]. The advantage of using a solid-phase synthesis is that products do not need to be purified after each reaction step since the product molecules are immobilised and the excess reagents can simply be washed away. Whilst phosphochloridite chemistry can be applied to solid-supported methodology, the reactivity of the starting materials meant that the use of this technology on a solid-support was not widely adopted.

Today, oligonucleotide synthesis is almost exclusively carried out using solid-supported synthesis in which the 3′ end of the chain is attached by a chemical linker to a polymer support. The oligonucleotide is then synthesised by the addition of one nucleotide at a time to the 5′ end of the growing polymer. The coupling reactions of these monomer units vary depending on both the methodology used and the starting material (Fig. 12).
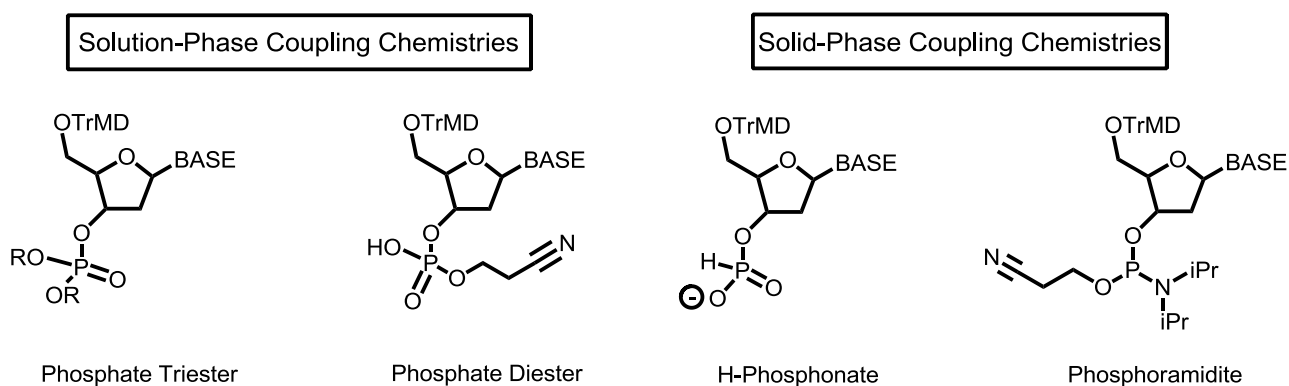
Figure 12: Coupling reagents used in various methods of oligonucleotide synthesis

18

1.5 H-Phosphonate Method
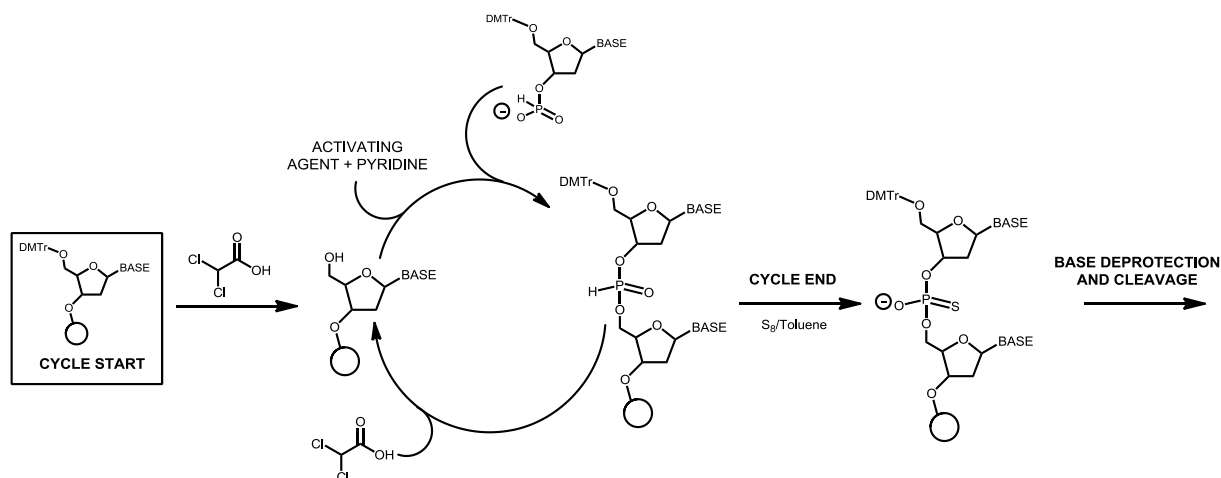
Scheme 4: General scheme for phosphorothioate synthesis via the H-phosphonate method

The H-phosphonate method of oligonucleotide synthesis was first proposed in 1957 but was not actually implemented until 1986[71]. This method consists of two basic steps: activation withactivating agent such as 2,4,6-triisopropylbenzenesulfonyl chloride, *N,N*-bis(2-oxo-3-oxazolidinyl)- phosphorodiamidic chloride, diphenylchlorophosphate or pivaloyl chloride and then reaction with a 5´-deprotected nucleoside. This cycle is repeated until the desired chain length is attained. When the desired chain length is achieved, the resulting oligonucleotide is followed by a functionalisation or oxidation step. Synthesis of oligonucleotides containing full phosphorothioate backbones is possible using this method when the resulting H-phosphonate oligonucleotides are treated with a solution of S_8 in toluene[72,73] (scheme 4). Oxidation to the natural phosphate backbone is achieved by treating the H-phosphonate oligonucleotide with a solution of I_2 in water.

The disadvantage of this cycle is that, unlike with the phosphoramidite method, no mixed functionality can be achieved as only one oxidation step is carried out per synthesis. A further disadvantage of this method is that the reagents are susceptible to side reactions with the activators such as acylation[72-75]. However, H-phosphonates are extremely stable starting materials requiring no careful solvent drying or special handling procedures. They are unreactive towards any nucleophilic impurities in solution (including water) meaning that coupling reactions using H-phosphonate nucleotides does not require the large excess of starting material that, for example, coupling phosphoramidites requires, making the H-phosphonate method an attractive alternative to other popular synthesis methodologies.

1.6 Phosphoramidite Method

The phosphoramidite method of synthesising oligonucleotides is currently the most commonly used method of synthesising long-chain oligonucleotides for pharmaceutical application. The modern incarnation of this method is a solid-phase synthesis whereby the growing oligonucleotide chain is bonded to a polymer support. The synthesis comprises four steps (scheme 5) which are repeated until the desired chain length is reached. Once the desired chain length is reached the oligonucleotides are cleaved from the polymer support and deprotected using base[70,76]. The newly synthesised oligonucleotides are then subjected to various purification steps.
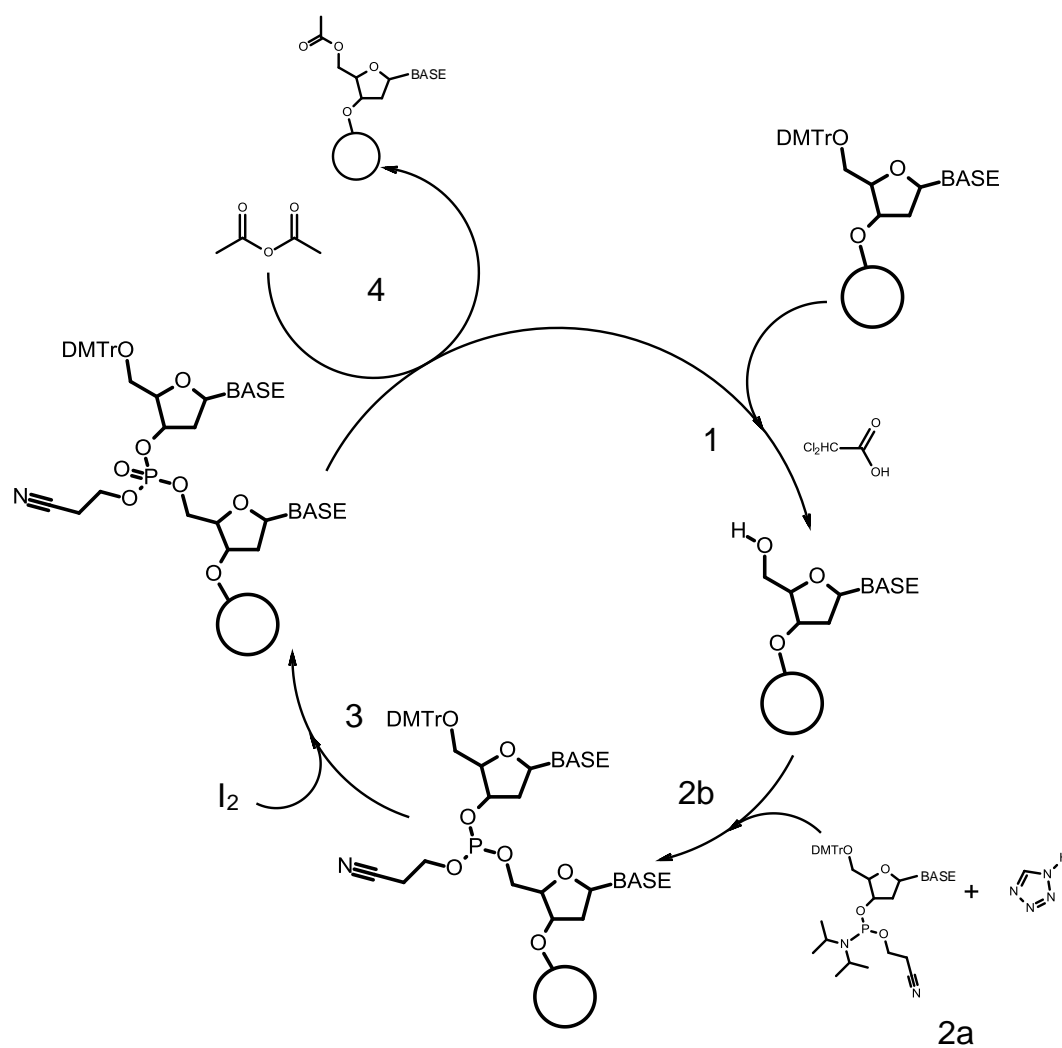
Scheme 5:The synthesis cycle of a DNA oligonucleotide with phosphate backbone using tetrazole as the activator. 1. Deprotection with dichloroacetic acid in toluene, 2a. Activation with 1H-tetrazole, 2b. Coupling, 3. Oxidation with Iodine, 4. Capping with acetic anhydride.

This method is widely employed due to the ease with which it can be performed and the variety of functionality achievable via this method. The solid support methodology allows this synthesis to be fully automated and the step-wise nature of the synthesis allows various different oligonucleotides to be produced i.e. phosphorothioate, methylphosphonate, boranophosphate etc. It is possible to generate chains with mixed functionality using this method since functionalisation takes place directly after each coupling and not at the end of the synthesis as was the case with the H-phosphonate method. The ease of manipulating backbone modifications is an advantage of the initial generation of the P(III) linkage when using phosphoramidites as the coupling reagents.

This method was first developed by Caruthers in the 1980s. The original phosphoramidites used in this synthesis were N,N-dimethylaminophosphoramidites which were activated by N,N-dimethylaniline hydrochloride. However, since the introduction of the method, there has been a lot of focus on improving and refining the procedure to make it more suitable to the modern demand for these reagents. The nucleosides used in the synthesis are now generally 3′-β-cyanoethyl N,N-di-isopropylphosphoramidites. The bulkier isopropyl substituents on the amine group render the phosphorus centre in the molecule less reactive and therefore easier to handle[70,76].

The major disadvantage of using this chemistry is that activated phosphoramidites are highly susceptible to hydrolysis by the water which is present in the solvent and so careful drying of solvents and reagents must be carried out, though loss of yield due to hydrolysis is always expected (scheme 6). Therefore, when implemented in an industrial setting, a large excess of coupling reagents is used to force a complete reaction. This has major implications on the cost of the total synthesis as well as the environmental impact.
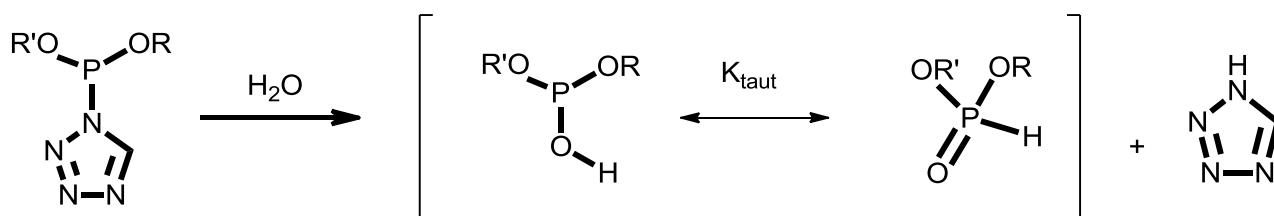
Scheme 6: Hydrolysis of a phosphoramidite activated by 1H-tetrazole

1.6.1 Activation and Coupling of Phosphoramidites

The coupling step of the phosphoramidite synthesis cycle consists of the alcoholysis of the 3′-β-cyanoethyl *N,N*-di-isopropyl phosphoramidite reagents by the free 5′-hydroxyl group of the growing oligonucleotide chain. This reaction is responsible for extending the oligonucleotide chain. Neutral phosphoramidites are generally quite resistant to nucleophilic attack and so this step only occurs in the presence of an activator. The high cost of the phosphoramidite reagents means the choice of activator is extremely important as the activator needs to afford high yielding coupling reactions with a fast rate in order to avoid side reactions whilst ensuring the maximal number of couplings[77].

Research by Caruthers into novel activators led to the discovery that 1H-tetrazole (Fig. 13)provided rapid rates of reaction with near quantitative conversion to the coupled dinucleotide whilst being commercially available. It is generally accepted that the mechanism of activation of phosphoramidites by 1H-tetrazole is one of general acid catalysis in which the phosphoramidite group is protonated by the acidic activator (scheme 7.2). 1H-Tetrazole has a pK_a of 14.5 in ACN[78] which allows protonation of the phosphoramidite but does not cause any unwanted side reactions such as depurination or detritylation which occurs with the use of other, stronger acids[76,77,79]. This compound therefore remains a popular choice as an activator. Disadvantages of using 1H-tetrazole are that it is expensive, toxic and potentially explosive[70,76]. Therefore further research has gone into identifying alternative activators.

.
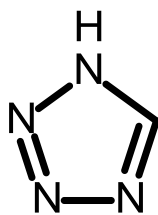
Figure 13: 1H-Tetrazole

1.6.1.2 Nucleophilic substitution during coupling

The reaction of the activated amidite with the 5′OH group of the oligonucleotide chain occurs via a nucleophilic substitution reaction. This could either occur by direct attack of the alcohol group on the phosphorus or it could proceed via an intermediate formed by reaction with the activator i.e. by nucleophilic displacement of the amine group of the amidite by the conjugate base of the deprotonated activator. It is worth noting that an attractive proprty of tetrazoles in this regard is that whilst they are relatively acidic, the conjugate base of these acids (tetrazolide ions) are also reasonable nucleophiles. To determine whether the alcoholysis occurs by attack directly at the phosphoromadite or whether is occurs via a tetrazolide intermediate, nucleoside tetrazolide species were synthesised and isolated. The ^{31}P NMR shifts of these compounds are similar to those found in reaction mixtures when tetrazole is used as an activator during the reaction. This is indicative of nucleophilic attack by the tetrazolide on the protonated phosphoramidite[70,79] (scheme 7).

Regardless of the mechanism of nucleophilic attack, every coupling step generates one molar equivalent of di-isopropylamine. The nature of the tetrazole-based activator system is such that a salt is formed between the acidic activator and the basic leaving group[80,81]. This stops the activator from acting as a catalyst since one molar equivalent of activator becomes involved in acid-base equilibria with the amine leaving group. Studies have shown that removing the generated amine with 10Å molecular sieves allows the activator to act catalytically[80].

1.6.1.3 Phosphoramidite protonation

It has been proposed that protonation of the amidite could occur either at the phosphorus centre[77,82] or on the nitrogen atom of the di-isopropylamine group[83]. Molecular modelling work however has shown that protonation of the phosphorus shortens, and therefore strengthens, the P-N bond whereas protonation of the nitrogen lengthens and therefore weakens the P-N bond. This therefore indicates that protonation of the nitrogen generates a more reactive species than a P-protonated system[84,85]. This was supported by work done by Nurminen *et al* who showed by NMR that the rate of coupling was slower when P protonation occurred[78,83]. During this work, Nurminen also showed that P-protonation was indeed possible, however, this requires acids with pK_a in acetonitrile of less than 10. The use of acids of this strength is undesirable under the conditions of the phosphoramidite synthesis as it increases the risk of side reactions occurring including depurination.
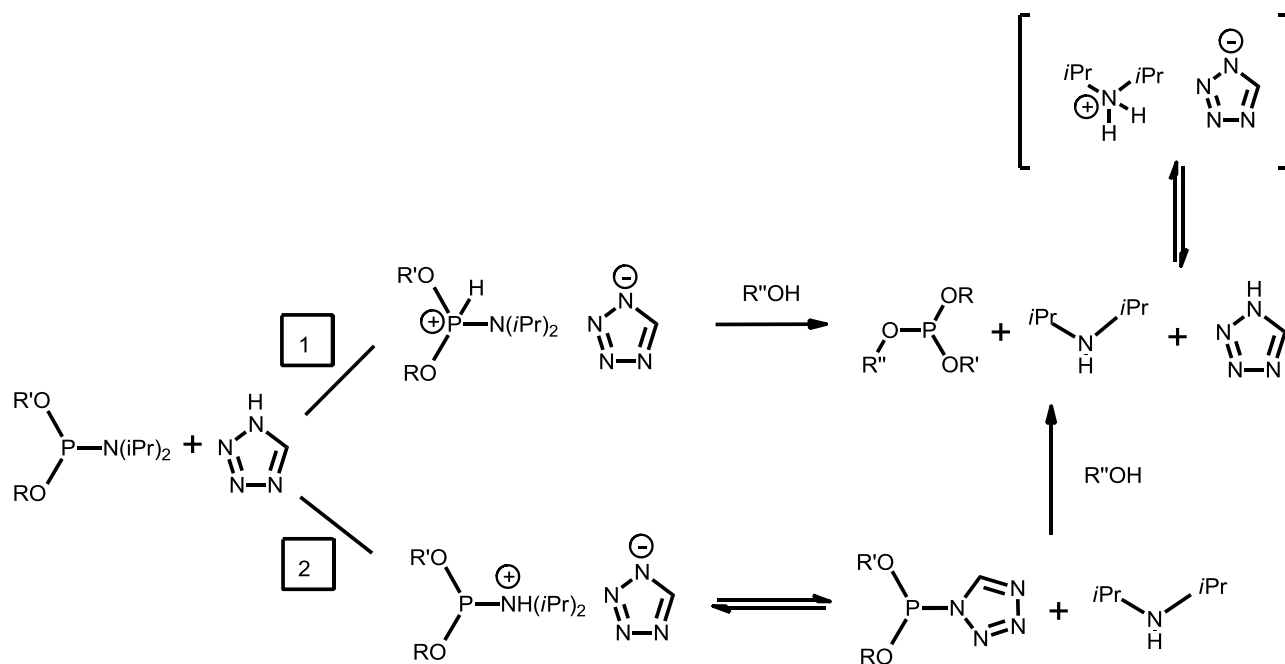
Scheme 7: Scheme showing the different possible pathways of phosphoramidite protonation. Direct P-Protonation (1) and protonation of the di-isopropylamine group (2).

1.6.1.4 Choosing an activator

A good activator must be acidic enough to protonate the amine group of the amidite whilst not being too acidic so as to cause phosphorus protonation, depurination or detritylation. Upon disassociation of the acid, a nucleophile must be generated with sufficient nucleophilicity to displace the amine group from the phosphoramidite via nucleophilic substitution i.e. a weak acid with a strongly nucleophilic conjugate base. This has led to the discovery of a number of acidic activators including (but not limited to) 2,4-dinitrophenol[85,86], various 5-substituted tetrazoles (5-ethylthio-1H-tetrazole[87], 5-benzylthio-1H-tetrazole (ETT)[88], substituted 5-phenyl-1H-tetrazoles[89], 5-(benzylmercapto)-1H-tetrazole[90]) and various carboxylic acids[80].

1.6.2 Sulfurisation step

Phosphorothioate modified oligonucleotides are extremely popular structures to use as potential therapeutic agents due to their increased nuclease resistance and their improved cell uptake compared to the wild-type phosphate oligonucleotides. These molecules can be readily synthesised on a solid support. If using the phosphoramidite method, sulfurisation involves the oxidative transfer of sulfur to the P(III) inter-nucleotide linkage from an appropriate sulfur transfer reagent after each coupling reaction.

Traditionally, elemental sulfur[91] was used as the sulfurising agent in such reactions. However, inefficient sulfur transfer and the general low solubility of sulfur in most solvents led to the development of other more efficient sulfurising agents such as 3H-1,2-benzodithiol-3-one 1,1-dioxide (Beaucage reagent)[92], 3-amino-1,2,4-dithiazole-5-thione (Xanthane Hydride)[93], 3-Methyl-l,2,4-dithiazolin-5-one (MEDITH)[94], 3-ethoxy-1,2,4-dithiazoline-5-one (EDITH)[95] and phenylacetyl disulfide (PADS). The most notable of these is the 'Beaucage Reagent' (Fig. 14). This compound was widely adopted as the sulfurising agent of choice because of its extremely efficient sulfurising ability. However, synthesis of this compound requires a long, multi-stage synthetic process and it is therefore fairly expensive. Sulfurisation using this compound also forms potentially oxidising side products. More recently, the industry has largely moved away from using this compound and now favours the cheap and efficient phenylacetyl disulfide (PADS) which can be easily synthesised from Na_2S_2 and phenylacetic acid[96-98].
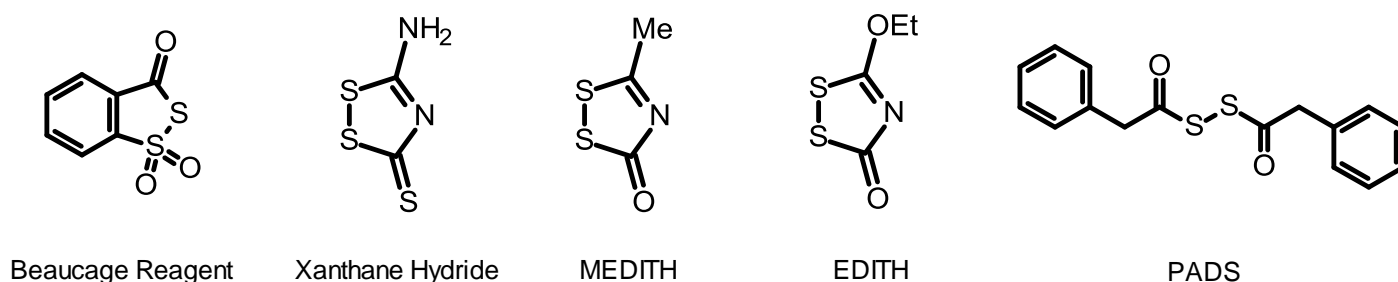
Figure 14: Various novel sulfur-transfer reagents used in phosphorothioate synthesis

The common feature amongst these novel sulfur transfer reagents is the presence of a sulfur-sulfur bond. Largely, the proposed mechanism for sulfurisation of phosphite linkages is that of nucleophilic attack on the sulfur-sulfur bond (contained in all of these molecules) by the nucleophilic phosphorus(III) centre[93,99].

1.6.2.1 Overview of Disulfides

Disulfide bonds are ubiquitous in nature. They are important structural elements in the quaternary structure of proteins, for example the hormone insulin, and they are also found in a range of other naturally occurring compounds such as several toxins and various seaweed and plant extracts[100].

Disulfide bonds are the third strongest homo-covalent bonds known with a bond dissociation energy of 265 kJmol^{-1} [101]. The strength and length of the S-S bond is also fairly independent of the electronic or steric properties of the groups bonded to the sulfur atoms with the bond lengths of Cl_2S_2, Me_2S_2 and H_2S_2 varying by only $0.01\overset{\circ}{A}$[100].
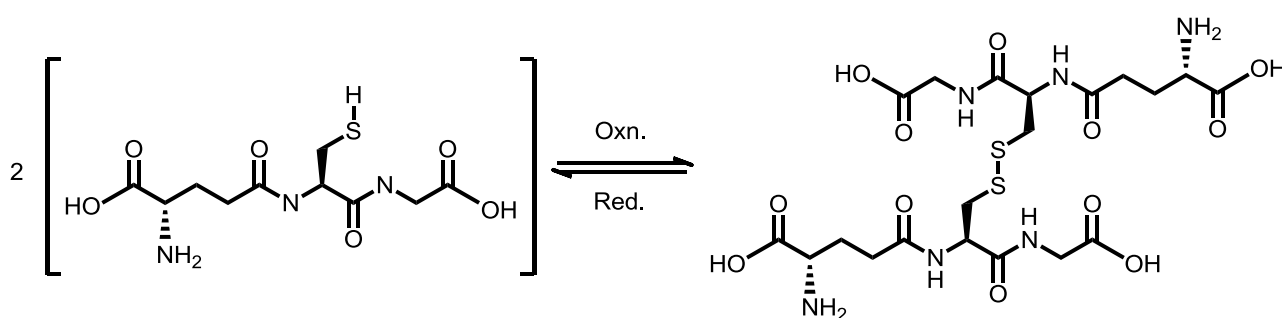
Figure 15: Oxidation of glutathione to form glutathione disulfide.

In proteins, disulfide bonds are formed by the oxidation of thiol groups in cysteine residues in the protein. This thiol-disulfide interchange also plays a key role in the function of the anti-oxidant glutathione (Fig. 15)[102], however, this is not limited to biological systems. Data have shown that many thiols will readily form disulfides with mercaptoethanol and dithioethreitol, oxidising at neutral pH in 50% v/v methanol/water at 25°C[103]. This suggests a high reactivity of disulfides towards sulfur nucleophiles.

Though disulfides show reactivity towards strong electrophiles and radicals, the broadest category of reactivity of disulfides is towards nucleophiles. Disulfides show excellent reactivity towards a broad range of nucleophiles, the most thiophilic nucleophiles being phosphites[100]. Reaction of phosphites with disulfides usually proceeds via nucleophilic attack by phosphorus to generate a phosphonium intermediate followed by decomposition to form a phosphorothioate[104] (scheme 8).

$$P(OR')_3 + RSSR \longrightarrow R\text{-}S\text{-}P^+(OR')_3 + RS^- \longrightarrow RSR + (R'O)_3P=S$$

$$RSSSR' + R^- \longleftarrow \boxed{RSSR + R'S^-} \longrightarrow RSSR' + RS^-$$
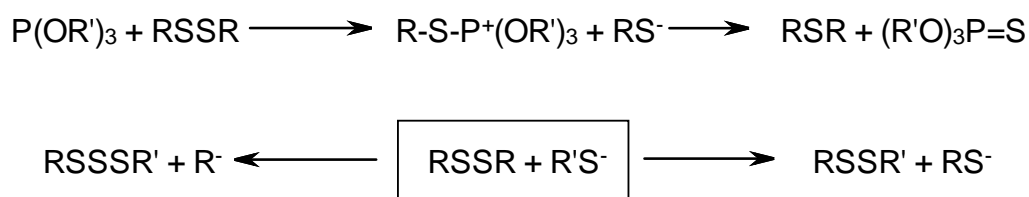
Scheme 8: General scheme for reaction of phosphites and sulfide anions with disulfides

However, a further important class of disulfide reactions is that with sulfur nucleophiles, particularly S^- anions and $S\cdot$ raidcals, mentioned previously. Disulfides are known to react with sulfide ions to form asymmetrical disulfides or polysulfides[105] , the reaction products are dependent upon the stability of the leaving group.

Polysulfides are highly reactive species and are known to be formed in many biological systems[106]. Thermal studies of organic polysulfides have shown that, upon heating, these molecules are able to disproportionate and form an equilibrium between species with varying numbers of sulfur atoms. For example, a solution of Me_2S_3 in CCl_4 heated to 80^oC for a period of 20 days was found to contain a mixture of Me_2S_2 (21%), Me_2S_3 (62%), Me_2S_4 (14%) and Me_2S_5 (3%) determined by monitoring the slightly different chemical shifts of the methyl protons in ^{1}H NMR spectra of these mixtures. The mechanism of this disproportionation is unclear, both radical and ionic mechanisms have been proposed as the addition of a radical inhibitor is able to block the generation of the S_{4+} species when starting with S_3 or S_2 by quenching the $S_3\cdot$ radical, thus preventing the disproportionation reaction. Also, sulfide anions are known to have poor delocalisation of charge with neighbouring atoms. This is not the case with sulfur radicals and so the radical species are stabilised to a greater extent than the anions with increasing sulfur chain length[101]. However, the initiation of the degradation of these alkyl polysulfides in the presence of heat is reported to be via homolytic cleavage of and S-S bond and not via the cleavage of the C-S bond[107].

1.6.2.2 Sulfurisation of Phosphites Using PADS

Very few mechanistic studies have been undertaken on the sulfurisation of phosphites by PADS. Nevertheless, the mechanism of action of PADS has been proposed (scheme 9)[108]:
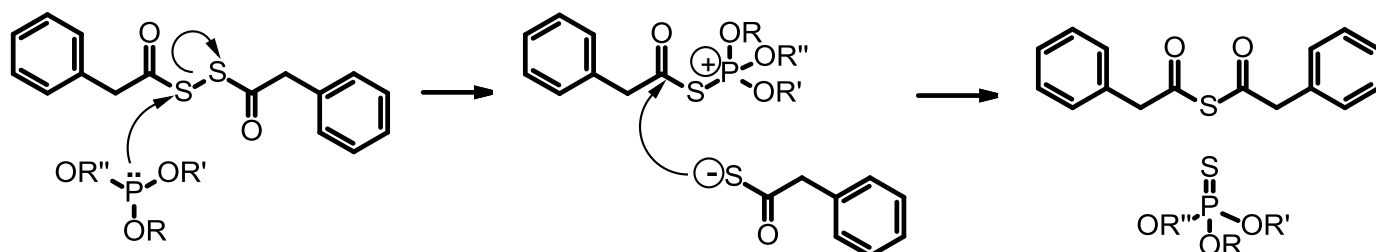
Scheme 9: Literature proposed mechanism for the sulfurisation of phosphites using PADS

However, it is widely known that solutions of freshly made PADS are not optimal[96] sulfurising agents. PADS is often made up in solutions containing up to 50% v/v 3-picoline in ACN or other compounds such as pyridine or collidine[108]. One suggestion is that sulfurisation generally occurs more rapidly in solvents of higher dielectric constant[109] and so adding co-solvents such as these increases the dielectric constant and therefore the overall rate of reaction.

It is also widely accepted that the efficiency of PADS improves greatly upon ageing[96]. Sierzchala et al. stated that a solution of fresh PADS affords a 99.6% yield of phosphorothioate per cycle whereas an 'aged' solution affords a 99.89% yield. This difference may appear small however when extrapolated to afford, for example, a 20 nucleotide oligonucleotide this represents an overall yield difference of 7.5%. Chromatographic data of solutions of fresh PADS compared to chromatograms of 'aged' PADS show significant differences in the chemical composition[96] such as the formation of unidentified peaks in the chromatograms. Visual inspection of aged PADS solutions suggests significant chemical change as there is a very distinct colour change from a pale yellow to a blue-black colour with PADS solutions aged in 50% v/v 3-picoline/acetonitrile solution over 48 h. Therefore in order to elucidate a mechanism of action of PADS it is important to quantify these changes and identify any new compounds present in aged solutions of PADS.

1.7 General Aims of the Work

The general aims of the work are to investigate the mechanisms of the reactions involved in the phosphoramidite method of oligonucleotide synthesis. The work will focus particularly on the formation of new inter-nucleotide linkages via coupling of nucleoside phosphoramidites and the sulfurisation of the newly-formed linkages using the sulfur transfer reagent PADS.

The investigation into the coupling reaction aims to analyse the kinetics of the activation of phosphoramidites by tetrazole activators (mainly ethylthio tetrazole). Using NMR spectroscopy the work aims to investigate the effect of substituents on the tetrazole ring and use these observations to infer details of the transition state during the activation process. The work also aims to investigate the ion-pairing behaviour between the acidic activator and the basic amine leaving group liberated during this process by means of conductivity.

The majority of this thesis aims to elucidate the mechanism of sulfurisation of phosphites by the sulfur-transfer reagent PADS under basic conditions. The work initially aims to identify and characterise the active sulfur transfer species generated during the 'ageing' of PADS. Using intermediate-trapping experiments and the synthesis of mechanistic probes the work also aims to identify the mechanism by which the aging of PADS.

Using linear-free energy relationships the work aims to identify the mechanism of sulfur transfer from PADS to phosphites to generate phosphorothioates. Of particular interest in this work is the difference between the mechanisms of sulfur transfer using fresh PADS and aged PADS in order to identify the origin of the vast differences in the rate of reaction using these species. The work aims to make an accurate assessment of the role of the various pyridine bases used in both the aging of PADS and the subsequent reaction between PADS and phosphites.

2. Experimental

2.1 Materials

All materials used during the work were of an analytical or equivalent grade if available. All reagents and solvents were supplied by Aldrich, Fisher, Avocado, Alfa Aesar, Glenn Research and Fluorochem with PADS being supplied by Carbosynth. Deuterated solvents were supplied by Goss Scientific. All reagents were used as provided with no further purification. All solvents used were stored over 3Å molecular sieves which were activated by heating to 280°C overnight and cooled under an atmosphere of nitrogen.

2.2 HPLC Method and Specification

All HPLC traces were acquired using a Shimadzu SIL 50AH instrument. The column used in all cases was a Phenomenex Luna 5μ C18 4.67 × 250mm. The detection method used was a diode array UV-Vis detector. Chromatograms were recorded at a wavelength of 260 nm. The method was a gradient of water and acetonitrile as follows:

Time (min)	% Acetonitrile	Flow Rate (ml/min)
0	30	1
15	95	1
20	95	1
21	30	1
30	30	1

2.3 NMR Specification

All NMR experiments were performed using a 400 MHz Bruker Avance DP X400 NMR machine unless stated otherwise. All solvents were deuterated and purchased from Goss Scientific unless stated otherwise.

2.4 Infra-Red Spectroscopy

I.R. spectroscopy was performed using a Thermo-Electron Nicolet 380 'Smart Orbit' FT-IR ATR spectrometer.

2.5 Mass Spectrometry LC-MS Methods and Specification

Mass spectra were recorded using an Agilent 6210 tine-of-flight mass spectrometer. Data was acquired at a 2 GHz dynamic range scanning at a rate of 5.00 spectra per second with a m/z range of 80-1700 m/z. Gas flow was kept at 10 L per minute at a temperature of $350^{\circ}C$. When LC-MS was performed the HPLC system was an Agilent 1200 series HPLC using a diode array detector. This was fitted with a Phenomenex Luna 5μ C18 2.4 x 250mm column and the method used was as follows:

Time (min)	% Acetonitrile	Flow Rate (ml/min)
0	30	0.2
15	95	0.2
20	95	0.2
21	30	0.2
30	30	0.2

2.6 Conductivity Measurements

Conductivity measurements were taken using a Metrohm five-ring conductivity cell with 856 conductivity module using *tiamolight* software for kinetics measurements. All conductivity measurements were recorded in a 20 ml jacketed cell kept at a constant temperature of $25^{\circ}C$.

2.7 General Method of Generating Aged PADS Solutions

A solution of PADS (1 M) was made up in a solution of 3-picoline (5 M) in acetonitrile and left to age for 48 h. At T=*n* h a 1 ml sample of this was removed and quenched in dilute hydrochloric acid (10 ml, 2 M) in order to remove the 3-picoline as the protonated pyridinium species. The organic species were then extracted with DCM (2×10ml). The aqueous layer was discarded. The organic layers were collected and dried over anhydrous sodium sulfate which was removed by gravity filtration. The solvent was then removed under vacuum. The resulting oil was then made up to 1 ml in deuterated acetonitrile.

2.8 General HPLC Degradation Kinetics Method

A solution of PADS (1000 ppm, 3.3 mM) was made up in a solution of 3-picoline (0.5-5 M) in HPLC-grade acetonitrile. Naphthalene (100 ppm, 0.8 mM) was added as an internal standard. Due to the size of the HPLC vials used and the sample sizes required, it was necessary to split this solution between two HPLC vials which were inserted into an auto-samplerand chromatograms were recorded every 30 min for 48 h. The chromatographic method is stated in section 2.2.

2.9 General NMR Sulfurisation Kinetics Method

A mixed equimolar solution of triaryl phosphite and triphenyl phosphine oxide (0.05-1 M, 50-200 µL) in deuterated acetonitrile was added to an NMR tube (note that the triphenyl phosphine oxide was added as an internal standard). This was mixed with 3-picoline (0.5-10.2 M, 8-200 µL) in deuterated acetonitrile. At T=0 PADS solution (50-200 µL, 0.5-3 M) was added to the mixture. If necessary deuterated acetonitrile was also added in order to make-up a total reaction volume in all cases of 600 µL. ^{31}P NMR spectra were recorded approximately every 90 s until the reaction was deemed complete. The reaction was deemed complete when the peak corresponding to the phosphite starting material was no longer visible.

2.10 Experimental – Ageing PADS

2.10.1 Analysis of Aged PADS Solutions

A solution of PADS (1000 ppm, 3.3 mM) was made-up in a solution of 3-picoline (5 M) in HPLC-grade acetonitrile and were left for 1 week. At t=n h 20 µL aliquots of these solutions were analysed using the HPLC system and method described in section 2.2. At these time points, 20 µL samples were also submitted for LC-MS analysis using the method detailed in section 2.4. To analyse aged PADS mixtures by NMR, a solution of PADS (0.2 M) and 3-picoline (0.4 M) was made up in deuterated acetonitrile and left for 1 week. Again, at t=n h ^{1}H and ^{13}C NMR spectra were recorded.

2.10.2 Dependence of PADS Decomposition on 3-Picoline Concentration

Seven solutions of PADS were analysed as described in section 2.6; each solution contained a different concentration of 3-picoline such that solutions containing 0 M, 0.5 M, 1 M, 1.5 M, 2 M, 2.5 M and 5 M 3-picoline were analysed. The rate of reaction was assessed by monitoring the change in the ratio of the peak area of the peaks corresponding to PADS and to that of the internal standard (naphthalene) over time.

2.10.3 Effect of Pyridine pK$_a$ on the Rate of Degradation

A solution of PADS (1 M, 300 µL) in deuterated acetonitrile was added to an NMR tube. At T=0 a solution of 3-picoline (5 M, 300 µL) was added to this and a ^{1}H NMR spectrum of this solution was taken. Further ^{1}H NMR spectra were taken periodically over a period of 48 h. The concentration of PADS was assessed by monitoring the change in the ratio of the PADS methylene peak and the PADS aromatic peak region. This was repeated several times under identical conditions but the 3-picoline was replaced for an equimolar amount of 4-pyridinecarbonitrile, 3-pyridinecarbonitrile, 3-chloropyridine, pyridine, 3-methoxypyridine, 4-methoxypyridine, 2,6-dimethylpyridine and triethylamine. Note that the data for triethylamine are not included as the reaction was too fast to monitor the disappearance of PADS.

2.10.4 Reaction of 3-Picoline with Phenylacetyl Chloride
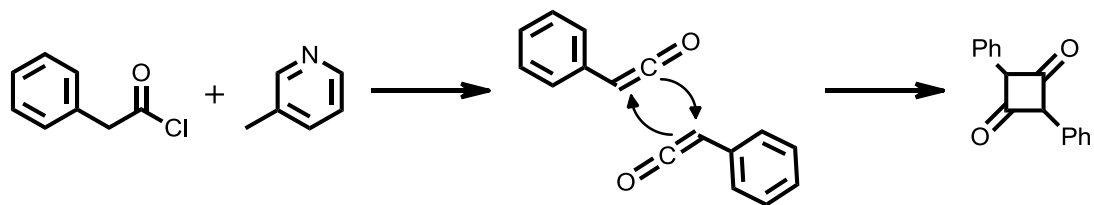
To a 5 ml vial was added phenylacetyl chloride (100 µL, 116.9 mg, 0.75 mmol) and the solution was stirred. To this, 3-picoline (146 µL, 140 mg, 1.5 mmol) was added dropwise. The reaction was complete almost instantaneously as the reaction mixture solidified. This was diluted to 5 ml using HPLC-grade acetonitrile and were further diluted by a factor of 100. This solution was then analysed by mass spectrometry and the products identified as stated in the discussion.

2.10.5 Assessment of the Rate of Decomposition of Phenyl-Substituted PADS Analogues

The rates of decomposition of 2,2´-(4-fluorophenyl)acetyl disulfide (section 2.11.16),, 2,2´-(4-chlorophenyl)acetyl disulfide (section 2.10.19), 2,2´-(3-chlorophenyl)acetyl disulfide (section 2.11.17) were assessed via the method described in section 2.6. The concentration of 3-picoline in these solutions was 1 M.

2.10.6 Deuterium Exchange with PADS

A solution of PADS (0.2 M, 400 µl) in deuterated acetonitrile was added to an NMR tube with D_2O (50 µl). At T=0 3-picoline (15.5 µl, 16.2 mg, 0.17 mmol) was added to the reaction mixture and the tube inverted to mix. ^1H NMR spectra of this mixture were recorded approximately every 2 min until no signal corresponding to the PADS CH_2 or CHD could be observed and the reaction was complete.

This process was repeated twice under identical conditions but using 31 µl and 7.5 µl of 3-picoline. This process was also repeated replacing the D_2O with an equal volume of ultra-pure H_2O.

2.10.7 Deuterium Exchange with Phenyl-Substituted PADS Analogues

The above reaction (2.10.6) was repeated several times under identical conditions replacing PADS with an equimolar amount of 2,2´-(4-methoxyphenyl)acetyl disulfide (section 2.10.21), 2,2´-(4-chlorophenyl)acetyl disulfide (section 2.10.19) and 2,2´-(4-cyanophenyl)acetyl disulfide (section 2.10.20).

2.10.8 Trapping the Ketene Generated During Ageing of 2,2´-diallyl-2,2´-phenylacetyl disulfide

The cycloaddition product 7,7a-dihydro-1H-cyclobuta[a]inden-2(2aH)-one was synthesised according to the method described in section 2.9.16. This was characterised by NMR and M.S. which were used as reference spectra in order to identify the presence of this species in aged PADS mixtures.
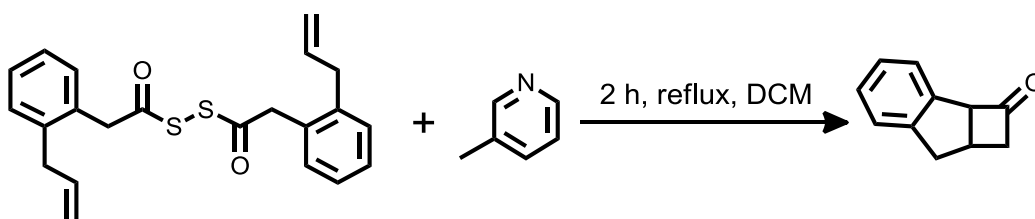
A mixture of 2,2'-(σ -allylphenyl)acetyl disulfide (330mg, 0.852mmol) and 3-picoline (165.6 µl, 1.7 mmol) in acetonitrile (10 ml) was heated to reflux for 2 h. The reaction was followed by HPLC and was complete after 2 h. This reaction was not purified further as mass spec and NMR analysis showed evidence of the product 7,7a-dihydro-1H-cyclobuta[a]inden-2(2aH)-one. HRMS (m/z): [M+H]$^+$ for $C_{11}H_{10}O$, calculated 159.0809, measured 159.0804.

36

2.10.9 Separation of the Products of PADS Ageing by HPLC

A solution of PADS (3 M, 1 ml) was aged for 48 h and the products extracted according to the method described in section 2.6. This solution was then separated using an Agilent 1200 series HPLC system using the column and method described in section 2.2. This system was fitted with an Agilent 1200 series quantitative fraction collector. Ten unique fractions were collected, concentrated and fractions were combined over many runs. Due to the small load capacity of the column, over 100 runs were required to get a useable sample size.
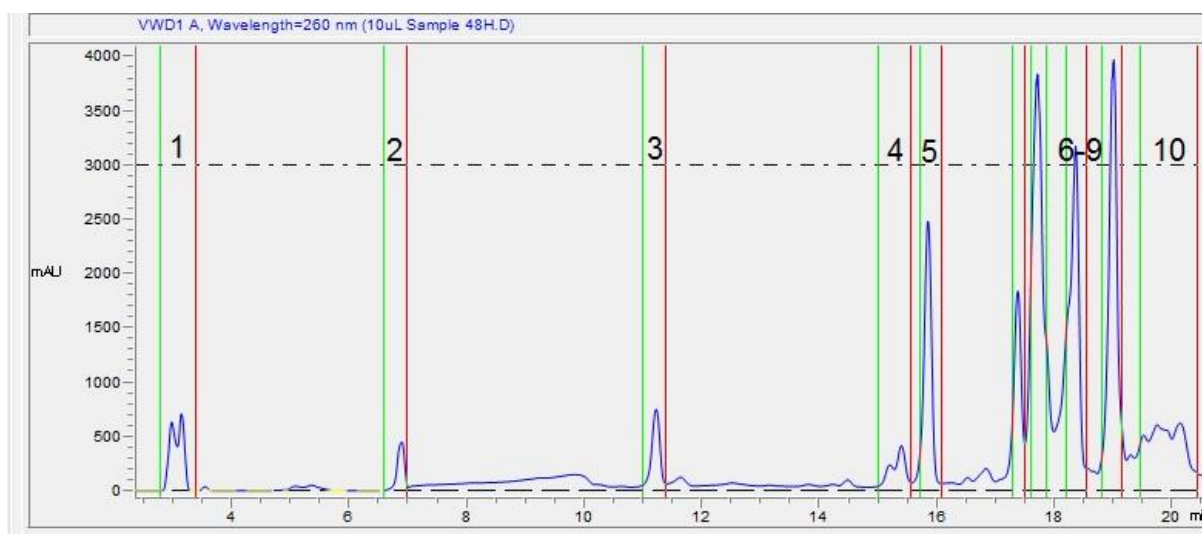
^ HPLC fractions collected
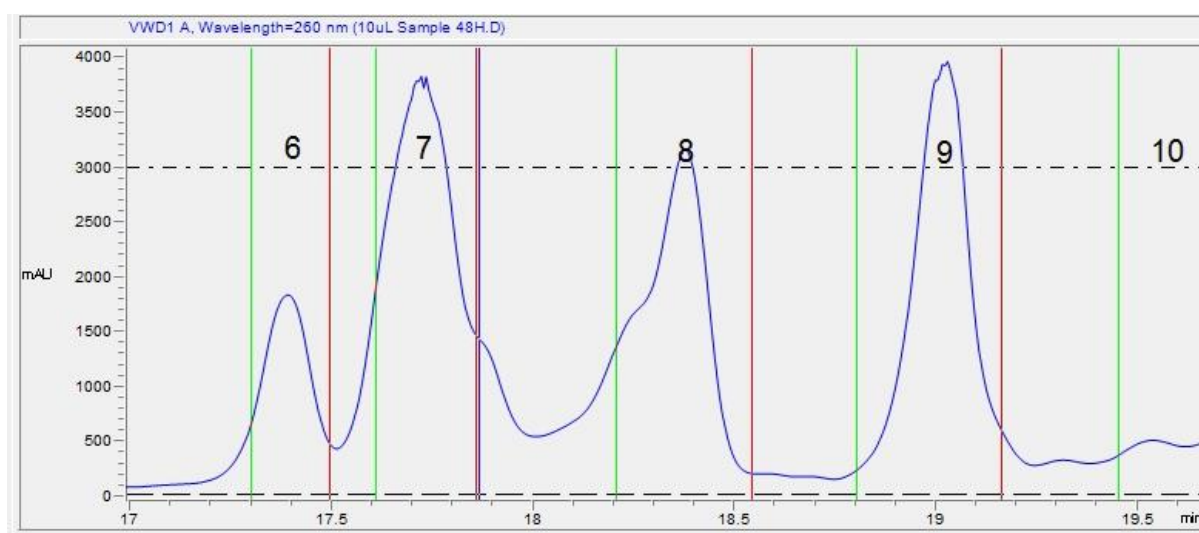
Expanded: Region containing fractions 6-9

2.10.10 Assessment of Sulfur-Transfer Activity of Aged PADS Fractions

An arbitrarily-sized sample of each of the combined fractions recovered from the aged PADS solution was taken and made up in deuterated acetonitrile. 20 µL of each sample was analysed by HPLC in order to ensure an adequate concentration and homogeneity of material. To each of these, excess triphenyl phosphite (50 µl) and 3-picoline (50 µl) were added. After 1 h tese reaction mixtures were analysed by ^{31}P NMR to assess whether any of the phosphite had been converted to the phosphorothioate. Phosphorothioate was detected in 5 samples (fractions 5, 7, 8, 9, 10). These were deemed the active sulfur transfer reagents.

2.10.11 Quantification and Kinetic Measurements of Sulfur Transfer with Fractions from Aged PADS Solutions

The reactive fractions collected from aged PADS solutions were made up to 0.5 ml in deuterated acetonitrile. To these solutions naphthalene (100 ppm) was added as an internal standard. These solutions were then analysed by HPLC and the ratio of the peak area of the active species and the standard was calculated. It was assumed that these species had a similar UV response to PADS. The concentrations of these solutions were calculated by comparing the ratios of species/standard to the ratios of the peak areas of known concentrations of PADS to the standard (naphthalene, 100 ppm). These solutions were then diluted to a concentration of 35 mM based on the calibration with the reference PADS solution. Sulfurisation kinetics were measured as described in section 2.8 using triphenyl phosphite (3.5 mM, 200 µl) and 3-picoline (70 mM, 200 µl) and replacing PADS with the appropriate fraction (35 mM, 200 µl).

A reference experiment using PADS (35 mM, 200 µl) was also performed using the same method.

2.10.12 Assessment of the Rate of Decomposition of PADS in the Presence of BHT

Two separate degradation experiments were run according to the method described in section 2.7 using 3-picoline at a concentration of 1 M. To one of these experiments was added butylated hydroxyl toluene (3.3 mM). The concentrations of PADS in each were monitored simultaneously by HPLC.

2.10.13 Synthesis of Methyl *o*-iodophenylacetate
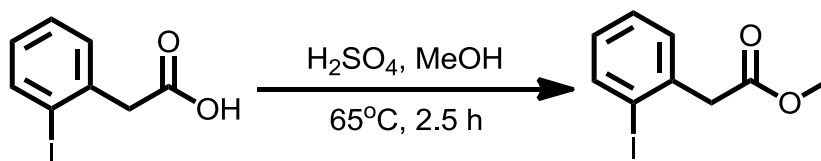
To a clean, dry, 25 ml round-bottomed flask *o*-iodophenylacetic acid (5.01 g, 19.1 mmol) and H_2SO_4 (98%, 1.25 ml) were added. This mixture was then added to methanol (7.5 ml). The reaction mixture was stirred for 2.5 h at 65°C after which time the reaction mixture was diluted with DCM (250 ml). This was extracted with water (2 × 100 ml) and brine (50 ml). The resulting organic solution was dried using anhydrous $MgSO_4$ and filtered before DCM was removed under vacuum. The product was obtained as a pale yellow oil (4.88 g, 93% yield). HPLC retention time 5.4 min; ^1H NMR (CDCl$_3$, 400MHz) δ 3.69 (s, 3H, CH$_3$), 3.79 (s, 2H, CH$_2$), 6.92-6.96 (m, 1H, ArH), 7.22-7.32 (m, 2H, ArH), 7.83 (d, 1H, *J* 7.9Hz, ArH) ppm; ^{13}C NMR (CDCl$_3$, 100 MHz) δ 46.1 (CH$_3$), 52.2 (CH$_2$), 101.1 (CI), 128.5 (CH), 128.9 (CH), 130.7 (CH), 137.7 (Cq), 139.5 (CH), 171.0 (CO) ppm; IR (film) 1732 cm^{-1}.

2.10.14 Synthesis of Methyl 2-(2′-allylphenyl)acetate
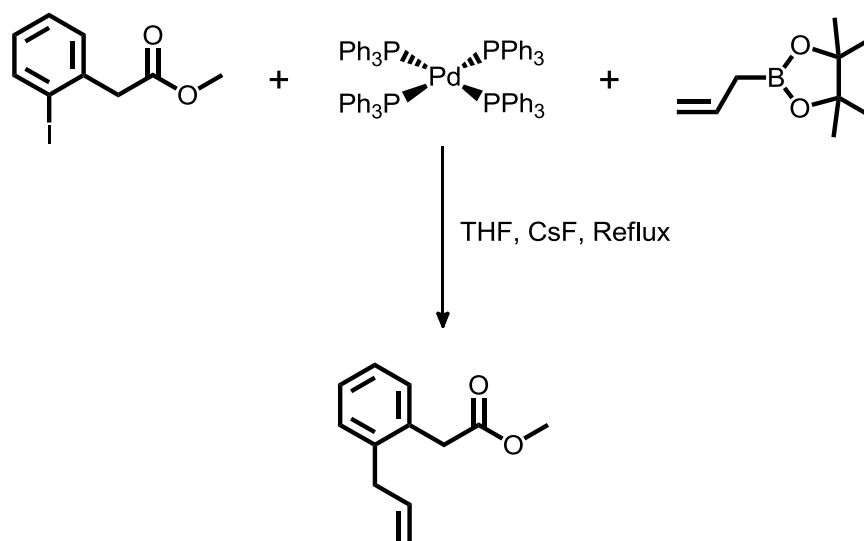
Methyl o-iodophenylacetate (3 g, 10.9 mmol), CsF (6.6 g, 43.6 mmol), and Pd(PPh$_3$)$_4$ (0.63 g, 0.55 mmol) were added to a 2-neck round-bottom flask and dissolved in THF (250 ml). This solution was stirred for 30 min at room temperature. A solution of allylboronic acid pinacol ester (3.3 ml, 21.8 mmol) in THF (50 mL) was added and the resulting reaction mixture was heated under reflux for 24 h. During the course of the reaction a yellow inorganic precipitate was formed in the flask. After 24 h the reaction mixture was diluted with petroleum ether (bpt. 60–80°C, 300 mL). This was extracted with H$_2$O (2 x 200 ml) and the combined aqueous layer was washed with petroleum ether (bpt. 60-80°C, 100 ml). The organic layers were combined and washed with H$_2$O (100 mL), brine (100 mL) and then dried using anhydrous MgSO$_4$. The solvent was removed under vacuum to give the crude product as an orange oil (2.5 g) containing impurities. The crude mixture was purified using a Biotage SP4 chromatography system fitted with a Biotage Snap 10 column eluting with heptane and varying percentages of ethyl acetate: 0% for 2 column volumes then 0-20% over 15 column volumes followed by isocratic elution for 5 column volumes. This gave the product ester as a yellow oil (1.6 g, 77% yield). HPLC retention time 5.6 min; ^{1}H NMR (CDCl$_3$, 400 MHz) δ 3.39 (dt, 2H, J_1 6.3 Hz, J_2 1.4 Hz CH$_2$), 3.61 (s, 2H, CH$_2$), 3.65 (s, 3H, CH$_3$), 4.94-5.06 (m, 2H, CH$_2$), 5.87-5.97 (m, 1H, CH), 7.14-7.23 (m, 4H, ArH) ppm; ^{13}C NMR (CDCl$_3$, 100 MHz) δ 37.4 (CH$_2$), 38.5 (CH$_2$), 51.9 (CH$_3$), 116.0 (CH$_2$), 126.7 (CH), 127.6 (CH), 129.9 (CH), 130.7 (CH), 132.7 (Cq), 136.6 (CH$_2$), 138.4 (Cq), 172.0 (CO) ppm; IR (film) 1734 cm^{-1}.

2.10.15 Synthesis of 2-(2´-allylphenyl)acetic acid
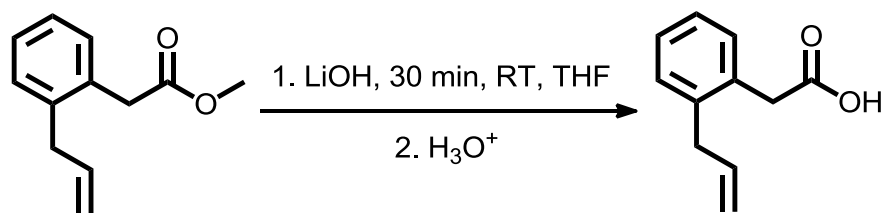
Methyl 2-(2´-allylphenyl)acetate (1.7 g, 8.9 mmol) was added to a round-bottom flask and dissolved in THF (20 ml). To this was added an aqueous lithium hydroxide solution (0.4 M, 20 ml). The solution was stirred at room temperature for 3 h. After the reaction was complete (monitored by HPLC) the reaction mixture was diluted with water (40 ml) and extracted with DCM (2 x 20 ml). The pH of the aqueous layer was then lowered to around pH 1. This was then re-extracted with DCM (2 x 20ml). The 2 layers from the acidified aqueous extraction were then combined and dried using $MgSO_4$. The solvent was then removed under vacuum giving the product as a brown oil (1.7 g, 9.7 mmol, 83% yield). HPLC retention time 4.6 min; ^{1}H NMR (CDCl$_3$, 400 MHz) δ 3.38 (dt, 2H, J_1 6.4 Hz, J_2 1.6 Hz, CH$_2$), 3.65 (s, 2H, CH$_2$), 4.94-5.06 (m, 2H, CH$_2$), 5.86-5.96 (m, 1H, CH), 7.14-7.23 (m, 4H, ArH), 10.76 (bs, 1H, OH) ppm; ^{13}C NMR (CDCl$_3$, 100 MHz) δ 37.5 (CH$_2$), 38.5 (CH$_2$), 116.22 (CH$_2$), 126.8 (CH), 128.0 (CH), 130.1 (CH), 130.9 (CH), 132.1 (Cq), 136.5 (CH), 138.6 (Cq), 178.4 (CO) ppm; IR (film) 1702cm^{-1}.

2.10.16 Synthesis of 7,7a-dihydro-1H-cyclobuta[a]inden-2(2aH)-one
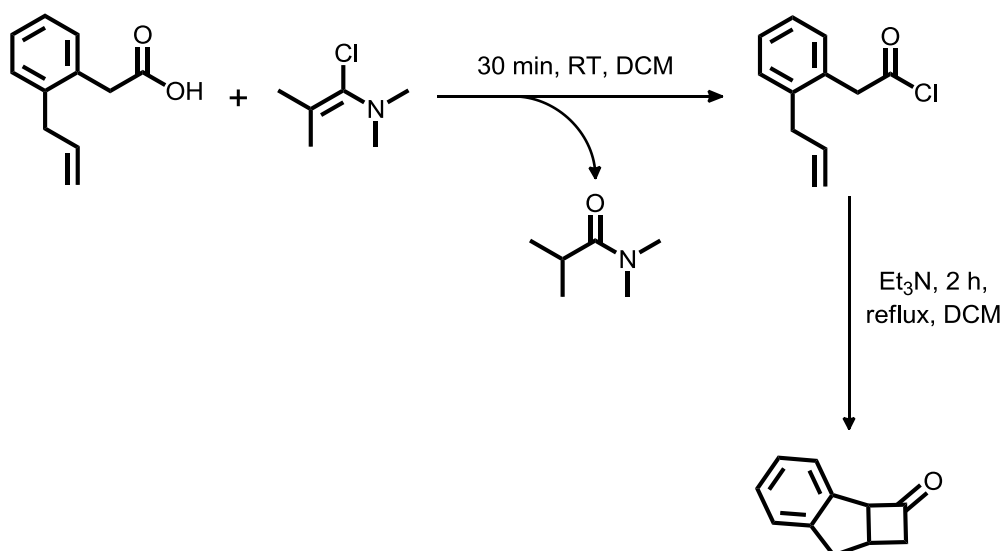
To a clean, dry 25 ml double-necked round-bottomed flask 2-(2′-allylphenyl)acetic acid (100 mg, 0.514 mmol) was added. This was dissolved in DCM (4 ml). To this 1-chloro-*N,N-2*-trimethyl-1-propenylamine (74.7 μl, 0.56 mmol) was added. The reaction mixture was stirred for 30 min at room temperature. Conversion of the acid (retention time 4.6 min) to the acid chloride was determined by quenching samples of the reaction with methanol. This converted the product acid chloride to the corresponding methyl ester (retention time 5.6 min) and allowed the reaction to be monitored by HPLC. Once the reaction was complete the flask was fitted with a condenser and brought to reflux. To this a solution of triethylamine (78 μl, 0.56 mmol) in DCM (4 ml) was added drop-wise via a dropping funnel and the reaction was stirred at reflux for 2 h. Once the reaction was complete the reaction mixture was cooled and extracted with dilute hydrochloric acid (2 M, 20 ml) to remove the amine. The crude product mixture (a brown oil) was purified using a Gilson preparative. HPLC system using a gradient of 50-100% acetonitrile (0.05% TFA) in water (0.05% TFA) over 15 min, then isocratic elution at 50% acetonitrile (0.05% TFA) in water (0.05% TFA) for a further 3 min. The product eluted at 7.5 min, all fractions were collected to give the product as a white, crystalline solid (34 mg, 42% yield). HPLC retention time 4.8 min; ^{1}H NMR (ACN-d$_3$, 400 MHz) δ 2.75-2.87 (m, 1H, CH$_2$), 3.05 (d, 1H, *J* 16.7, CH$_2$), 3.11-3.18 (m, 1H, CH), 3.30-3.42 (m, 1H, CH$_2$), 3.38-3.45 (m, 1H, CH$_2$), 4.71 (bs, 1H), 7.23-7.36 (m, 4H, ArH); ^{13}C NMR (ACN-d$_3$, 100 MHz) δ 26.2 (CH), 38.8 (CH$_2$), 52.3 (CH$_2$), 71.8 (CH), 124.5 (CH), 125.5 (CH), 126.8 (CH), 127.5 (CH), 137.6 (Cq), 143.4 (Cq), 206.1 (CO); IR (film) 1771 cm^{-1}.

2.10.17 Synthesis of 2,2´-di(σ-allylphenyl)acetyl disulfide
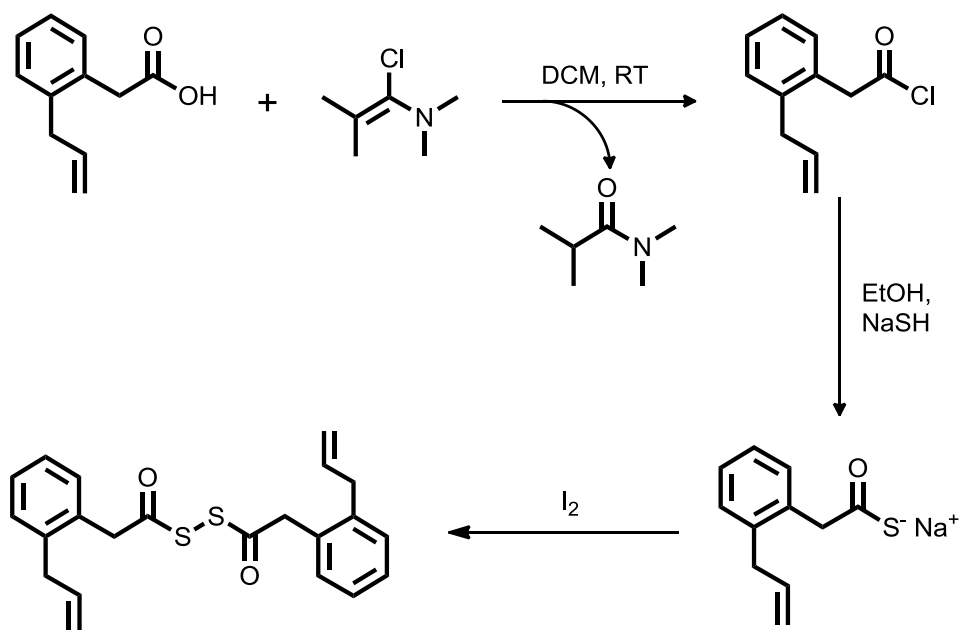
In a clean, dry, 25 ml round bottom flask sodium hydrosulfide (798 mg, 14.25 mmol) was dissolved in ethanol (5 ml) and chilled over ice. Working in a well-ventilated fume hood this flask was fitted with an exhaust line allowing any gasses generated to be scrubbed by sodium hypochlorite. Into a separate 25 ml round bottom flask 2-(2´-allylphenyl)acetic acid (1 g, 5.7 mmol) was dissolved in dichloromethane (10 ml). To this, 1-chloro-*N,N*-2-trimethyl-1-propenylamine (1.04 g, 1.03 ml, 8.5 mmol) was added and stirred at room temperature for 30 min. After the reaction was complete the solvent was removed under vacuum to yield an orange oil. This oil was added to the ethanolic sodium hydrosulfide, the solution instantly turned yellow and a precipitate (sodium chloride) was formed. This precipitate was removed under vacuum filtration and was washed with ice cold ethanol (1.5 ml). The resulting yellow solution was recovered from the Buchner flask, added to a clean 25 ml round bottomed flask and stirred over ice. To this solution, iodine was slowly added until the colour of the suspension changed from white to pale brown (approximately 1 g, 7.8 mmol) after around 60 s. The resulting reaction mixture was diluted with dichloromethane (10 ml) and was washed twice with saturated sodium thiosulfate solution (2 x 15 ml). The organic layer was then concentrated under vacuum to yield the crude product as a brown oil. This was purified using a Biotage SP4 chromatography system fitted with a Biotage Snap 10 column eluting with 25% ethyl acetate in hexane (*rf*. Product = 0.41). This gave the product as a clear oil (384 mg, 1 mmol, 14.1% yield). HPLC retention time 7.6 min; ^{1}H NMR (CDCl$_3$, 400 MHz) δ 3.41 (d, 4H, *J* 6.3 Hz, CH$_2$),

4.00 (s, 4H, CH$_2$), 4.96-5.60 (m, 4H, CH$_2$), 5.88-5.98 (m, 2H, CH), 7.17-7.30 (m, 8H, ArH) ppm; ^{13}C NMR (CDCl$_3$, 100 MHz) δ 37.5 (CH$_2$), 46.7 (CH$_2$), 116.6 (CH$_2$), 127.0 (CH), 128.6 (CH), 130.2 (CH), 130.88 (Cq), 131.5 (CH), 136.1 (CH), 139.1 (Cq), 191.8 (CO) ppm. HRMS (m/z): [M+NH4]$^+$ for C$_{20}$H$_{22}$O$_2$S$_2$, calculated 400.1399, measured 400.1356; IR: 1796 cm^{-1} (film).

2.10.18 Synthesis of Bis-benzoyl disulfide
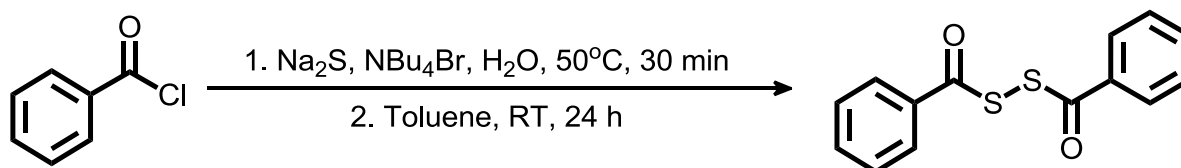
Sodium sulfide (1.84 g, 23.6 mmol) was dissolved in water (12ml) and heated to 50°C. To this tetra-N-butylammonium bromide (380 mg, 1.18 mmol) was added and stirred at 50°C for 30 min. In a separate flask, benzoyl chloride (2 ml, 1.6 5g, 11.8 mmol) was dissolved in toluene (12 ml) and rapidly stirred. In a well-ventilated fume hood this flask was fitted with an exhaust line allowing any gasses generated to be scrubbed by sodium hypochlorite and chilled in an ice bath. After 30 min the sodium sulfide solution was cooled to room temperature and slowly added to the rapidly stirring, chilled benzoyl chloride solution under a nitrogen atmosphere. A yellow precipitate immediately precipitated out of solution. This two-phase system was stirred for 24 h. After 24 h the organic and the aqueous layer were separated, the aqueous layer washed with portions of toluene (2 × 5 ml) and the organic layers combined. The toluene was then removed under vacuum giving the product as white crystals (738 mg, 46% yield, M.P. 129-30°C [132]) from which a single crystal X-ray diffraction pattern was resolved (see appendix 1). Please note that the aqueous layer contains residual Na$_2$S which will generate extremely toxic H$_2$S gas if exposed to acid. This must be disposed of extremely carefully. ^{1}H NMR (CDCl$_3$, 400MHz) δ 7.52 (t, 4H, *J* 7.6 Hz, ArH), 7.66 (t, 2H, *J* 7.6 Hz, ArH), 8.08 (d, 4H, *J* 8.1, ArH) ppm; ^{13}C NMR (CDCl$_3$, 100MHz) δ 127.9 (CH), 128.8 (CH), 134.0 (CH), 136.6 (Cq), 190.4 (CO) ppm.

2.10.19 Synthesis of 2,2,2´,2´-tetramethyl-2,2´-phenylacetyl disulfide
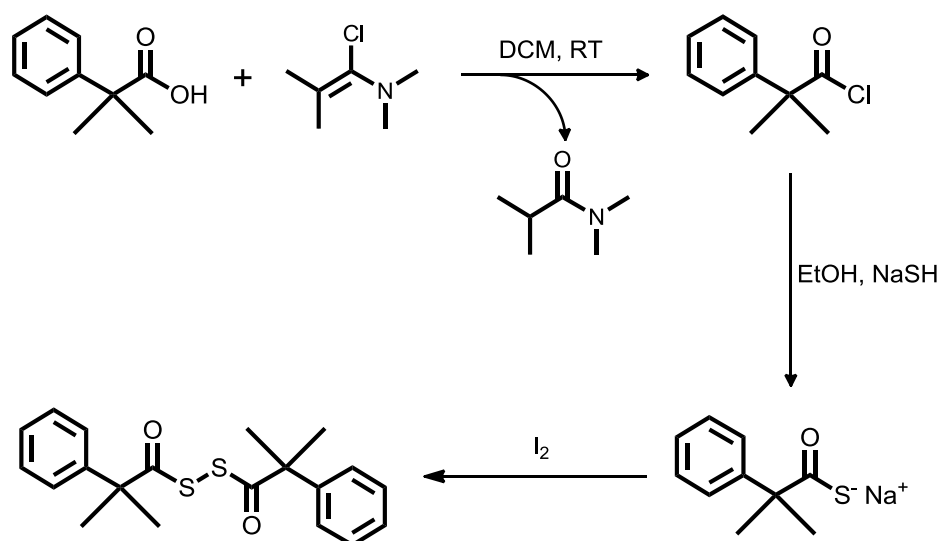
In a clean, dry, 50 ml round bottom flask sodium hydrosulfide (4.2 g, 75 mmol) was dissolved in ethanol (30 ml) and chilled over ice. Working in a well-ventilated fume hood this flask was fitted with an exhaust line allowing any gasses generated to be scrubbed by sodium hypochlorite. Into a separate 50 ml round bottom flask 2-phenyl*iso*butyric acid (5 g, 30 mmol) was dissolved in dichloromethane (20 ml). To this, 1-chloro-*N,N-2*-trimethyl-1-propenylamine (6.16 g, 5.6 ml, 45 mmol) was added and the solution stirred at room temperature for 30 min. After the reaction was complete (determined by HPLC) the solvent was removed under vacuum to yield an orange oil. The oil was added to the ethanolic sodium hydrosulfide, the solution instantly turned yellow and a precipitate (sodium chloride) was formed. This precipitate was removed under vacuum filtration and was washed with ice cold ethanol (1.5 ml). The resulting yellow solution was recovered from the Buchner flask, added to a clean 50 ml round bottomed flask and stirred over ice to ensure that the temperature was kept below 15°C. To this solution iodine was added (2 g, 15.6 mmol) and the product precipitated out of solution. Iodine was slowly added until the colour of the suspension changed from white to pale brown (approximately 1 g, 7.8 mmol) after around 60 s. The precipitate was collected by vacuum filtration and washed with ice-cold ethanol (5 ml) and water (10ml) to give a waxy yellow solid (2.2 g, 5.9 mmol, 39.3 % yield). HPLC retention time 7.6 min; ^{1}H NMR (ACN-d$_3$, 400 MHz) δ 1.69 (s, 12H, CH$_3$), 7.35–7.49 (m, 10H, ArH) ppm; ^{13}C NMR (CDCl$_3$, 100 MHz) δ 26.3 (CH$_3$), 54.2 (Cq) , 127.3 (CH), 128.0 (Cq), 128.8 (CH), 142.3 (CH), 198.8 (CO) ppm. HRMS (m/z): [M+NH4]$^+$ for C$_{20}$H$_{22}$O$_2$S$_2$, calculated 390.0782, measured 390.0788; IR: 1707 cm^{-1} (film).

2.10.20 Synthesis of 2,2´-(4-chlorophenyl)acetyl disulfide
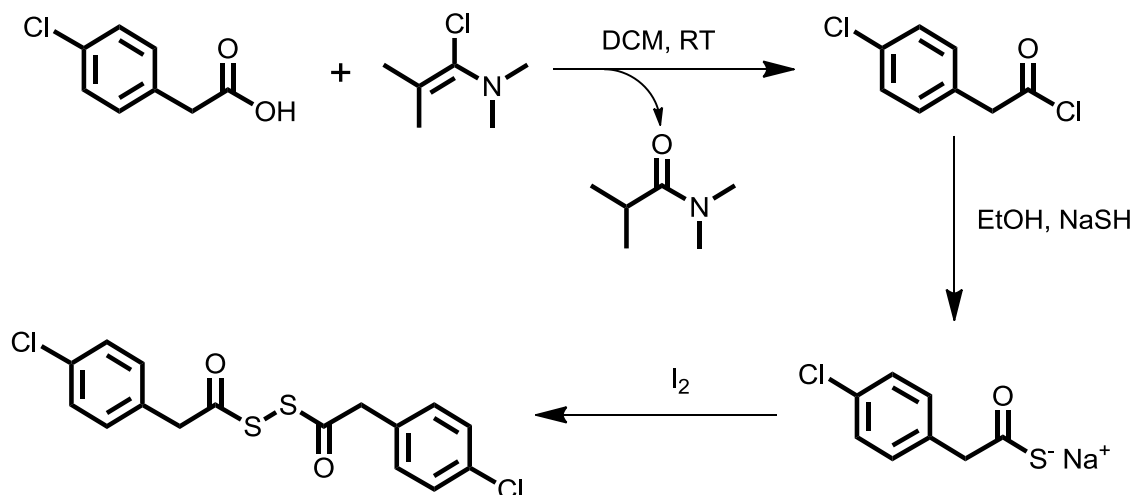
Into a clean, dry, 50 ml round bottom flask sodium hydrosulfide (1.6 g, 29.25 mmol) was dissolved in ethanol (15 ml) and chilled over ice. Working in a well-ventilated fume hood this flask was fitted with an exhaust line allowing any gasses generated to be scrubbed by sodium hypochlorite. Into a separate 50 ml round bottom flask 2-(4-chlorophenyl)acetic acid (2 g, 11.7 mmol) was dissolved in dichloromethane (15 ml). To this, 1-chloro-*N,N*-2-trimethyl-1-propenylamine (1.72 g, 1.57 ml, 12.9 mmol) was added and the mixture was stirred at room temperature for 30 min. After the reaction was complete (determined by HPLC) the solvent was removed under vacuum to yield a pale-brown oil. This oil was added to the ethanolic sodium hydrosulfide, the solution instantly turned yellow and a precipitate (sodium chloride) was formed. This precipitate was removed under vacuum filtration and was washed with ice cold ethanol (1.5 ml). The resulting yellow solution was recovered from the Buchner flask, added to a clean 50 ml round bottomed flask and stirred over ice to ensure that the temperature was kept below 15°C. To this solution iodine was added (0.5 g, 3.9 mmol) and the product precipitated out of solution. Iodine was slowly added until the colour of the suspension changed from white to pale brown (approximately 1 g, 7.8 mmol). The precipitate was collected by vacuum filtration and was washed with ice-cold ethanol (2.5 ml) and water (10 ml) to give off-white crystals (1.5 g, 4.1 mmol, 70 % yield). HPLC retention time 7.3 min; ^{1}H NMR (CDCl$_3$, 400 MHz) δ 3.94 (s, 4H, CH$_2$), 7.22 (d, 8H, *J* 8.3 Hz, ArH) and 7.32 (d, 8H, *J* 8.28 Hz, ArH) ppm; ^{13}C NMR (CDCl$_3$, 100 MHz) δ 48.4 (CH$_2$), 129.1 (CH), 130.5 (Cq), 131.1 (CH), 134.1 (Cq), 190.8 (CO) ppm. HRMS (m/z): [M+NH$_4$]$^+$ for C$_{16}$H$_{12}$Cl$_2$O$_2$S$_2$, calculated 387.9994, measured 388.0000; IR: 1720cm^{-1} (film).

2.10.21 Synthesis of 2,2´-(4-cyanophenyl)acetyl disulfide

In a clean, dry, 50 ml round bottom flask sodium hydrosulfide (2.4 g, 43 mmol) was dissolved in ethanol (20 ml) and chilled over ice. Working in a well-ventilated fume hood this flask was fitted with an exhaust line allowing any gasses generated to be scrubbed by sodium hypochlorite. Into a separate 50 ml round bottom flask 2-(4-cyanophenyl)acetic acid (2.753 g, 17.1 mmol) was dissolved in dichloromethane (150 ml). To this, 1-chloro-*N,N-2*-trimethyl-1-propenylamine (3.432 g, 3.120 ml, 25.7 mmol) was added and the mixture was stirred at room temperature for 30 min. After the reaction was complete (determined by HPLC) the solvent was removed under vacuum to yield a bright green oil. This oil was added to the ethanolic sodium hydrosulfide, the solution instantly turned yellow and a precipitate (sodium chloride) was formed. This precipitate was removed under vacuum filtration and was washed with ice cold ethanol (1.5ml). The resulting yellow solution was recovered from the Buchner flask, added to a clean 50 ml round bottomed flask and stirred over ice. To this solution iodine was added (0.5 g, 3.9 mmol) and the product precipitated out of solution. Iodine was slowly added until the colour of the suspension changed from white to pale brown (approximately 1 g, 7.8 mmol). The precipitate was collected by vacuum filtration and washed with ice-cold ethanol (2.5 ml) and water (10 ml) to give a yellow powder (1.6 g, 4.6 mmol, 53.8 % yield). HPLC retention time 6.0 min; ^{1}H NMR (CDCl$_3$, 400 MHz) δ 4.08 (s, 4H), 7.41 (d, 8H, *J* 8.1 Hz, ArH) and 7.64 (d, 8H, *J* 8.06 Hz, ArH) ppm; ^{13}C NMR (CDCl$_3$, 100 MHz) δ 48.8 (CH$_2$), 112.1 (CN), 118.4 (Cq), 130.5 (CH), 132.7 (CH), 137.3 (Cq), 189.76 (CO) ppm. HRMS (m/z): [M+NH$_4$]$^+$ for C$_{18}$H$_{12}$N$_2$O$_2$S$_2$, calculated 370.0678, measured 370.0692; IR: 1716 cm^{-1} (film).

2.10.22 Synthesis of 2,2´-(4-methoxyphenyl)acetyl disulfide

In a clean, dry, 50 ml round bottom flask sodium hydrosulfide (4.26 g, 75.3 mmol) was dissolved in ethanol (20 ml) and chilled over ice. Working in a well-ventilated fume hood this flask was fitted with an exhaust line allowing any gasses generated to be scrubbed by sodium hypochlorite. Into a separate 50 ml round bottom flask 2-(4-methoxyphenyl)acetic acid (5 g, 30.1 mmol) was dissolved in dichloromethane (150 ml). To this, 1-chloro-*N,N*-2-trimethyl-1-propenylamine (8.03g, 7.96 ml, 60.2 mmol) was added and stirred at room temperature for 30 min. After the reaction was complete (determined by HPLC) the solvent was removed under vacuum to yield a pale yellow oil. This oil was added to the ethanolic sodium hydrosulfide, the solution instantly turned yellow and a precipitate (sodium chloride) was formed. This precipitate was removed under vacuum filtration and washed with ice cold ethanol (2 × 1.5 ml). The resulting yellow solution was recovered from the Buchner flask, added to a clean 50 ml round bottomed flask and stirred over ice. To this solution iodine was added (1 g, 7.8 mmol) and the product precipitated out of solution. Iodine was slowly added until the colour of the suspension changed from white to pale brown (approximately 0.5 g, 3.9 mmol). The precipitate was collected by vacuum filtration and washed with ice-cold ethanol (2 × 2.5ml) and water (10 ml) to give a yellow powder (1.19 g, 3.28 mmol, 11 % yield). ^{1}H NMR (CDCl$_3$, 400 MHz) δ 3.79 (s, 6H, CH$_3$), 3.92 (s, 4H, CH$_2$), 6.89 (d, 8H, J 8.8 Hz,ArH) and 7.16 (d, 8H, J 8.8 Hz, ArH) ppm; ^{13}C NMR (CDCl$_3$, 100MHz) δ 48.6 (CH$_3$), 55.2 (CH$_2$), 114.7 (CH), 124.5 (Cq), 131.1 (CH), 159.5 (Cq), 192.5 (CO) ppm; HRMS (m/z): [M+NH$_4$]$^+$ for C$_{18}$H$_{18}$O$_4$S$_2$, calculated 362.0647, measured 362.0634.

2.11 Experimental: Sulfurisation with Fresh and Aged PADS

2.11.1 Varying 3-Picoline Concentration in Sulfurisation with Fresh PADS

Several ^{31}P NMR experiments were run in order to assess the dependence of the rate of the sulfurisation reaction on 3-picoline concentration. A mixed solution of triphenyl phosphite and triphenyl phosphine oxide (0.6 M, 100 µL) was added to an NMR tube. Varying amounts of 3-picoline were added to this as follows to make a total reaction volume of 600 µL.

3-Picoline concentration (M)	Volume (µL)	
	3-Picoline	ACN-d$_3$
0.5	29.2	270.8
1.0	58.3	241.7
1.5	87.5	212.5
2.0	116.6	183.4
2.5	145.8	154.2
3.0	174.9	125.1
3.5	204.1	95.9
4.0	233.2	66.8

At T=0 PADS (3 M, 200 µL) was added to this and ^{31}P NMR spectra were acquired approximately every 90 s until the phosphite starting material had been consumed.

2.11.2 Varying PADS Concentration in Sulfurisation Reaction with Fresh PADS

Several ^{31}P NMR experiments were run in order to assess the dependence of the rate of reaction on PADS concentration. A mixed solution of triphenyl phosphite and triphenyl phosphine oxide (1.2 M, 50 µL), 3-picoline (116.6 µL) and varying quantities of deuterated acetonitrile (see below) were added to an NMR tube. At T=0 varying quantities of PADS were added to this and ^{31}P NMR spectra were run approximately every 90 s until the phosphite starting material had been consumed.

PADS Reaction Conc. (M)	Volume (µL)	
	PADS (5 M)	ACN-d3
1.0	120	314
2.0	240	194
2.5	300	134
3.0	360	74
3.5	420	14

2.11.3 Sulfurisation Reaction in the Presence of BHT (1 M)

To an NMR tube, a mixed solution of triphenyl phosphite and triphenyl phosphine oxide (0.6 M, 100 µL), 3-picoline (100 µL, 6 M) and butylated hydroxy toluene (3 M, 100 µL) were added to an NMR tube. At T=0 PADS (3 M, 200 µL) was added and ^{31}P NMR spectra were run approximately every 90 s until the phosphite starting material had been consumed.

2.11.4 Sulfurisation Reaction in the Presence of BHT (0.1 M)

To an NMR tube, a mixed solution of triphenyl phosphite and triphenyl phosphine oxide (0.6 M, 100 µL), 3-picoline (100 µL, 6 M) and butylated hydroxy toluene (3 M, 10 µL) and deuterated acetonitrile (90 µL) were added to an NMR tube. At T=0 PADS (3 M, 200 µL) was added and ^{31}P NMR spectra were run approximately every 90 s until the phosphite starting material had been consumed.

2.11.5 Sulfurisation of Aryl Phosphites with Fresh PADS in Acetonitrile-d$_3$

Solutions of several differently substituted aryl phosphites (x= *p*-OMe, *p*-Me, H, *p*-F, *p*-Cl, *m*-Cl) were made up in acetonitrile-d$_3$ with an equimolar concentration of triphenyl phosphine oxide (0.3 M) in acetonitrile-d$_3$. Aliquots of these solutions (200 µL) were added to NMR tubes with 3-picoline (6 M, 200 µL). At T=0 PADS (3 M, 200 µL) was added and ^{31}P NMR spectra were run approximately every 90 s until the phosphite starting material had been consumed.

2.11.6 Sulfurisation of Aryl Phosphites with Fresh PADS in Toluene-d$_8$

Solutions of several differently substituted aryl phosphites (x= *p*-OMe, *p*-Me, H, *p*-F, *p*-Cl, *m*-Cl) were made up in toluene-d$_8$ with an equimolar concentration of triphenyl phosphine oxide (0.1 M) in toluene-d$_8$. Aliquots of these solutions (200 μL) were added to NMR tubes with 3-picoline (2 M, 200 μL). At T=0 PADS (1 M, 200 μL) was added and ^{31}P NMR spectra were run approximately every 90 s until the phosphite starting material had been consumed.

2.11.7 Sulfurisation of Aryl Phosphites with Fresh PADS in CDCl$_3$

Solutions of several differently substituted aryl phosphites (x= *p*-OMe, *p*-Me, H, *p*-F, *p*-Cl, *m*-Cl) were made up in CDCl$_3$ with an equimolar concentration of triphenyl phosphine oxide (0.1 M) in CDCl$_3$. Aliquots of these solutions (200 μL) were added to NMR tubes with 3-picoline (2 M, 200 μL). At T=0 PADS (1 M, 200 μL) was added and ^{31}P NMR spectra were run approximately every 90 s until the phosphite starting material had been consumed.

2.11.8 Sulfurisation of Aryl Phosphites with Fresh PADS in DMSO-d$_6$

Solutions of several different substituted aryl phosphites (x= *p*-OMe, *p*-Me, H, *p*-F, *p*-Cl, *m*-Cl) were made up in DMSO-d$_6$ with an equimolar concentration of triphenyl phosphine oxide (0.1 M) in DMSO-d$_6$. Aliquots of these solutions (200 μL) were added to NMR tubes with 3-picoline (2 M, 200 μL). At T=0 PADS (1 M, 200 μL) was added and ^{31}P NMR spectra were run approximately every 90 s until the phosphite starting material had been consumed.

2.11.9 Sulfurisation of Alkyl Phosphites with Fresh PADS in CDCl$_3$

Solutions of several different alkyl phosphites (R= MeO, EtO, 2-ClEtO, F$_3$EtO) were made up in CDCl$_3$ with an equimolar concentration of triphenyl phosphine oxide (0.1 M) in CDCl$_3$. Aliquots of these solutions (200 μL) were added to NMR tubes with 3-picoline (2 M, 200 μL). At T=0 PADS (1 M, 200 μL) was added and ^{31}P NMR spectra were run approximately every 90 s until the phosphite starting material had been consumed.

2.11.10 Sulfurisation of Phosphites in Acetonitrile-d$_3$ Using Fresh PADS with Various Substituted Pyridines

Sulfurisation kinetic experiments were run in acetonitrile-d$_3$ according to the method detailed in section 2.8 using triphenyl phosphite (0.3 M, 200 µL) and PADS (3 M, 200 µL). In place of 3-picoline various substituted pyridines were used (6 M, 200 µL) where x = *p*-CN, *p*-OMe, H, *m*-CN, *m*-Cl, *m*-OMe and *m*-Me.

2.11.11 Sulfurisation of Phosphites Using 2,2,2´2´-tetramethyl-2,2´-phenylacetyl disulfide with Various Substituted Pyridines

Sulfurisation kinetic experiments were run in acetonitrile-d$_3$ according to the method detailed in section 2.8 using triphenyl phosphite (0.07 M, 200 µL). PADS was replaced in this experiment set with 2,2,2'2'-tetramethyl-2,2'-phenylacetyl disulfide (0.7 M, 200 µL). In place of 3-picoline various substituted pyridines were used (1.4 M, 200 µL) where x = *p*-CN, *p*-OMe, H, *m*-CN, *m*-Cl, *m*-OMe and *m*-Me.

2.11.12 Sulfurisation of Phosphites Using Dibenzoyl disulfide with Various Substituted Pyridines

Sulfurisation kinetic experiments were run in acetonitrile-d$_3$ according to the method detailed in section 2.8 using triphenyl phosphite (0.025 M, 200 µL). In these experiments, PADS was replaced with dibenzoyl disulfide (0.25 M, 200 µL). In place of 3-picoline various substituted pyridines were used (0.5 M, 200 µL) where x = *p*-CN, *p*-OMe, H, *m*-CN, *m*-Cl, *m*-OMe and *m*-Me.

2.11.13 Sulfurisation of Phosphites in Acetonitrile-d$_3$ Using Fresh PADS with Various Substituted Pyridines

Sulfurisation kinetic experiments were run in acetonitrile-d$_3$ according to the method detailed in section 2.8 using triphenyl phosphite (0.3 M, 200 µL) and PADS (3 M, 200 µL). In this experiment, 3-picoline was replaced with triethyl amine (167 µL). Acetonitrile-d$_3$ (33 µL) was added to make the total reaction volume up to 600 µL.

2.11.14 Sulfurisation of Phosphites in Acetonitrile-d₃ Using Various Phenyl Substituted PADS with 3-Picoline

Sulfurisation kinetic experiments were run in acetonitrile-d_3 according to the method detailed in section 2.8 using triphenyl phosphite (0.3 M, 200 μL) and 3-picoline (6M, 200 μL). In this series of experiments, PADS was replaced with various phenyl substituted PADS compounds (3M, 200 μL) where x = *p*-OMe, *p*-F, *p*-Cl, *p*-CN and *m*-Cl.

2.11.15 Synthesis of tris-(4-methoxyphenyl)phosphite

In a clean, dry 250 ml three-necked round-bottom flask a solution of 4-methoxyphenol (9.77 g, 78.7 mmol) and pyridine (8.10 ml, 7.92 g, 100 mmol) was prepared in diethyl ether (80 ml). To this, phosphorus trichloride (1.74 ml, 2.74 g, 20.0 mmol) was added dropwise at room temperature under nitrogen atmosphere and stirred for 1.5 h. When the reaction was complete, the reaction mixture was quenched with water (100 ml). The reaction mixture was transferred to a separating funnel. The organic phase was separated and washed with water (50 ml) and brine (50 ml). This was then dried with magnesium sulfate, and the solvent was removed under vacuum. The crude mixture was purified by silica gel column chromatography using chloroform as the eluent to give the product as a colourless oil (4.87 g, 4.03 ml, 12.2 mmol, 61 % yield). ^{1}H NMR (CDCl₃, 400 MHz) δ 3.78 (s, 9H, CH₃), 6.87 (d, 6H, *J* 9.1 Hz, ArH) and 7.11 (d, 6H, *J* 9.1 Hz, ArH) ppm; ^{13}C NMR (CDCl₃, 100 MHz) δ 55.6 (CH₃), 114.7 (CH), 121.7 (CH), 145.1 (Cq), 156.3 (Cq) ppm; ^{31}P NMR (CDCl₃, 400 MHz), δ 128.9 ppm, HRMS (m/z): [M+H]$^+$ for C₂₁H₂₁O₃P, calculated 401.1149, measured 401.1150.

2.11.16 Synthesis of 2,2′-(4-fluorophenyl)acetyl disulfide
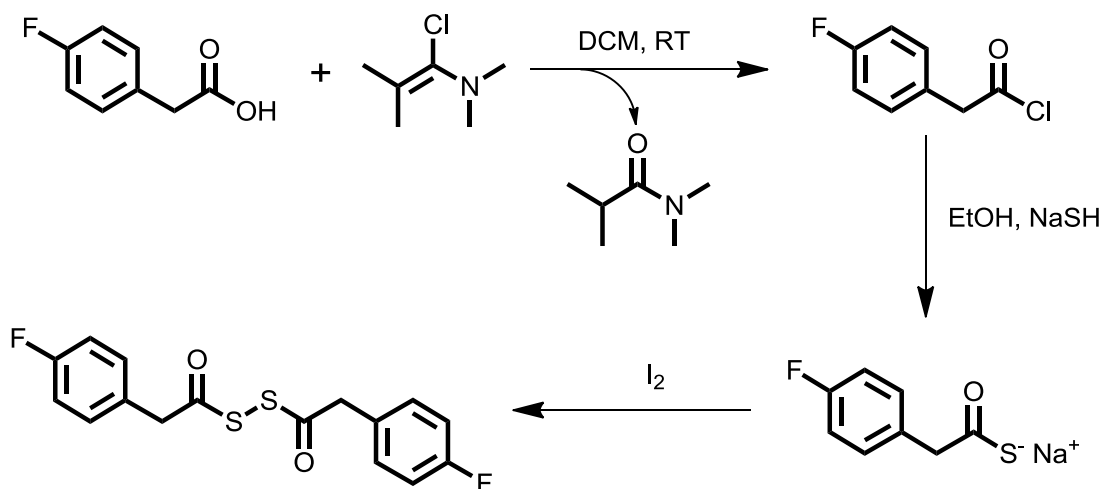
Into a clean, dry, 50 ml round bottom flask sodium hydrosulfide (1.8 g, 33.3 mmol) was dissolved in ethanol (15 ml) and chilled over ice. This flask was fitted with an exhaust line allowing any gasses generated to be scrubbed by sodium hypochlorite in a well-ventilated fume hood. Into a separate 50 ml round bottom flask 2-(4-fluorophenyl)acetic acid (2 g, 13.2 mmol) was dissolved in dichloromethane (15 ml). To this, 1-chloro-*N,N*-2-trimethyl-1-propenylamine (1.9 g, 1.73 ml, 14.0 mmol) was added and stirred at room temperature for 30 min. After the reaction was complete (determined by HPLC) the solvent was removed under vacuum to yield a dark-brown oil. This oil was added to the ethanolic sodium hydrosulfide, the solution instantly turned yellow and a precipitate (sodium chloride) was formed. This precipitate was removed under vacuum filtration and washed with ice cold ethanol (1.5ml). The resulting yellow solution was recovered from the Buchner flask, added to a clean 50 ml round bottomed flask and stirred over ice to ensure that the temperature was kept below 15°C. To this solution excess iodine was added (1.5 g, 11.7 mmol) until the colour of the solution changed from white to pale brown and the product precipitated out of solution. The precipitate was collected by vacuum filtration and washed with ice-cold ethanol (2.5ml) and water (10ml) to give off-white crystals (1.5 g, 4.4 mmol, 67% yield). HPLC retention time 6.7 min; ^{1}H NMR (CDCl$_3$, 400MHz) δ 3.94 (s, 4H, CH$_2$), 7.01 and 7.24 (2t, 8H, *J* 7.3, ArH) ppm; ^{13}C NMR (CDCl$_3$, 100MHz) δ 48.2 (CH$_2$), 115.8 (d, J 21.2 Hz, CH), 127.9 (d, 3.3 Hz, Cq), 131.5 (d, 8.1 Hz, CH), 162.1 (d, *J* 246.9 Hz, CF), 191.3 (CO) ppm. HRMS (m/z): [M+NH$_4$]$^+$ for C$_{16}$H$_{12}$F$_2$O$_2$S$_2$, calculated 338.0247, measured 338.0254; IR: 1719 cm^{-1} (film).

2.11.17 Synthesis of 2,2′-(3-chlorophenyl)acetyl disulfide
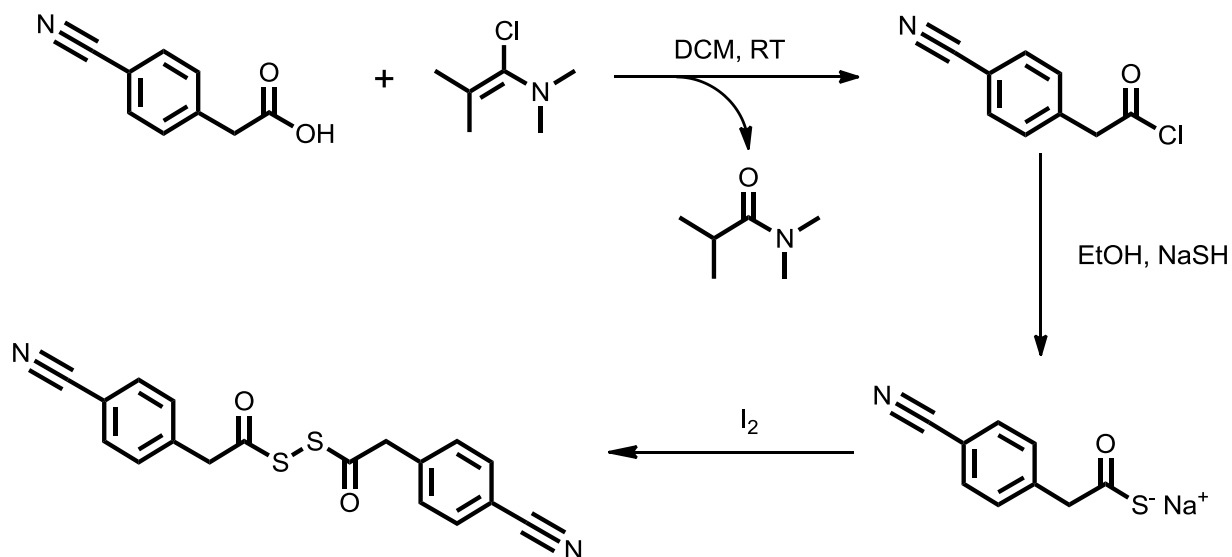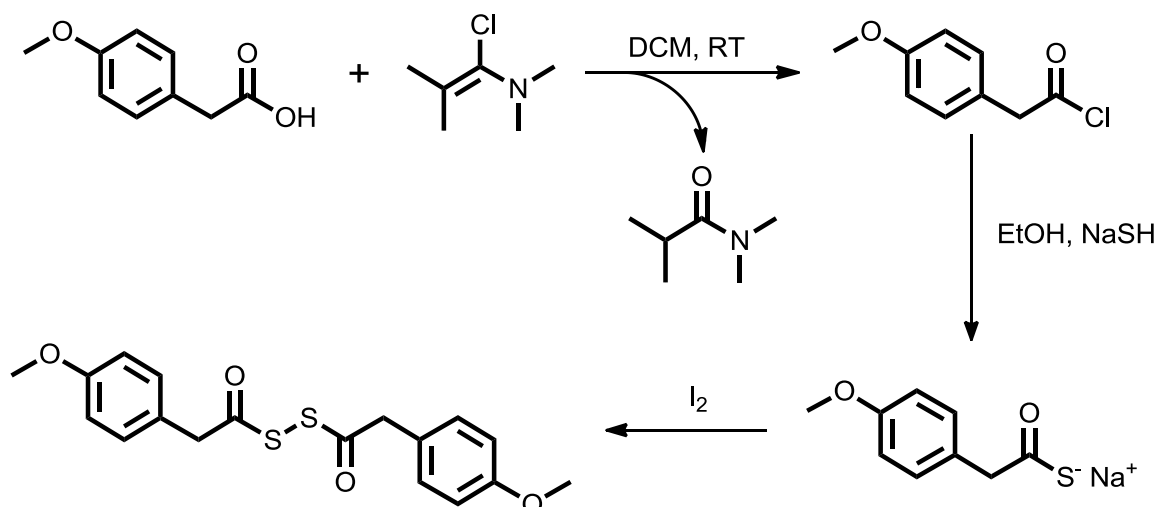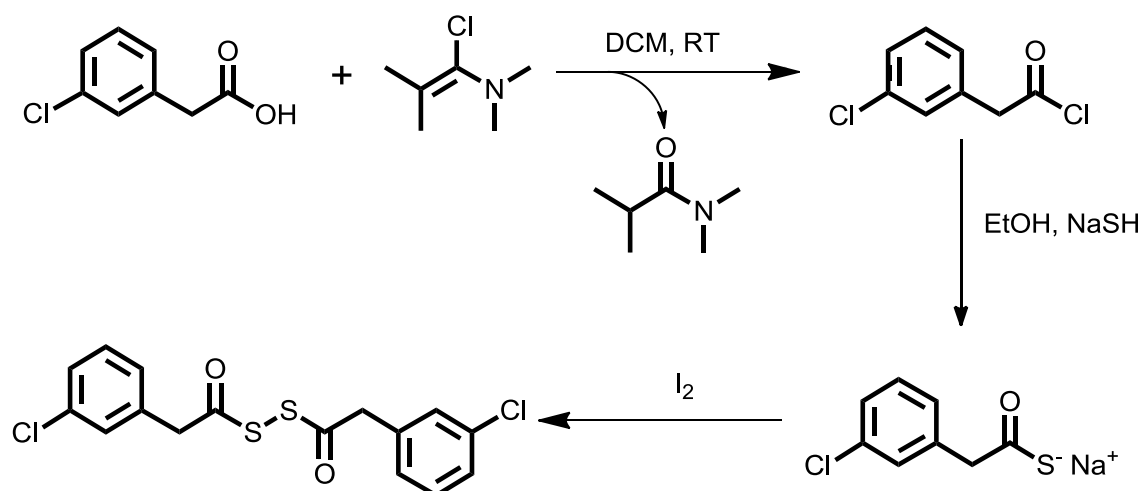

Into a clean, dry, 50 ml round bottom flask sodium hydrosulfide (1.6 g, 29.25 mmol) was dissolved in ethanol (15 ml) and chilled over ice. This flask was fitted with an exhaust line allowing any gasses generated to be scrubbed by sodium hypochlorite in a well-ventilated fume hood. Into a separate 50 ml round bottom flask 3-chlorophenylacetic acid (2 g, 11.7 mmol) was dissolved in dichloromethane (15 ml). To this, 1-chloro-*N,N*-2-trimethyl-1-propenylamine (1.72 g, 1.57 ml, 12.9 mmol) was added and stirred at room temperature for 30 min. After the reaction was complete (determined by HPLC) the solvent was removed under vacuum to yield a pale-orange oil. This oil was added to the ethanolic sodium hydrosulfide, the solution instantly turned yellow and a precipitate (sodium chloride) was formed. This precipitate was removed under vacuum filtration and washed with ice cold ethanol (1.5ml). The resulting yellow solution was recovered from the Buchner flask, added to a clean 50 ml round bottomed flask and stirred over ice to ensure that the temperature was kept below 15°C. To this solution iodine was added (0.5 g, 3.9 mmol) and the product crashed out of solution. Iodine was slowly added until the colour of the suspension changed from white to pale brown (approximately 1 g, 7.8 mmol). The precipitate was collected by vacuum filtration and washed with ice-cold ethanol (2.5ml) and water (10ml) to give a white powder (1.7 g, 4.6 mmol, 79 % yield). HPLC retention time 7.1 min; ^{1}H NMR (CDCl$_3$, 400MHz) δ 3.96 (s, 4H, CH$_2$), 7.16–7.30 (m, 8H, ArH); ^{13}C NMR (CDCl$_3$, 100MHz) δ 48.6 (CH$_2$), 129.9 (CH), 128.3 (CH), 129.8 (CH), 130.2 (CH), 133.9 (Cq), 143.7 (Cq), 190.6 (CO) ppm. HRMS (m/z): [M+NH$_4$]$^+$ for C$_{16}$H$_{12}$Cl$_2$O$_2$S$_2$, calculated 369.9656, measured 369.9660; IR: 1720 cm^{-1} (film).

2.11.18 Synthesis of tris(3-chlorophenyl)phosphite
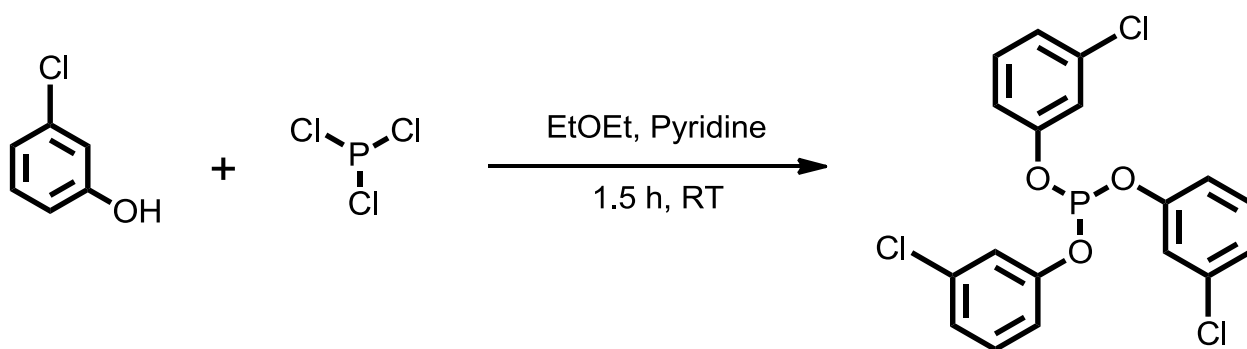
In a clean, dry 250 ml three-necked round-bottom flask a solution of 3-chlorophenol (14.04 g, 112.8 mmol) and pyridine (10.8 ml, 10.58 g, 141 mmol) was prepared in diethyl ether (120 ml). To this, phosphorus trichloride (4.0 ml, 3.87 g, 28.2 mmol) was added dropwise at room temperature under nitrogen atmosphere and stirred for 1.5 h. When the reaction was complete, the reaction mixture was quenched with water (150 ml). The reaction mixture was transferred to a separating funnel. The organic phase was separated and washed with water (50 ml) and brine (50 ml). This was then dried with magnesium sulfate, and the solvent was removed under vacuum. The crude mixture was purified by silica gel column chromatography using chloroform as the eluent to give the product as a yellow oil (9.1 g, 6.8 ml, 22 mmol, 78 % yield). ^{1}H NMR (CDCl$_3$, 400 MHz) δ 7.01–7.29 (m, 12H, ArH) ppm; ^{13}C NMR (CDCl$_3$, 100 MHz) δ 118.8 (d, J_{C-P} 7.5 Hz, CH), 121.2 (d, J_{C-P} = 6.6 Hz, CH), 124.9 (CH), 130.6(CH), 135.1 (Cq), 151.8 (Cq) ppm; ^{31}P NMR (CDCl$_3$, 400 MHz), δ 126.5 ppm, HRMS (m/z): [M+H]$^+$ for C$_{18}$H$_{12}$O$_3$Cl$_3$P, calculated 412.9662, measured 411.9672.

2.11.19 Preparation of tris (4-chlorophenyl)phosphite
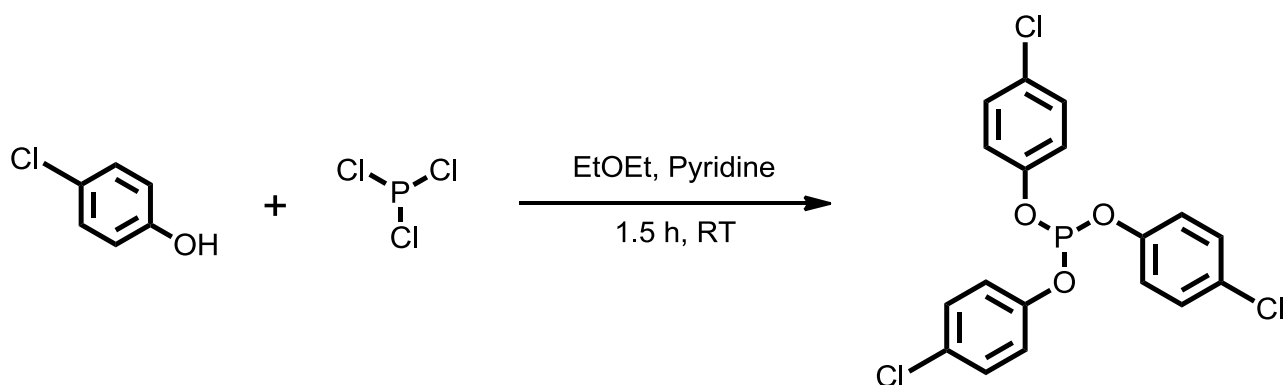
In a clean, dry 250 ml three-necked round-bottom flask a solution of 4-chlorophenol (10.3 g, 80 mmol) and pyridine (8.10 ml, 7.92 g, 100 mmol) was prepared in diethyl ether (80 ml). To this, phosphorus trichloride (1.74 ml, 2.74 g, 20.0 mmol) was added dropwise at room temperature under nitrogen atmosphere and stirrer for 1.5 h. When the reaction was complete, the reaction mixture was quenched with water (100 ml). The reaction mixture was transferred to a separating funnel. The organic phase was separated and washed with water (50 ml) and brine (50 ml). This was then dried with magnesium sulfate, and the solvent was removed under vacuum. The crude mixture was purified by silica gel column chromatography using chloroform as the eluent to give the product as a white solid (5.06 g, 12.2 mmol, 61 % yield). ^{1}H NMR (CDCl$_3$, 400 MHz) δ 7.17 (2d, J = 8.8 Hz, 12H, ArH) ppm; ^{13}C NMR (CDCl$_3$, 100 MHz) δ 121.9 (d, J_{C-P} 6.6 Hz, Cq), 129.9 (CH), 149.8 (d, J_{C-P} = 2.8 Hz, Cq) ppm; ^{31}P NMR (CDCl$_3$, 400 MHz), δ 126.8 ppm, HRMS (m/z): [M+H]$^+$ for C$_{18}$H$_{12}$O$_3$Cl$_3$P, calculated 412.9662, measured 412.9665.

2.11.20 Preparation of tris (4-fluorophenyl)phosphite
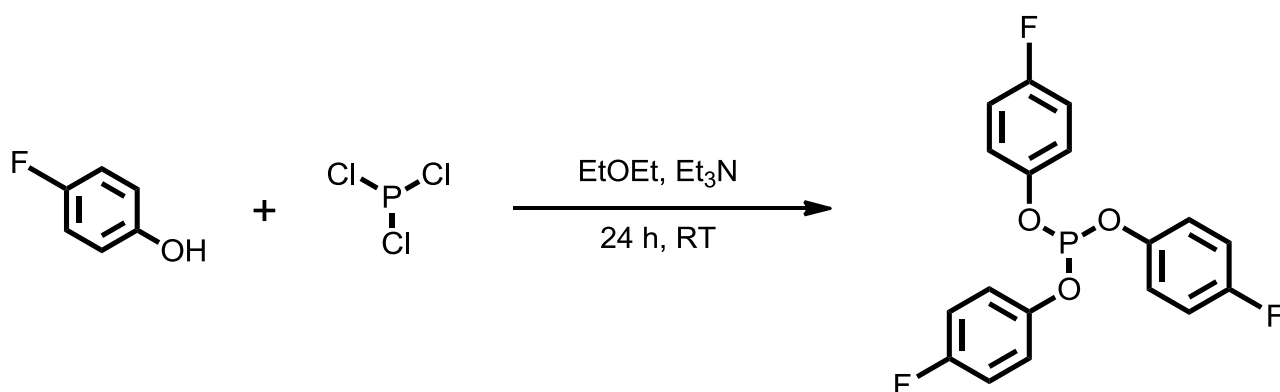
In a clean, dry 250 ml three-necked round-bottom flask a solution of 4-fluorophenol (4.41 g, 39.3 mmol) and triethylamine (5.6 ml, 4.06 g, 40 mmol) was prepared in diethyl ether (40 ml). To this, phosphorus trichloride (0.87 ml, 1.37 g, 10.0 mmol) was added dropwise at room temperature under nitrogen atmosphere and stirrer for 24 h. After 24 h the solid precipitate from the reaction was removed by vacuum filtration and washed with diethyl ether (2 ×10ml). The filtrate was then transferred into a round-bottomed flask and the solvent was removed under vacuum. The crude product was purified by silica gel column chromatography eluting with chloroform to give the product as a white solid (4.77 g, 13.1 mmol, 71% yield). ^{1}H NMR (CDCl$_3$, 400 MHz) δ 7.01 – 7.13 (m, 12H, ArH) ppm; ^{13}C NMR (CDCl$_3$, 100 MHz) 116.4 (d, J_{C-F} = 23 Hz, CH), 122.0 (t, J_{C-F} = 7.4 Hz, J_{C-P} = 7.3 Hz, CH), 147.2 (d, J_{C-F} = 2.9 Hz, J_{C-P} = 3.0 Hz, Cq), 159.5 (d, J_{C-F} = 243 Hz, CF) ppm; ^{31}P NMR (CDCl$_3$, 400 MHz) δ 127.5 (127.8) ppm, HRMS (m/z): [M+H]$^+$ for C$_{18}$H$_{12}$O$_3$F$_3$P, calculated 365.0476, measured 365.0550.

2.12 Experimental – Activation and Coupling

2.12.1 Solubility of ETTH in Acetonitrile at 25°C

Acetonitrile (ca. 10 ml) was accurately weighed and added to a 25 ml round-bottomed flask. ETTH (ca. 10 g) was accurately weighed and added to this. The mixture was kept at 25°C in a water bath and stirred for 24 h. After 24 h the solution was filtered under vacuum and the recovered solid masswas dried overnight in an oven set at 80°C. The solubility was calculated by subtracting the remaining solid from the total solid added as follows:

$$Solubility_{max}\ (g) = \frac{\left(\dfrac{Mass\ ETTH_{total}\ (g) - Mass\ ETTH_{recovered}\ (g)}{RMM\ of\ ETTH\ (130.03gmol^{-1})}\right)}{\left(\dfrac{Mass\ of\ ACN}{density\ of\ ACN\ (0.786\ gml^{-1})}\right)}$$

2.12.2 Solubility of [ETTHDIA] in Acetonitrile at 25°C

A saturated solution of ETTH was prepared (1.6 M, 50 ml) in acetonitrile. To this, di-isopropyl amine was added in excess. As amine was added, ETTHDIA precipitated as white crystals. This mixture was then filtered under vacuum and the solid washed with ice-cold acetonitrile (2 × 5 ml). The solid was collected and dried in an oven set to 80°C overnight. The maximum solubility of [ETTHDIA] was calculated in the same way as the maximum solubility of ETTH in section 2.10.1.

2.12.3 Calculation of ETTH pK$_a$ in H$_2$O

Solutions of ETTH (0.1 M, 250 ml) and NaOH (0.1 M, 250 ml) were prepared in ultra-pure water. A portion of the ETTH solution (25 ml) was added to a 250 ml beaker which was suspended in a water bath kept at 25°C. This was then equipped with a stirrer bar and a pH probe was placed in the solution to monitor the pH. Above this, a burette was kept in place using a clamp stand. This was filled with the NaOH solution. Small amounts of NaOH were then added to the ETTH solution and the pH was monitored throughout. The titration ended when the pH of the solution remained stable upon the addition of NaOH. The pK$_a$ of ETT was then determined using the Henderson-Hasselbach equation.

$$\text{pH} = \text{p}K_a + \log\frac{[A^-]}{[HA]}$$

2.12.4 Calculation of pK$_a$ of Several Tetrazoles in 10% v/v DMSO/H$_2$O

Solutions of *x*-tetrazole (0.1 M, 250 ml) and NaOH (1 M, 250 ml) were prepared in a solvent mixture of 10% v/v DMSO/H$_2$O. A portion of the *x*-tetrazole solution (25 ml) was added to a 250 ml beaker equipped with a stirrer bar and a pH probe was placed in the solution to monitor the pH and was incubated in a water bath at 25°C. Above this, a burette was kept in place using a clamp stand. This was filled with the NaOH solution. Small amounts of NaOH were then added to the substituted tetrazole solution and the pH was monitored throughout. The titration was ended when the pH of the solution remained stable upon the addition of NaOH. The pK$_a$ of the substituted tetrazole was then determined using the Henderson-Hasselbach equation.

2.12.5 Conductance Measurements of ETTH Solutions in Acetonitrile

Several solutions of ETTH were made up in acetonitrile (10 – 100 mM, 10 ml) and placed in a jacketed flask, equipped with a stirrer bar, with the temperature maintained at 25°C. Once at temperature the conductance probe was submerged in the solution and allowed to equilibrate for 5 min before values were recorded.

2.12.6 Conductance Measurements of ETTHDIA Solutions in Acetonitrile

ETTHDIA was prepared as described in section 2.12.2. Solutions of ETTHDIA were prepared in acetonitrile (0.5 – 5 mM, 10 ml). Conductance measurements were taken in the same way as that described for ETTH in section 2.12.5.

2.12.7 Conductance Measurements of ETTHDIA Solutions with Excess ETTH in Acetonitrile

Several solutions of ETTH were made up (0 – 30 mM, 10 ml) in acetonitrile. Each solution was added individually to a jacketed vessel, equipped with a stirrer bar, with the temperature maintained at 25°C. To these solutions, ETTHDIA was added (250 µL, 0.2 M). Once at temperature the conductance probe was submerged in the solution and allowed to equilibrate for 5 min before the value was recorded.

2.12.8 Activation of UAm Using ETTH Monitored by Conductivity

Into a jacketed reaction vessel, a solution of UAm in acetonitrile (5 mM, 30ml) was added and kept at a constant 25°C. The conductivity probe was inserted to monitor the conductivity and temperature. Once the solution had reached temperature, varying amounts of ETT (0.1-1 M, 3 ml) were added and the conductivity was recorded every 0.1 s until the conductivity stabilised and the reaction was complete.

2.12.9 Methanolysis of UAm Activated by ETTH Monitored by Conductivity

A solution of methanol in acetonitrile was prepared (5% v/v, 1.2 M, 50 ml). Into a jacketed reaction vessel, a solution of UAm in acetonitrile (5 mM, 30ml) was mixed varying amounts of the 5% methanol solution (0-1.25 ml) and kept at a constant 25°C. The conductivity probe was inserted to monitor the conductivity and temperature. Once the solution had reached temperature, ETT (1 M, 1.5 ml) was added and the conductivity was recorded every 0.1 seconds until the conductivity stabilised and the reaction was complete.

2.12.10 Investigation into the Acitvation Equillibrium by ^{31}P NMR

A solution of UAm (0.1 M, 500 µL) in acetonitrile-d$_3$ was added to an NMR tube and a ^{31}P NMR spectra recorded. To this, three aliquots of ETTH (1 M, 50µL) were added periodically with ^{31}P NMR spectra being taken after each addition. To the resulting solution, DIA (2 M, 25 µL) was added again periodically with ^{31}P NMR spectra being taken after each addition.

2.12.11 Kinetics of Activation of di-*tert*-butyl *N,N*-di-isopropyl phosphoramidite (DBAm) with Various Substituted Tetrazoles. Reactions Followed by ^{31}P NMR Using Samples Quenched With Diethyl amine

Solutions of various substituted tetrazoles were made up in acetonitrile-d$_3$ (10 mM, 5 ml). A solution of DBAm (5 mM, 5 ml) was also made up in acetonitrile-d$_3$. Aliquots of the UAm solution (300 µL) were added to a 5 ml reaction vial. At t=0 the substituted tetrazole (300 µL) was added. At t=*n* diethyl amine (31 µL) was added neat and thoroughly mixed. These solutions were transferred to separate NMR tubes and ^{31}P NMR spectra were recorded. This allowed the concentration of DBAm to be plotted as a function of time for these reactions.

3. Results and Discussion: Ageing PADS

3. Ageing PADS

Phosphorothioate oligonucleotides are synthesised via sulfurization of newly formed phosphite linkages between coupled nucleotides. In the phosphoramidite method of oligonucleotide synthesis this is done immediately after the linkage is formed.

Currently, the most popular reagent used to perform this sulfurization is phenylacetyl disulfide (PADS). PADS is used because it gives low PO:PS ratio (95-99% PS) and reaction with PADS does not generate any oxidizing by-products unlike other sulfur transfer reagents such as the Beaucage[92]. PADS also gives rapid rates of reaction, affording almost full conversion of starting material to products with contact times of around 3 mins[96].
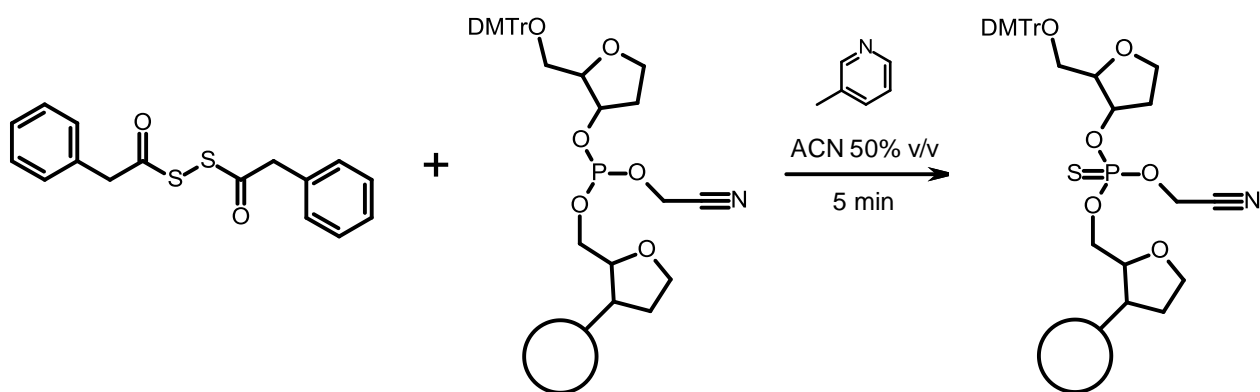
Scheme 10: General scheme for reaction of PADS with inter-nucleotide phosphite linkage.

Despite the efficiency of this reaction it is well known that the reaction rate and yield can be improved by 'ageing' PADS[97]. This involves preparing a solution of PADS in a 50% vol/vol mixture of acetonitrile and a pyridine (usually 3-picoline[97] although bases such as pyridine and collidine[108] have been used). This solution is then allowed to 'age' for around 48 h. This process generates a more efficient sulfurisation mixture (with the yield of phosphorothioate increasing from 99.5% yield with fresh PADS to 99.8% yield using aged PADS)[96]. Though this process is widely adopted and accepted to be of value, little is known about the products or mechanism of the process. It has been suggested that this process generates acylpolysulfides and that these are the active sulfur transfer reagents in these mixtures.

3.1 Analysis of Aged PADS Solutions

Solutions of PADS made up in acetonitrile with 3-picoline (5 M) exhibit multiple colour changes over time, changing from a pale-yellow through green/blue to brown/black. As well as the colour change, a further observation to be made looking at these solutions is that elemental sulfur crystallises out of the mixture after around 48 h. It is worth noting that PADS is stable in acetonitrile with no base present and that these changes are dependent on the presence of base.

In the current work, solutions of PADS aged in acetonitrile with 3-picoline (5 M) were analysed by HPLC, ^{1}H and ^{13}C NMR and mass spectrometry was performed in order to identify the products of the ageing process. HPLC analysis showed that under these conditions PADS degraded completely in 48 h and NMR analysis shows the disappearance of the peak corresponding to the methylene group of PADS at δ ^{1}H 4.1, ^{13}C 48.4 ppm (Fig. 16). All analytical methods show the generation of multiple degradation products, rather than one single species.
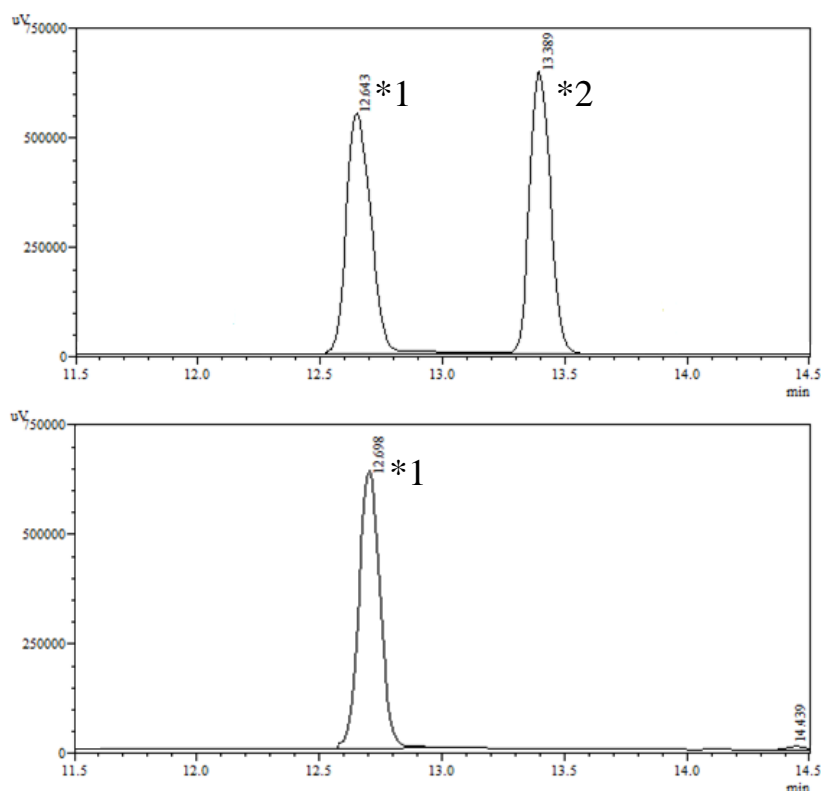
*Figure 16: HPLC chromatograms of PADS (3.3 mM) in a solution of 3-picoline (5M) in ACN (naphthalene internal standard at T=0 (top) and T=48 h (bottom) showing PADS degradation.*1 = Naphthalene (internal standard), *2 = PADS*

65
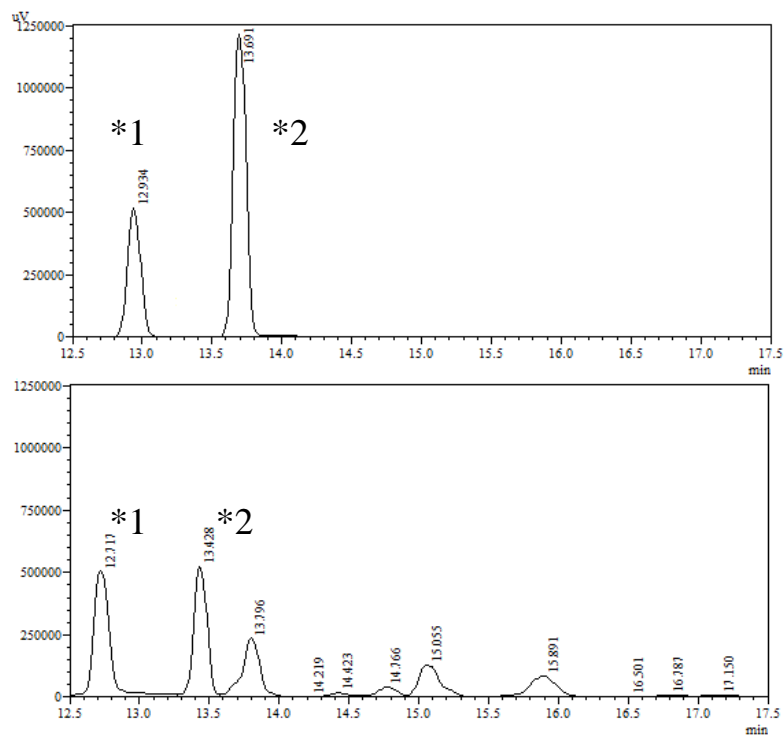
*Figure 17: HPLC chromatograms of PADS (3.3 mM) in a solution of 3-picoline (5M) in ACN (naphthalene internal standard at T=0 (top) and T=24 hours (bottom) showing non-polar degradation products. *1 = Naphthalene (internal standard), *2 = PADS*
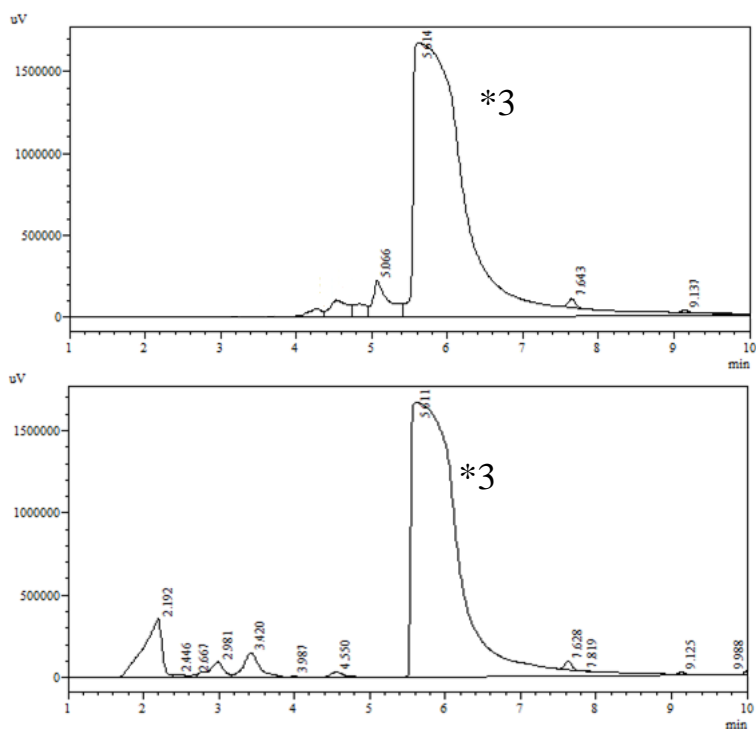
*Figure 18: HPLC chromatograms of PADS (3.3 mM) in a solution of 3-picoline (5M) in ACN (naphthalene internal standard at T=0 (top) and T=24 hours (bottom) showing polar degradation products. *3 = 3-picoline*
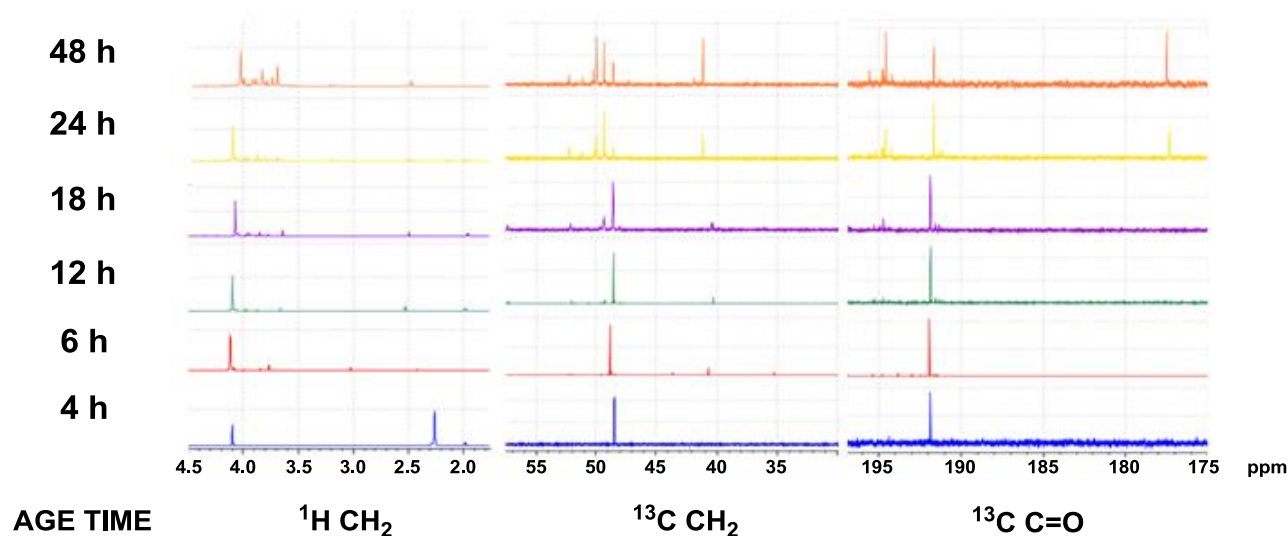
Figure 19: ^1H and ^{13}C NMR spectra of PADS (0.2M) in 3-picoline (0.4M) in ACN at T=n h

The NMR spectra in figure 19 show that the products of ageing are somewhat similar in structure to PADS itself, i.e. multiple methylene and carbonyl peaks are generated in close proximity to the original peaks. Similarly, the HPLC chromatograms show that multiple sharp peaks are generated with progressively longer retention times than PADS. Mass spectral analysis of these mixtures suggests that these degradation products are acylpolysulfides.
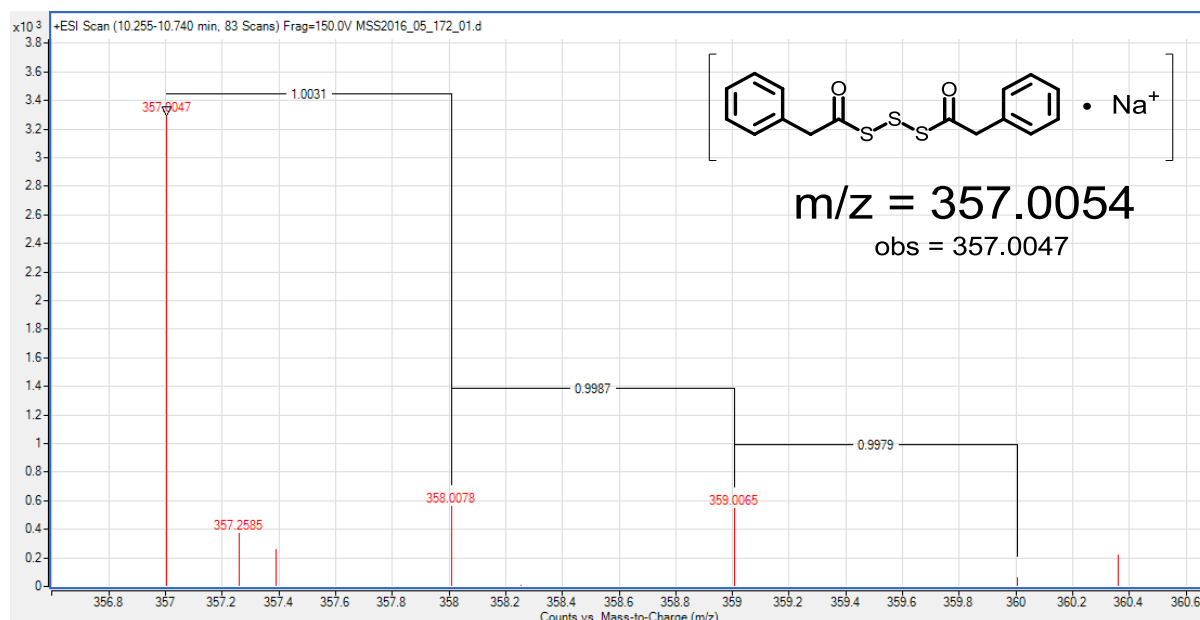
Figure 20: Mass spectrum of sodium adduct of bis-phenylacetyl trisulfide. $m/z_{exp} = 357.0054$, $m/z_{obs} = 357.0047$.
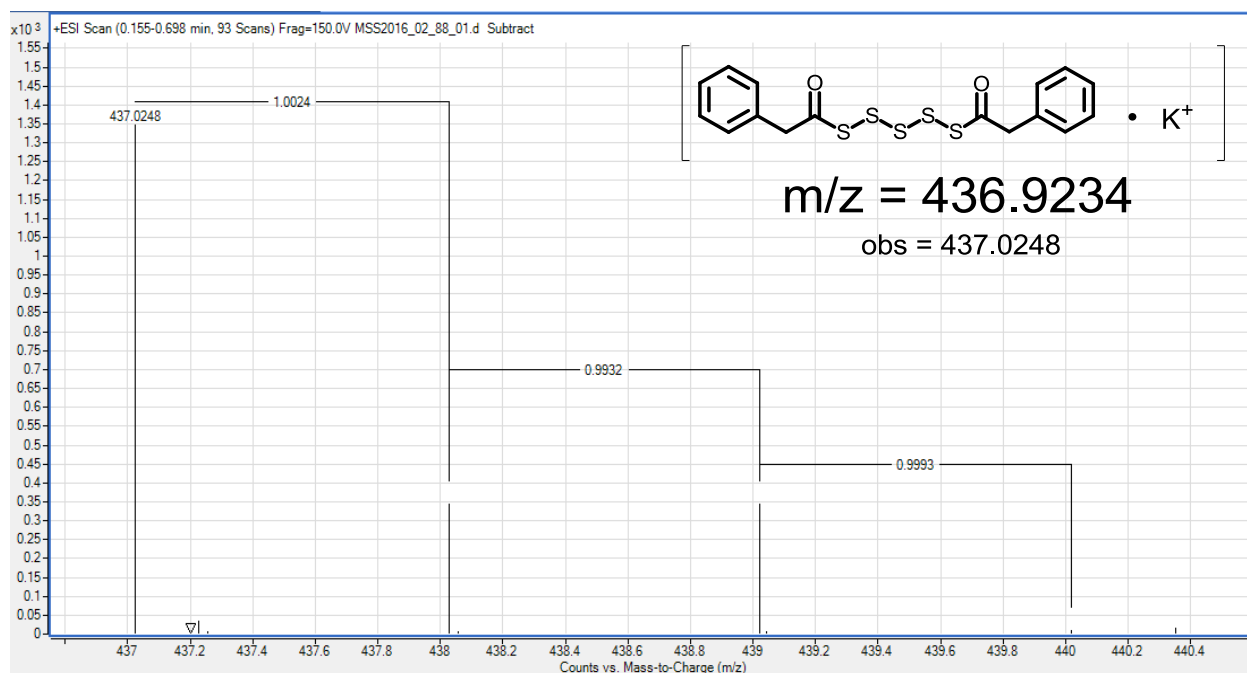
Figure 21: Mass spectrum of potassium adduct of bis-phenylacetyl pentasulfide. $m/z_{exp} = 436.9234$, $m/z_{obs} = 437.0248$
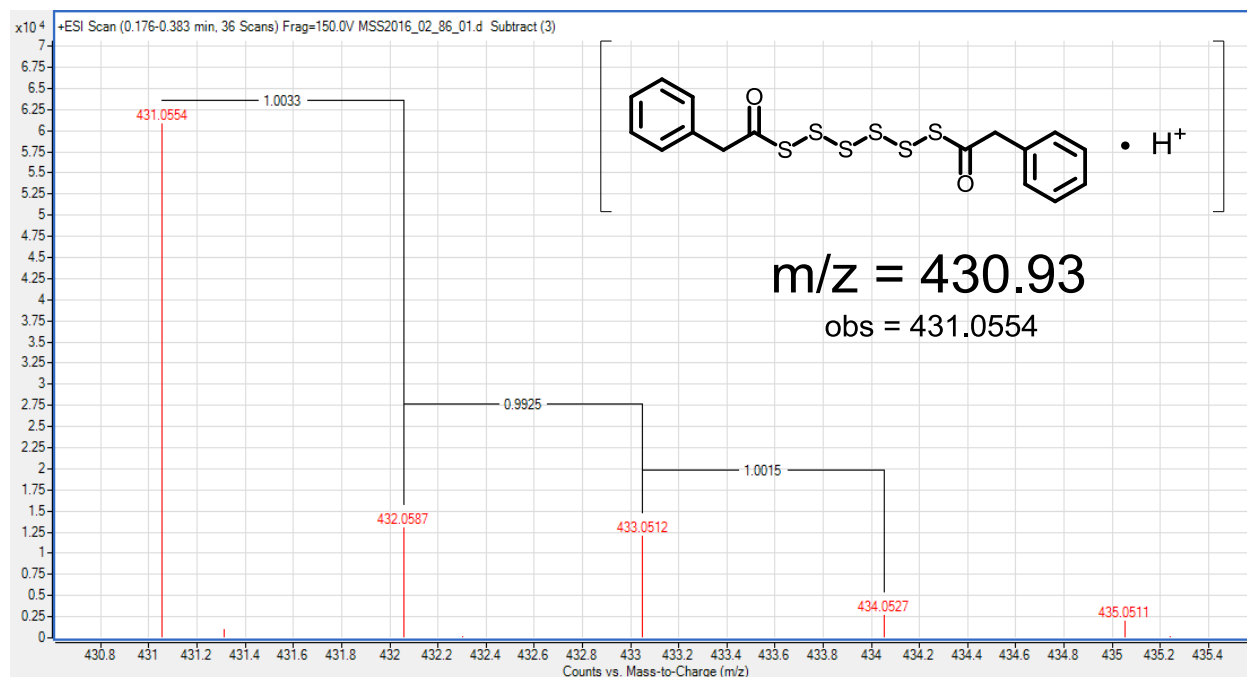
Figure 22: Mass spectrum of proton adduct of bis-phenylacetyl hexasulfide. $m/z_{exp} = 430.9300$, $m/z_{obs} = 431.0554$

The components responsible for these peaks were isolated by preparative HPLC. Reaction of these fractions with triphenylphosphite in the presence of 3-picoline showed that these acylpolysulfides are all active sulfur transfer reagents. Due to the fact that PADS degrades completely in acetonitrile with 5M 3-picoline it can be assumed that these species are the active sulfur transfer reagents in aged PADS solutions.

It is likely that the mechanism of formation of these polysulfides proceeds via nucleophilic attack of polysulfide anions on PADS and various other polysulfides (scheme 11)[110].

Though attempts to isolate these anions from aged PADS mixtures have been unsuccesful HPLC analysis of these solutions shows the presence of peaks eluting at a much lower retention time than PADS (i.e. much more polar) with similar UV absorbtion profiles (Fig. 18). These are thought to be the various polysulfide anions formed during PADS degradation as the mobile phase is much more polar earlier in the chromatogram.
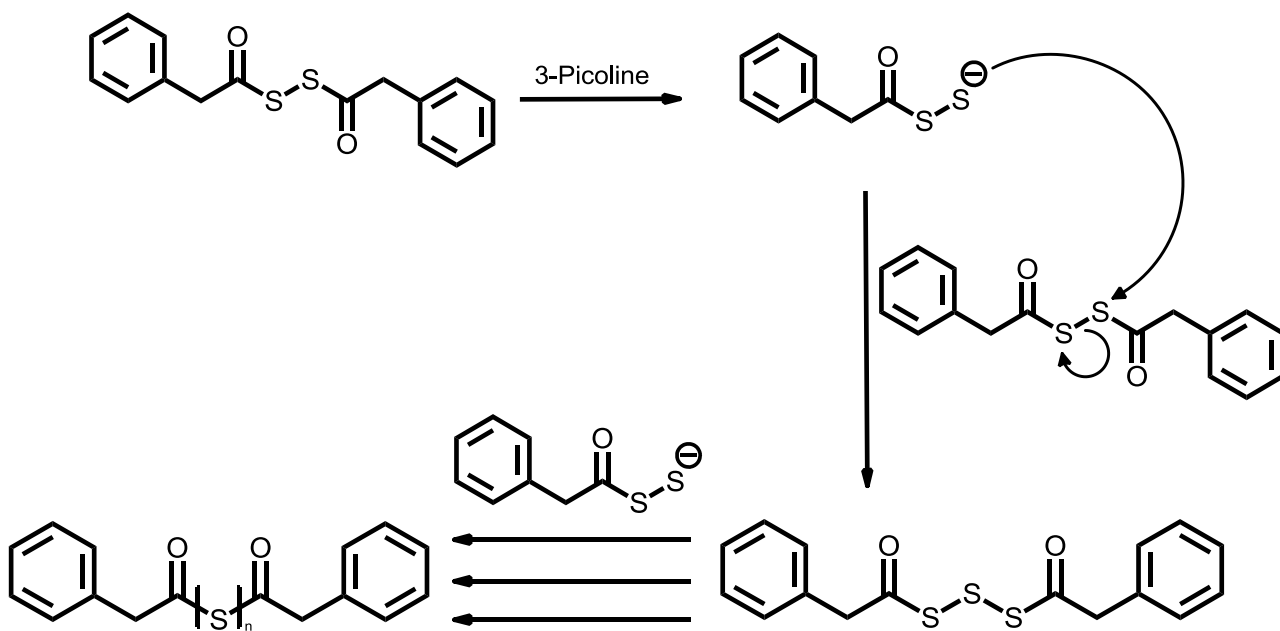
Scheme 11: Proposed general mechanism for the formation of acylpolysulfides during ageing of PADS in solutions of 3-picoline in acetonitrile.

3.2 Dependence of PADS Decomposition on 3-Picoline Concentration

It has been proposed in the literature that the enhanced rate of decomposition of PADS in solutions of 3-picoline is due to an increase in the dielectric of the solvent when 3-picoline is added[108]. In order to investigate this, a solution of PADS (3.3 mM) was made up in 10% v/v dimethyl sulfoxide in acetonitrile. This solvent was chosen due to its extremely high dielectric constant and low nucleophilicity and basicity. HPLC analysis showed that PADS is stable in this solution for at least one week. Due to this observation, it is unlikely that the effect of 3-picoline is due solely to a dielectric effect.

The effect of the concentration of 3-picoline on the rate of decomposition of PADS was investigated by HPLC in which PADS (3.3 mM) in acetonitrile was made up in solutions of varying concentrations of 3-picoline (Figure 23). It was found that the pseudo first–order rate constants for the degradation of PADS were linearly related to 3-picoline concentration meaning that the reaction is first order with respect to picoline with an overall second-order rate constant of 1.29×10^{-5} M^{-1}. The rate equation for the degradation of PADS can be written as:

$$Rate = k_{deg}[PADS][Picoline]$$

The fact that the rate of the degradation is related to picoline concentration suggests a reaction pathway proceeding via a polar transition state. Further evidence of this can be seen in the literature in which it has been reported that PADS solutions made up in less polar solvents with high concentrations of base (e.g. 5 M 3-picoline in toluene) degrade at a much slower rate[96].

Pseudo First-Order Rate Constants (k_{obs} /s^{-1}) for Decomposition of PADS (3.3 mM) as a Function of 3-Picoline Concentration (M) in Acetonitrile at 25°C

$$k_{obs} = (1.29 \times 10^{-05}) \times [\text{Picoline}]$$

$$R^2 = 7.64\text{E-}01$$
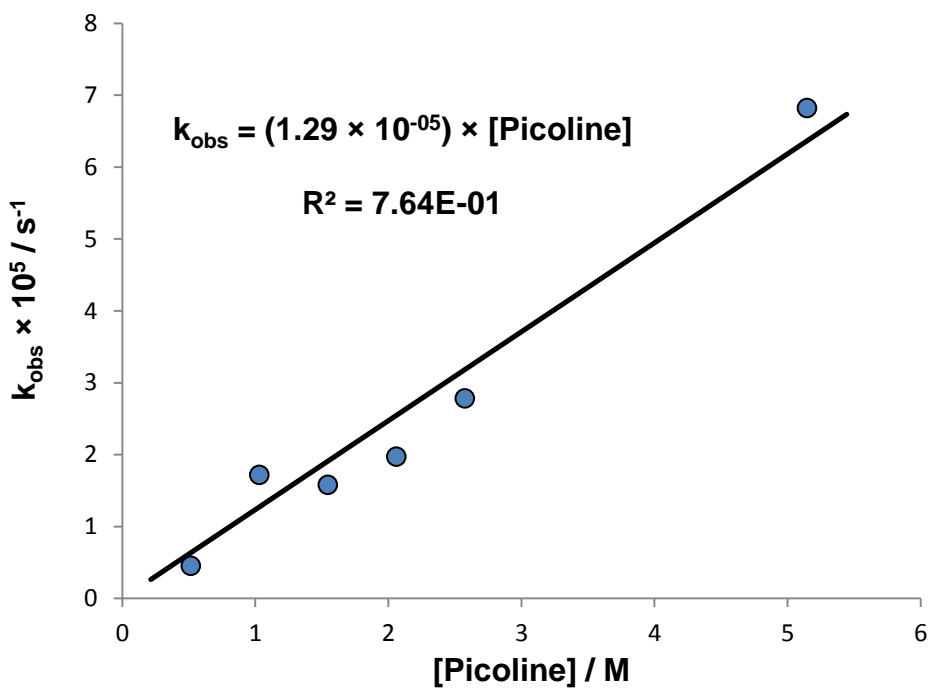
Figure 23: Pseudo first-order rate constants of degradation of PADS (3.3mM) in various concentrations of 3-picoline in acetonitrile monitored by HPLC at 25°C.

3.3 Effect of Pyridine pK_a on the Rate of Degradation

Since the rate of degradation of PADS is related to the concentration of 3-picoline it is important to assess the role of 3-picoline in the reaction. If degradation is due to a solvent effect then altering the pK_a of the pyridine used as a catalyst in this process should have a random effect, not proportional to the substituent since solvent dielectric constant is not related to the acidity or basicity of the solvent molecules. PADS (0.2 M) was made up in solutions of several different pyridines (2.5M) in ACN-d_3 and the pseudo first-order rate constants for the degradation of PADS were determined by ^{1}H NMR and the corresponding second order rate constants plotted as a function of the pK_a of the base (Fig. 24).
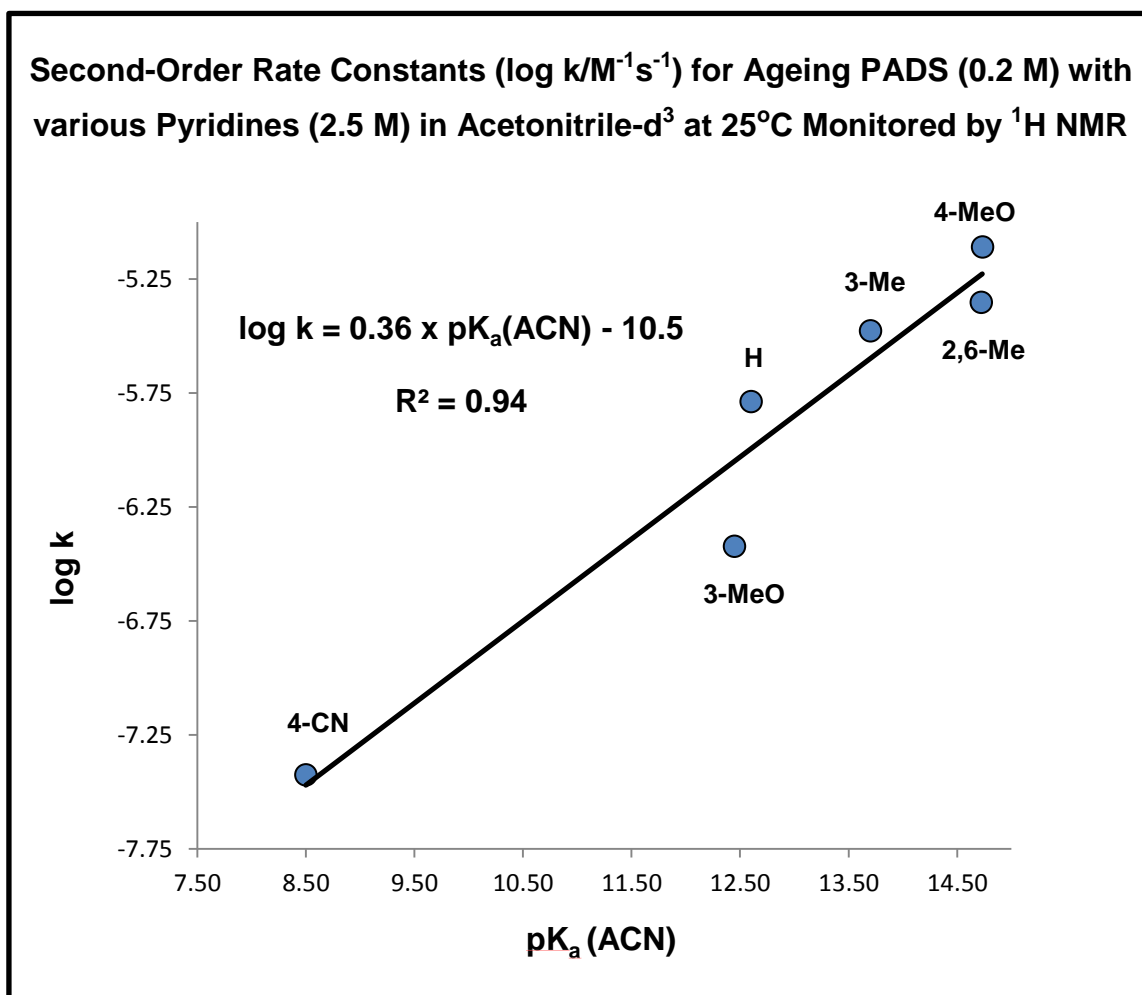
Figure 24: Brønsted plot of log of the second-order rate constants for the degradation of PADS (0.2 M) with various pyridines (2.5 M) determined by ^{1}H NMR in acetonitrile-d_3 at 25°C

Inspection of Fig. 24 shows that PADS degradation is linearly related to the pK_a of the pyridine catalyst used and the rate constants increase with increasing basicity of the catalyst. This makes it unlikely that the role of 3-picoline in the ageing process is entirely a solvent effect. Instead, these data suggest that these pyridine catalysts act as either a base of a nucleophile (Scheme 12). The slope of the Brønsted plot gives a β_{Nuc} value of 0.37 which suggests only partial build-up of positive charge on the pyridine nitrogen in the transition state of the reaction if it is acting as a nucleophile. However, since pK_a can be indicative of both the relative nucleophilicity and basicity, it is not possible to ascertain the exact role of 3-picoline directly from these data.
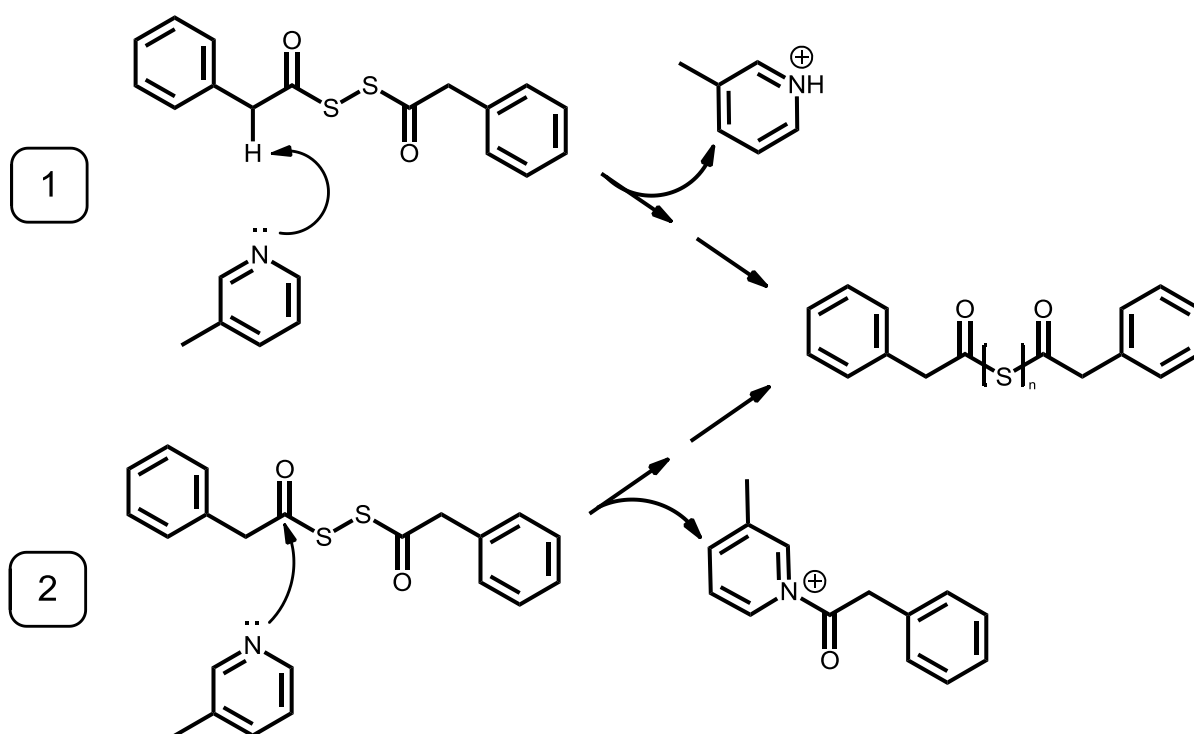
Scheme 12: Possible mechanisms of attack of 3-picoline on PADS as (1) a base and (2) a nucleophile.

3.4 Nucleophilic or General Base Catalysis by 3-Picoline

As mentioned previously, the rate of decomposition of PADS is linearly related to the pK_a of the pyridine catalyst used. If catalysis involved nucleophilic attack on PADS by 3-picoline then the first step in the mechanism proceeds as illustrated in Scheme 13, producing the acylpyridinium cation as one of the major products.
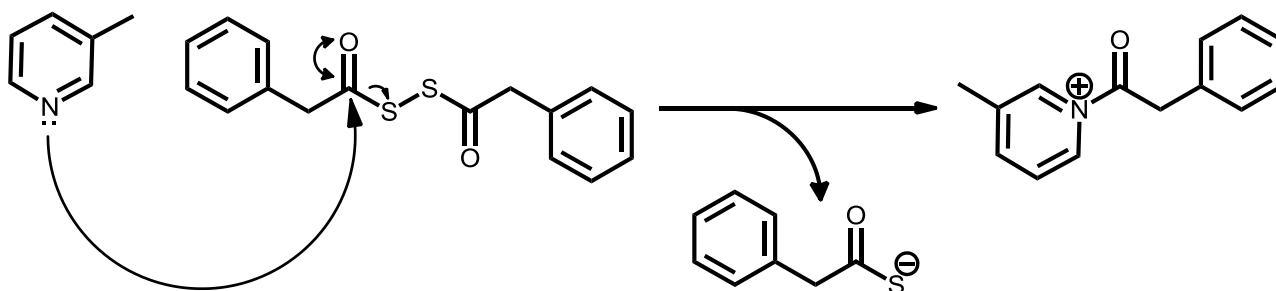
Scheme 13: Nucleophilic attack by 3-picoline on PADS

Mass spectral analysis of multiple solutions of aged PADS was not able to detect the presence of the acylpyridinium ion. An attempt was therefore made to synthesise this species by reacting 3-picoline with phenylacetyl chloride since the carbonyl carbon is extremely electrophilic. However, rather than acting as a nucleophile the 3-picoline acted as a base, removing the proton alpha to the carbonyl group. This generated the ketene (Scheme 13) and multiple cyclo-addition products (Figure 25). This result suggests that 3-picoline may not act as a nucleophile in the pyridine catalysed decomposition of PADS and instead acts as a base.

Further evidence for picoline acting as a base and not a nucleophile can be seen when using non-nucleophilic pyridines as the catalyst. Using either two equivalents of triethylamine or di-isopropyl ethyl amine (Hünug's Base) gives complete degradation of PADS within 5 minutes. Similarly, using 2,6-lutidine, a sterically hindered pyridine, causes degradation at a rate which fits the linear correlation of the Brønsted plot (Figure 24). If the reaction mechanism involved nucleophilic catalysis then using these sterically hindered bases would be expected to hinder catalysis.
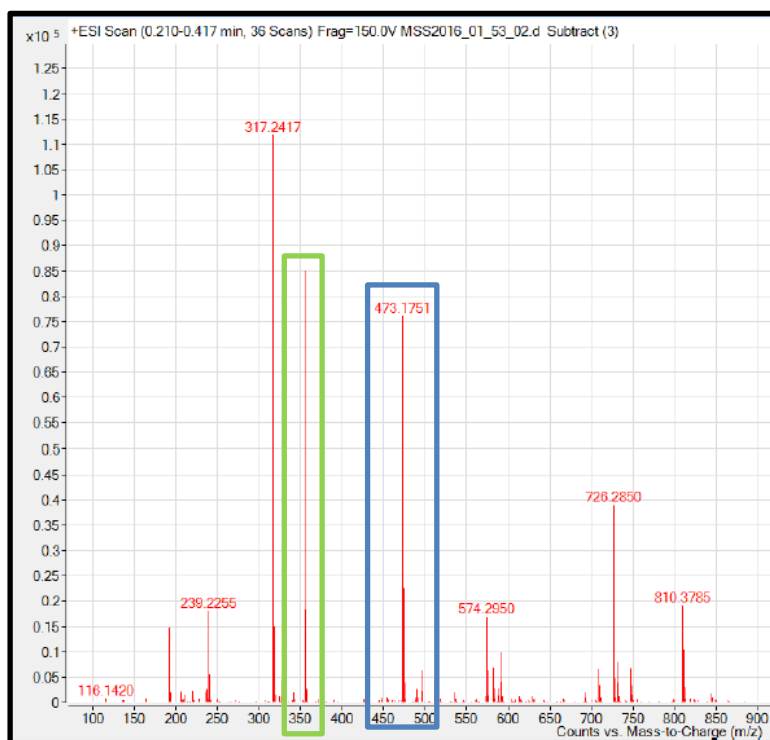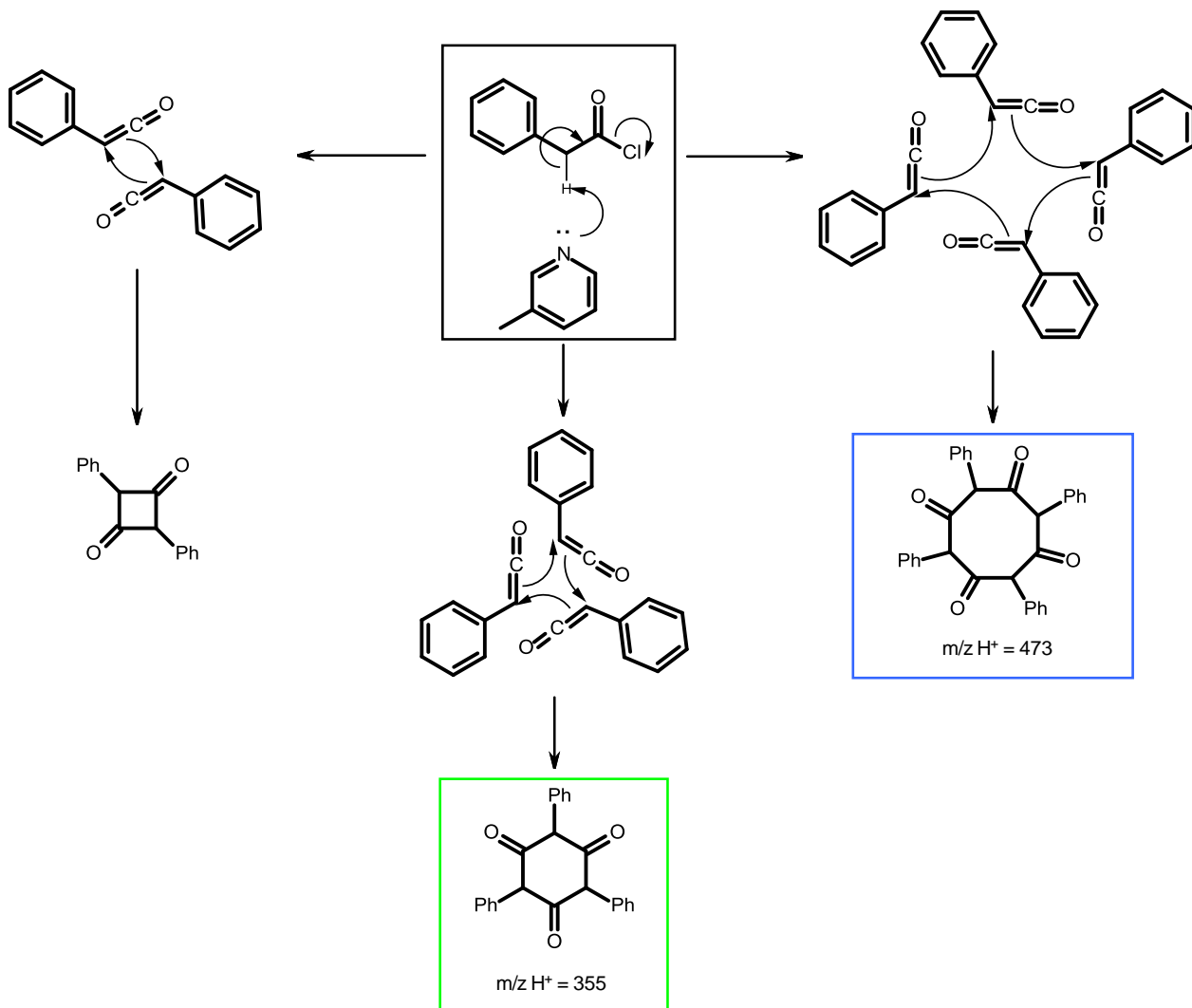
Figure 25: Reaction of 3-picoline with phenylacetyl chloride and subsequent polymerisation of the ketene product.

3.5 Possible Mechanisms Proceeding With 3-Picoline Acting as a Base

The experimental evidence so far suggests that nucleophilic attack by picoline during PADS degradation does not occur. Therefore it is likely that picoline acts as a base in this process, removing the proton adjacent to the carbonyl group in PADS (Scheme 12). This proposal is supported by the reaction of 3-picoline with phenylacetyl chloride (Figure 25). Electron withdrawing substituents in the aromatic ring of PADS increase the rate of degradation. This is expected if these substituents increase the acidity of the PADS CH_2 hydrogens (figure 26). These substituents would have little effect on the electrophilicity of the carbonyl carbon and therefore any reaction proceeding via a nucleophilic pathway would be little affected by this.
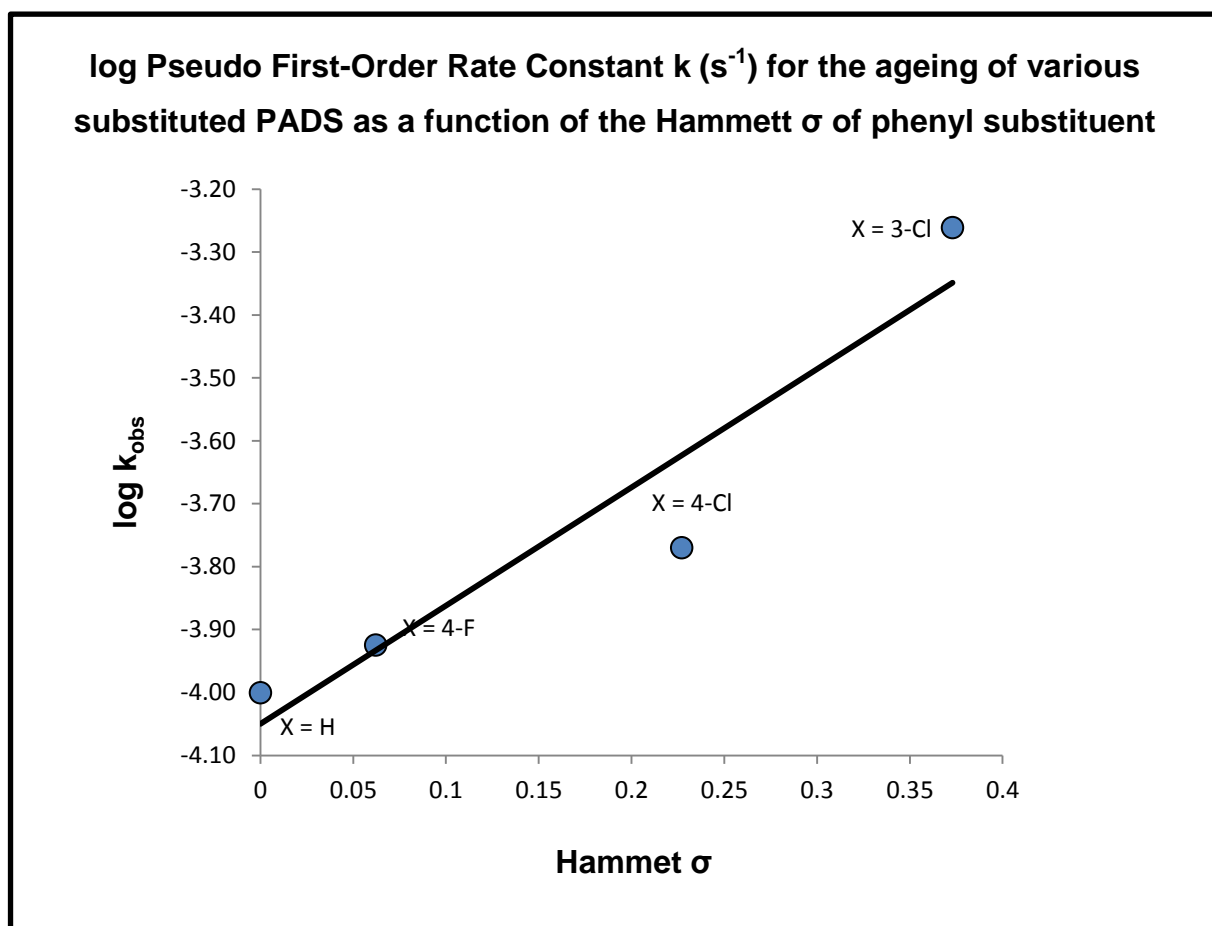
Figure 26: log of the pseudo first-order rate constants for the decomposition of various substituted PADS analogues (3.3 mM) with 3-picoline (1 M) as a function of the Hammett σ value of the PADS phenyl substituent

There are two ways in which this base catalysis could proceed, both involving elimination mechanisms: an E2 mechanism in which the proton abstraction and C-S bond fission occur simultaneously, or an E1cB mechanism in which the proton is abstracted to yield an intermediate which degrades in the rate-limiting step (Scheme 14). In both cases, the suggested products of the degradation are the ketene (**2**) and the acyl disulfide anion (**1**).
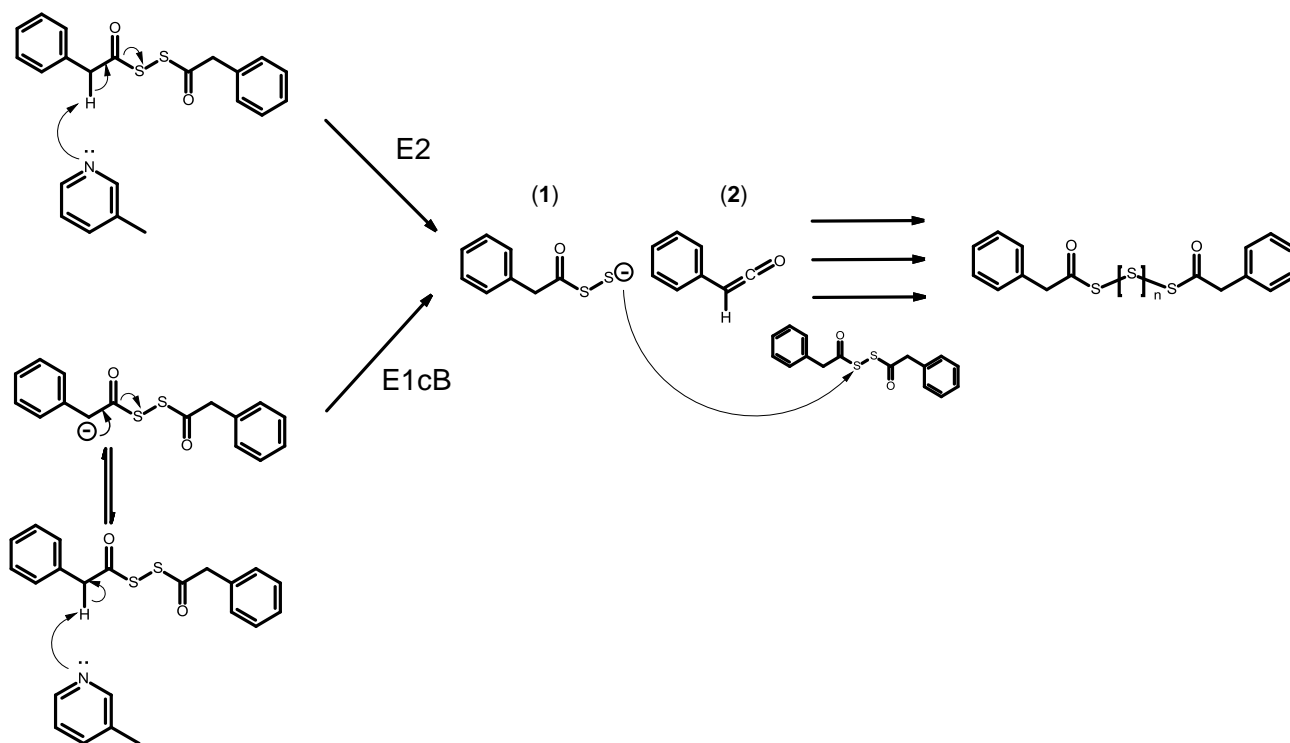
Scheme 14: Possible mechanisms for the base catalysed degradation of PADS

As mentioned previously, attempts to isolate the acyl polysulfide anionic species have been unsuccessful, however, HPLC analysis of aged PADS solutions suggests that they may exist in small quantities (Figure 18). Therefore, in order to distinguish between these two mechanisms and to justify the proposed mechanistic pathway other species generated in the mechanism needed to be identified or trapped.

3.6 Trapping the Carbanion Intermediate with D₂O Exchange

In order to distinguish between the E1cB and the E2 mechanisms of base catalysed decomposition (Scheme 14) the carbanion intermediate generated from proton abstraction needed to be detected by trapping experiments. This was done using a D_2O exchange experiment which was monitored by ^{1}H NMR. If the E1cB mechanism is dominant then a decrease in the CH_2 signal (singlet) of PADS should be observed along with the appearance of a CHD signal (triplet). This is because the carbanion formed during the E1cB mechanism can form a dissociative ion pair with the protonated pyridine. When this ion pair dissociates it is possible for the carbanion to form another ion pair with a D^+ source (in this case, the deuterated pyridinium) and an equilibrium between the D^+ source and deuterated PADS will be established according to the relative pK_as of the two species (Scheme 15). As the E_2 mechanism is a single-step process, no intermediate can be trapped if the reaction proceeds via this mechanism.
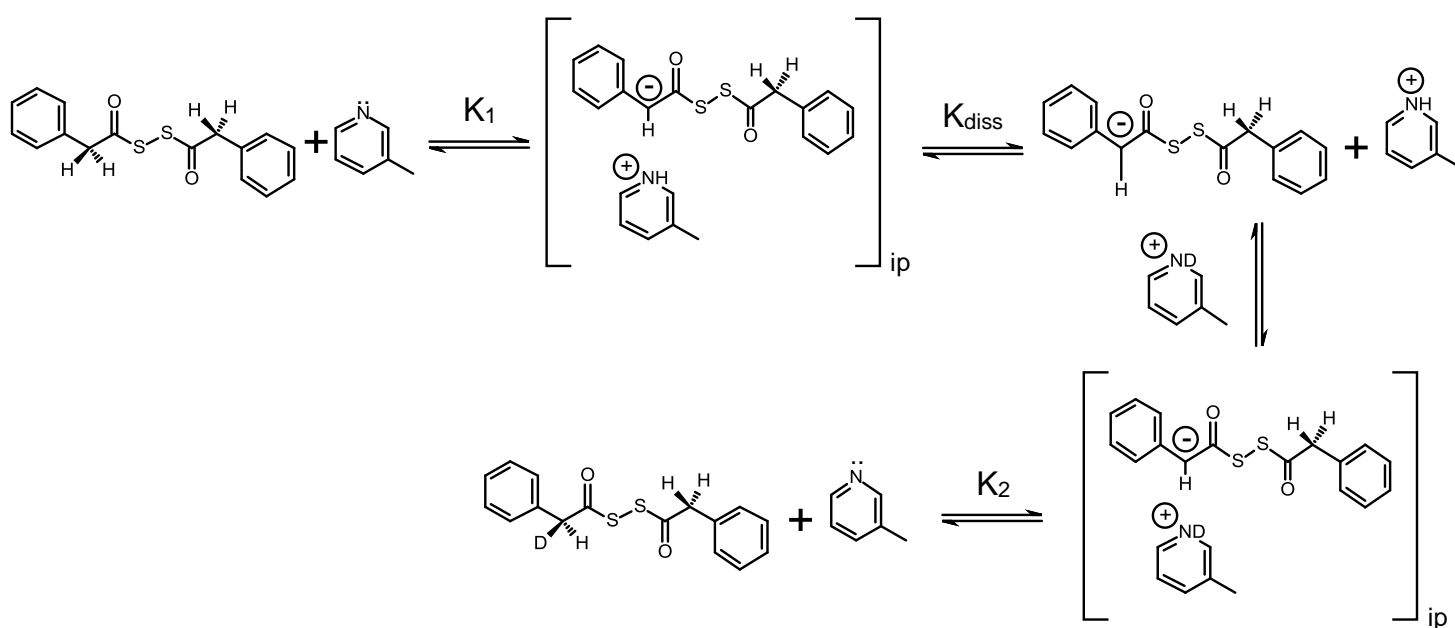
Scheme 15: Mechanism of deuterium exchange between PADS and D₂O catalysed by 3-picoline.

Inspection of the ^{1}H NMR showed that it was indeed possible to trap the carbanion using D_2O (Fig. 27) and this provided the possibility that PADS ageing is initiated by an E1cB mechanism and not an E2 mechanism. By measuring the rates of H/D exchange, pseudo first order rate constants were obtained.
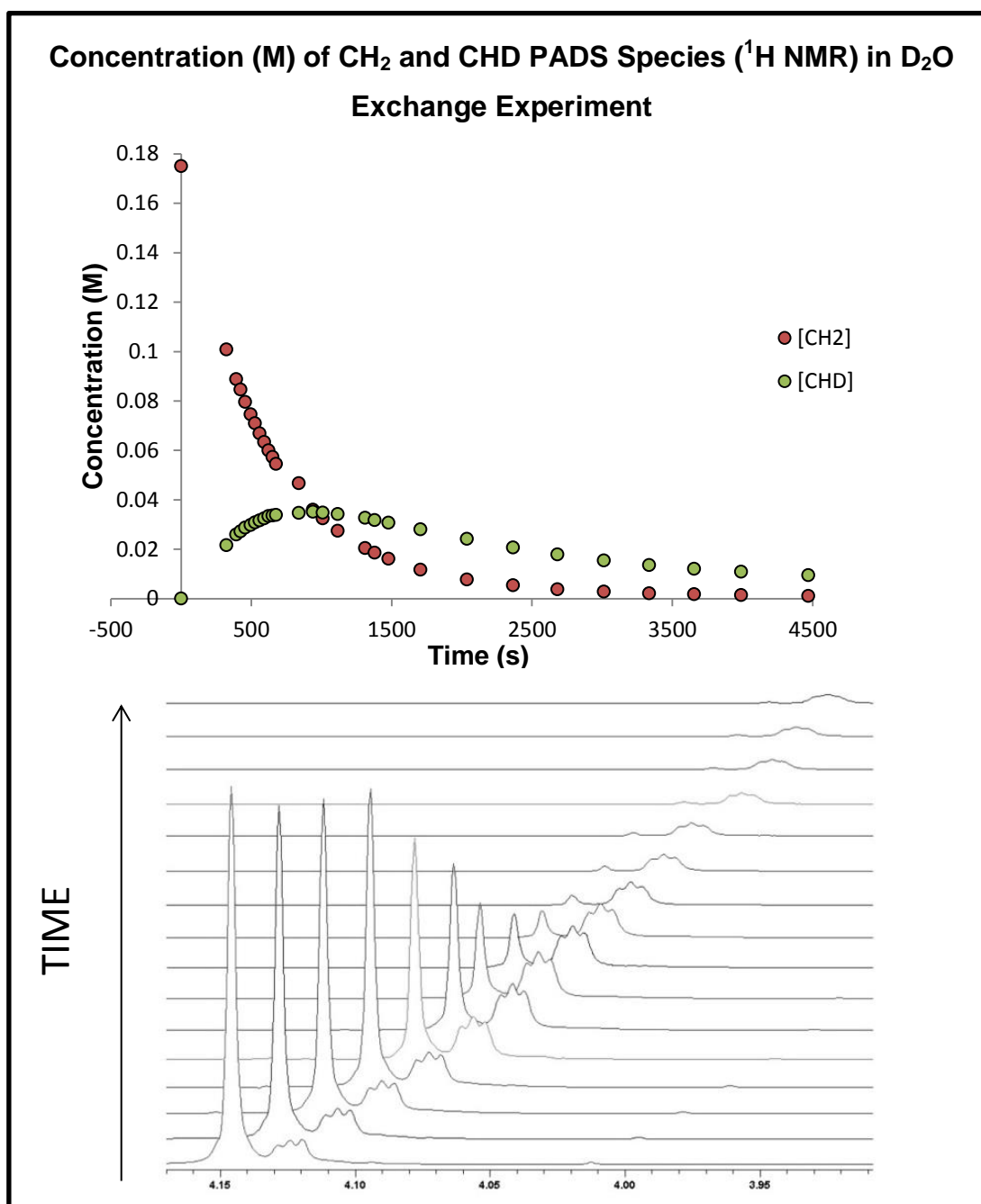
Figure 27: Concentration of PADS CH₂ and CHD as a function of time for 3-picoline catalysed PADS deuterium exchange.

R = Me or H
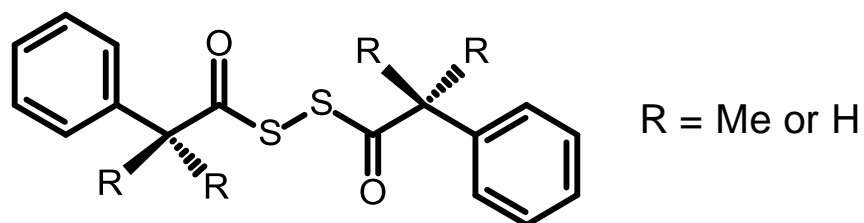
(3)

Further experiments demonstrated that these pseudo first-order rate constants for carbanion formation, like PADS decomposition, is linearly related to the concentration of 3-picoline and is therefore a second order process in which the rate is proportional to the concentration of PADS and of the base catalyst (Fig. 28). The corresponding second order rate constant for exchange is 5.69 x 10^{-3} $M^{-1}s^{-1}$ at 25°Cin 12% D_2O in acetonitrile-d_3.

Pseudo First-Order Rate Constants (k_{obs}/s^{-1}) for Deuterium Exchange as a function of 3-Picoline Concentration at 25°C in 12% D_2O in Acetonitrile-d_3

$k_{obs} = (5.69 \times 10^{-3}) \times$ [Picoline]

$R^2 = 0.96$
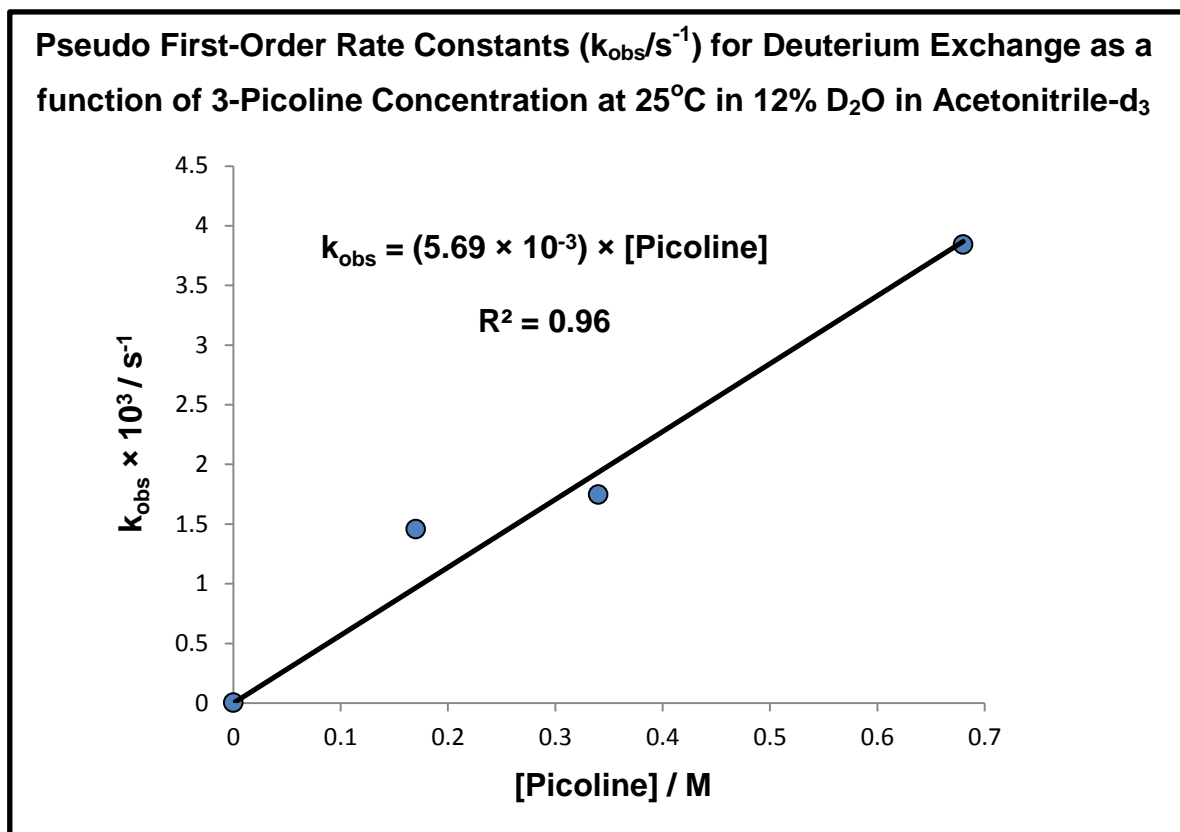
Figure 28: Pseudo first-order rate constants for deuterium exchange as a function of 3-picoline concentration determined by ^1H NMR at 25°C in 12% D_2O in acetonitrile-d_3

Analysis of the ^1H NMR spectra for the deuterium exchange experiment (Fig. 27) not only shows loss of the CH_2 signal but also the rise and subsequent loss of the CHD signal. In order for this carbanion formation to be relevant to PADS ageing it must be much faster than the ageing process. To ensure this is the case, a similar experiment was performed substuting D_2O for H_2O, under the same conditions as the deuterium exchange experiment. The ^1H NMR spectra showed that loss of the CH_2 signal still occurs due to decomposition and is around 500 times slower than the rate of exchange with pseudo first-order rate constants k_{obs} (D_2O) = 1.75×10^{-3} s^{-1} and k_{obs} (H_2O) = 6.30×10^{-6}. This difference in the observed pseudo first-order rate constants is adequate to assume that carbanion formation is relevant to the ageing process.

Finally in a separate experiment to establish the intermediate formation of a carbanion, an attempt was made to quench ageing PADS mixtures with methyl triflate which trapped the carbanion yielding a mixture of the varying degrees of α-methylated PADS species (**3**).

From the above data, it is possible to calculate the rate of decomposition of the carbanion intermediate if the pK_a of PADS were known. This is important information as for the mechanism to be classified as an E1cB mechanism and not a concerted E2 mechanism, the intermediate must have a reasonable lifetime (i.e. longer than the time taken for a C-H bond vibration but short enough to give the observed decomposition).
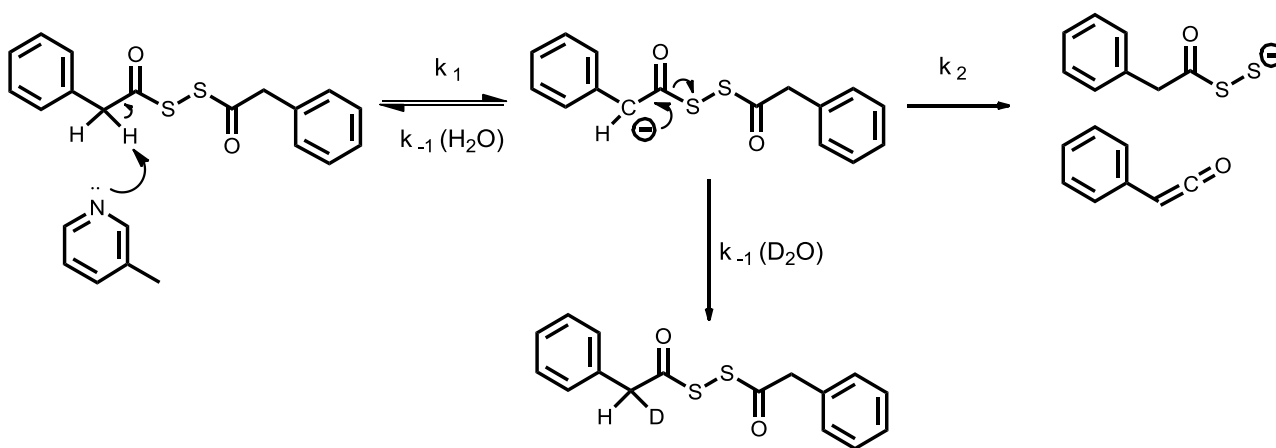
Scheme 16: E1cB initiated degradation of PADS

The proposed mechanism of PADS degradation by an E1cB mechanism is illustrated in Scheme 16. The rate of degradation of PADS determined from the experiment performed with 12% H_2O in acetonitrile—d3 is equal to the overall rate of degradation whereas the rate observed from the D_2O experiment is the rate of carbanion formation i.e:
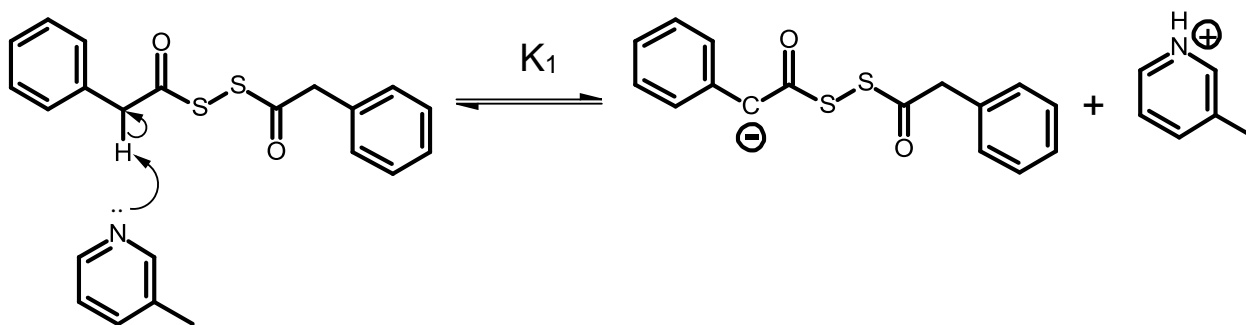
$$k_{obs}^{degrad.} = K_1 \times k_2$$

$$k_{obs}^{ex-} = k_1$$

Where $K_1 = k_1 / k_{-1}$

Therefore the rate of degradation of the carbanion can be calculated as shown below. k_{-1} is assumed to be diffusion controlled[111] and therefore $\approx 1 \times 10^{10} M^{-1}s^{-1}$. The rate of the diffusion controlled process may be expected to vary slightly as the viscosity of acetonitrile is lower than that of water however the value of 10^{10} can be used as a minimum value.

$$k_{obs}^{degrad.} = K_1 \times k_2 = 6.30 \times 10^{-6} \ s^{-1}$$

$$K_1 = k_{obs}^{ex} / k_{-1} = (5.69 \times 10^{-3})/(10^{10}) = 5.69 \times 10^{-13}$$

$$\text{Calculated } k_2 = k_{obs}^{degrad.} / K_1$$

$$= (6.30 \times 10^{-6})/(5.69 \times 10^{-13})$$

$$= 1.12 \times 10^7 \ s^{-1}$$

The value of $\sim 10^7 \ s^{-1}$ for the degradation of the carbanion is reasonable and shows the reversibility of the carbanion formation.

3.7 Calculation of the pKₐ of PADS

In order to test the validity of the suggested E1cB mechanism the deuterium exchange data can be used to estimate the pK_a of PADS under the solvent conditions of the experiment (i.e. acetonitrile-d_3 with ~12% D_2O).

As mentioned earlier, equilibrium between deuterated PADS and deuterated picoline is established according to the relative pK_as of the two species i.e:

$$K_1 = \frac{[\text{PADS}^-][\text{PicH}^+]}{[\text{PADS}][\text{Pic}]}$$

$$K_a^{\text{PicH+}} = \frac{[\text{Pic}][\text{H}^+]}{[\text{PicH}^+]} \qquad K_1 = \frac{[K_a^{\text{PADS}}]}{[K_a^{\text{PicH+}}]}$$

$$K_a^{\text{PADS}} = \frac{[\text{PADS}^-][\text{H}^+]}{[\text{PADS}]}$$

Since the pK_a of 3-picoline is known in pure acetonitrile[111] then the pK_a of PADS can be calculated as follows:

$$pK_a \text{ of 3-picoline ACN} = 13.7$$

$$K_a \text{ of 3-picoline in ACN} = 2 \times 10^{-14}$$

$$K_1 = 5.69 \times 10^{-13}$$

$$K_a^{\text{PADS}} = (K_a^{\text{PicH+}}) \times (K_1) = (2 \times 10^{-14}) \times (5.69 \times 10^{-13})$$

$$K_a^{\text{PADS}} = 1.138 \times 10^{-26}$$

$$\boldsymbol{pK_a^{\text{PADS}} = 25.9}$$

In order to see if this value is reasonable it is possible to compare it to the pK_a of similar compounds and assess how substituents affect the pK_a of these derivatives. The pK_a values of several esters are listed in Table 1.
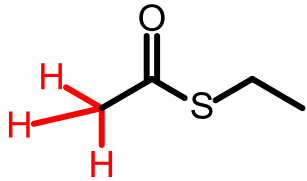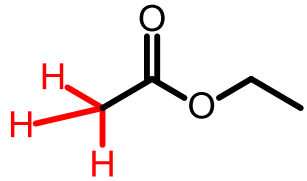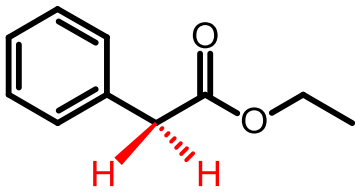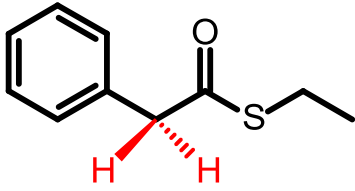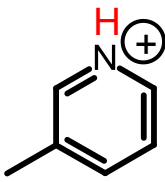
Compound	pK$_a$ in Solvent		
	Water	DMSO	ACN
1	21	24.9	37.8
2	25.6	29.5	
3	18.7	22.6	
4	14.1	18	30.9
5	5.7	3.7	13.7

Table 1: Table of calculated and literature reported pK$_a$s of various ethyl esters in various solvents[111].

The black values are reported in the literature whilst the red values are estimated based on looking at the effects of structural changes in compounds of known pK$_a$. For example, changing the ester group (2) for a thioester group (1) decreases the pK$_a$ of the α-protons by 4.6 units, changing the solvent from water to DMSO increases the pK$_a$ of the ethylester (2) by 3.9 units and replacing one of the α-protons with a phenyl ring decreases the pK$_a$ of the remaining α-protons in the ethyl ester (3) by 6.9 units. Assuming that these changes are roughly uniform and can be applied to derivatives within the same series, the approximate pK$_a$ values of the phenyl substituted ethyl thioester (4) can be estimated (30.9). The chemical environment in which the α-protons in this molecule are situated

is very similar to the environment in which the α-protons in PADS are situated and therefore this can be considered a good comparison, since no data is available for the pK_a of acyldisulfides or peroxides.

The measured value of 25.9 for the pK_a of PADS is slightly lower than the calculated value for that of the thioester (8) in Table 1. This could be due to one of two or both of the following factors:

1. The measured value for PADS was measured in a solution containing ~12% D_2O. This would be expected to lower the pK_a by several units. There is little to no data on the pK_a in binary solvents of this type and due to the macro behaviour of solvent molecules it is not easy to predict what this change might be.

2. The model compound is a thioester whereas PADS is an acyl disulfide in which the adjacent sulfur and acyl group would be expected to be more electron withdrawing than the ethyl group in the model. This also lowers the pK_a.

In summary the calculated pK_a value for PADS as a carbon acid of ~26 is a reasonable value.

3.8 Deuterium Exchange with Phenyl Substituted PADS Species

Further evidence for a base-catalysed mechanism for the degradation of PADS can be seen when investigating the rate of degradation of phenyl substituted PADS species. Adding substituents to the phenyl rings of PADS should alter the pK_a of the methylene CH_2 protons whilst leaving the electrophilic carbonyl carbon largely unaffected. If the process is indeed base-catalysed then adding electron withdrawing groups to the phenyl ring of PADS should increase the rate of proton-transfer and degradation. To investigate this, various phenyl substituted PADS compounds were synthesised[112] and the rates of deuterium exchange and proton transfer were assessed under identical conditions as those used for PADS.

Pseudo First-Order Rate Constants (Log k_{obs}/s^{-1}) for H/D Exchange for Various Phenyl Substituted PADS as a Function of Hammett σ Value of PADS Substituent in 12% D_2O/acetonitrile

log k_{obs} = (2.06 × Hammett σ) - 2.72
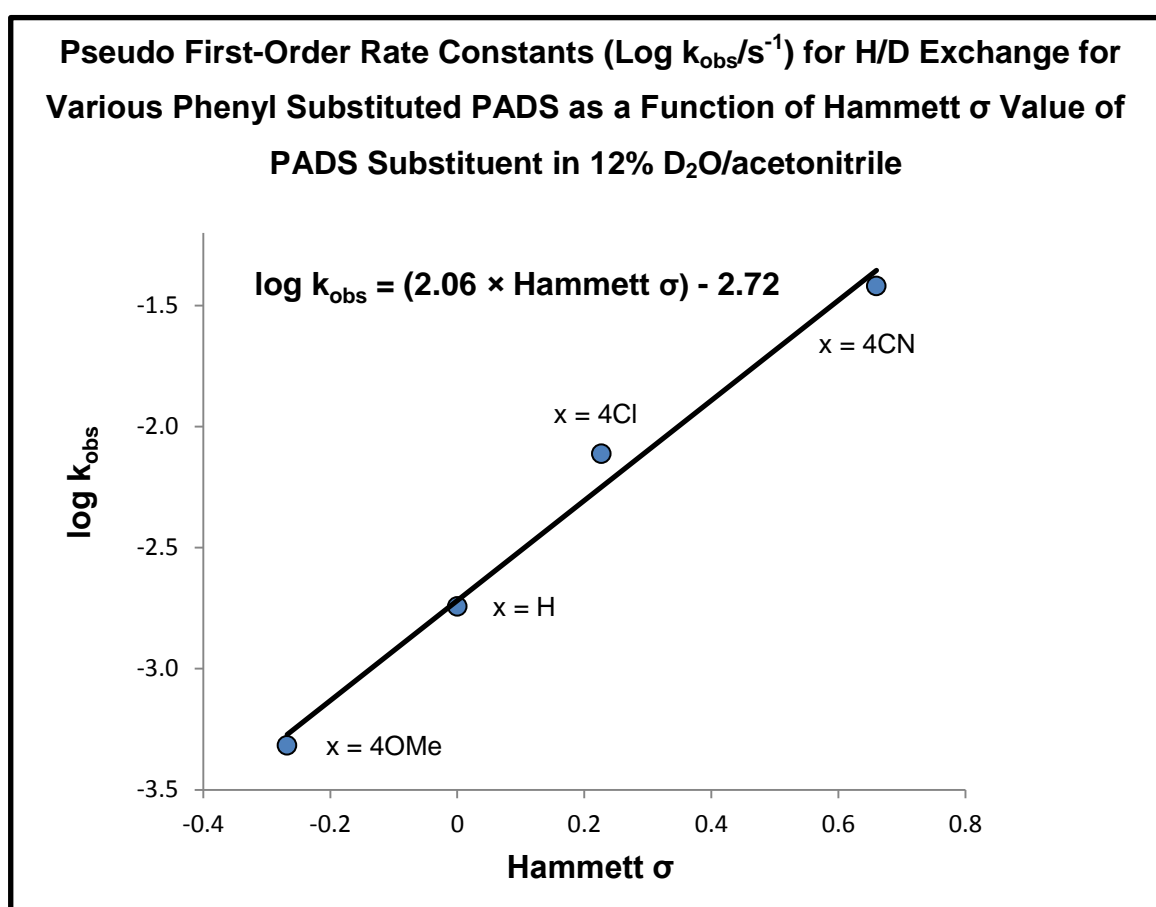
Figure 29: log of the pseudo first-order rate constants for H/D exchange of methylene protons in various substituted PADS analogs (0.17 M) with 3-Picoline (0.35 M) monitored by ^1H NMR at 25°C in deuterated acetonitrile with 12% D_2O

From these data, the pK_as of the various substituted PADS analogues can be calculated based onsimilar calculations to those used for PADS in section 3.7. These data can then be used to construct a Brønsted plot of degradation of substituted PADS analogues vs their $pK_{a\ calc}$.

Subst.	σ	$k_{exchange}$ (M^{-1}s^{-1})	log $k_{exchange}$	pK$_{a \ calc}$
MeO	-0.27	1.38×10^{-3}	-2.86	26.56
H	+0.00	5.16×10^{-3}	-2.29	25.99
4Cl	+0.23	2.20×10^{-2}	-1.66	25.36
4CN	+0.66	1.09×10^{-1}	-1.42	24.66

Table 2: Table of the second-order H/D exchange rate constants determined by ^{1}H NMR at 25°C in 12% D$_2$O in acetonitrile-d$_3$ and calculated pK$_a$ of several substituted PADS analogues in 12% D$_2$O in Acetonitrile-d$_3$.

Brønsted Plot of Degradation of Substituted PADS Analogues as a Function of pK$_{a \ calc}$ in 12% D$_2$O in Acetonitrile-d$_3$

$$\log k_{obs} = (-0.49 \times pK_{a \ calc.}) + 7.75$$
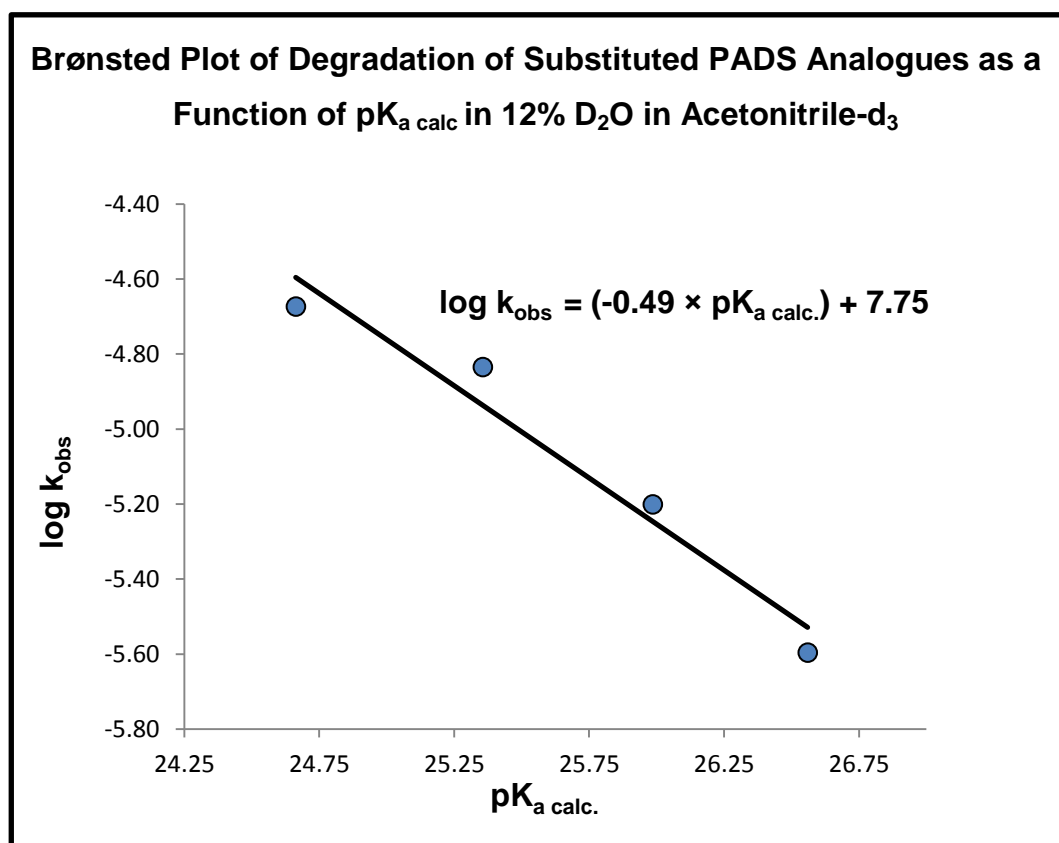
Figure 30: Brønsted plot showing the log of the observed pseudo first-order rate constants of the degradation of substituted PADS analogues (0.17 M) as a function of pK$_{a \ calc}$ in 12% D$_2$O in Acetonitrile-d$_3$ using 3-Picoline (0.35 M) as the base. Pseaudo first-order rate constants determined by ^{31}P NMR

The inverse relationship between pK$_a$ and the rate of degradation seen in Fig 30 is indicative of negative charge build-up on the methylene CH$_2$ of PADS as would be the case with base-catalysed carbanion formation. This further supports the idea that the degradation of PADS proceeds via an E1cB mechanism.

3.9 Ageing PADS Analogues without Dissociable Protons

Experimental evidence suggests that the ageing of PADS is initiated via an E1cB mechanism in which the α-protons of the PADS molecule are removed by the base catalyst (Scheme 16).

In order to confirm this and to assess whether an alternative mechanism can occur, PADS analogues with no dissociable α-protons were synthesised: 2,2,2′,2′-tetramethyl 2,2′phenylacetyl disulfide (**4**) and bis-benzoyl disulfide (**5**). Solutions of these were made in a solution of 3-picoline (5M) in acetonitrile. The concentration of these species was monitored over the course of 1 week.

Figure 31: Acyldisulfide compounds synthesised without dissociable protons

NMR and HPLC analysis showed that these molecules were stable in 5 M 3-picoline acetonitrile solution under the same conditions which caused the degradation of PADS. This therefore further suggests that the predominant mechanism of PADS degradation is initiated by picoline acting as a base.

3.10 Trapping the Ketene By-Product

The suggested E1cB mechanism of PADS degradation involves the asymmetrical degradation of the PADS molecule generating two major by-products: a disulfide anion and a ketene.
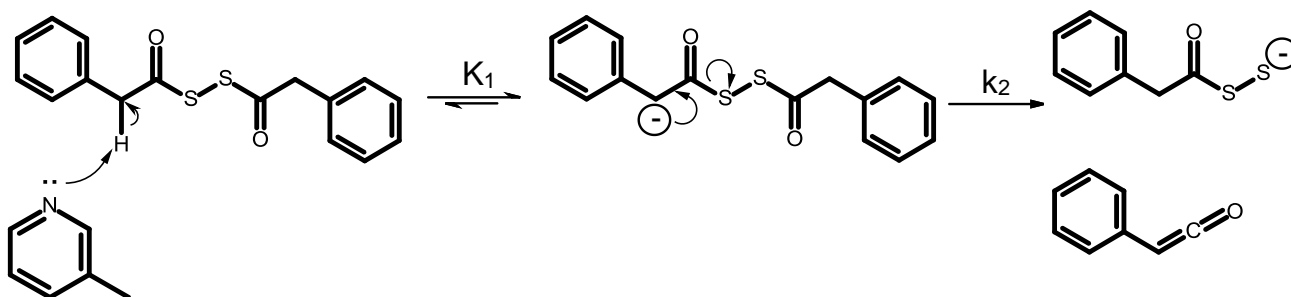
Scheme 17: E1cB initiated degradation of PADS

As previously mentioned, attempts to isolate the disulfide anions were unsuccessful, however the presence of acyl polysulfides and sulfur in aged PADS solutions suggests their existence. Therefore an attempt was made to detect the ketene by-product by trapping it via a [2+2]-cycloaddition reaction. This was done by synthesising an *o*-allyl substituted PADS molecule and ageing this in the usual way.
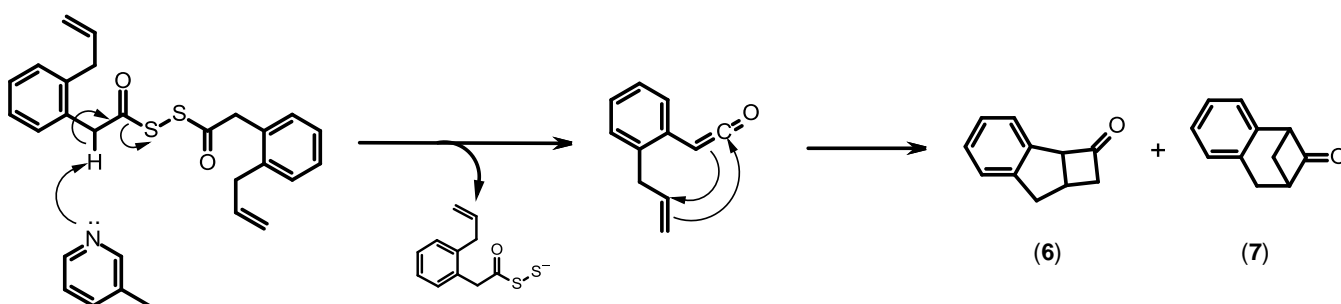
Scheme 18: Mechanism of [2+2]-intramolecular cycloaddition reaction trapping the ketene intermediate.

Initially, the desired cyclo-addition product was synthesised using 2-(*o*-allylphenyl)-acetylchloride using diethyl amine as the base catalyst in DCM. A pure sample of the cyclo-addition product (**6**) was isolated by preparative HPLC and analysed by ^{1}H NMR (figure 32) so that this could be used as a reference sample for analysis of crude ageing PADS mixtures.
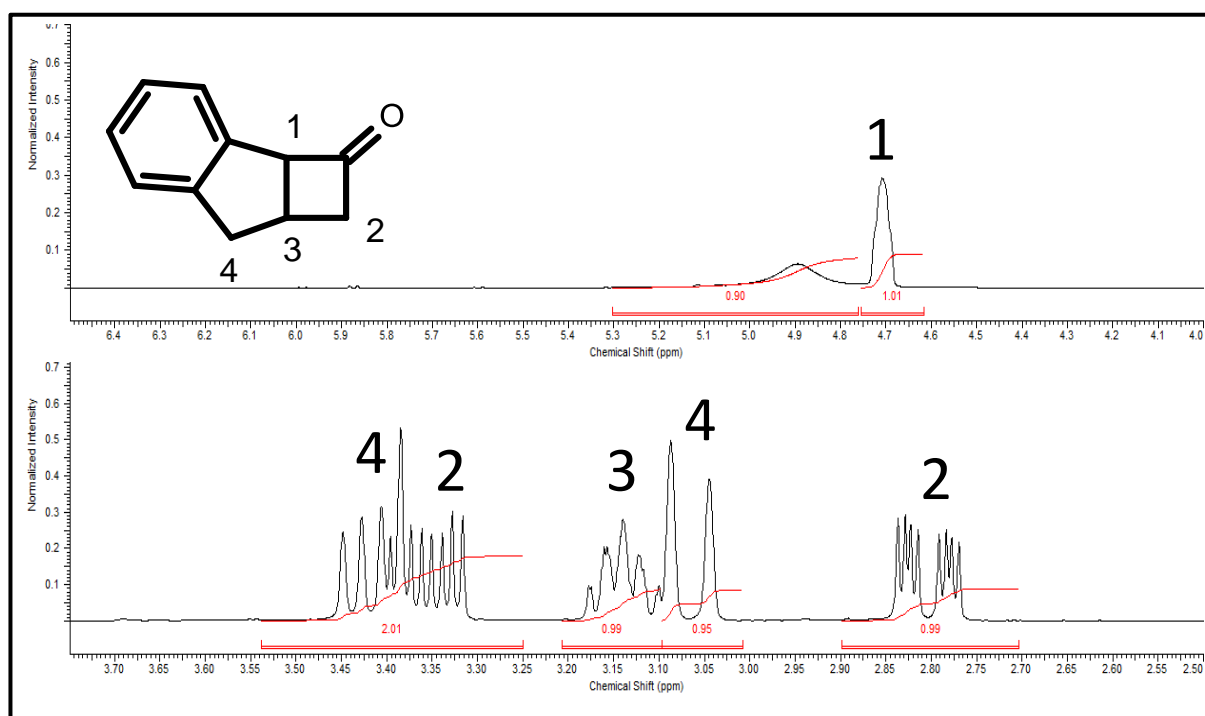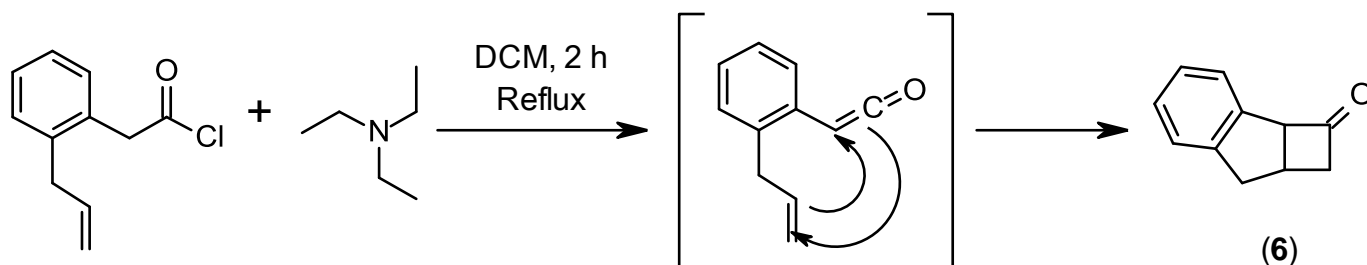
*Figure 32: Synthesis and ^{1}H NMR spectrum of cycloaddition product (**6**)*

^{1}H NMR Analysis of aged PADS solutions showed the presence of this cyclo-addition product (figs33 and 34) amongst other ageing products. Mass spectral analysis of these solutions also showed evidence of the cyclo-addition product and the expected mass spectra fragments. This further supports the proposed mechanism of PADS ageing.
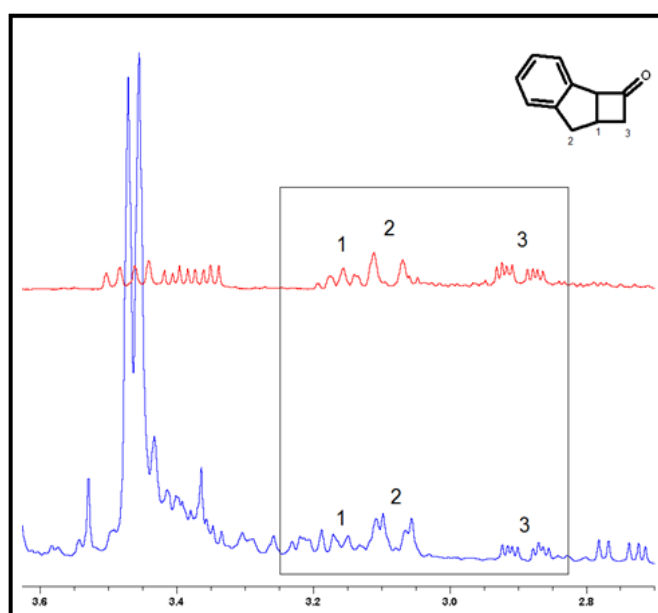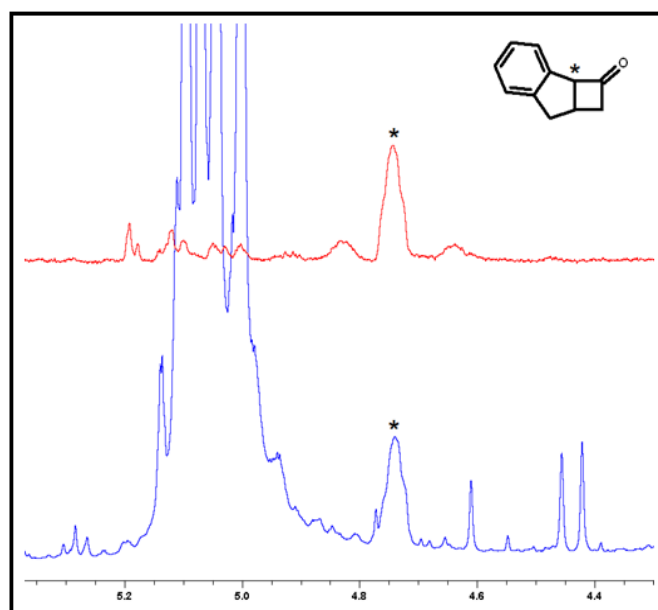
*Figure 33: ^{1}H NMR spectra of crude solutions of 2,2´-(allylphenyl)acetyl disulfide(bottom, blue) and pure, isolated cycloaddition product (**6**) (top, red)*
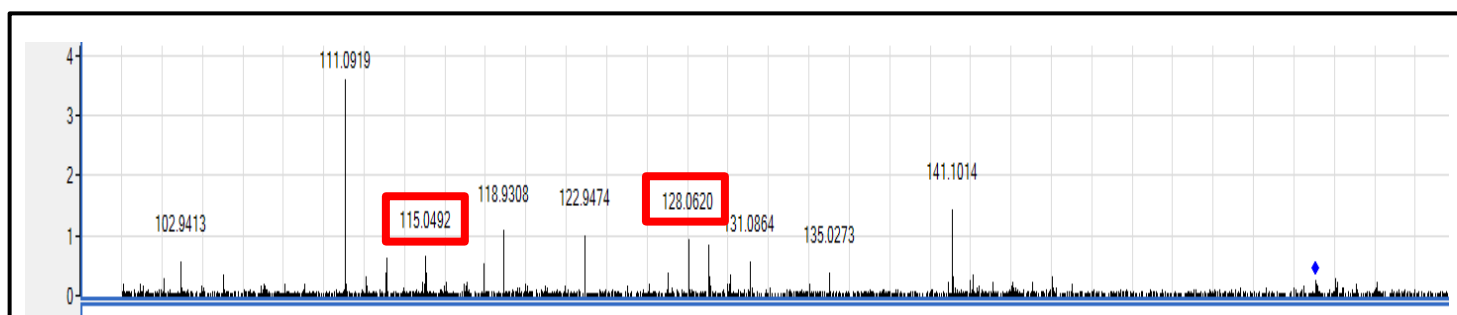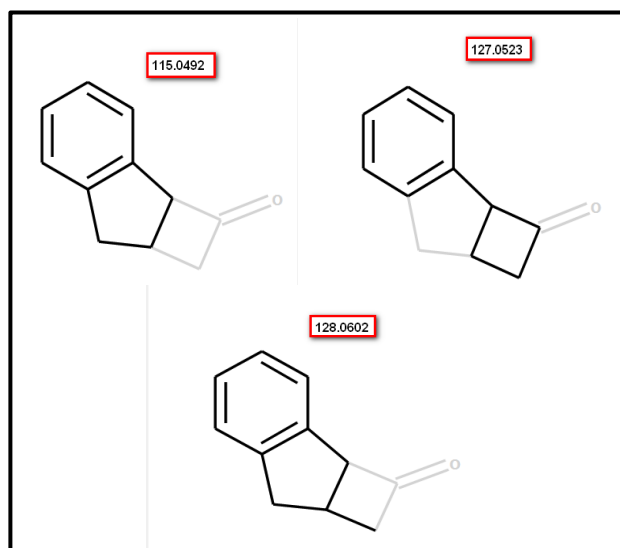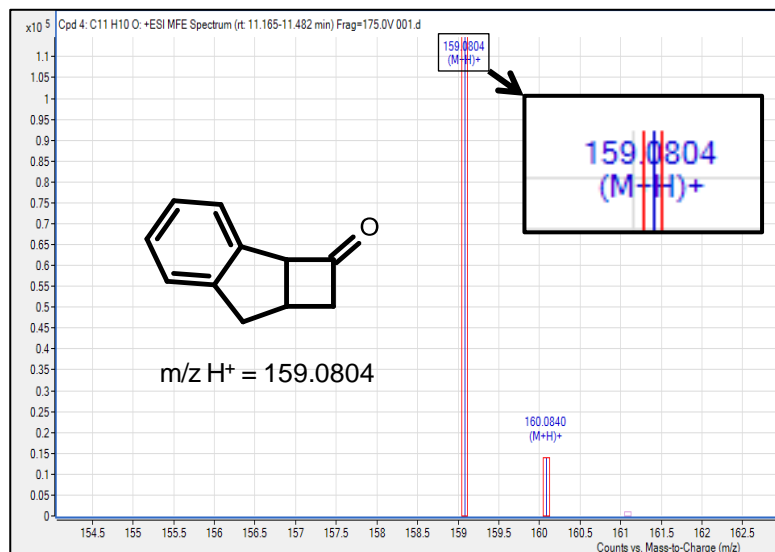
Figure 34: Mass spec. analysis of cyclo-addition product (**6**) degradation fragments.

3.11 Isolation of the Products of Ageing by Preparative HPLC

A sample of PADS (1 M, 1 ml) was made up in acetonitrile with 3-picoline (3 M) and was allowed to age for 48 h. After 48 h the solution was quenched with HCl (2 M, 10 ml) and the aqueous solution was extracted with DCM (30ml). The organic layer was retained and the solvent removed to give a solution of aged PADS in which the 3-picoline and any very polar degradation products had been removed (Fig. 35).
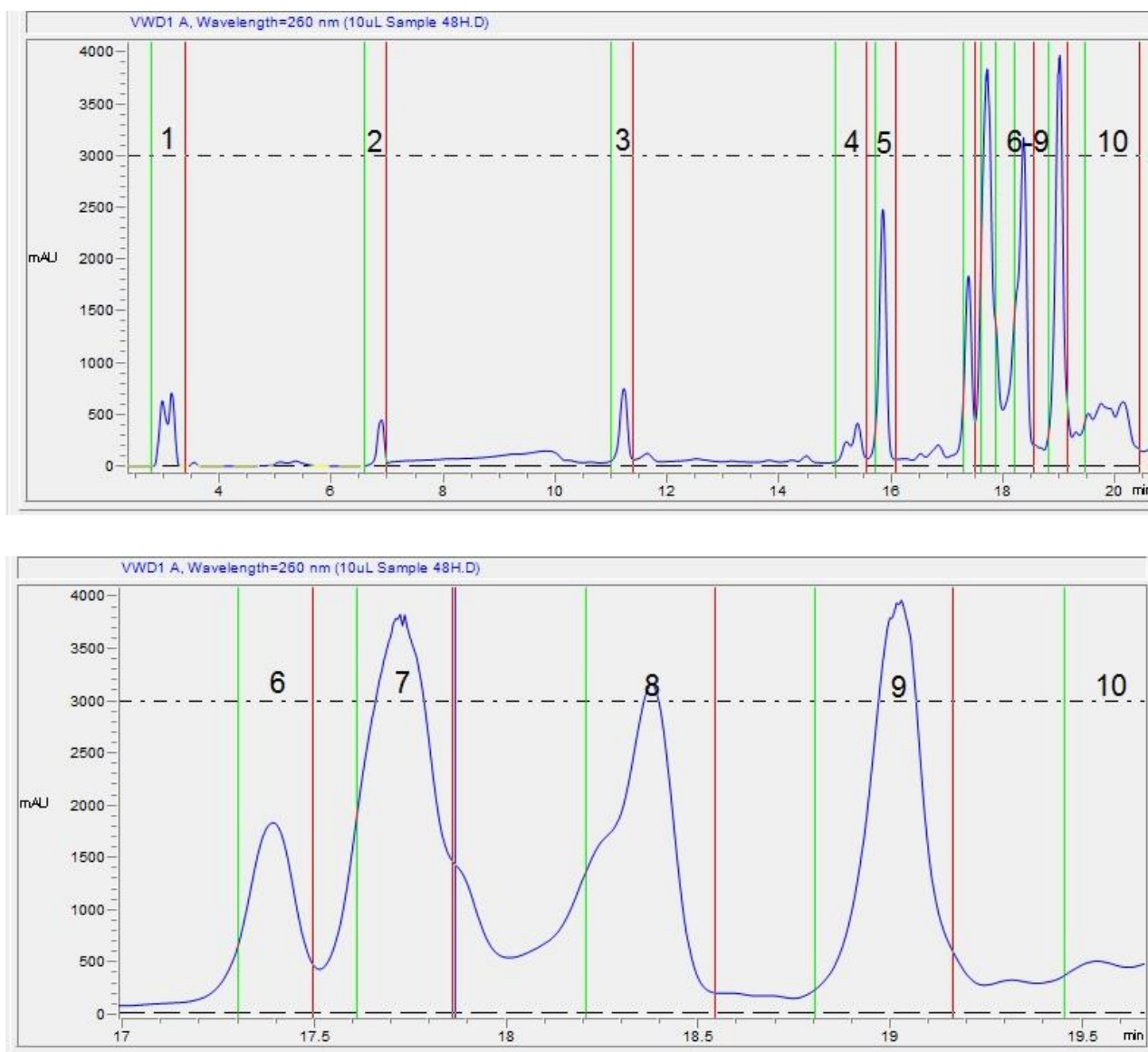
Figure 35: Above - HPLC chromatogram of a solution of PADS aged for 48 h and extracted with dilute HCl. Below: Expansion of fractions 6-10 from the chromatogram above

Using a HPLC equipped with a fraction collector the crude aged PADS mixture was separated according to the fractions illustrated in Fig. 35. Before further analysis each fraction was mixed with an excess of triphenyl phosphite and 3-picoline in order to assess whether these fractions were active sulfur transfer reagents or not. ^{31}P NMR analysis of these reaction mixtures found that triphenyl phosphorothioate ((PhO)$_3$PS) was only present in the reactions of fractions 5, 7, 8, 9 and 10. Therefore fractions 1, 2, 3, 4 and 6 were discarded and were not collected. (note: the concentration of the reactant in the fractions was not standardised at this point as the test merely aimed to qualitatively assess which fractions were active and so some fractions were more concentrated than others hence the large difference in the amount of conversion to product).
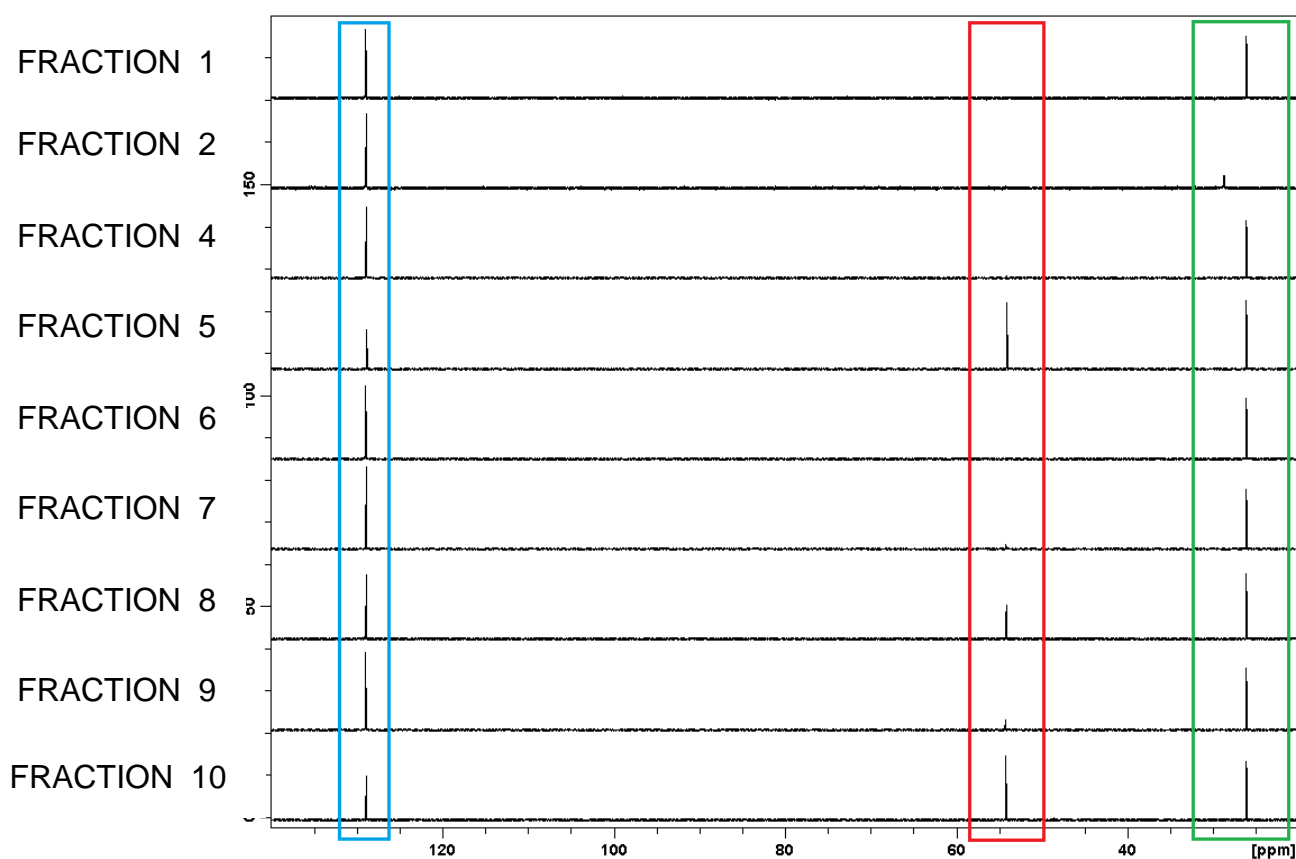
Figure 36: ^{31}P NMR analysis of reactions of HPLC fractions of aged PADS solution with triphenyl phosphite in the presence of 3-picoline. Blue- triphenyl phosphite, red- triphenyl phosphorothioate, green- triphenyl phosphine oxide (internal standard).

Fraction no.	Integration		% Reaction
	Phosphite	P=S	
1	1.53	0.00	0.00
2	1.50	0.00	0.00
4	1.43	0.00	0.00
5	1.06	0.60	**36.14**
6	1.54	0.00	0.00
7	1.57	0.07	**4.27**
8	1.05	0.68	**39.31**
9	1.46	0.25	**14.62**
10	0.95	0.99	**51.03**

Table 3: Table of data from sulfurisation reactions using fractions from aged PADS reaction.

It was difficult to obtain reliable mass spectral data for phenylacetyl polysulfides. This, coupled with the small amount of material collected during these separations, meant that no mass spectral data was generated for these fractions. However, previous LC-MS (Fig. 20-22) suggests that these fractions are polysulfides. Similarly, small amount of material collected meant that full 2D NMR analysis of these fractions was not possible. Careful analysis of the acyl CH_2 region of the ^{1}H NMR spectra (figure 37), however, show similar patterns to that of aged PADS i.e. the CH_2 signals move further and further upfield with the remainder of the spectrum remaining very similar to that of PADS itself (Fig. 19).
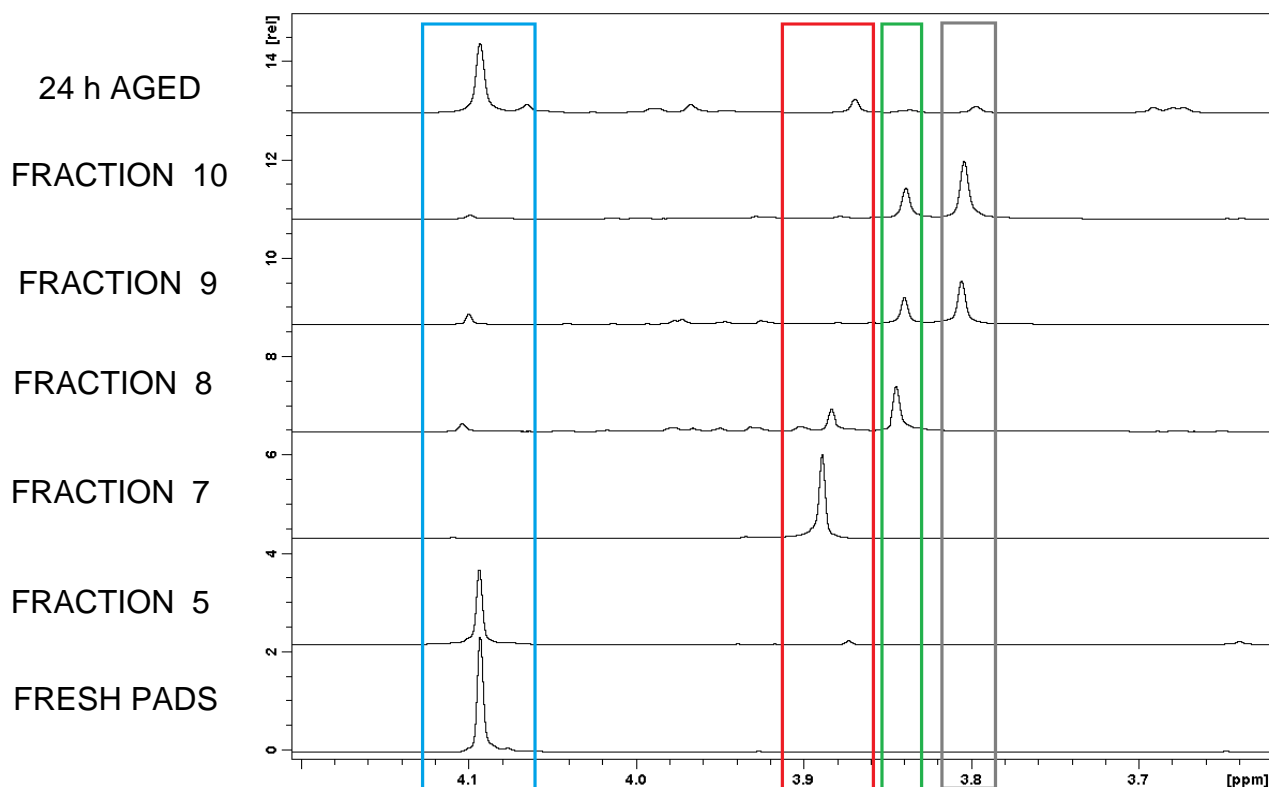
Figure 37:Acyl CH_2 region of various PADS species isolated from aged PADS mixtures by HPLC

Once the reactive fractions in the aged PADS mixtures were identified solutions of each (35 mM calculated by HPLC) were made up in acetonitrile-d_3. The relative rates of reaction of these compounds were then assessed using ^{31}P NMR by reaction with triphenyl phosphite as the limiting reagent. The experiment showed that each of these compounds show a pseudo first-order rate profile due to the excess of the sulfur transfer reagent and 3-picoline. The data also showed that each of these compounds generally showed a similar rate of reactivity towards triphenyl phosphite to PADS under the same conditions. Some fractions (fractions 5, 9 and 10) show a slight increase in rate over PADS but their concentrations in degraded PADS are not known, other than they must be less than that of PADS itself.

Species	k_{obs} (s^{-1})	Ratio k_{frac}/k_{PADS}
PADS	7.46×10^{-5}	1.00
Frac. 5	8.72×10^{-5}	1.17
Frac. 7	1.83×10^{-5}	0.25
Frac. 8	2.65×10^{-5}	0.36
Frac. 9	4.23×10^{-4}	5.67
Frac. 10	1.09×10^{-4}	1.46

Table 4: Table of pseudo first-order rate constants for the reaction of triphenyl phosphite (3.5mM) with various PADS species (35 mM) in the presence of 3-picoline (70 mM) determined by ^{31}P NMR at 25°C in acetonitrile-d_3.

3.12 Ageing PADS in the Presence of the Radical Trap Butylated Hydroxytoluene

The mechanism of ageing of PADS proposed here is initiated by base and proceeds via charged intermediates as suggested by all previous experimental data. There are several reports in the literature, however, of disproportionation of polysulfides via pathways involving polysulfide radicals[107]. In order to assess whether there is any radical involvement in the ageing of PADS two samples of PADS (3.3mM) were made up in solutions of 3-picoline (1 M) in acetonitrile. To one of the solutions, the radical trap butylated hydroxytoluene (BHT) was added (3.3 mM). The concentration of PADS in these solutions was monitored simultaneously by HPLC over 60 hours. If PADS degradation proceeds via a radical mechanism then the addition of BHT would be expected to slow or stop degradation by quenching the radical products of degradation and forming the stable BHT radical (Fig. 38).
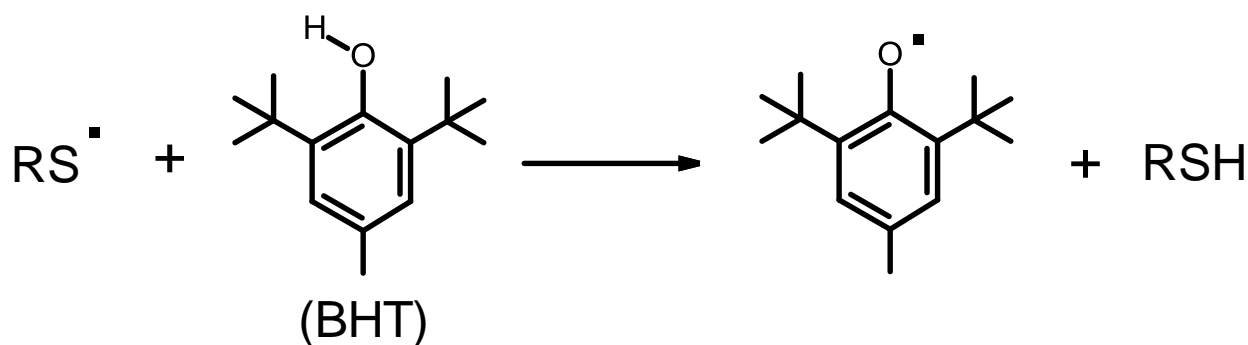
Figure 38: Mechanism of quenching radicals by butylated hydroxytoluene[113].

97

In[PADS] as a Function of Time for Degradation of PADS (3.3 mM) in 3-picoline (1 M) in acetonitrile with (right) and without (left) BHT (3.3 mM)

ln [PADS] = (-4.91 × 10^{-6}) × Time - 5.94

ln [PADS] = (-5.69 × 10^{-6}) × Time - 5.98
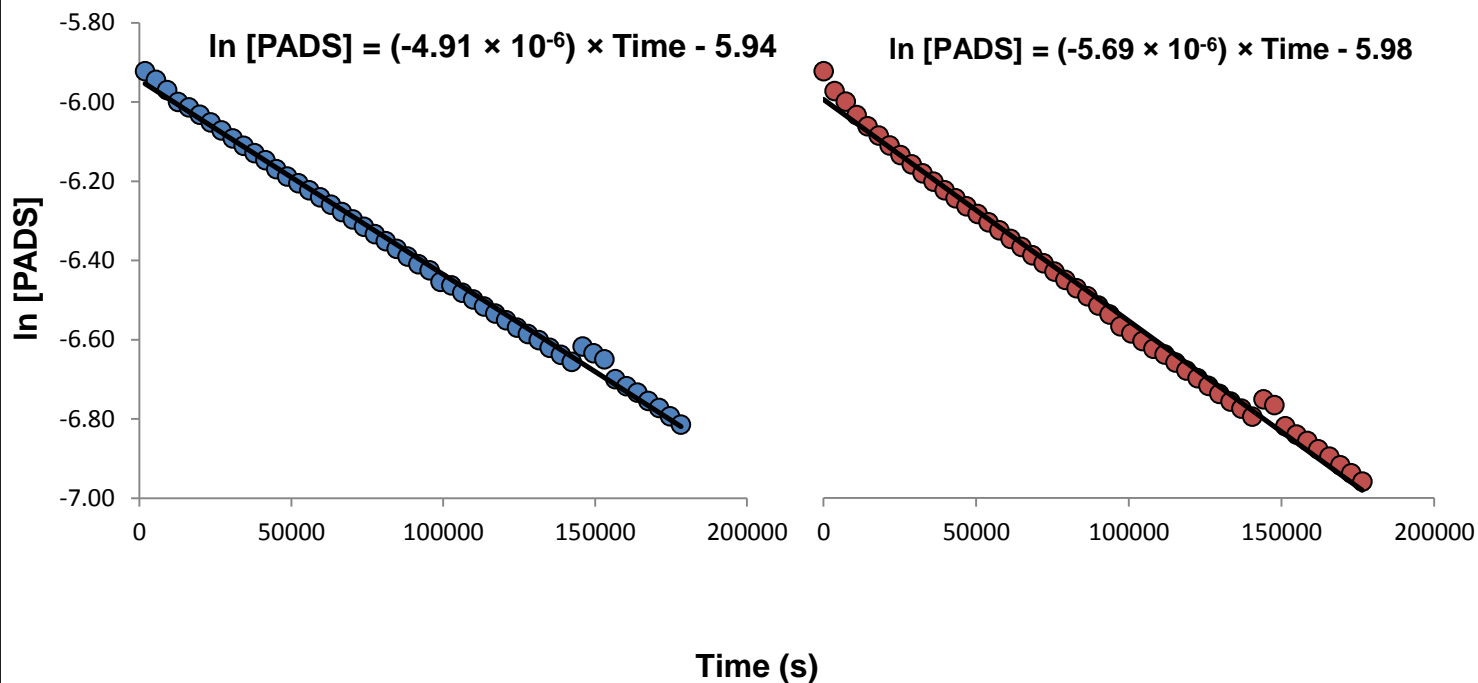
Concentration of BHT (mM)	k_{deg} (s^{-1})
0	5.69×10^{-6}
3.3	4.91×10^{-6}

Figure 39: ln Concentration of PADS as a function of time during ageing with 3-picoline (1 M) in acetonitrile-d₃ at 25°C both with (left) and without (right) BHT (3.3mM)

Figure 39 shows that the addition of BHT into the system made no significant difference to the rate of degradation of PADS. It can be assumed that there is no radical involvement in the ageing of PADS.

4. Results and Discussion: Sulfurisation

PADS is widely used as a sulfur transfer reagent. As seen in the previous chapter, before PADS is used industrially, it is 'aged' in basic acetonitrile to yield polysulfides[114]. These species are more active sulfur transfer reagents than PADS and therefore the rate of sulfurisation increases with ageing (figure 40). However, fresh solutions of PADS are still active sulfur transfer reagents.
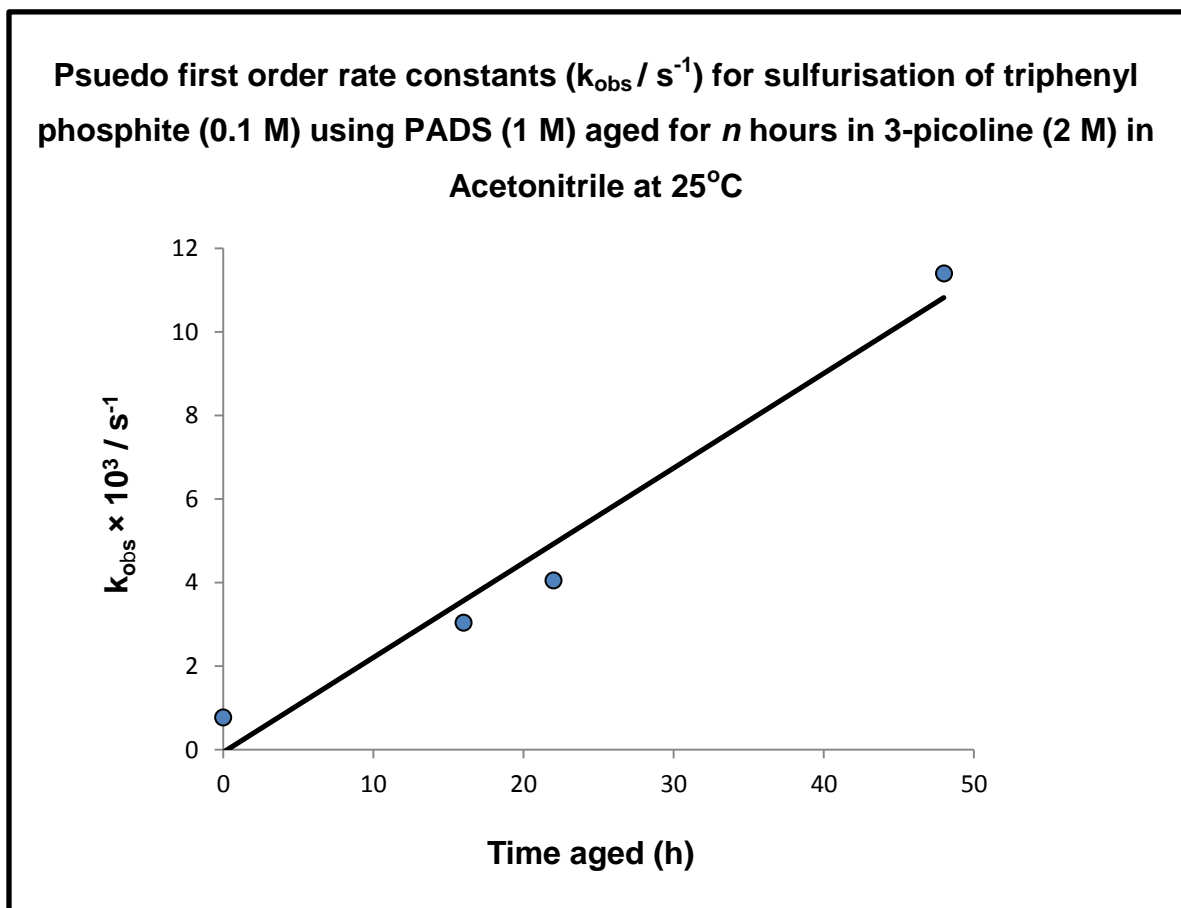
Figure 40: Pseudo first-order rate constants for sulfurisation of (PhO)$_3$P (0.1 M) using PADS (1 M) aged for n h in 3-picoline (5 M) in acetonitrile at 25°C determined by ^{31}P NMR

There has been speculation about the mechanism of sulfur transfer using PADS in the literature[108] but no detailed kinetic or mechanistic studies have been performed. The following chapter describes a study of the mechanism of sulfur transfer using both fresh and aged PADS and also describes the differences in their reaction mechanisms.

4.1 Fresh PADS

4.1.1 Determination of the Order of the Sulfurisation Reaction

The mechanism of sulfurisation of phosphites by PADS has been presumed in the literature to involve nucleophilic attack of the phosphite on PADS to form a phosphonium ion intermediate. This is followed by attack of a thiocarboxylate ion at the thioester to generate the thiophosphate product and the monosulfur acid anhydride species (Fig. 41)[108].
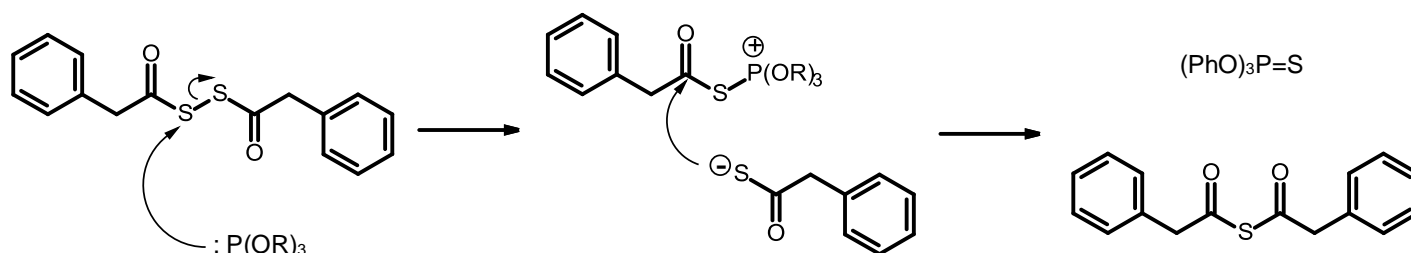
Figure 41: Literature[106] reported mechanism of sulfurisation of phosphites by PADS.

However, since the reaction is always performed in the presence of a large amount of organic base, it is important to assess whether or not the base plays a part in the mechanism or is simply present as a co-solvent. In order to assess this, the rates of sulfurisation reactions were determined with varying concentrations of 3-picoline (Fig. 42) under pseudo first-order conditions. It was found that the rate constants for pseudo first-order sulfurisation were linearly proportional to the concentration of 3-picoline. This suggests that the organic base is involved in the mechanism of the reaction and, more importantly, acts before or during the rate limiting step and therefore appears in the rate equation. As the relationship between the rate and the concentration of 3-picoline is linear (i.e. the rate increase is directly proportional to the 3-picoline concentration) the reaction must be first order with respect to picoline. It has been suggested in the literature[106] that this relationship is due to a solvent effect as a solution of 5 M 3-picoline is around 50 % v/v. The dielectric constant of 3-picoline is 10 and the dielectric constant of acetonitrile is 37.5[115]. Adding 3-picoline to acetonitrile would therefore lower the overall dielectric constant of the solution. As will be shown later in this section, sulfurisation reactions proceed faster in *higher* dielectric solutions and therefore the effect of 3-picoline is unlikely to be a solvent effect.

It is also worthy of note that the sulfurisation reactions detailed within this report are performed under pseudo first-order conditions i.e. all reagents except the phosphite are in excess. During the course of the reaction the concentration of the phosphite (the rate limiting reagent) decreases exponentially and so the reaction is also first order with respect to phosphite.

Pseudo first-order rate constants (k_{obs} / s^{-1}) for sulfurisation of P(OPh)$_3$ (0.1 M) Using Fresh PADS (1 M) with Varying Concentrations of 3-Picoline in Acetonitrile at 25°C

$$k_{obs} = (3.56 \times 10^{-4}) \times [\text{Picoline}]$$
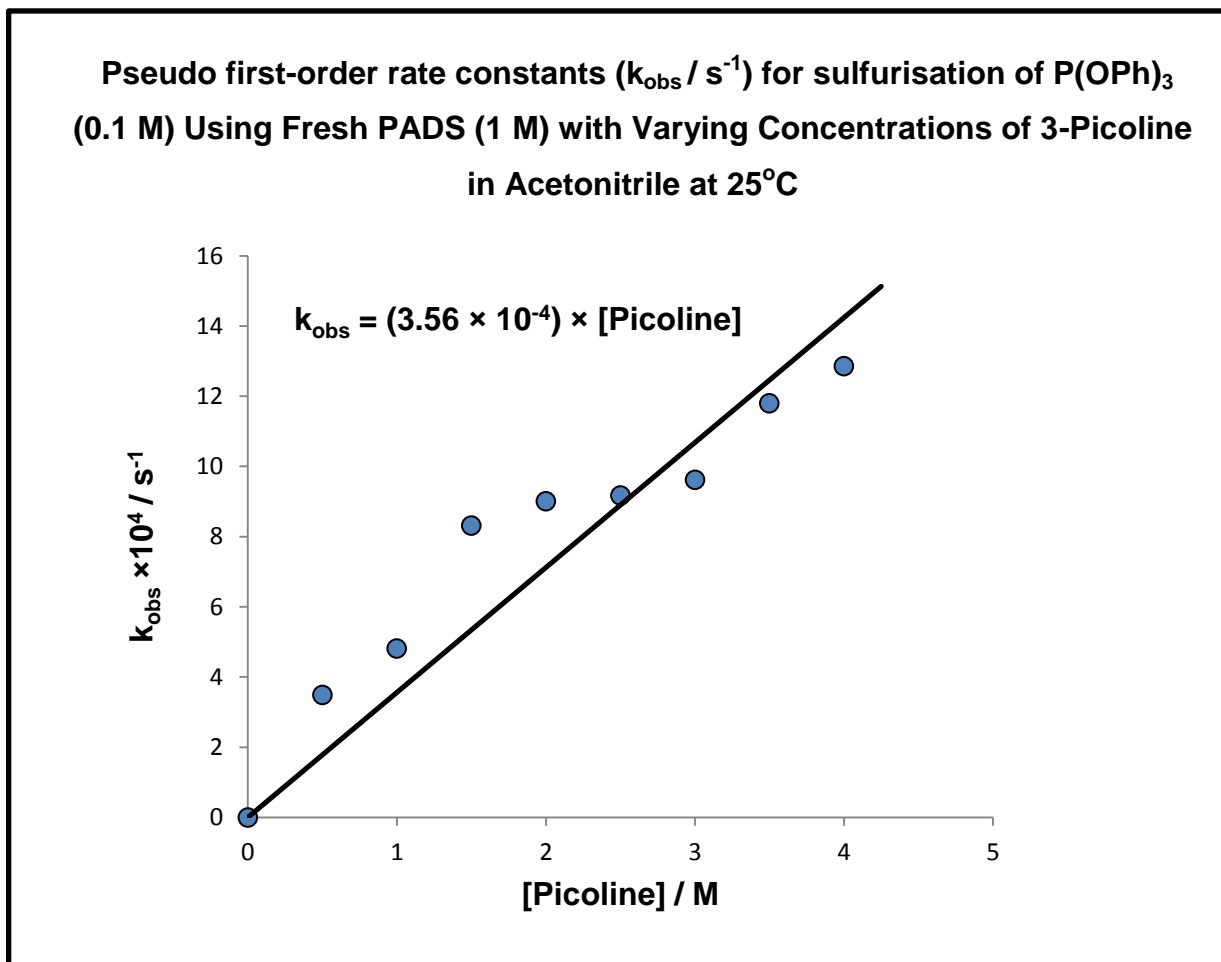
Figure 42: Pseudo first-order rate constants (s^{-1}) for sulfurisation of (PhO)$_3$P (0.1 M) using PADS (1 M) with varying concentrations of 3-Picoline determined by ^{31}P NMR at 25°C in acetonitrile-d$_3$

Finally, the dependence of the rate of sulfurisation on the concentration of PADS was assessed (Scheme 19) and again, the rate was found to be linearly dependent on the concentration of PADS and the reaction is therefore first order with respect to PADS. This suggests an overall third order process in which the rate of reaction is proportional to the concentration of all three reaction components: phosphite, PADS and base. A rate law for the reaction is as follows:

Rate = k [Phosphite] [PADS] [Base]

Figure 43: Pseudo first-order rate constants for sulfurisation of (PhO)₃P (0.1 M) using 3-picoline (2 M) with varying concentrations of PADS

4.1.2 Distinction between PADS and Polysulfides as Active Sulfurisation Agent in Fresh PADS Solution

Although showing lower reactivity than aged solutions, fresh solutions of PADS are active sulfur transfer reagents. The sulfur transfer reaction is base catalysed. Since the decomposition of PADS to generate polysulfides is also base catalysed it is important to make a distinction as to whether the active sulfur transfer reagent in fresh PADS solutions is phenylacetyl disulfide (bottom route in scheme 19) or the phenylacetyl polysulfides generated via ageing (top route in scheme 19). Since the rate of reaction of fresh solutions is slower than with aged solutions it could be possible that this difference in rate is due to the fact that PADS must first be converted to polysulfides before the sulfurisation reaction can occur.
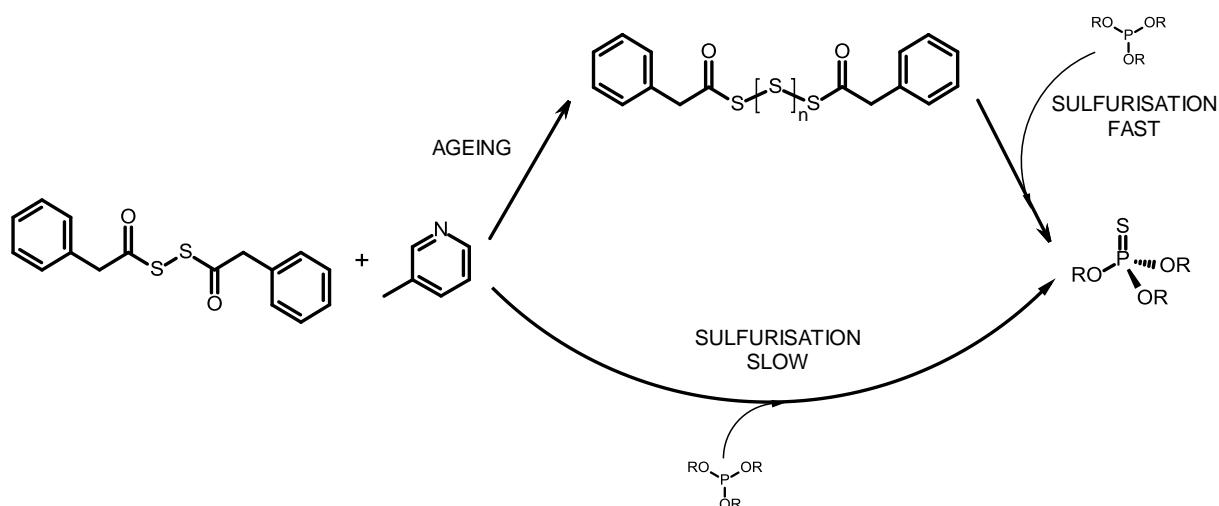
Scheme 19: possible pathways for the sulfurisation of phosphites using fresh PADS

In order to assess which route is active, two simultaneous reactions were performed in which PADS (1 M) was mixed with 3-picoline (2 M) and to one of the reactions triphenyl phosphite (0.1M) was added (herein labelled solution A and B respectively). Using ^{1}H NMR, the concentration of PADS was followed in solution A, whilst the concentration of phosphite was followed using ^{31}P NMR in solution B (Fig. 44).
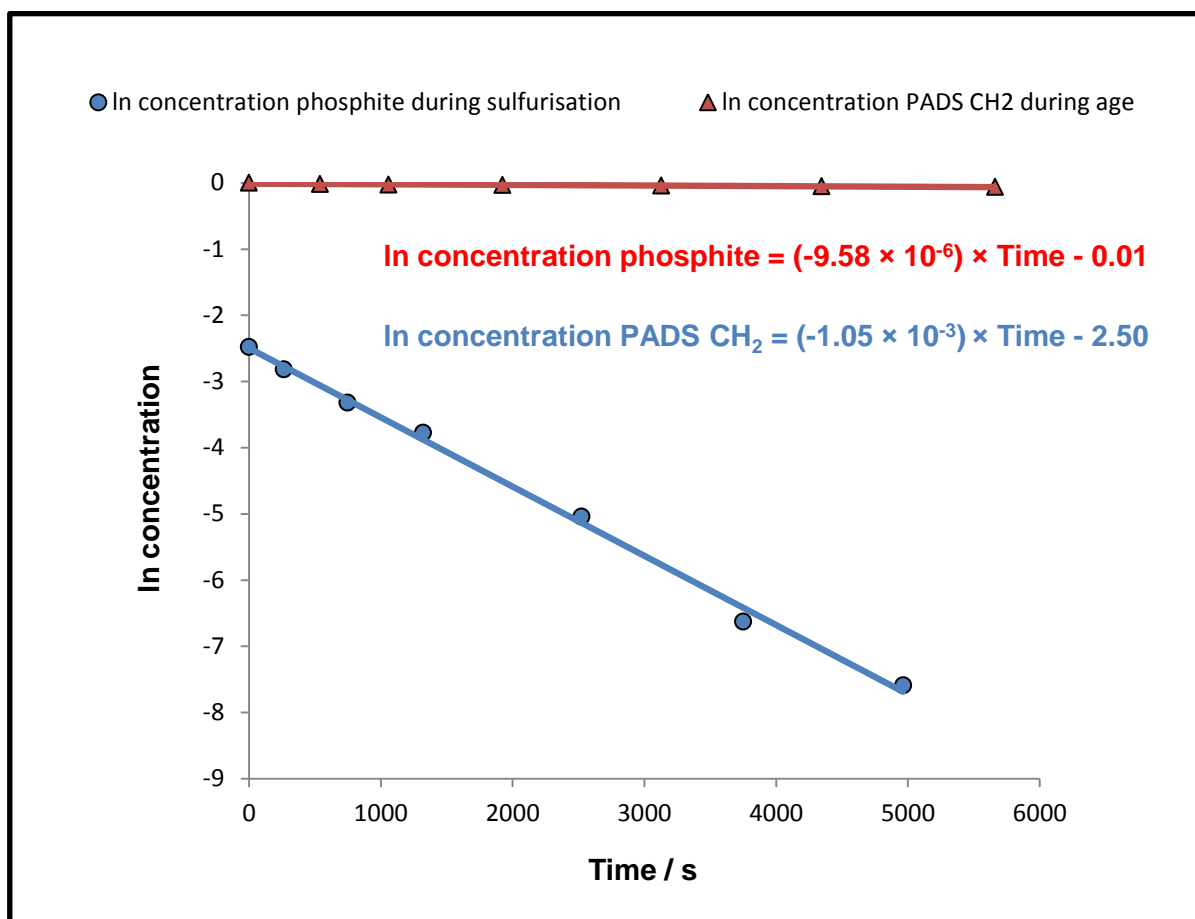
Figure 44: rate profiles of the decomposition of PADS and the sulfurisation of triphenyl phosphite in two parallel reactions containing fresh PADS (1M), 3-picoline (2M) and, in solution B only, triphenyl phosphite (0.1M). Reactions were performed at 25°C in acetonitrile

The data showed that under identical conditions, the rate of ageing is 2 orders of magnitude slower than that of sulfurisation. Therefore it is unlikely that sulfurisation using fresh PADS is dependent on the ageing of PADS and the generation of an active sulfur transfer species. These data also, therefore, suggests that the PADS molecule itself acts as a sulfur transfer reagent under these experimental conditions.

4.1.3 Distinction between a Radical and an Ionic Pathway

The oxidation of phosphites by disulfides is well known[93,97]. The mechanism of this process, however, is not easy to discern as there are potentially two different pathways i.e. nucleophilic attack by phosphorus[93](Scheme 20 B) or single electron, radical mechanisms[116] (scheme 20 A).
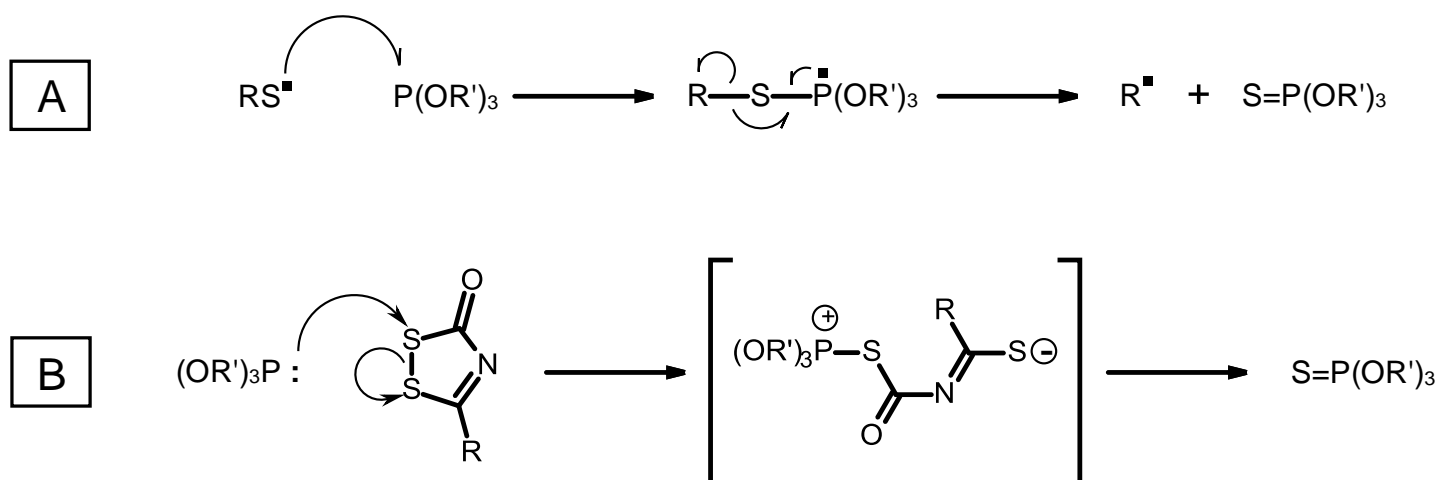
Scheme 20: Reported mechanisms of sulfurisation of phosphites by disulfides.

In order to distinguish between an ionic and a radical mechanism several sulfurisation reactions were performed in the presence of the radical trap butylated hydroxyl toluene. If there is radical involvement in the pathway then including this species should stop, or at least slow the reaction.
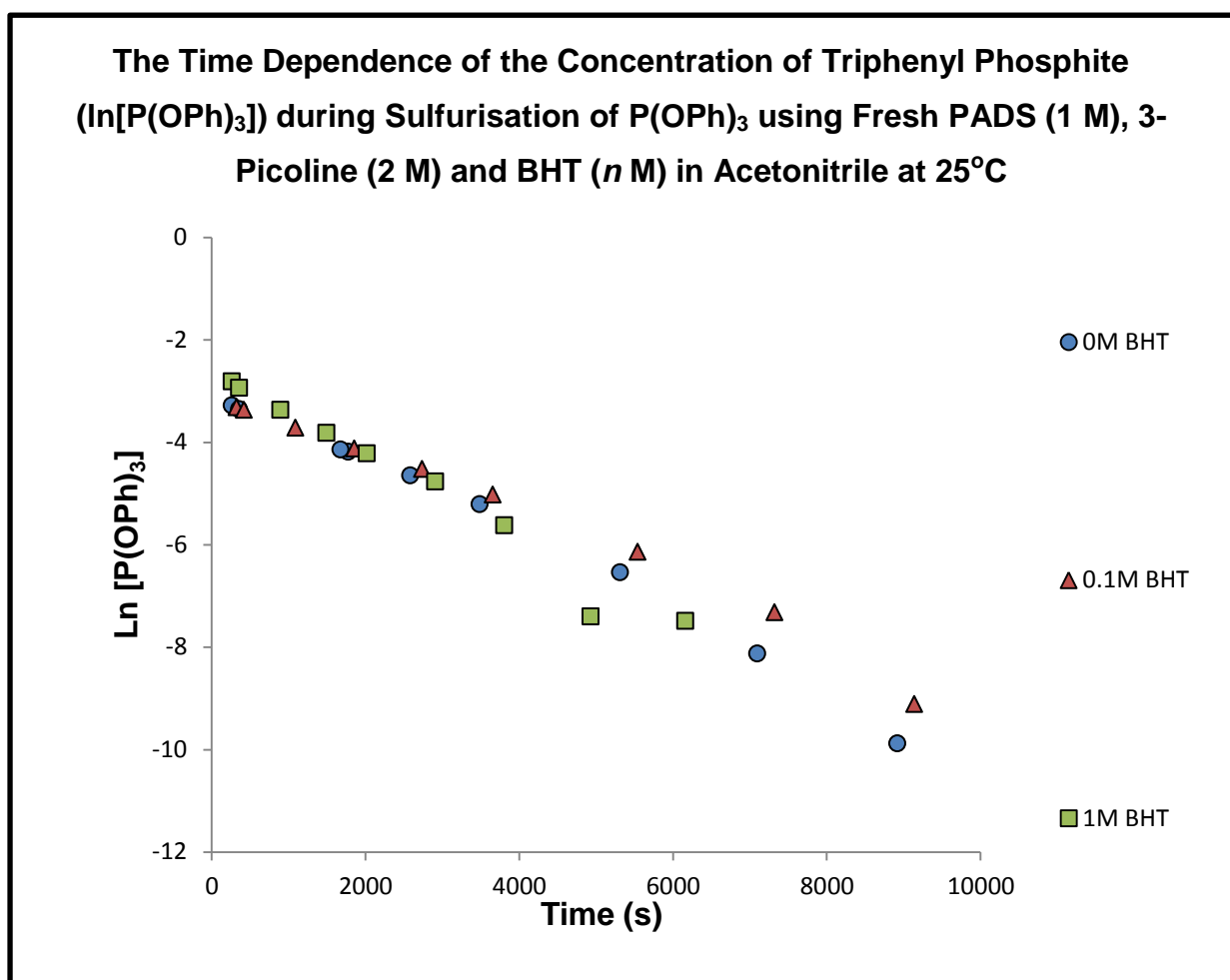
Figure 45: Concentration of triphenyl phosphite (ln[P(OPh)$_3$]) during sulfurisation with PADS (1 M) and 3-Picoline (2 M) in the presence of BHT (n M) in Acetonitrile at 25°C determined by ^{31}P NMR.

Concentration of BHT (M)	k_{obs} (s^{-1})
0	7.46×10^{-4}
0.1	6.26×10^{-4}
1	$8.46 \times [\# \ 10^{-4}$

Table 5: Pseudo first-order rate constants for sulfurisation of triphenyl phosphite (0.1 M) with fresh PADS (1 M) and 3-picoline (3 M) in the presence of BHT (n M). Reactions followed by ^{31}P NMR at 25°C in acetonitrile-d$_3$

Inspection of the results of these experiments (Fig. 45) clearly shows that adding BHT to the sulfurisation reaction has no effect on the rate of the reaction. Therefore it is unlikely that the sulfurisation reaction proceeds via a radical process and is instead likely to be an ionic mechanism. Further evidence for this can be seen when looking at the effect of solvent properties on the rate of the reaction.

Industrially, the sulfurisation reaction is carried out in a solvent of 50% (5 M) 3-picoline in acetonitrile. In order to assess whether or not the reaction proceeds with significant charge generation, the reaction was carried out in various solvents and the rates of the reactions were assessed.

Solvent	Dielectric Constant	k / $M^{-2}s^{-1}$	log k
Toluene	2.38	1.62×10^{-4}	-3.79
Chloroform	4.81	5.90×10^{-4}	-3.23
ACN	37.5	1.54×10^{-3}	-2.81
DMSO	46.7	4.13×10^{-3}	-2.38

Table 6: Third-order rate constants for sulfurisation of (PhO)$_3$P as a function of the solvent dielectric constant for sulfurisation with 10eq PADS and 20eq 3-Picoline. Reactions followed by ^{31}P NMR at 25°C.

Inspection of the rate constants measured for the different solvent systems (Table 6) shows that the sulfurisation of triphenyl phosphite by PADS proceeds faster in more polar solvents. This suggests the generation of a significant amount of charge during the reaction which is stabilised by the solvent. These data favour the proposal that the sulfurisation reaction proceeds via an electron pair exchange (i.e. an ionic mechanism) rather than exchange of a single electron in a radical mechanism since polar solvents solvate charged species more easily. As previously mentioned in section 4.1.1 the solvent effect observed here contradicts the theory proposed in the literature that the influence of 3-picoline on this reaction is simply a solvent effect since adding 3-picoline would lower the dielectric constant of the solvent and, as suggested by the data in table 6, slow the rate of reaction. It therefore follows that the role of 3-picoline in this process is as a reagent and not simply a solvent.

4.1.4 Phosphite Substituent Effects on the Rate of Sulfurisation with Fresh PADS

The sulfurisation reaction probably proceeds via nucleophilic attack either by phosphite on PADS or by PADS on the phosphite. In order to distinguish between a nucleophilic phosphite and an electrophilic phosphite several substituted aryl phosphites were synthesised in order to assess the effect of substituents on the rate of the sulfurisation reaction. The reaction was followed by ^{31}P NMR, monitoring the consumption of the phosphite under pseudo first-order conditions in which the concentrations of phosphite, PADS and 3-picoline were 0.1 M, 1 M and 2 M respectively (Fig. 46).
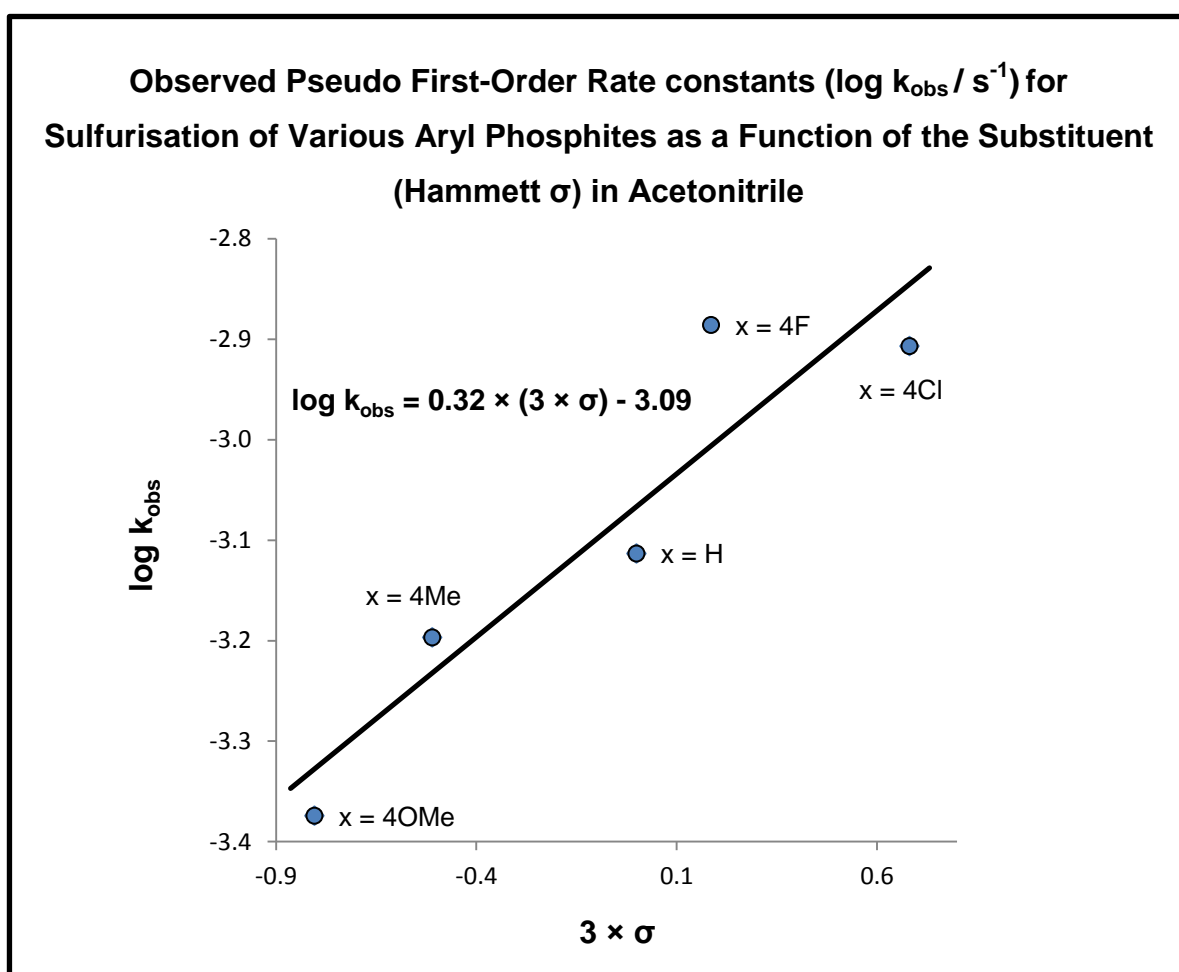
Figure 46: log of the observed pseudo first-order rate constants for the sulfurisation of various triaryl phosphites (0.1 M) with PADS (1 M) and 3-Picoline (2 M) as a function of the Hammett σ value of the substituent in acetonitrile-d_3 at 25°C.

Subst.	σ	k / s^{-1}	log k
4-OMe	-0.804	4.22×10^{-4}	-3.374
4-Me	-0.51	6.36×10^{-4}	-3.197
H	0	7.70×10^{-4}	-3.113
4-F	0.186	1.30×10^{-3}	-2.886
4-Cl	0.681	1.24×10^{-3}	-2.907

Table 7: Data from Hammett plot for the sulfurisation of various tris-aryl phosphites (0.1 M) with PADS (1 M) and 3-Picoline (2 M) in acetonitrile-d_3 at 25°C.

A Hammett plot for the data (Fig. 46) shows that electron-withdrawing groups increase the rate of reaction. This could suggest a build-up of negative charge on phosphorus in the transition state of reaction relative to the reactant state, i.e. phosphorus acting as an electrophile. However, the small value of the reaction constant (ρ = 0.32) suggests either a small build-up of negative charge (unlikely in a mechanism involving nucleophilic attack on phosphorus) or a multi-step reaction in which the ρ_{obs} is the sum of opposing ρ values of each step (Scheme 21). However, when looking at the individual rate constants of these reactions (Table 7) there is only a 3 fold increase in rate from the most electron donating substituent to the most electron withdrawing substituent, which is not very significant. Similarly, as previously mentioned, the magnitude of the reaction constant is not very large. For example, the ρ value for the reaction of substituted triaryl phosphites with aryl selenoxides, in which the phosphite is an electrophile is +2.3[117]. In reactions involving triaryl phosphites as nucleophiles, for example reaction with diphenyl trisulfide, the ρ value is -1.1[117]. The ρ_{obs} in this case is obviously much lower than these values.

$$\rho_{obs} = \rho_1 + \rho_2$$
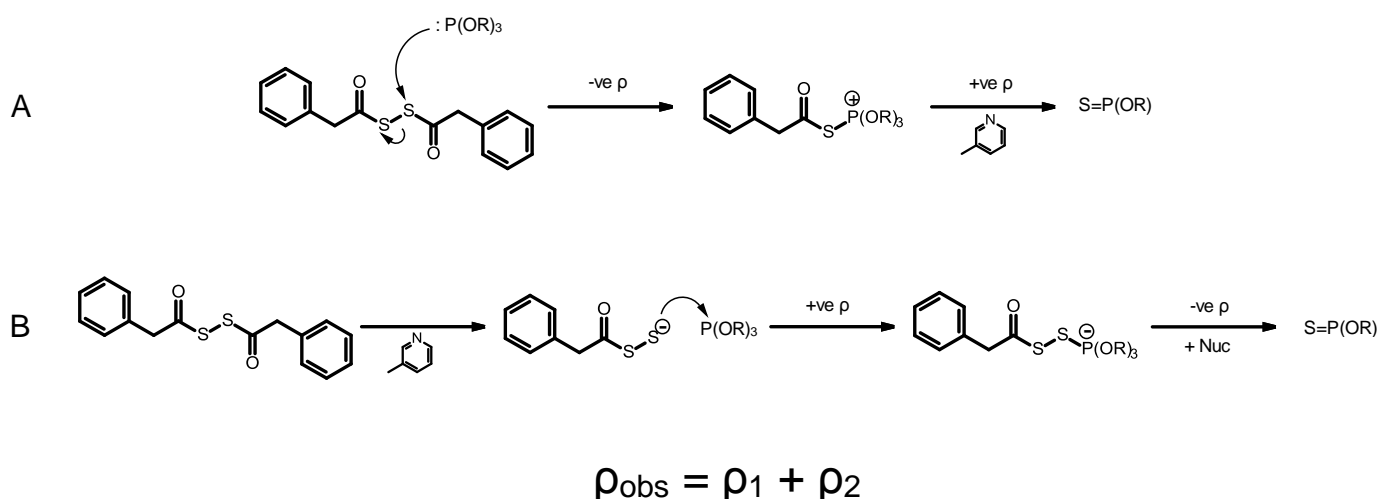
Scheme 21: Possible mechanisms of sulfurisation of phosphites by PADS in 3-Picoline/Acetonitrile.

Due to this low dependence of the rate of sulfurisation on phosphite substituent effect, the effect of alkoxy substituents was assessed. It is possible that the small effect of aryl substituents is due to the distance of the phosphorus centre from the *m-* and *p-* substituents as seen in the relative sensitivities of the ionisation of benzoic acid and phenylacetic acid in which the acid group in the benzoic acid is closer to the substituent and so the substituent has a larger effect[118]. This is minimised when using alkoxy phosphites. Also, not only are the reactions of alkoxy phosphites with PADS much faster than those of the aryl phosphites, the alkoxy species offer a much wider range of the strength of the nucleophiles. The Br∅nsted pK_a range of the corresponding alcohols of the alkoxy substituents investigated spans over 3 units whereas the pK_a range of the corresponding phenols of the alkoxy substituents barely spans 0.6 units (note pK_a values refer to aqueous acidity). However, due to the rapid rates of reaction of these compounds in acetonitrile, it was necessary to perform the reactions in chloroform at a lower concentration.
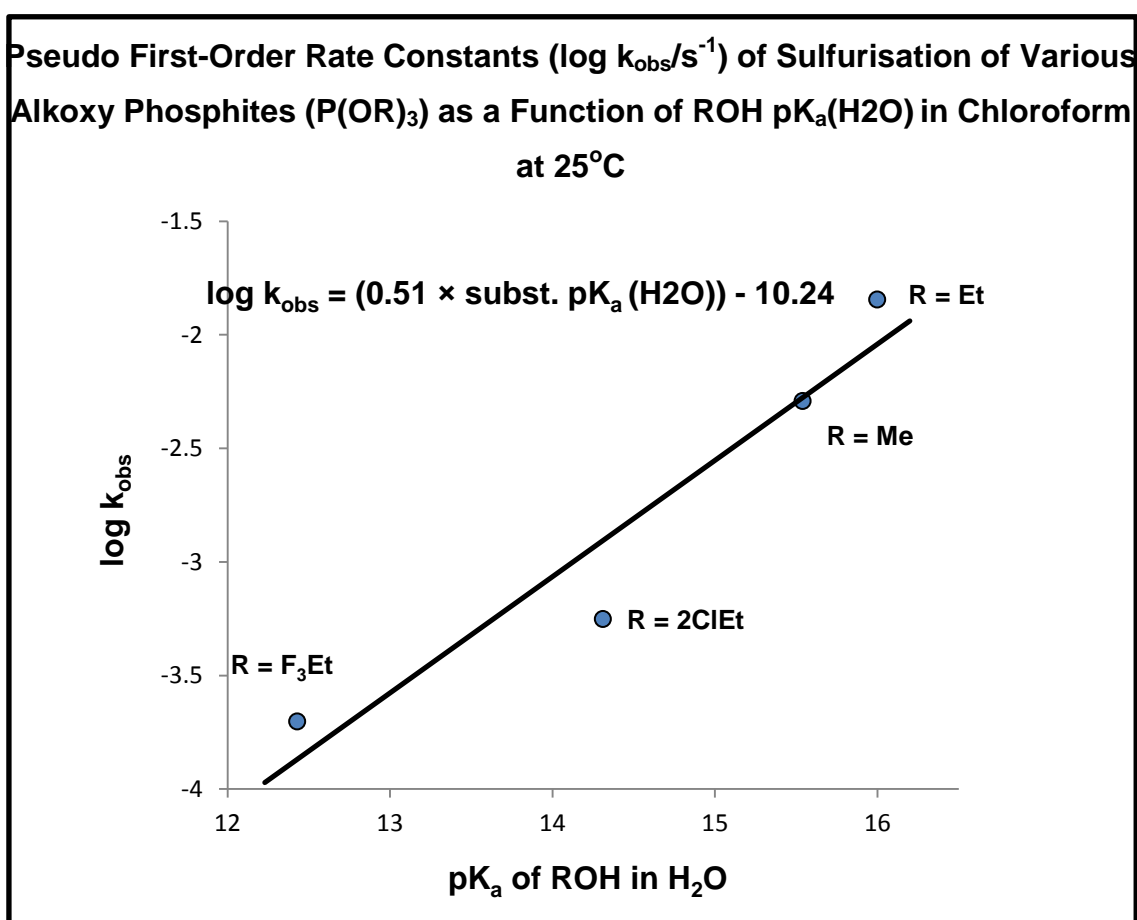
Figure 47: Brønsted plot for the sulfurisation of various alkoxy phosphites (0.03 M) with PADS (0.3 M) and 3-Picoline (0.6 M) determined by ^{31}P NMR in Chloroform at 25°C

R	pK$_a$(H2O)	k$_{obs}$ /s^{-1}	log k
Me	15.54	5.10×10^{-3}	-2.29
Et	16.00	1.43×10^{-2}	-1.84
F$_3$Et	12.43	1.98×10^{-4}	-3.70
2ClEt	14.31	5.60×10^{-4}	-3.25

Table 8: Table of observed pseudo first-order rate constants determined by ^{31}P NMR for the sulfurisation of various alkoxy phosphites (0.03 M) with PADS (0.3 M) and 3-Picoline (0.6 M) in CDCl$_3$ at 25°C

The Brønsted β$_{nuc}$ value +0.51 (Fig. 47) is much more definitive and mechanistically useful than the value of the reaction constant determined with aryl phosphites. The β$_{nuc}$ value of +0.51 indicates a build-up of positive charge on phosphorus in the transition state. This is in-line with a reaction mechanism proceeding via nucleophilic attack by phosphorus on one of the sulfur atoms in the PADS disulfide bond (Scheme 21, A). This is consistent with either rate-limiting nucleophilic attack with a transition state in between the phosphite and the phosphonium or with rate-limiting cleavage of the phosphonium species.

4.1.5 The Effect of Pyridine pK_a on the Rate of Reaction

As mentioned in section 4.1.1, the sulfurisation of phosphites by PADS is a third-order process which is first-order in respect to phosphite, PADS and the pyridine base. Therefore, the pyridine (in this work so far: 3-picoline) must be involved in a step preceding or including the rate-limiting step. In order to further probe the role of 3-picoline in this reaction an investigation was undertaken to study how using various different substituted pyridines, with varying pK_as, influenced the rate constant for the reaction (Fig. 48, Table 9).
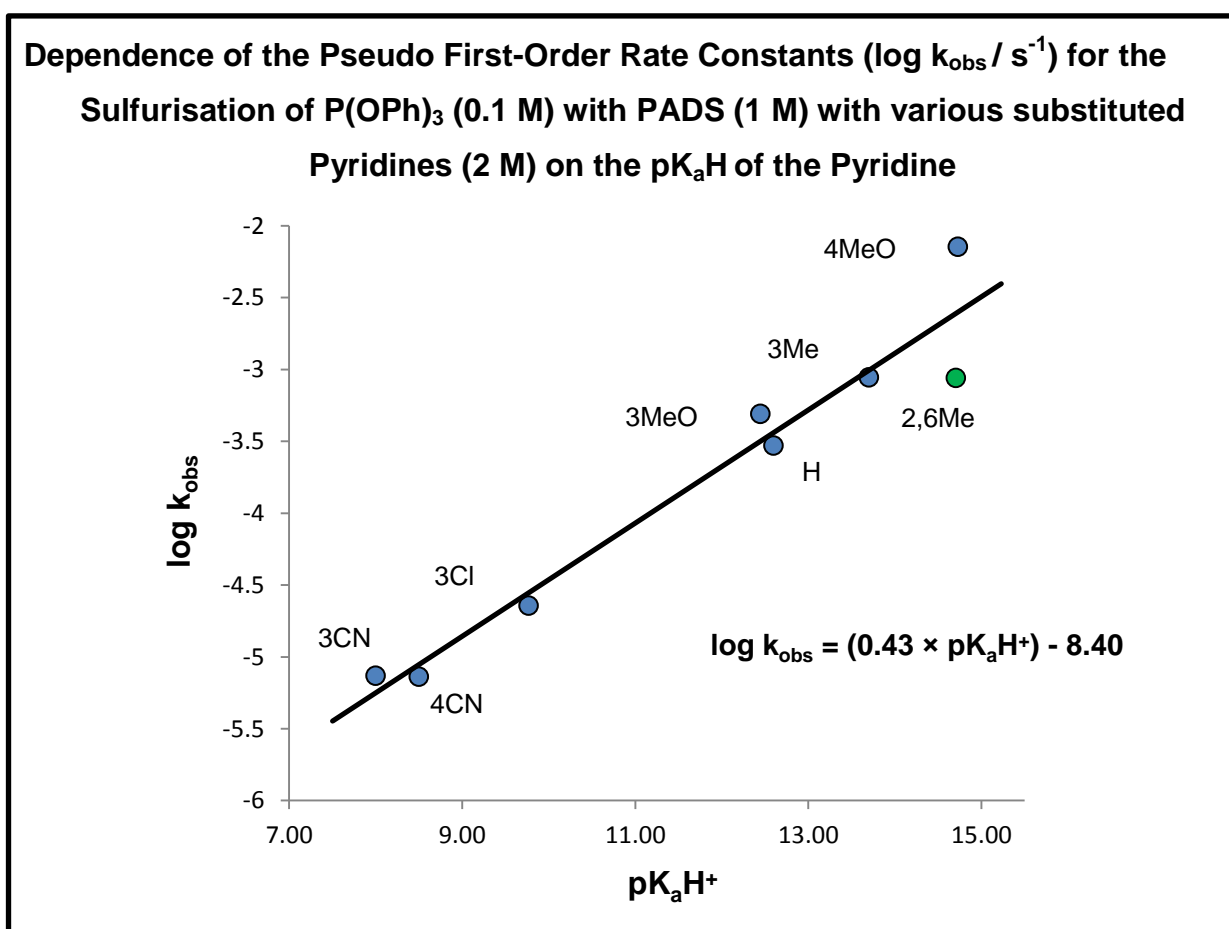
Figure 48: Dependence of the pseudo first-order rate constants for sulfurisation of triphenyl phosphite (0.1 M) with PADS (1 M) on the pK_a [111] of the pyridine catalyst used (3 M) in acetonitrile at 25^oC. Reactions followed by ^{31}P NMR.

113

Subst.	pK$_a$ ACN	k$_{obs}$ / s^{-1}	log k
4-MeO	**14.73**	7.15 × 10^{-3}	-2.15
2,6-Me	14.70	8.75 × 10^{-4}	-3.06
3-Me	13.70	8.81 × 10^{-4}	-3.06
H	12.60	2.96 × 10^{-4}	-3.53
3-MeO	**12.45**	4.92 × 10^{-4}	-3.31
3-Cl	**9.77**	2.27 × 10^{-5}	-4.64
4-CN	8.50	7.26 × 10^{-6}	-5.14
3-CN	8.00	7.38 × 10^{-6}	-5.13

Table 9: Observed pseudo first-order rate constants (k_{obs} / s^{-1}) for sulfurisation of triphenyl phosphite (0.1 M) with various pyridines (2 M) with fresh PADS (1 M) in acetonitrile at 25°C

The results of this investigation clearly show a positive correlation between the pK$_a$ of the pyridine and the rate of sulfurisation in which stronger bases afford faster rates of reaction. The β$_{nuc}$ value of +0.43 determined from the Brønsted plot (Fig. 48) is significant and suggests a reaction pathway that proceeds via a mechanism in which there is significant positive charge build-up on the pyridine nitrogen.

However, as discussed in the previous chapter, a positive correlation between pyridine pK$_a$ and rate of reaction is only indicative of the charge build-up during the reaction and does not give details about the role of the pyridine i.e. whether the pyridine acts as a nucleophile or as a base and since both routes are possible, further analysis of the data is required.
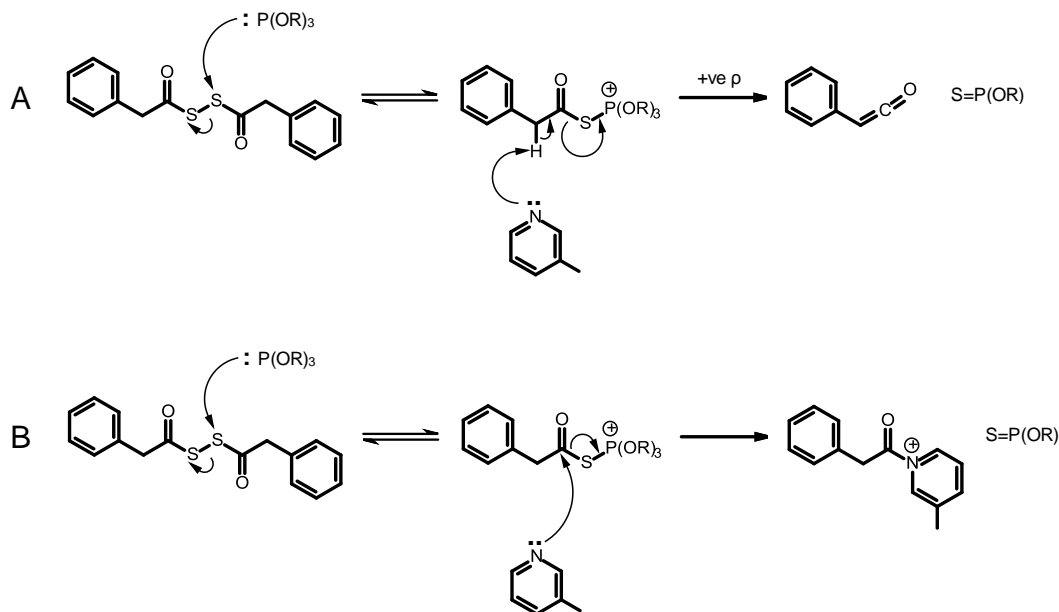
Scheme 22: Two possible mechanisms for the action of picoline in the sulfurisation reaction A: 3-picoline acting as a base, B: 3-picoline acting as a nucleophile

114

In general, pyridines become more nucleophilic as their pK_a increases. This therefore leads to ambiguity in determining the mechanistic role of pyridines in the sulfurisation reaction. However, with a non-nucleophilic base, 2,6-lutidine (**8**), the pseudo first-order rate constant (k_{obs}) for this reaction is still within the range predicted by the Brønsted plot for a pyridine of its pK_a. Similar reactions were also run with other hindered bases such as triethyl amine which is extremely basic ($pKaH(H2O) = 10.75$[111]) and affords a rapid rate of reaction ($t_{1/2} \approx 18$ s). This, therefore suggests that in the sulfurisation of phosphites using fresh PADS, the role of the pyridine is as a base and they are involved in abstraction of the α-protons which leads to the decomposition of the phosphonium intermediate (Scheme 22,A). This is supported by the literature reports of pyridine catalysed proton abstraction from carbon acids, in which the relative rates of deprotonation by lutidine and pyridine is proportional to the pK_as of the two compounds[119]. Whereas in the nucleophile catalysed hydrolysis of acetic anhydride[120] and acetyl fluoride[121] $k_{pyridine}$ is far greater than $k_{lutidine}$ despite its lower pK_a.
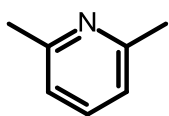
(8)
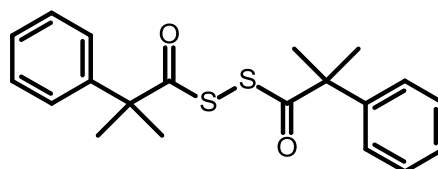
(4)
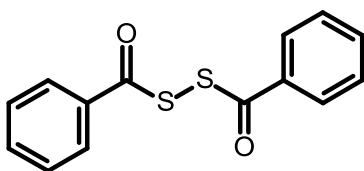
(5)
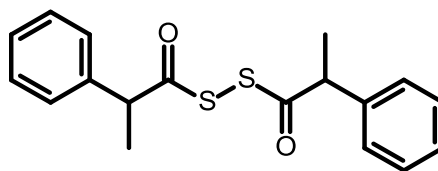
(9)

Further evidence for a mechanism involving base-catalysed decomposition of the phosphonium intermediate can be seen when comparing the dependence of the rate of sulfurisation of phosphites using the compounds 2,2,2′,2′-tetramethyl-2,2′phenylacetyl disulfide (**4**) and bis-benzoyl disulfide (**5**) in which the protons α to the carbonyl are missing. Under the same reaction conditions, not only are the relative rates of reaction of these compounds much slower (k_{obs} for reaction with $(PhO)_3P$ (0.1 M), 3-Picoline (2 M) and either PADS, (**4**) or (**5**) $\approx$ 46:4:1 respectively) but the dependence of the rate of these reactions on the pK_a of the base (β value) is much lower (Table 10).

Sulfurising Agent	β_{nuc}
PADS	+0.43
(4)	+0.30
(5)	+0.16

Table 10: β_{nuc} values from Brønsted plots for the sulfurisation of P(OPh)$_3$ using vaious different sulfur transfer reagents with different substituted pyridines in acetonitrile at 25°C

The difference in the Brønsted β values indicates an alternative mechanism of reaction when moving from PADS to (4) or (5). Equally important is the fact that there is no reaction observed when using the tetramethyl derivative (4) as the sulfur transfer reagent and with 2,6-lutidine (8) as the base. This is to be expected since there are no dissociable protons in (4) and therefore the reaction must proceed via nucleophilic attack rather than proton transfer. The non-nucleophilic 2,6-lutidine is therefore incapable of catalysing this reaction.

Further evidence that the pyridines act as bases in reactions with fresh PADS can be seen when comparing the rates of reaction between 2,2′-methyl-2,2′-phenylacetyl disulfide (9). Though the reaction with (9) is slower than that of PADS, the replacement of one of the methyl groups of (4) with a proton increases the rate by a factor of 4.5. This is due to the fact that the pyridine is now able to act as a base. The difference in rate between fresh PADS and (9) can be explained by the fact that the α-proton in (9) is expected to be much less acidic than that of PADS due to electron donating nature of the methyl group (for example adding a methyl group to the secondary carbon in *i*PrOH increases the pK_a $_{H2O}$ from 16.5 to 17.0[111]).

Compound	k_{obs} / s^{-1}	log k_{obs}	k_{obs}/k_{PADS}
PADS	8.81×10^{-4}	-3.06	1.00
(9)	3.27×10^{-4}	-3.49	0.37
(4)	7.07×10^{-5}	-4.15	0.08

Table 11: k_{obs} for sulfurisation of (PhO)$_3$P (0.1 M) with fresh PADS, (2) and (3) (1 M) with 3-picoline (2 M).

4.1.7 The Effect of PADS Phenyl Substituents on the Rate of Reaction

In the work so far, the effects of substituents on two of the components of the sulfurisation reaction have been assessed i.e. in the phosphite and the pyridine. In order to complete the data set and to fully understand the effect of substituents on the sulfurisation reaction, several more substituted PADS compounds were synthesised in order to construct a linear-free energy relationship and assess the effect of PADS phenyl substituents on the rate of reaction.

Pseudo First-Order Rate Constants (log k_{obs} / s^{-1}) for Sulfurisation of P(OPh)$_3$ (0.1 M) with Various Phenyl Substituted PADS Derivatives (1 M) and Pyridine (2 M) as a Function of the Substituent Hammett σ at 25°C in Acetonitrile-d$_3$

x = 4Cl
x = 3Cl
x = 4CN
x = 4F
x = H
x = 4OMe

Solid Line: log k_{obs} = (0.45 × σ) - 2.50

Dotted Line: log k_{obs} = (2.34 × σ) - 3.03
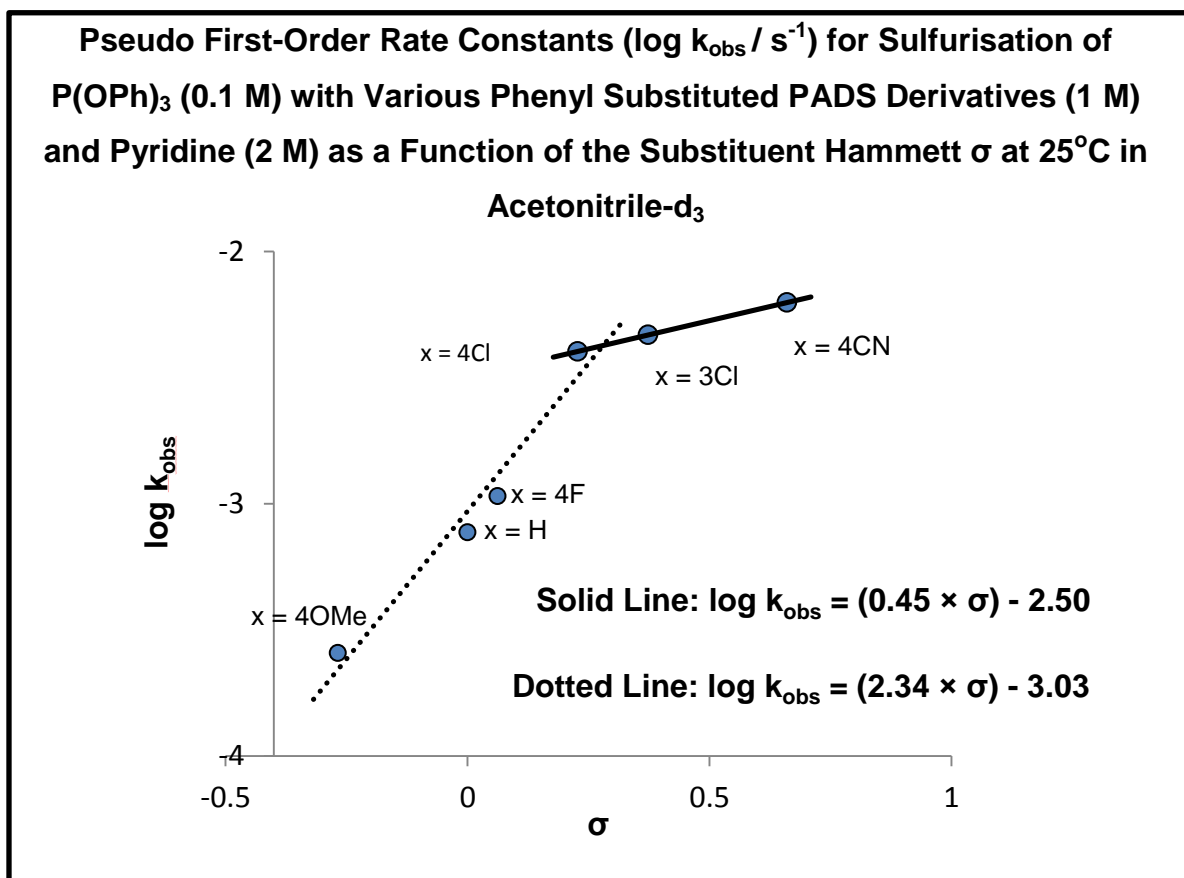
Figure 49: Linear free-energy relationship for sulfurisation of P(OPh)$_3$ (0.1 M) with 3-Picoline (2 M) using various substituted PADS analogues

Whilst the Hammett plot is non-linear (Fig. 49) the results suggest that electron withdrawing substituents increase the rate of the sulfurisation reaction. A non-linear Hammett plot tending towards a decreased slope indicates a change in the rate-limiting step of the reaction. It is possible to envision two initial steps for the reaction (Scheme 21); the first is nucleophilic attack by the phosphite at one of the sulfur atoms of PADS to generate a phosphonium intermediate. The second is a mechanism in which the phosphite acts as an electrophile and is attacked by an in-situ generated disulfide anion to generate a phosphide intermediate, generating a positive ρ value. Since decomposition of this phosphide intermediate to afford the phosphorothioate product involves the

transfer of negative charge from the phosphorus onto the phenylthioacetate group, electron withdrawing groups would have a rate enhancing effect on this pathway, generating a negative ρ value.

However, the magnitude of the initial ρ value (dotted line in Fig. 49) indicates the generation of a significant amount of negative charge close to the phenyl ring. This build-up of a significant negative charge is more consistent with a mechanism in which one of the methylene protons is removed in the rate-limiting step. This suggests a mechanism in which the pyridine present acts as a base to remove these protons in a step preceding the rate-limiting step.

In the linear-free energy relationship (Fig.49) there is a change in the gradient of the slope, i.e. the rate becomes less dependent on the PADS phenyl substituent for the most electron withdrawing substituents. This is most likely explained by a change in the rate-limiting step of the reaction in which k_2 (the decomposition of the phosphonium to form products) becomes greater than k_{-1} (the reverse reaction of the nucleophilic attack by the phosphite on PADS). This would be expected as adding electron withdrawing groups decreases the pK_a of the methylene protons. This could result in a pathway in which the phenylthioacetate by-product of the nucleophilic decomposition of PADS is now basic enough to remove these protons ($pK_aH(ACN)3$-picoline= 13.7, $pK_a(ACN)$ 2-phenylthioacetic acid $\approx 20^{111}$). This changes the rate-limiting step of the reaction from k_2 to k_1.

Scheme 23: Alternative mechanisms of phosphonium degradation with substituted phenyl PADS analogues
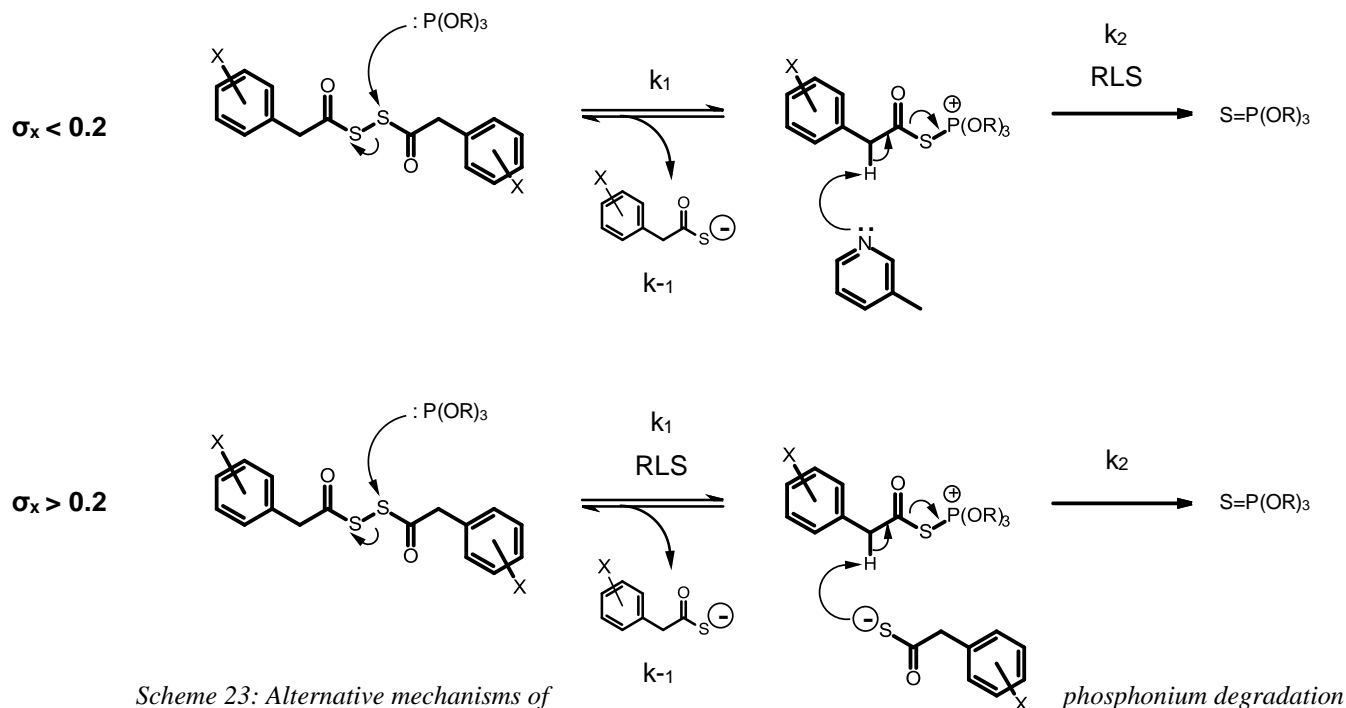
4.1.8 Summary of the Mechanism of the Sulfurisation of Phosphites using Fresh PADS

As discussed in previous sections, the sulfurisation of phosphites using fresh PADS in the presence of a pyridine is a third-order process which is first-order with respect to each component: phosphite, PADS and pyridine. Substituent effects on the phosphite and pyridine show Brønsted β_{nuc} values of +0.51 and +0.43 respectively, indicating a reaction mechanism pathway in which substantial positive charge is transferred or generated on the pyridine nitrogen and phosphite phosphorus atoms. Adding electron withdrawing substituents to the phenyl rings of PADS affords an increase in the rate of reaction with a Hammett ρ value of +2.34 indicating a build-up of significant negative charge next to the PADS phenyl ring in the rate-limiting step. This suggests that the role of the pyridine in this process is as a base, not a nucleophile. The mechanism of sulfurisation using fresh PADS is proposed as follows:
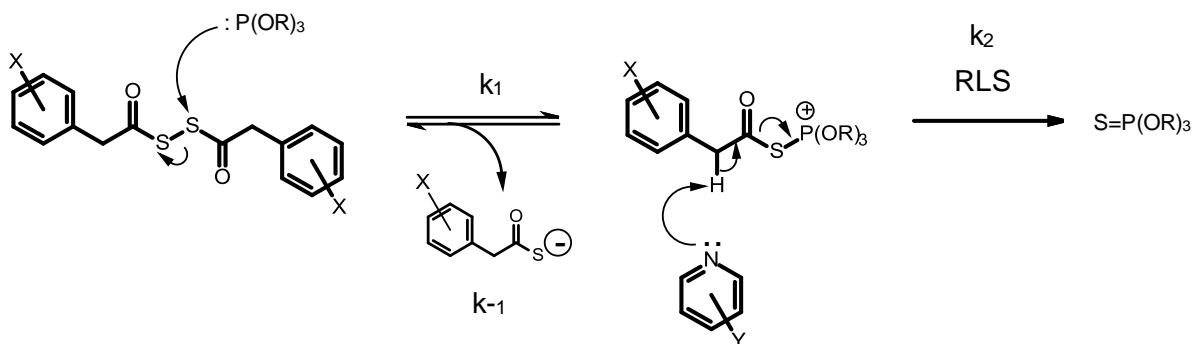
Scheme 24: Mechanism of sulfurisation of phosphites using fresh PADS in the presence of a pyridine base.

The linear free-energy relationship correlating the rate of reaction with PADS substituents also shows a change in the rate limiting step. Therefore, the rate law for the rate of the reaction can be written as follows:

$$\sigma_x > 0.2 \ then \ k_{-1} \ll k_2 \ so \ Rate = \ k_1 \ [PADS][Phos]$$

$$\sigma_x < 0.2 \ then \ k_{-1} \gg k_2 \ so \ Rate = \frac{k_1 k_2 [PADS][Phos][Pyr]}{k_{-1}[S^-]}$$

Where: [Phos] = Phosphite, [SH] = 2-phenylthioacetate and [Pyr] = pyridine.

4.2 Aged PADS

As discussed previously, sulfurisation of phosphites with PADS solutions that have been aged are much more efficient than using fresh PADS solutions, with rate increases of 13-fold when aged for 48 h. Using aged PADS has also been shown to improve the ratio of PS/PO phosphate esters present in the backbone of the oligonucleotide chain by a significant 0.2%[96]. When PADS is aged in the presence of a pyridine it decomposes and forms polysulfides. This, coupled with the increase in rate, suggests a somewhat different mechanism of sulfurisation when using aged PADS solutions compared with fresh PADS. In the following sections, the acyl polysulfide products of PADS ageing will be generally represented diagrammatically with 2,2′-phenylacetyl **tri**sulfide, however, as seen in the mass spectra in the previous chapter, these polysulfides vary in the number of sulfur atoms in the polysulfide chain. Furthermore the second and third order rate constants reported are based on the starting concentration of PADS and as the actual concentrations of the polysulfides must be smaller than this, the reported constants are the minimum values.

Structurally, there is not a big difference between the disulfide PADS and the phenylacetyl polysulfides generated by ageing except that they vary in the number of sulfur atoms the molecules contain. However, this increase in the number of sulfur atoms allows for a more facile pathway of sulfurisation. In terms of reaction initiation, it is proposed that this remains very much the same as in PADS; i.e. nucleophilic attack from the lone pair of the phosphite on one of the sulfur atoms in the molecule. However, since the symmetry of the polysulfides is slightly different to that of PADS, there are more possible sites for phosphite attack; i.e. the phosphite can either attack a terminal sufur or a sulfur in the middle of the polysulfide chain (Fig 50).

The possible phosphonium products of phosphite attack on the polysulfide ageing products (simply represented here by the trisulfide) are illustrated in figure (50). This process is slightly more complicated as there are now potentially 4 products. Which sulfur is likely to be attacked by phosphorus in this case is mechanistically important as the ease (and therefore the rate) of product formation from these two different sets of reactions is different. The attack of phosphorus on phenylacetyl trisulfide has been expanded below.
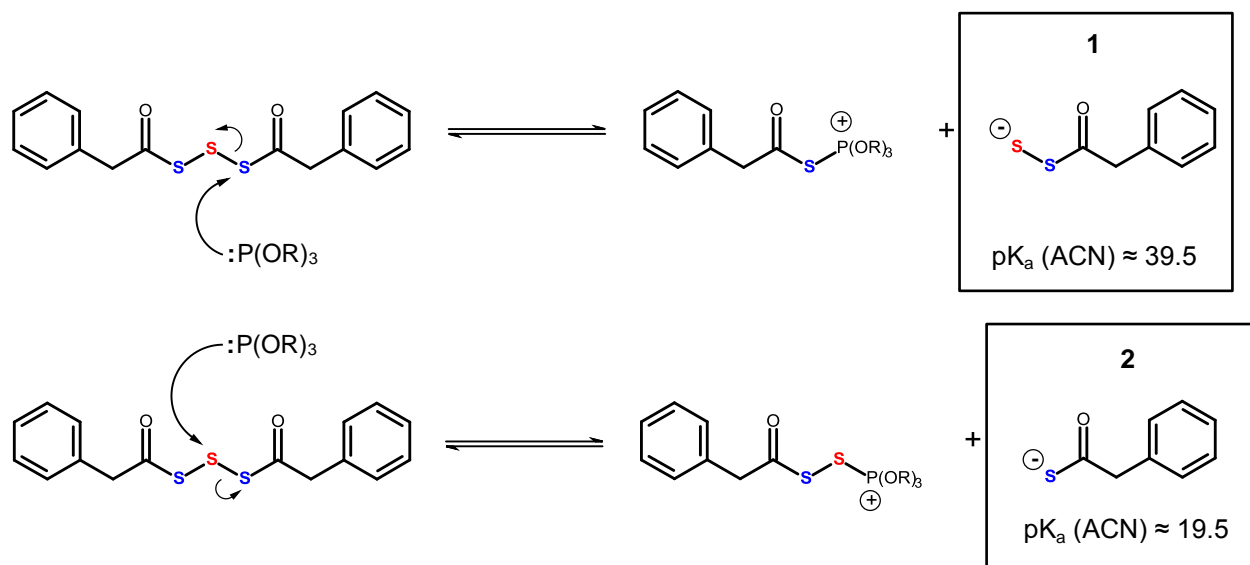
Figure 50: Nucleophilic attack by phosphites on sulfur atoms in 2,2´-phenylacetyl trisulfide.

Figure 50 shows not only the products of the nucleophilic attack on the trisulfide species but also the pK_a of the corresponding eliminated thioacid and acylthiol products. Attack at the different sites (Fig. 50) generates different sulfur leaving group species which have different pK_as. The pK_a of the acyldisulfide anion has been calculated based on the literature values for the pK_as of thioacetic acid, phenylacetic acid and peracetic acid[122] and literature correlations between aqueous pK_as and those in acetonitrile for carboxylic acids. Though oxygen acids and thio acids are different in terms of structure and polarizability, using the oxygen acid system as a model for the thio system is sufficient for the purposes of this approximation.

Compound	pKa	
	H₂O	**ACN**
Acetic acid	4.8	23.5
Phenylacetic Acid	4.3	**21.8**
Peracetic acid	8.2	**28.0**
Thioacetic Acid	3.3	**20.2**
Phenylthioacetic Acid	**2.9**	**19.5**
Phenylperthioacetic Acid	**15.4**	**39.5**

$$pK_a(ACN) = 1.6 \times pK_a(H_2O) + 14.9$$

Table 12: table of pK_as of oxyacids and thioacids in water and in acetonitrile. Red values have been calculated using the above correlation equation[111].

It has been assumed in the calculation that the effect that the disulfide bond has on the pK_a of the perthioacetic acid relative to the thioacetic acid is equal to the effect the peroxide bond has on the pK_a of peracetic acid relative to acetic acid (Table 12). Despite the approximations used it is clear that the thioacid leaving group ($PhCH_2COS^-$) is much less basic than the disulfide anion ($PhCH_2COSS^-$).

Looking at the pK_as of the protonated forms of the two anionic leaving groups of the possible, alternate reaction pathways it can be seen that the corresponding thioacid is several orders of magnitude more acidic than the acyldisulfide anion. This mean that the thioacetate has a much more delocalised charge and is not only much more stable in acetonitrile but is also a much better leaving group and weaker nucleophile than the acyldisulfide anion. It is proposed therefore that this is the most likely way in which the reaction will proceed: i.e. the phosphorus will likely always attack at the position which will cause the formation of the most stable transition state and products and is less likely to give a reversible step. In this particular case this means that the reaction is likely initiated by attack by the phosphorus on the sulfur adjacent to the thiocarboxyl group. This generates the phenylthioacetate species and a phenylthioacyl phosphonium containing n-1 sulfur atoms (where n is the total number of sulfur atoms in the polysulfide).

This is consistent with the literature surrounding desulfurisation of ^{35}S-labelled alkyl trisulfides with phosphites and phosphines where it was found that the nucleophile removes the central sulfur atom and not the terminal sulfur atom. These reactions however do require the addition of an external nucleophile as the thiol by-products of these reactions are poorer leaving groups than the thioacid by-products in the case of acylpolysulfides and are therefore also better nucleophiles. It is proposed that, in the case of alkyl polysufides, a tight ion-pair is formed between the leaving group and the phosphonium which facilitates product formation[123].

4.2.1 Effect of Phosphite Substituents on the Rate of Sulfurisation Using Aged PADS

Due to the increased activity of aged PADS solutions reaction with alkyl phosphites were too fast to monitor by ^{1}H NMR and HPLC, even in solvents which would usually slow the rate of reaction enough to measure e.g. chloroform. It is not possible to monitor these reactions by UV due to the fact that the λ_{max} of all three components occurs within the same region. This does not allow for the reaction to be monitored under pseudo first-order conditions. Therefore the only data that could be obtained was the effect of phosphite substituents in reactions with aryl phosphites.
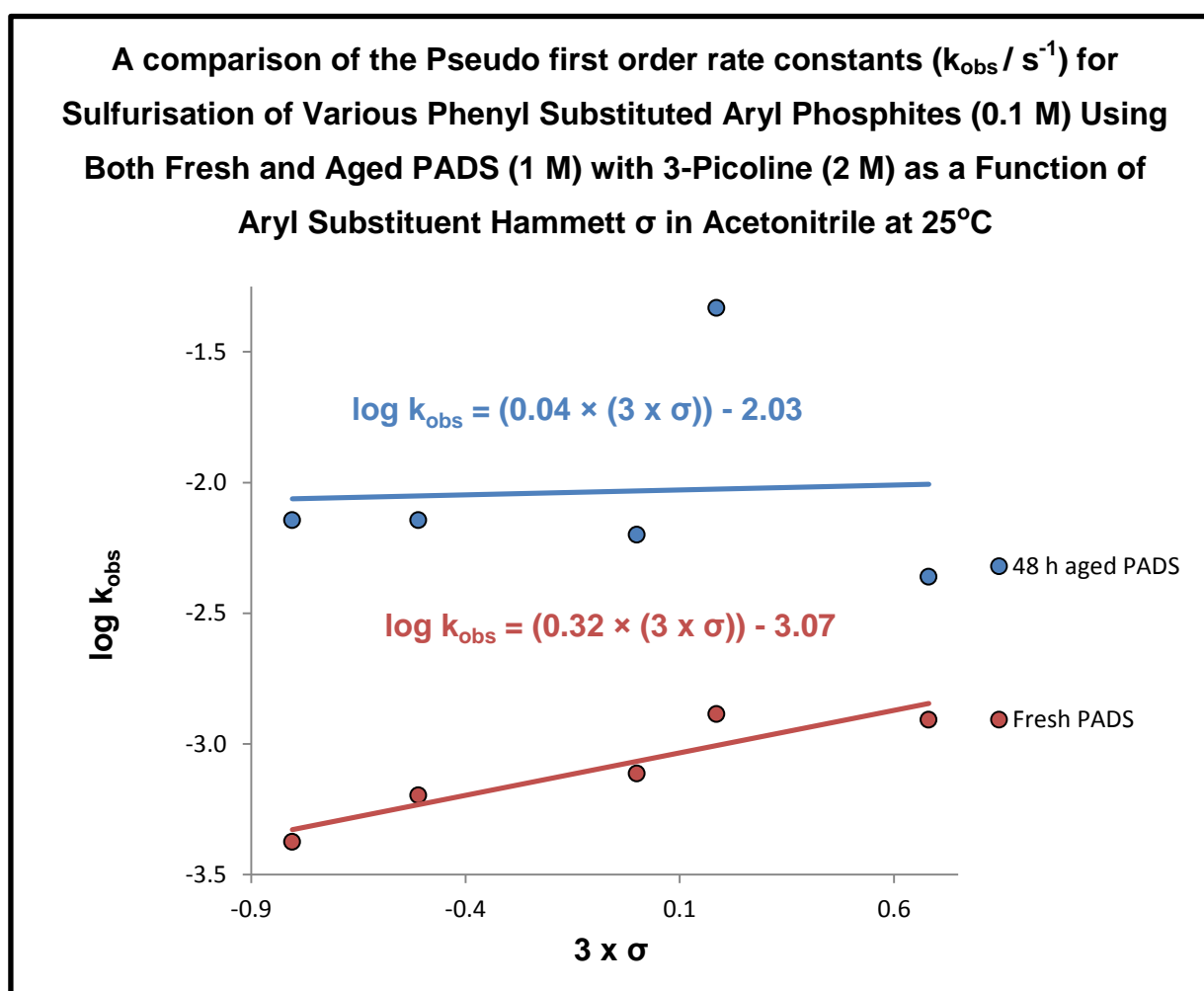
Figure 51: Hammett plot for sulfurisation of various substituted phenyl phosphites (0.1 M) using fresh and aged PADS (1 M) with 3-picoline (2 M) in acetonitrile-d$_3$ at 25°C

Subst.	Hammett σ	log k_{obs}	
		Fresh PADS	**48 h Aged PADS**
4-OMe	-0.80	-3.37	-2.14
4-Me	-0.51	-3.20	-2.14
H	0.00	-3.11	-2.20
4-Cl	0.68	-2.91	-2.36
4-F	0.19	-2.89	-1.33

Table 13: log of the pseudo first-order rate constants for sulfurisation of various substituted triaryl phosphites (0.1 M) with PADS (1 M) and 3-picoline (2 M) determined by ^{31}P NMR at 25°C in acetonitrile-d_3.

In our earlier experiments it was found that the effect of substituents on aryl phosphites with fresh PADS was relatively small. The results with aged PADS show that this effect is in fact even smaller, by a factor of almost 10 fold. It can be said therefore that the rate of reaction of phosphites with PADS aged for 48 h is independent of the phenyl substituent. The fact that alkoxy phosphites still present a faster rate of reaction than phenyl phosphites is still indicative of a mechanism proceeding via nucleophilic attack by the phosphite as these species are generally more nucleophilic than aryl phosphites. However, the fact that the reaction shows little dependence on the phosphite substituent is indicative of a process in which the transition state for the rate-limiting step is different to that with fresh PADS where it was shown that with phenyl phosphites electron withdrawing groups aid the decomposition of the phosphonium intermediate. The data indicate that, with aged PADS, the overall change in charge on the phosphite is small when moving from reactant to the highest energy transition state.
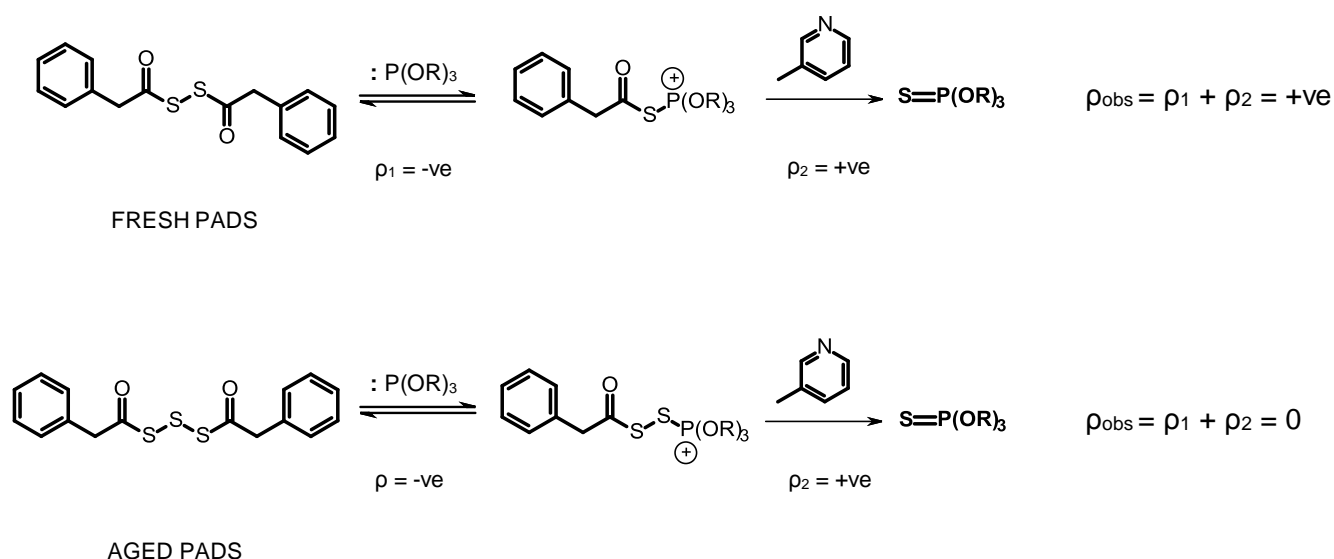
Scheme 25: General scheme of reactions of substituted phosphites with both fresh PADS and aged PADS.

124

4.2.2 Dependence of the Rate of Sulfurisation Using Aged PADS on Base pK_a

A study of the observed pseudo first-order rate constants of the sulfurisation of phosphites using aged PADS (Fig. 52) demonstrated that the reaction can be catalysed by the presence of a pyridine, much like fresh PADS. However, when using aged PADS solutions, the dependence of the rate of reaction on the pK_a of the pyridine used is not as great (Fig. 52). The measured β_{nuc} values are much lower and more closely match those measured for 2,2,2´,2´-tetramethyl PADS (**4**) and dibenzoyl disulfide (**5**) than fresh PADS.
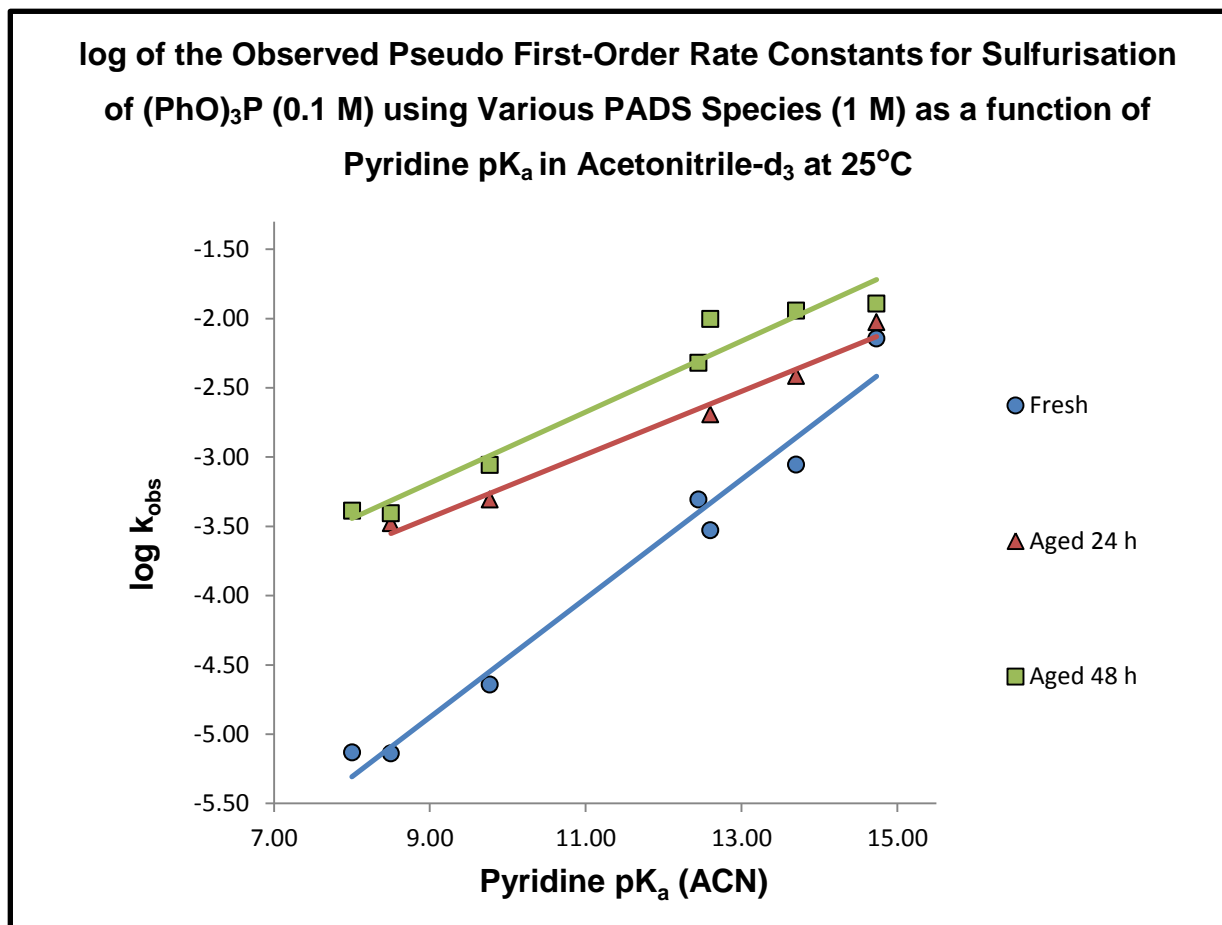
Figure 52: log of the observed pseudo first-order rate constants for sulfurisation of (PhO)₃P (0.1 M) using various PADS species (1 M) as a function of pyridine pKa. Reactions followed by ^{31}P NMR in acetonitrile-d3 at 25°C

Sulfurising Agent	β_{nuc}
Fresh PADS	0.43
24 h Aged PADS	0.23
48 h Aged PADS	0.26
2,2,2´,2´-tetramethyl PADS (**4**)	0.30
DBDS (**5**)	0.16

Table 14: β_{nuc} values for sulfurisation of (PhO)₃P (0.1 M) using various sulfurising agents (1 M) whilst varying the base catalyst (2 M)

Previously (section 4.1) it was suggested that the mechanism of sulfurisation of phosphites using fresh PADS proceeds via a pathway in which the pyridine acts as a base to remove one of the methylene protons from the phenylacetyl- group of the phosphonium intermediate (Scheme 24). The pK_a of these protons in the intermediate formed by attack of the phosphite on PADS and the intermediate formed by attack of the phosphite on the polysulfides present in aged PADS solutions can be expected to be very similar due to the similar electronic environment. Therefore, since the pK_a values of the respective pyridines remain constant throughout the experiment, if decomposition of the polysulfide phosphonium proceeded via a base catalysed mechanism (as seen with fresh PADS) the dependence of the rate of reaction on the pK_a of the base would be expected to be roughly the same as the pK_a ratios remain the same. As can be seen from the results (Fig. 52), however, the dependence on pyridine pK_a is much lower in aged PADS than in fresh PADS. In fact, the β_{nuc} values for aged PADS solutions are more similar to those seen when using 2,2,2′,2′-tetramethyl-2,2′-phenylacetyl disulfide (**4**) and dibenzoyl disulfide (**5**), molecules that react by a nucleophilic mechanism due to the absence of the methylene protons.

This set of results suggests that the decomposition of the phosphonium intermediate when using aged PADS solutions occurs via a different mechanism to that seen in fresh PADS i.e. not base catalysed. It is likely that the operating mechanism therefore involves nucleophilic attack of the pyridine on the sulfur adjacent to the P-S bond.
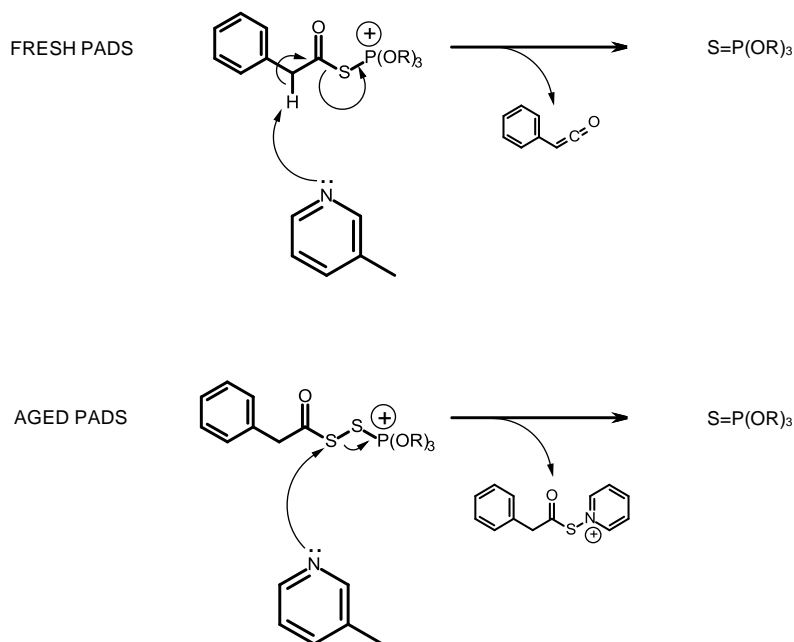
Scheme 26: Base catalysed decomposition of the phosphonium intermediate generated from fresh PADS and nucleophile catalysed decomposition of the phosphonium intermediate formed using aged PADS.

126

A further observation to be made about the effect of the pyridine substituents on the rate of reaction with aged PADS is the effect of using the non-nucleophilic base 2,6-lutidine.

Sulfurising Agent	k_{obs} / s^{-1}
Fresh PADS	5.47×10^{-4}
24 h Aged PADS	7.97×10^{-4}

Table 15: Pseudo first-order rate constants (k_{obs}/s^{-1}) for sulfurisation of (PhO)$_3$P (0.1 M) using fresh PADS (1 M) and PADS aged for 24 h (1 M) using 2,6-lutidine (2 M) as the base catalyst followed by ^{31}P NMR at 25°C in acetonitrile-d$_3$

Using the equation of the correlation line of the Brønsted plot of the dependence of the rate of sulfurisation of PADS aged for 24 h on the basicity of the pyridine base the observed pseudo first-order rate constant, k_{obs}, for the reaction using 2,6-lutidine as the base would be expected to be ca. 7.33×10^{-3} s^{-1}. The value actually observed of 7.97×10^{-4} s^{-1} is ten-fold slower than this. Since 2,6-lutidine is unable to act as a nucleophile due to the steric bulk around the nucleophilic nitrogen atom, it can be assumed that the observed value of $k_{obs} = 7.97 \times 10^{-4}$ s^{-1} is the rate constant for base catalysed decomposition of the polysulfide phosphonium intermediate. The fact that this value is approximately the same as the value observed using fresh PADS ($k_{fresh}/k_{aged} \approx 0.7$) is further evidence that the rate-limiting steps of the reaction of fresh PADS and aged PADS with phosphites proceeds via two different pathways.

It is likely that the change in the mechanism of the rate-limiting step (the breakdown of the phosphonium intermediate in both cases) in moving from fresh PADS to aged is the cause of the observed rate enhancement. The reason for this rate enhancement can be explained fairly simply when looking at the proposed mechanisms of each process (Scheme 26). The base catalysed degradation must proceed via the breakage of a carbon-sulfur bond ($\Delta H_{diss} = 272$ kJ.mol^{-1}) whereas the nucleophile catalysed process proceeds via the breakage of a sulfur-sulfur bond ($\Delta H_{diss} = 226$ kJ.mol^{-1})[101]. The difference in the bond dissociation energy of these two bonds makes the nucleophilic process energetically favoured. It is also worth noting that whilst the reactions of (**4**) and (**5**) also proceed via a nucleophilic catalysed process, these processes also require the breakage of a carbon-sulfur bond and are therefore slower. It may also be the case that in these systems there is a greater degree of reversibility in the breakdown of the phosphonium ion intermediate.

127
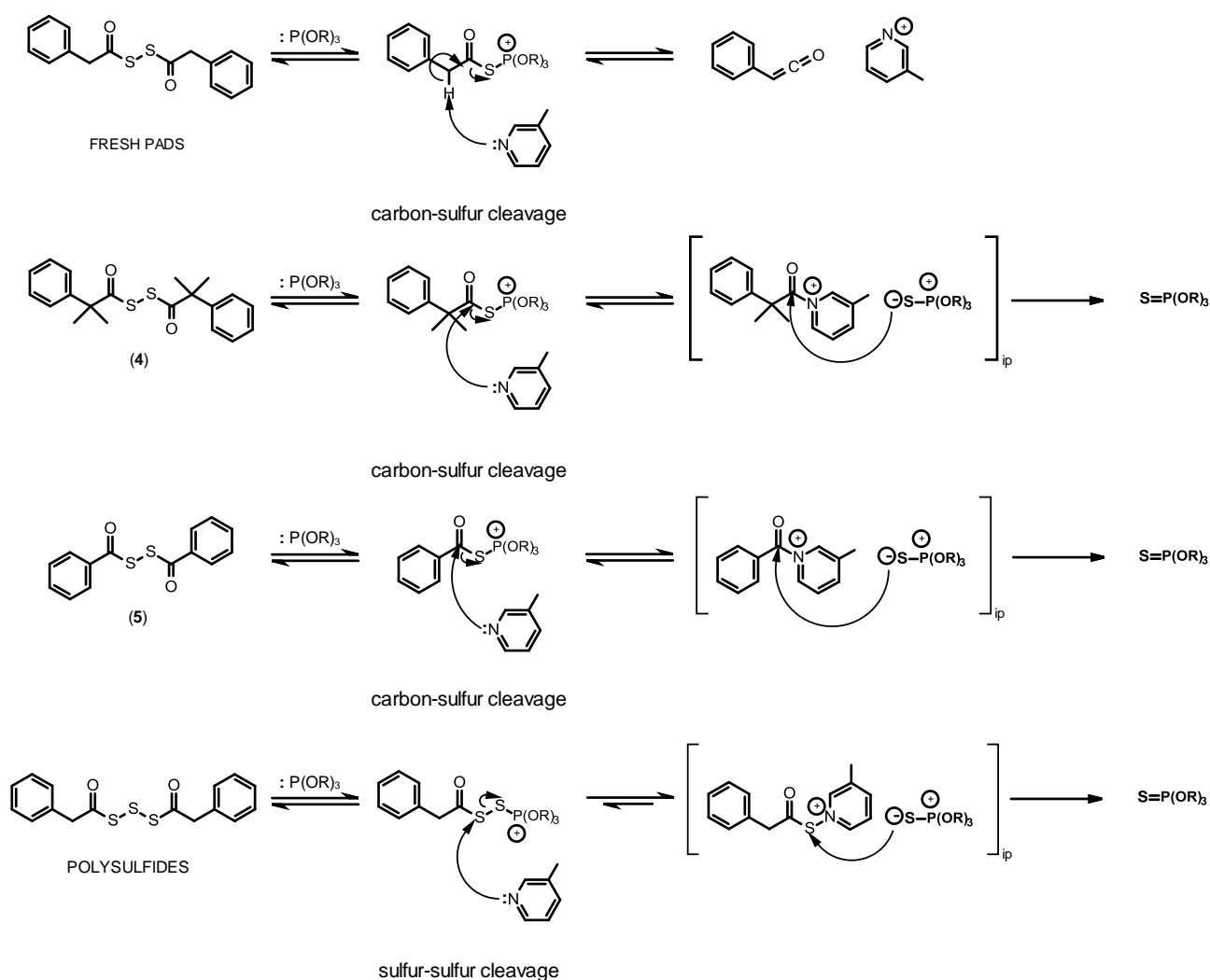
Scheme 27: The nucleophilic breakdown of the various phosphonium intermediates formed by reaction of fresh PADS, (4), (5) and polysulfides with phosphites.

The carbon atoms in the C-N bonds in the reactions of the tetramethyl PADS derivative (**4**) and dibenzoyl disulfide (**5**) have less electron density than the sulfur atom in the S-N bond due to the electronegative oxygen and nitrogen atoms bonded to it. Therefore this carbon is a better electrophile and is more susceptible to nucleophilic attack by the sulfide anion in the ion pair. Also, the formation of a carbon-sulfur bond ($\Delta H_{diss} = 272$ kJ.mol^{-1}) is more energetically favourable than the formation of a sulfur-sulfur bond ($\Delta H_{diss} = 226$ kJ.mol^{-1})[101].

4.2.3 Effect of 3-Picoline Concentration on the Rate of the Sulfurisation Reaction using Aged PADS

In earlier experiments it was shown that the sulfurisation of phosphites using aged PADS solutions can be catalysed by pyridines. When using aged PADS solutions it is possible for the reaction to proceed slowly without the presence of a pyridine. However, no reaction is observed with fresh PADS if there is no pyridine present. It is thought that this slow sulfurisation reaction with aged PADS could be due to the fact that during the ageing process, polysulfide anions are produced (see section 3 for further details). It is possible that, in the absence of a pyridine, these polysulfide anions could act as a nucleophile to facilitate the conversion of the reaction intermediates into products. Extending the sulfur chain in these anionic species drastically increases the pK_a, and thus the nucleophilicity, of the anionic sulfur. In fresh PADS, the thioacetate by-product is not a good enough nucleophile and no reaction is observed.

A further difference between the two systems can be seen by comparing the relative dependencies of the rates of reaction of fresh PADS and aged PADS solutions on the concentration of base. For aged PADS there is a non-linear dependence of the rate constant on the concentration of base (Fig. 53) whereas for fresh PADS, over the same concentration range, the correlation remains linear (Fig. 42).
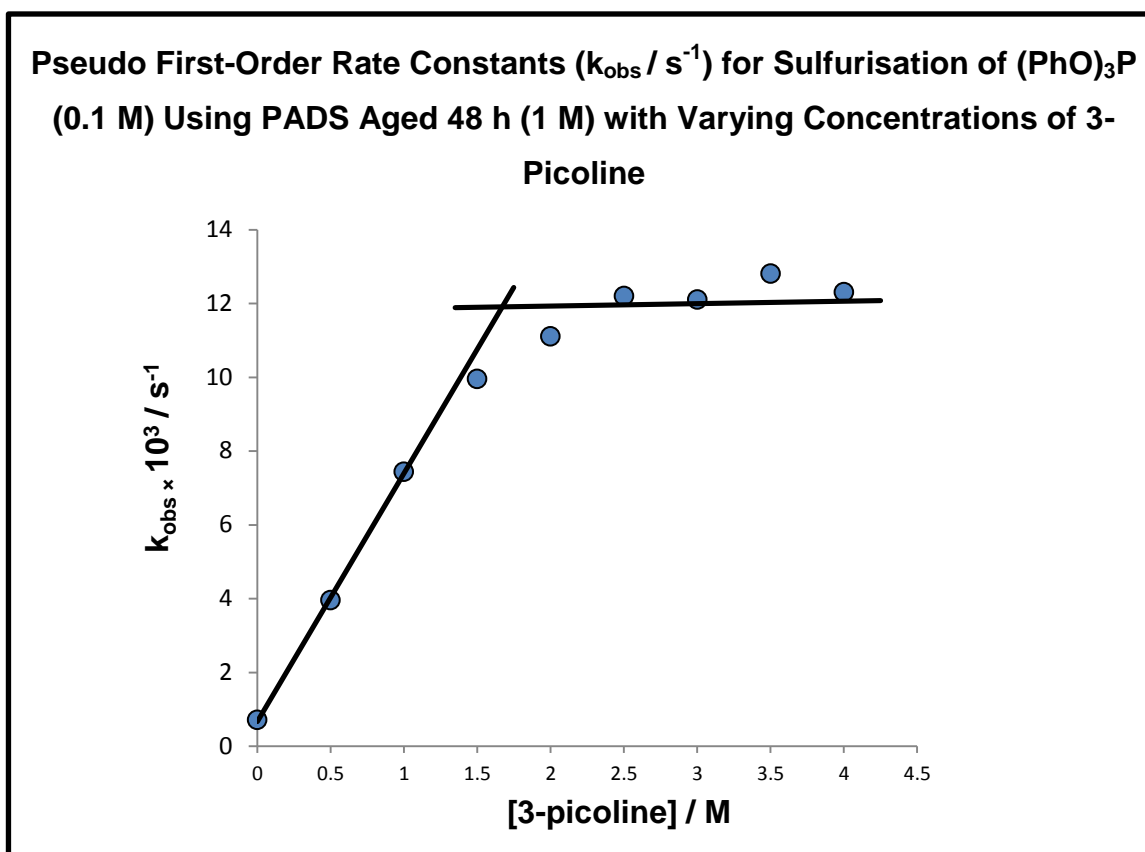
Figure 53: Observed pseudo first-order rate constants for the of sulfurisation of P(OPh)₃ (0.1 M) using PADS aged for
48 h (1 M) as a function of the concentration of 3-Picoline at 25°C in acetonitrile-d₃

For aged PADS, at low concentration of 3-picoline, the concentration of base has a large effect.
However, at high concentrations of 3-picoline, the rate constant appears to become near-
independent of base concentration. This is again indicative of an alternative mechanism of
phosphonium decomposition when moving from fresh PADS to aged PADS. The fact that the
reaction becomes independent of base concentration suggests a change in the rate limiting step due
to a more facile reaction pathway (i.e. the nucleophilic pathway suggested in section 4.2.2) and the
rate laws for these processes can be written as follows:

$$at\ low\ [3-Picoline]\ k_2[Pic] \ll k_{-1}[S^-]\ so\ Rate = \frac{k_1 k_2 [PADS][Phos][Pic]}{k_{-1}[S^-]}$$

$$at\ [3-Picoline]\ k_2[Pic] \gg k_{-1}[S^-]\ so\ Rate = k_1\ [PADS][Phos]$$

Where [Phos] = Phosphite, [S⁻] = 2-phenylthioacetate and [Pic] = 3-Picoline.

This change in the rate limiting step in moving from low to high concentration of 3-picoline can also be seen when looking at the effect of increasing the concentration of 3-picoline on the reactions of 2,2,2′,2′-tetramethyl PADS (**4**) and dibenzoyl disulfide (**5**) which, as mentioned earlier are only able to participate in mechanisms involving nucleophilic decomposition of the phosphonium intermediate (scheme 27).
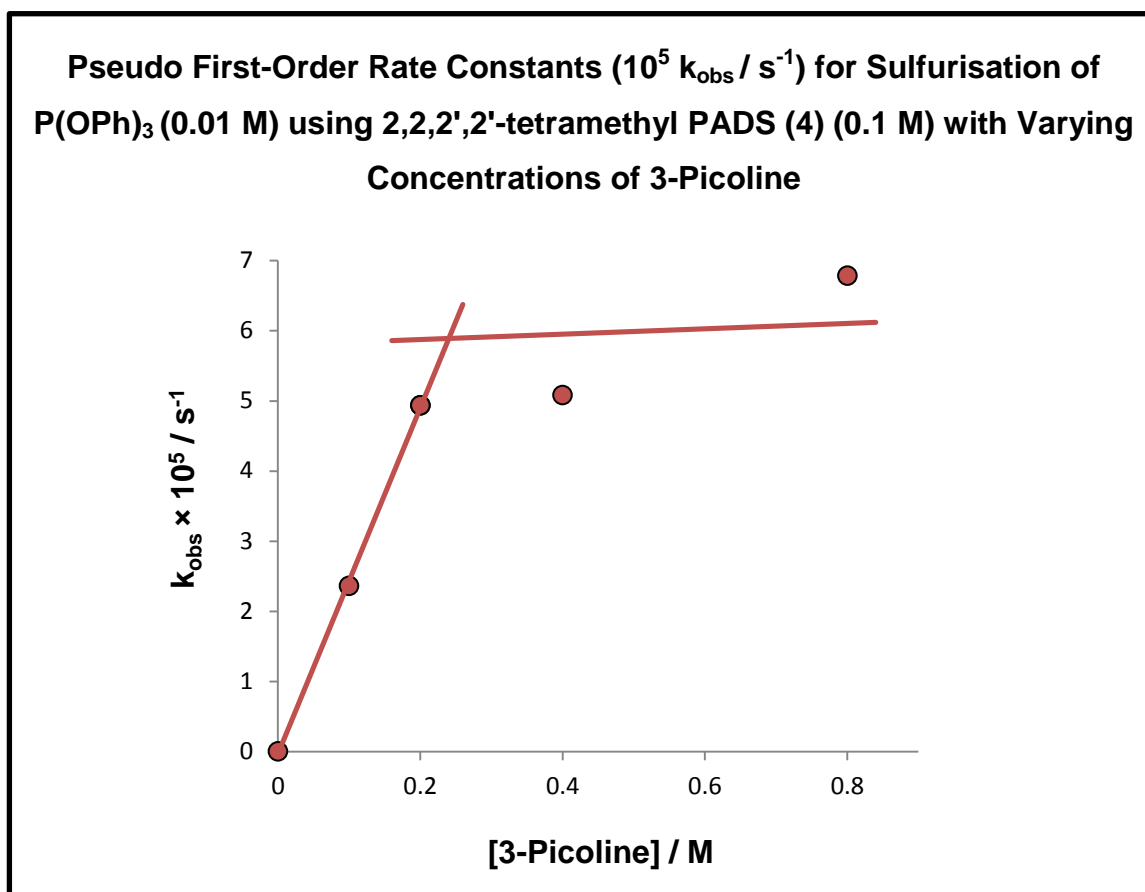
*Figure 54: Observed pseudo first-order rate constants for sulfurisation of (PhO)₃P (0.01 M) using 2,2,2′,2′-tetramethyl PADS (**4**) (0.1 M) with varying concentrations of 3-picoline in acetonitrile-d₃ at 25°C. Reactions followed by ³¹P NMR*
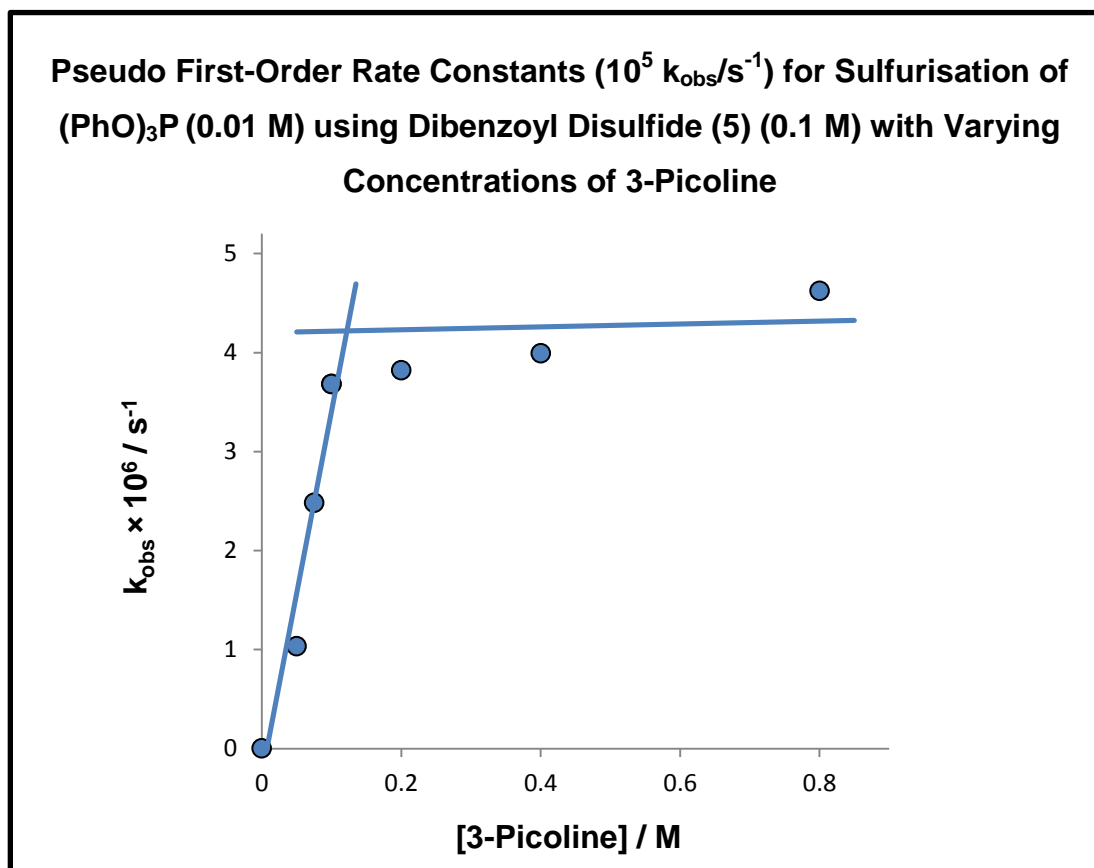
Figure 55: Observed pseudo first-order rate constants for sulfurisation of (PhO)₃P (0.01 M) using dibenzoyl disulfide (5) (0.1 M) with varying concentrations of 3-picoline in acetonitrile-d₃ at 25°C. Reactions followed by ³¹P NMR

A further observation can be made here about the fate of the pyridinium ion. All the kinetics studies were run under pseudo first order conditions i.e. reagents other than phosphite were in at least 10 fold excess in order to prevent the concentration of these species changing significantly throughout the course of the reaction and affecting the observed rate. However, analysis of aged PADS mixtures has shown that during sample preparation (see section 2.8 for details) up to 25% of the molar amount of the polysulfides present in solution can be lost. This changes the molar excess of the sulfurising agent from 10 fold to 7.5 which would no longer generate strictly pseudo first-order conditions. However, despite this the reactions using aged PADS solutions prepared in this way still exhibited good first-order kinetics. It can therefore be assumed that the concentration of **active** sulfur transfer reagent does not change regardless of the concentration, and this can be possible if reactive sulfurising species are regenerated (Scheme 28).
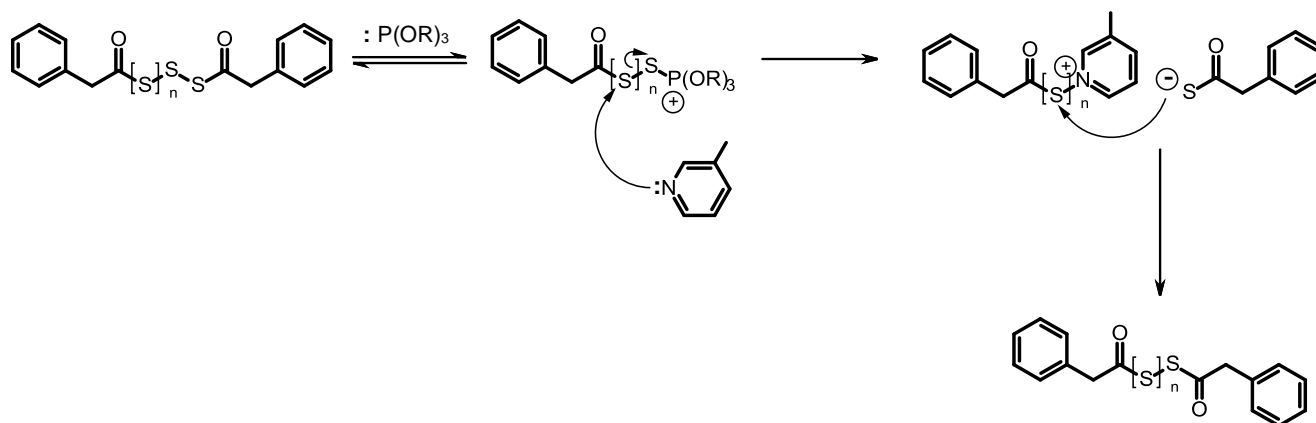
Scheme 28: Possible scheme for regeneration of an active sulfur transfer reagent during the reaction of phenylacetyl disulfide with a phosphite in the presence of a nucleophile.

This is possible due to the fact that the pK_a of the thioacid is approximately 7 units higher than that of 3-picoline in acetonitrile (Scheme 25). This reaction also neutralises the charged species present in solution which, in acetonitrile, would be relatively unstable.

4.2.4 Summary of the Mechanism of Sulfurisation of Phosphites by Aged PADS Solutions

As discussed in section 4.1, sulfurisation of phosphites using PADS analogues is a third order process in which the rate of the reaction is proportional to all three reaction components: phosphite, sulfurising agent and pyridine base. However, unlike with fresh PADS, the rate of reaction can become independent of base at high concentrations of the pyridine suggesting a change in the rate limiting step of the reaction when using aged PADS. The correlation between reaction rate and 3-picoline concentration using aged PADS (Fig. 53) shows a similar profile to those of the hindered sulfurising agents 2,2,2′,2′-tetramethyl phenylacetyl disulfide (**4**) and dibenzoyl disulfide (**5**) in which, as mentioned, breakdown of the phosphonium intermediate is only able to proceed via nucleophilic attack of the pyridine. This supports the hypothesis that the decomposition of the phosphonium intermediate in aged PADS solutions occurs through nucleophilic attack by pyridine. It is also proposed here that polysulfide anions produced from the ageing process present in aged PADS solutions are able to catalyse the conversion of the phosphonium intermediate to the product phosphorothioate at a much slower rate than 3-picoline, as evidenced by the fact that, unlike when using fresh PADS, a reaction still occurs without base present.

The observed β_{nuc} value when varying the pK_a of the base used in the reactions of aged PADS with phosphites is smaller than that observed when using fresh PADS. This is further support of the pyridines in these reactions acting as nucleophiles and not as bases since the observed β_{nuc} value is more similar to that of 2,2,2′,2′-tetramethyl phenylacetyl disulfide (**4**) and dibenzoyl disulfide (**5**) than to that of fresh PADS in which phosphonium breakdown is catalysed by a proton abstraction mechanism. Similarly, the effect of using hindered bases such as 2,6-lutidine supports the proposal that nucleophilic attack on the phosphonium products using aged PADS is the faster and preferred pathway since when a non-nucleophilic base is used, the rate of reaction becomes more similar to that of fresh PADS ($k_{fresh}/k_{aged} \approx 0.7$).

The rate enhancement seen in moving from fresh PADS to aged PADS has made studying the effect of alkyl substituents on the phosphite difficult. However, due to the fact that more nucleophilic phosphites (alkoxy phosphites) afford faster rates of reaction with aged PADS solutions it can be assumed that the reaction still proceeds via nucleophilic attack of the phosphite on the sulfurising agent.
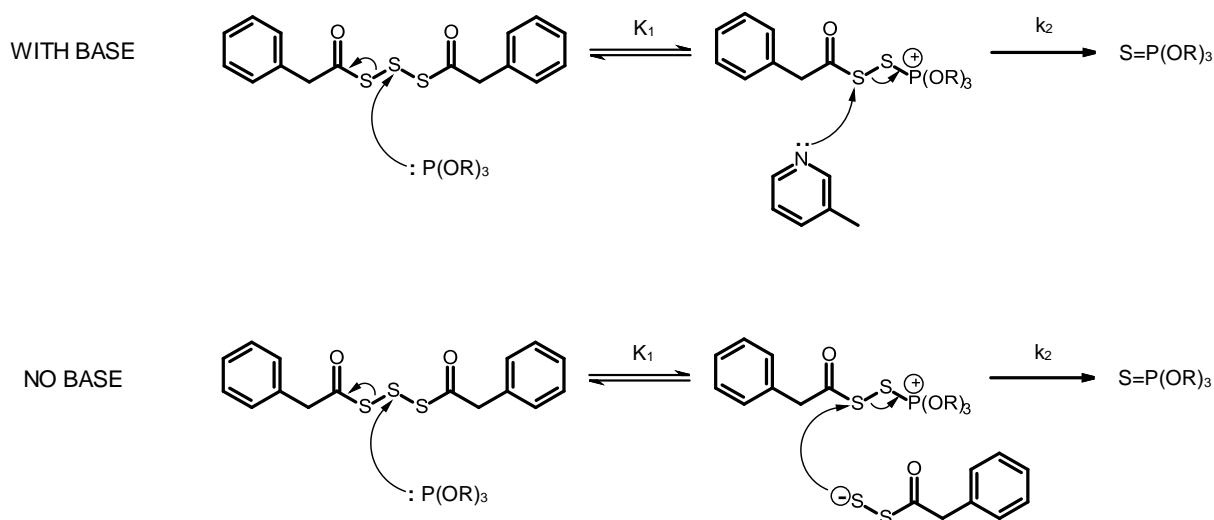
Scheme 29: Mechanism of sulfurisation of phosphites using aged PADS with and without 3-picoline.

Looking at the data therefore it is proposed that the mechanism of the sulfurisation of phosphites using aged PADS solutions is as follows: the phosphite acts as a nucleophile to attack the sulfur adjacent to the terminal sulfur to generate a phosphonium intermediate and phenylthioacetic acid as a by-product. The pyridine then acts as a nucleophile to attack the sulfur adjacent to the P-S bond in order to form the product phosphorothioate and a thio pyridinium derrivative which may react subsequently with the thioacid anion to generate polysulfides.

5. Results and Discussion: Activation and Coupling of Phosphoramidites

The coupling reaction is the second stage of the four-step synthesis of oligonucleotides and involves the reaction of the de-protected 5´ hydroxyl group of the growing oligonucleotide chain with free phosphoramidites that are introduced into the system (Scheme 30). Reactions of phosphoramidites with simple alcohols in the presence of an acid catalyst are extremely fast, this is due in part to the high enthalpy of formation of the P-O bond. For example, reactions of phosphoramidites with even bulky alcohols such as *t*-BuOH using a 1:1 mixture of a tetrazole and a tetrazolide-amine salt as the catalyst (referred to as an activator) display third-order rate constants of the order of 1.2 $M^{-2}s^{-1}$ [81]. However, phosphoramidites are very stable and in the absence of an activator are relatively unreactive.

Activation of phosphoramidites involves initial protonation of the amine group by an acid catalyst. This is followed by subsequent nucleophilic attack by the conjugate base of the acid, used in the initial protonation step, on the phosphorus centre to eliminate an amine, normally di-isopropylamine (Scheme 30) and to form an activated phosphorus species. The kinetics and mechanism of this process are dependent on the solvent, the pK_a of the activator, the pK_a of the amine leaving groups and the equilibrium formed between these two species. Understanding this relationship is key to fully understanding the mechanism of the phosphoramidite-activator system.

This study mainly focuses on understanding the nature of the equilibrium between activator and leaving group which are ethylthiotetrazole and di-isopropylamine respectively.
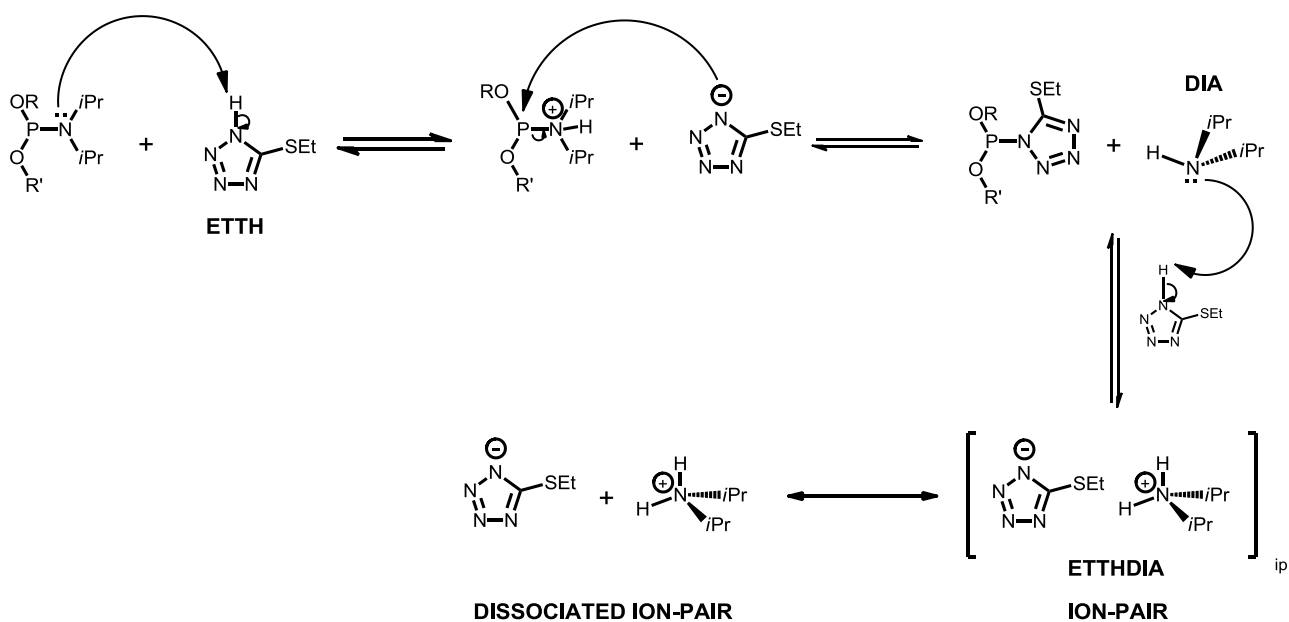
Scheme 30: Activation of di-isopropylphosphoramidites by ethylthiotetrazole

5.1 Determination of the Solubility of Ethylthiotetrazole (ETTH) and Di-isopropylammonium ethylthiotetrazolide salt (ETTHDIA)

In order to study the acid-base equilibrium between the activator and the phosphoramidite it was necessary to determine the solubility limits of the different species in solution. This was done simply by attempting to dissolve a known amount of material in a known volume of acetonitrile at $25^{o}C$ and then calculating the masses of dissolved and undissolved solid in the saturated solutions (Table 16).

	Repetition		
	1	**2**	**3**
Mass of ETTH added (g)	2.93	3.08	2.95
Vol. of ACN (ml)	9.98	10.22	9.96
Mass of undissolved solid measured (g)	0.77	0.90	0.93
Mass of dissolved solid calculated (g)	2.15	2.19	2.02
Moles of Dissolved ETTH (mol)	0.02	0.02	0.02
Concentration (M)	1.66	1.64	1.56
Max concentration	**1.62 M**		
	210.9 g/L		

Table 16: Data table from calculation of maximum solubility of ETTH in acetonitrile at $25^{o}C$

As the phosphoramidites used throughout this work are *N,N*-di-isopropyl phosphoramidites, unreacted or excess activator will form a salt with the di-isopropylamine leaving group. Since this salt formation can alter the equilibrium of the reaction and remove free activator, the solubility of this was also measured. The salt (ETTHDIA) was formed by making up a solution of ETTH in acetonitrile (1.5 M) and adding excess di-isopropylamine to it. Once the solubility limit of ETTHDIA was reached, excess salt precipitated out. This was vacuum filtered and washed with small amounts of ether to remove any excess ETTH or di-isopropylamine. This was dried in an oven and used as pure ETTHDIA in solubility studies. ^{1}H NMR analysis of this solid showed a 1:1 ratio of ETTH and DIA. The maximum solubility of the salt (ETTHDIA) in acetonitrile was found to be **0.22 M** (50.8 g/L).

5.2 Determination of the pK$_a$ of ETTH in Water

Because the activation of phosphoramidites is initiated by a proton transfer from the activator to the phosphoramidite (Scheme 30), this process is dependent on the pK$_a$ of the activator and, perhaps more importantly, the relative pK$_a$s of the activator and the amine leaving group.

Ionisation and ion-pair formation is very dependent on the nature of the solvent. Although the synthesis is conducted in the aprotic solvent acetonitrile it is simpler to measure pK$_a$s in water and so the pK$_a$ of ETTH was determined in water using a standard pH titration. Samples of ETTH (0.1 M, 25 ml) were titrated against NaOH (0.1 M) in deionised water. The pH was monitored throughout the experiment to give a pH profile (Fig. 56.)
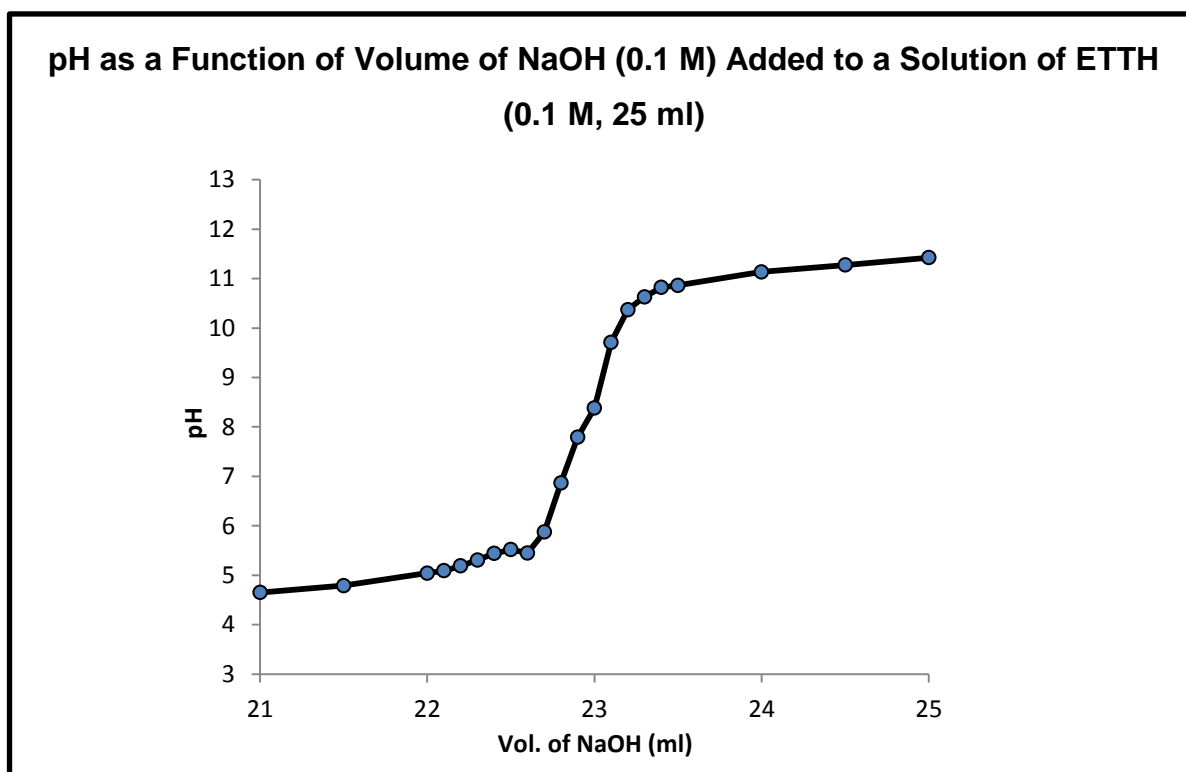
Figure 56: pH profile of titration of ETTH (0.1 M) with NaOH (0.1 M)

The data in the pH profile were fitted to the Henderson-Hasselbach equation which gives a pK_a value for ETTH in water of 3.61.

$$pH = pK_a + \log\frac{[A^-]}{[HA]}$$

Note: At the equivalence point of the reaction (the steepest part of the curve), [A⁻]/[HA] = 1 and so the term 'log ([A⁻]/[HA])' can be removed as log(1)= 0.

The measured pK_a of tetrazole itself in water is 4.5[86], the lower value of 3.6 for ETTH is to be expected since the sulfide group, β to the ionising NH, stabilises negative charge in such systems[124]. However, perhaps more important than the absolute value in determining the efficacy of ETTH as an activator is its pK_a relative to that of the di-isopropylamine leaving group. The free amine has a pK_a (H_2O) of 11.07[111], giving a Δ pK_a of around 7.5 units. This means that, in water, the activator would be expected to protonate the amine group of the amidite generating the positively charged amidite (Scheme 30). However, whilst pK_as in water can be indicative of what the pK_a of a certain species may be in other solvents, different classes of compounds often display varying responses in their pK_a in transferring from one solvent to another. For example, the pK_a of a carboxylic acid changes when moving from water to acetonitrile according to the equation pK_a(ACN) = 1.6 pK_a(H_2O) + 14.9 whereas the same change in solvent for phenols changes the pK_a according to the equation pK_a(ACN) = 1.8 pK_a + 9.6[111]. This means that a carboxylic acid and a phenol that have the same pK_a in water, for example pK_a(H_2O) = 5, would have pK_as that vary by 4.3 units in acetonitrile. This is an important consideration when considering acid-base equilibria in non-aqueous solvents.

5.3 Determination of the pK$_a$ of ETTH in Acetonitrile

An appreciation of the pK$_a$ of ETTH and di-isopropylamine in acetonitrile is essential in order to fully understand the acid-base equilibria in the coupling reaction. This is due to the fact that amines and tetrazoles are likely to respond to the change in solvent differently. Therefore, an attempt was made to determine the pK$_a$ of the activator ETTH in acetonitrile. Measuring the accurate pH of solutions in acetonitrile is difficult and requires specialist equipment; therefore the pK$_a$ could not be measured using the usual titrimetric or spectroscopic methods which require accurate pH. Similarly, since there are very few hydrogen or carbon atoms surrounding the acidic nitrogen in the tetrazole, the use of ^{1}H or ^{13}C NMR was also difficult.

A method using conductance, proposed by Nag and Datta[125] was employed in which the pK$_a$ is determined by looking at the conductance of solutions of various concentrations of the acid (Fig. 57). As only ionised species contribute to conductance, the conductance is proportional to the concentration of (in this system) the ETT$^-$ anion and ACNH$^+$. Using a correlation reported by Gearey[126] it is possible to relate the conductivity of acid solutions to the mole fraction of anion present and therefore to calculate the pK$_a$.
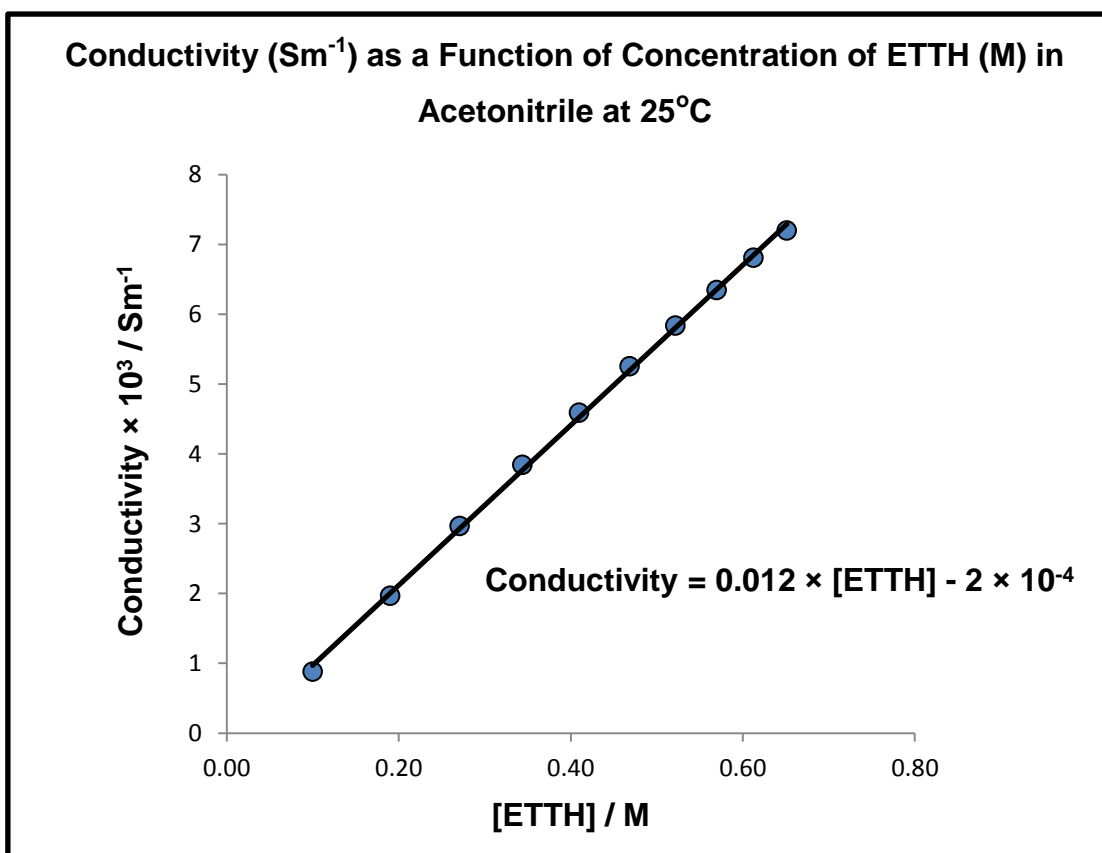
Figure 57: Conductivity (Sm^{-1}) of ETTH solutions as a function of concentration (M) of several solutions of ETTH in acetonitrile at 25°C

141

The data recorded for the conductivity of ETTH solutions can be fitted using the equation detailed by Gearey[126]. However, Gearey's equation takes the value for the average molar conductivity of a 1:1 electrolyte solution to be 140 Scm^2mol^{-1}. This value, however, takes into account strong and weak electrolytes which may have drastically different molar conductivities. Therefore the conductance of a 1 mM ETTHDIA solution was measured so that the molar conductivity of a 1:1 solution of ETT^- and $DIAH^+$ could be used in the calculation, rather than the generic value for 'strong electrolytes'.

The molar conductivity of a 1:1 solution of ETT^- and $DIAH^+$ was calculated as:

Conductivity of 1mM ETTHDIA   = (67.16/1,000,000)*(101.33/100) = **6.81 x 10^{-5} Scm^{-1}**
Molar Conductivity   = (6.81 x 10^{-5}) / (1/1,000,000) = **68.05 Scm^2mol^{-1}**

This value can now be put into the equation, an example is shown below using the values for 0.1 M ETTH.

Cell constant   = 101.33 m^{-1}

ETTH concentration   = 0.1moldm^{-3}

ETTH conductance (G)   = 9.61 µS

ETTH molar conductivity (Λ)   = $\dfrac{(G/1,000,000) \times (cell\ constant\ /\ 100)}{Concentration/1000}$

                                                             = 0.097 Scm^2mol^{-1}

Mole Fraction of ETT^- (F)   = Λ /68.05 = 1.43 x 10^{-3}

K_a = (Concentration x F^2) / (1-F)   = 2.05 x 10^{-7}

$pK_{a\ obs}$ = -LogK_a = **6.69**

The average pK_a ($pK_{a\ obs}$) when combining all the data together was 6.05 which would make ETTH a strong acid in acetonitrile. This is surprisingly low, the ionisation of neutral acids in acetonitrile generates ions which are not well solvated and involves the protonation of the weakly basic nitrile. Hence pK_a values of neutral acids are usually much higher in acetonitrile than they are in water. For example, the pK_a of dichloroacetic acid (pK_a (H_2O) = 1.42) has a pK_a in acetonitrile of 16.4[111]. An estimate of the pK_a can be obtained by looking at the correlation between pK_a (H_2O) and pK_a (ACN) for other similar, N-heterocyclic acids (Fig. 58).

Correlation between $pK_a(H_2O)$ and $pK_a(ACN)$ for various N-heterocyclic acids

$$pK_a(ACN) = (1.68 \times pK_a(H_2O) + 5.66$$
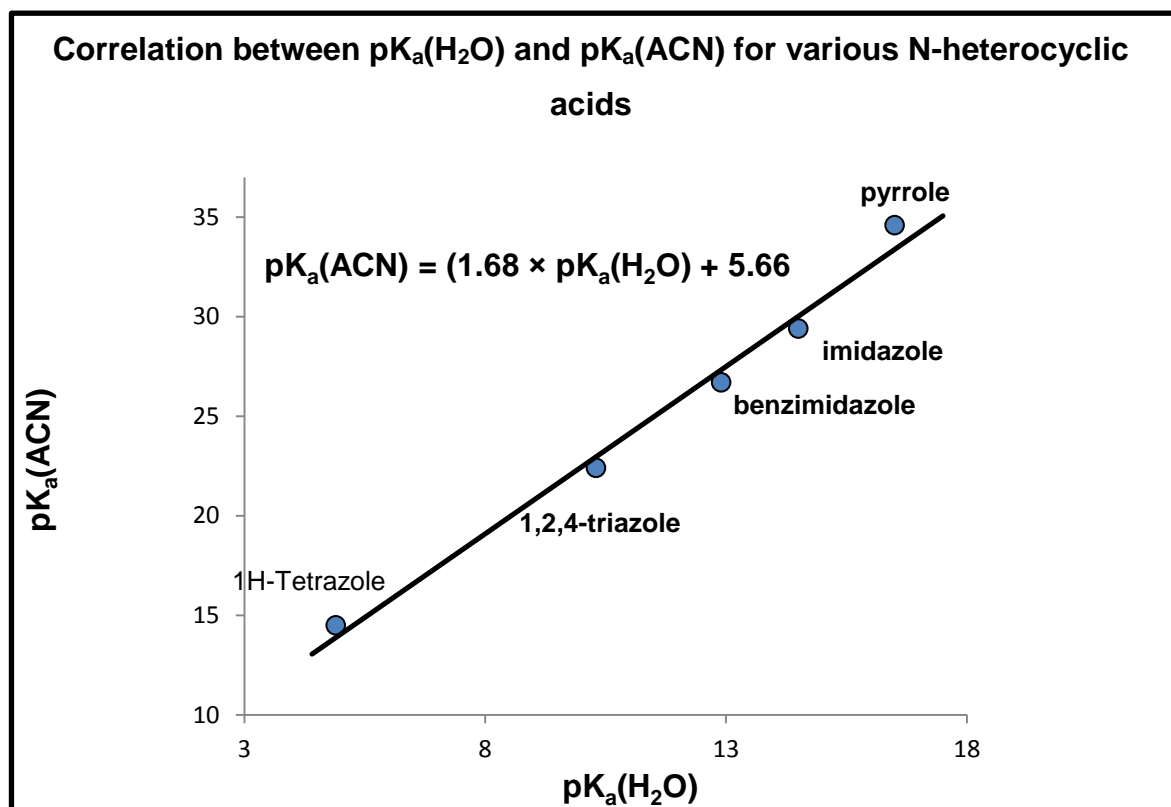
Figure 58: Correlation between pK_a (H_2O) and pK_a (ACN) for various N-heterocyclic acids.

Based on the correlation (Fig. 58), the pK_a (ACN) for ETTH would be expected to be 11.7. The closest compound to ETTH in the table above is 1H-Tetrazole which has a ΔpK_a (ACN-H_2O) of 9.6. The estimated pK_a value of ETTH taken from the graph is clearly vastly different from the experimental value of 6.05. The calculated value of 6.05, determined by conductance, is clearly erroneous.

One reason why these two values may vary so drastically is because tetrazoles exhibit a behaviour known as homo-conjugation in which tetrazolide anions hydrogen-bond to non-dissociated tetrazole molecules (Scheme 31). The effect of this phenomena is more pronounced in non-aqueous solvents as it helps to stabilise the charge of the anion formed by proton dissociation[127]. Since these homo-conjugates affect ion mobility and transport in solution it is possible that $K_{a\ obs}$ is actually an apparent value composed of a contribution from the actual pK_a and the homo-conjugation constant K_{homo}.
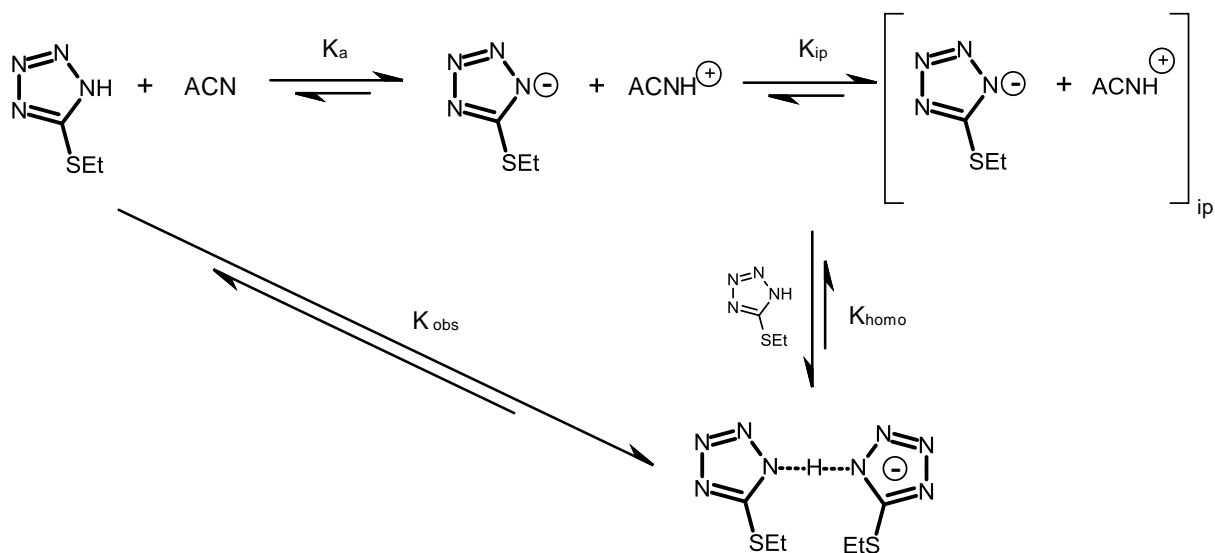
Scheme 31: Homo-conjugation of ETTH with ETT$^-$ [128].

If the above equilibria are active then it is possible to get a feel for the extent of homo-conjugation by estimating the homo-conjugation constant with the following equation:

$$K_{a\ obs} = K_a \times K_{ip} \times K_{homo}$$

If the pK$_a$ of ETTH is taken as the value obtained from the correlation graph (Fig. 58) of 11.7 and and K$_{ip}$ of the ETT$^-$ and ACNH$^+$ ions is taken to be around 10^3 M^{-1} (the order of magnitude expected for K$_{ip}$ in acetonitrile)[111] then the K$_{homo}$ can be estimated as:

$$2 \times 10^{-7} = (2 \times 10^{-12}) \times 10^3 \times K_{homo}$$

$$K_{homo} = \frac{9 \times 10^{-7}}{(2 \times 10^{-12}) \times 10^3}$$

$$K_{homo} = 10^2$$

This suggests that in acetonitrile, ETT$^-$ and ETTH would likely form homo-conjugates. This is likely to distort the conductivity measurements due to the difference in specific conductivity of the ETT$^-$ ion and the homo-conjugate. This could be responsible for the low value obtained for pK$_{a\ obs}$ for ETTH. Alternatively, this can be expressed by assuming the reasonable values of K$_{ip}$ = 10^3 M^{-1} and K$_{homo}$ = 10^2 so using the observed apparent K$_a$ gives a calculated pK$_a$ = 11.7.

5.4 Determination of the Ion-Pair Constant (K_{ip}) for the Acid-Base Equilibrium Between ETT⁻ and DIAH⁺ and [ETTHDIA]$_{ip}$

Another important factor affecting the acid-base equilibrium between activator and leaving group is the ion pairing of the deprotonated activator and the protonated basic leaving group. Examination of the conductivity behaviour of solutions of the ETTHDIA salt shows that the correlation between conductivity and concentration is non-linear which is probably due to ion-pairing.
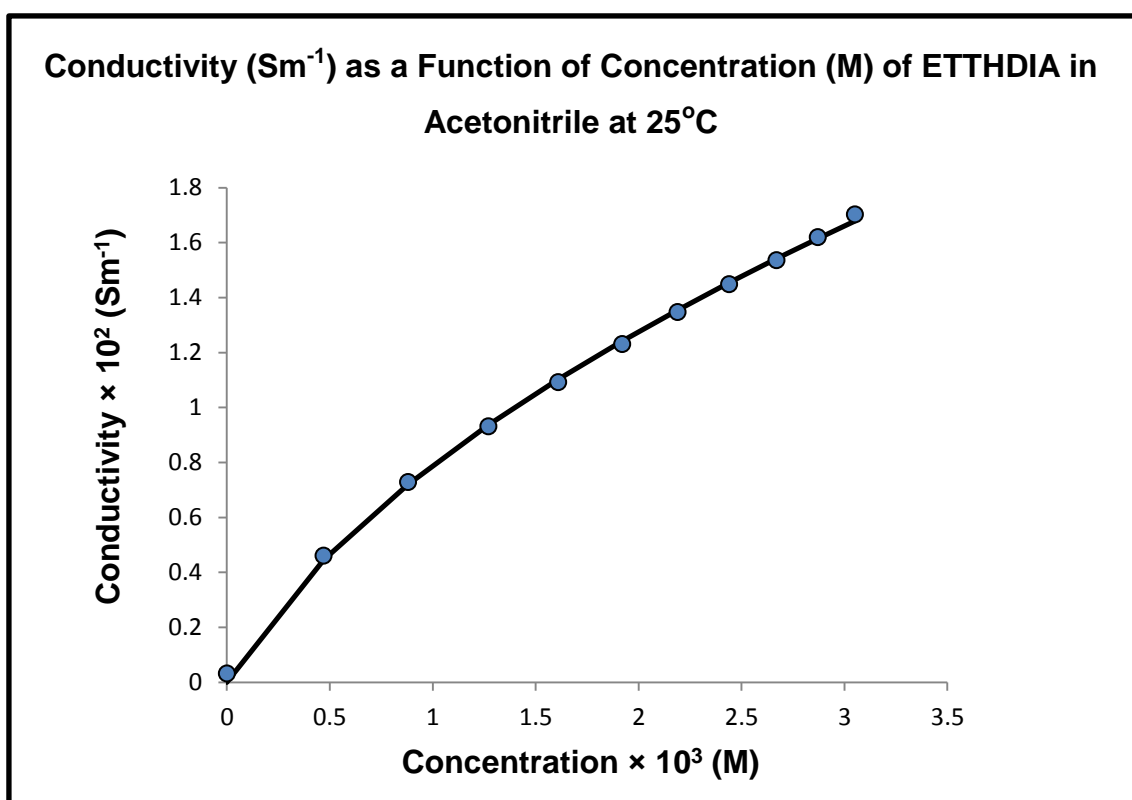
Figure 59: Conductivity (Sm⁻¹) as a function of concentration (M) of several solutions of ETTHDIA in acetonitrile at 25°C

The acid-base equilibria can be described as follows:

$$ETTH + DIA \underset{}{\overset{K_1}{\rightleftharpoons}} ETT^- + DIAH^+ \underset{}{\overset{K_{ip}}{\rightleftharpoons}} [ETTHDIA]_{ip}$$
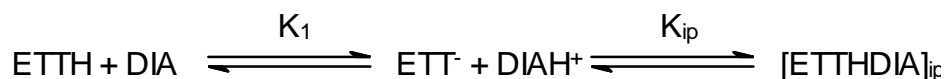
As the salt is a 1:1 mixture of ETTH and DIA, the concentrations of ETTH and DIA are equal, as are the concentrations of ETT⁻ and DIAH⁺.

$$K_1 = \frac{[ETT^-][DIAH^+]}{[ETTH][DIA]} = \frac{[ETT^-]^2}{[ETTH]^2} \qquad K_{ip} = \frac{[ETTHDIA]_{ip}}{[ETT^-][DIAH^+]} = \frac{[ETTHDIA]}{[ETT^-]^2}$$

The conductivity of the solution is proportional to the concentration of the ionic species only and is not affected by neutral acid or base or by ions involved in ion pairing interactions due to the fact that their charges are compensated by the counter-ion. Therefore in order to quantitatively analyse the conductivity data (Fig. 59), an expression for the concentration of the ionic species is required. Assessment and rearrangement of the mass balance of the equilibrium allows expressions for the concentration of the individual species. The mass balances are as follows:

$$[ETT]_{total} = [ETTH] + [ETT^-] + [ETTHDIA]_{ip}$$

$$[DIA]_{total} = [DIA] + [DIAH^+] + [ETTHDIA]_{ip}$$

The equilibrium constants can be rearranged and substituted into the mass balances to give an expression for the individual species in terms of [ETT⁻] or [DIAH⁺]. The concentrations are expressed in terms of the ionic species because these are the only species monitored by the conductivity measurements.

$$[ETT]_{total} = \frac{[ETT^-]}{\sqrt{K_1}} + [ETT^-] + K_{ip}[ETT^-]^2$$

This can now be rearranged into a quadratic equation of the form $0 = ax^2 + bx + c$ as follows:

$$0 = K_{ip}[ETT^-]^2 + [ETT^-] + \frac{[ETT^-]}{\sqrt{K_1}} - [ETT]_{total}$$

This can then be solved according to the following equation:

$$[ETT^-] = \frac{-b \pm \sqrt{b^2 - 4ac}}{2a}$$

Where: $x = [ETT^-]$ $a = K_{ip}$ $b = 1 + \frac{1}{\sqrt{K_1}}$ $c = -[ETT]_{total}$

The total conductivity of a solution (Λ) is equal to the background conductivity of the solution (λ_0) plus the sum of the conductivity of the ionic species multiplied by their individual specific conductivities (ε_x), in this case:

$$\Lambda = \lambda + (\varepsilon_{ETT-} \times [ETT^-]) + (\varepsilon_{DIAH+} \times [DIAH^+])$$

Since the specific conductivities for ETT⁻ and DIAH⁺ are unknown in acetonitrile, these terms must be combined in the equation into one variable term. The quadratic expression for the concentration of the ionic species can then be substituted into the conductivity equation to give the following equation:

$$\Lambda = \lambda + \left(\varepsilon_{total} \frac{-b \pm \sqrt{b^2 - 4ac}}{2a} \right)$$

Using the solver function in Microsoft Excel the data were modelled using a least squares method with the terms b, a and ε as variables whilst the conductivity (Λ), background conductivity (λ) and total concentration of species (c) were as measured during the experiment. This gave a fit (Fig. 59) with the following values for the variables:

K_1	0.36
K_{ip}	6540.02 M^{-1}
ε_{total}	32.50 $Sm^{-1}M^{-1}$

Table 17: Table of calculated equilibrium constants from the modelling of conductivity data of solutions of ETTHDIA

These values indicate that, when ionised, the charged species in the system are strongly ion paired due to the large value of K_{ip}. This is in the range typically expected for ions in acetonitrile[111]. When comparing the gradient of the slope between the conductivity of ETTH in acetonitrile alone (Fig. 57) with the slope of the linear section of the plot of concentration versus conductance measured for the ETTHDIA salt solution (0.9-3.3 mM) it is clear that the salt is around 400 times more conducting than ETTH alone. This is indicative of a much larger degree of ionisation of ETTH with added base despite the low value calculated for K_1. The pK$_a$H of di-isopropylamine has not been determined in acetonitrile but based on the values measured for other secondary amines it is

expected to be around 18 whilst the estimated value of the pK_a of ETTH from calibration data is 11.7. These values predict a favourable equilibrium constant (K_1) for salt formation of around $10^{6.}$

$$\text{ETTH} + \text{DIA} \; \xrightleftharpoons{K_1} \; \text{ETT}^- + \text{DIAH}^+ \xrightleftharpoons{K_{ip}} \; [\text{ETTHDIA}]_{ip}$$
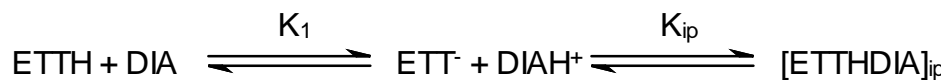
$$K_1 = \frac{[ETT^-][DIAH^+]}{[ETTH][DIA]} = \frac{K_{a\,ETTH}}{K_{a\,DIA}}$$

Conversely, if the pK_a of $DIAH^+$ in acetonitrile is taken to be 18 then, with the equilibrium constant K_1 for salt formation being 0.36, the estimated pK_a of ETTH would be 18.44. This suggests either an error or a more complicated equilibrium than the model is accounting for. This could be due to variances in the specific ion contributions or homo-conjugation of tetrazolide ions and free tetrazole molecules.

Homo-conjugation was briefly discussed in section 5.3.3 where the homo-conjugation constant was estimated to be in the order of $10^2 \, M^{-1}$. The effect of homo-conjugation on conductivity can be seen when adding excess ETTH to a solution of [ETTHDIA] i.e. adding free tetrazole to a solution of tetrazolide ions (Fig. 60). It is clear looking at the data in figure 60 that the conductivity behaviour of ETTH when added to solutions of ETTHDIA is very different from that of ETTH in acetonitrile alone. The first observation to be made from the data is that the relationship between conductivity and concentration of added ETTH is non-linear due to homo-conjugation between free ETTH molecules and deprotonated ETT$^-$ ions (Scheme 31).
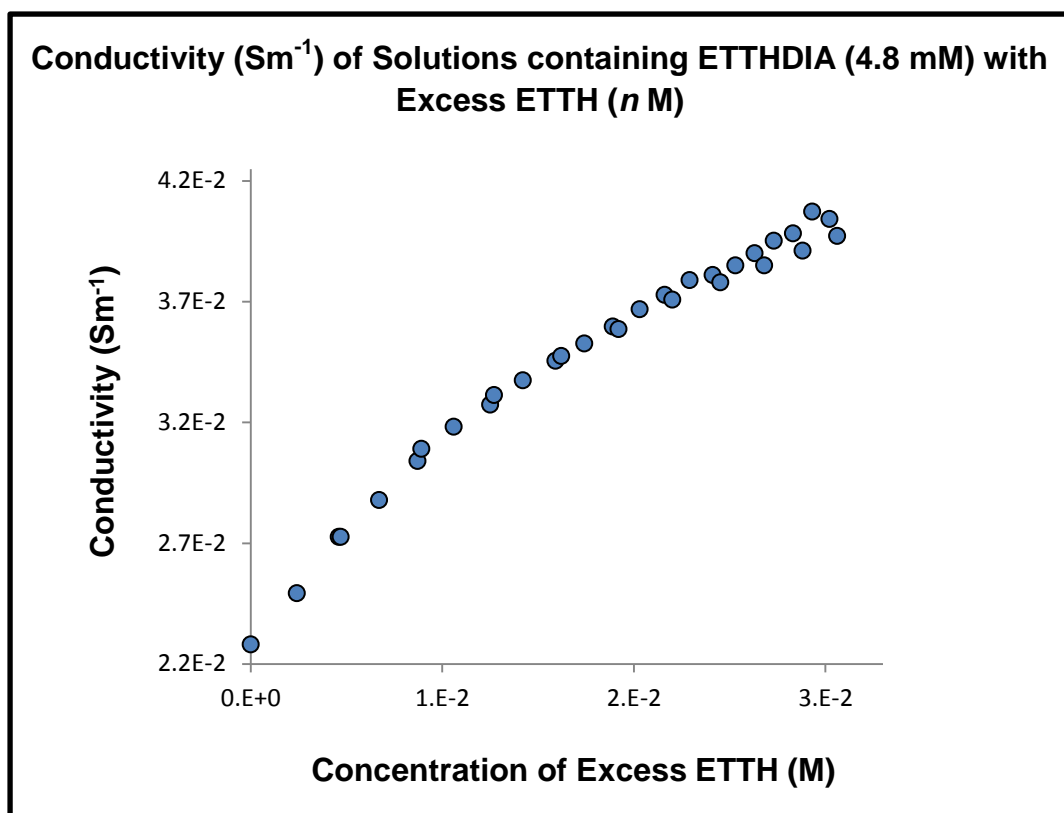
Figure 60: Conductivity (Sm^{-1}) of solutions containing ETTHDIA (4.8 mM) and ETTH (n M)

The second major observation to be made from figure 60 is that adding ETTH to solutions of ETTHDIA has a much larger effect than adding ETTH to acetonitrile alone. For example, adding a 0.01 M amount of ETTH to a 4.8 mM ETTHDIA solution in acetonitrile causes a conductivity increase of 8.78×10^{-4} mSm^{-1} whereas the same amount of ETTH in acetonitrile alone causes a conductivity increase of only 1.1×10^{-5} mSm^{-1}. This increase in conductivity could be due to the excess ETTH pushing the acid-base equilibrium between ETTH and DIA (K_1) towards the right, thus generating more ionic species. A possible further effect of adding ETTH to the ETTHDIA solution could be that excess ETTH disrupts ion pairing between ETT$^-$ and DIAH$^+$ thus generating more conducting species (scheme 31).

More work is needed before the values for K_{homo} can be accurately calculated.

5.5 Kinetics of Activation of 2´-Methoxy-5´-O-DMT-Uridine 3´-CE Phosphoramidite by ETT Followed by Conductivity
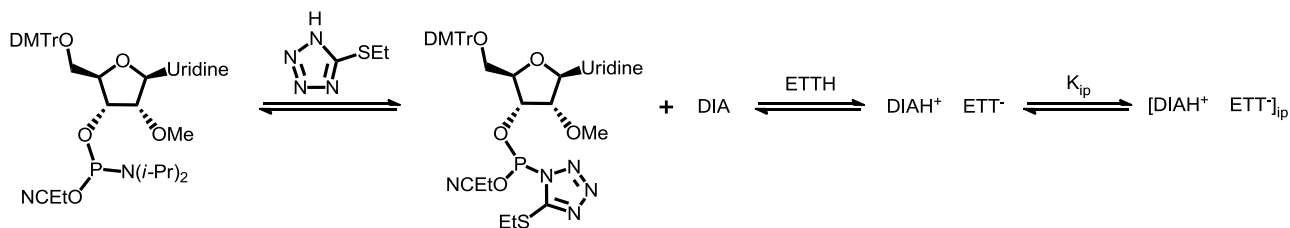
Scheme 32: Activation of UAm using ETT as the activator

The kinetics of activation and alcoholysis of phosphoramidites proved extremely difficult employing conventional methods such as NMR or UV stopped-flow spectroscopy due to the extremely fast reactions (too fast to measure on NMR) or due to the lack of a substantial change in the UV absorbance of the solution. However, it was found that the proton transfer involved in the pre-equilibrium between the activator and leaving group (in this case ethylthiotetrazole and di-isopropylamine) allowed the reaction to be monitored by conductivity measurements: the amine released from the phosphoramidite, reacts with excess ETTH generating ETT$^-$ and DIAH$^+$ and in doing so leads to an increase in conductance (Scheme 32). These measurements could be carried out rapidly and in real-time allowing kinetics to be measured. Since the conductivity behaviour of these solutions is complex and the ion-pairing behaviour of the protonated phosphoramidite is not understood, the conductivity values here have not been rationalised into accurate concentrations.

Several experiments were performed in which the conductivity was monitored of solutions containing 2'-deoxy-5'-O-DMT-uridine 3'-CE-phosphoramidite (5 mM) – referred to hereafter as UAm – with varying excess concentrations of ETTH in order to assess the order of the reaction with respect to ETTH in acetonitrile. The conductivity versus time profiles for these reactions showed a first-order relationship in which there was an exponential increase in conductivity and plots of the natural log of the conductance versus time were linear (Fig. 61).
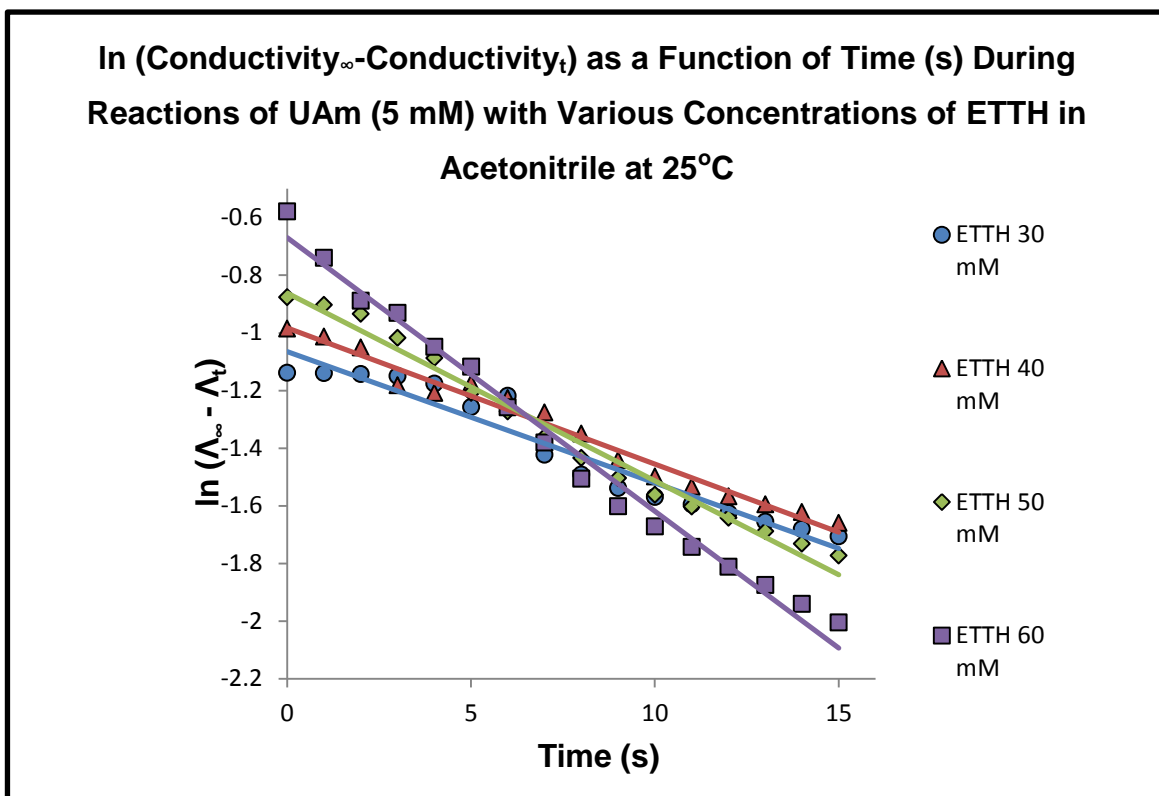
Figure 61: Conductivity measurements (Sm⁻¹) taken during the activation of Uam (5 mM) using varying concentrations of ETTH as a function of time in acetonitrile-d₃ at 25ºC. Concentrations determined by ³¹P NMR
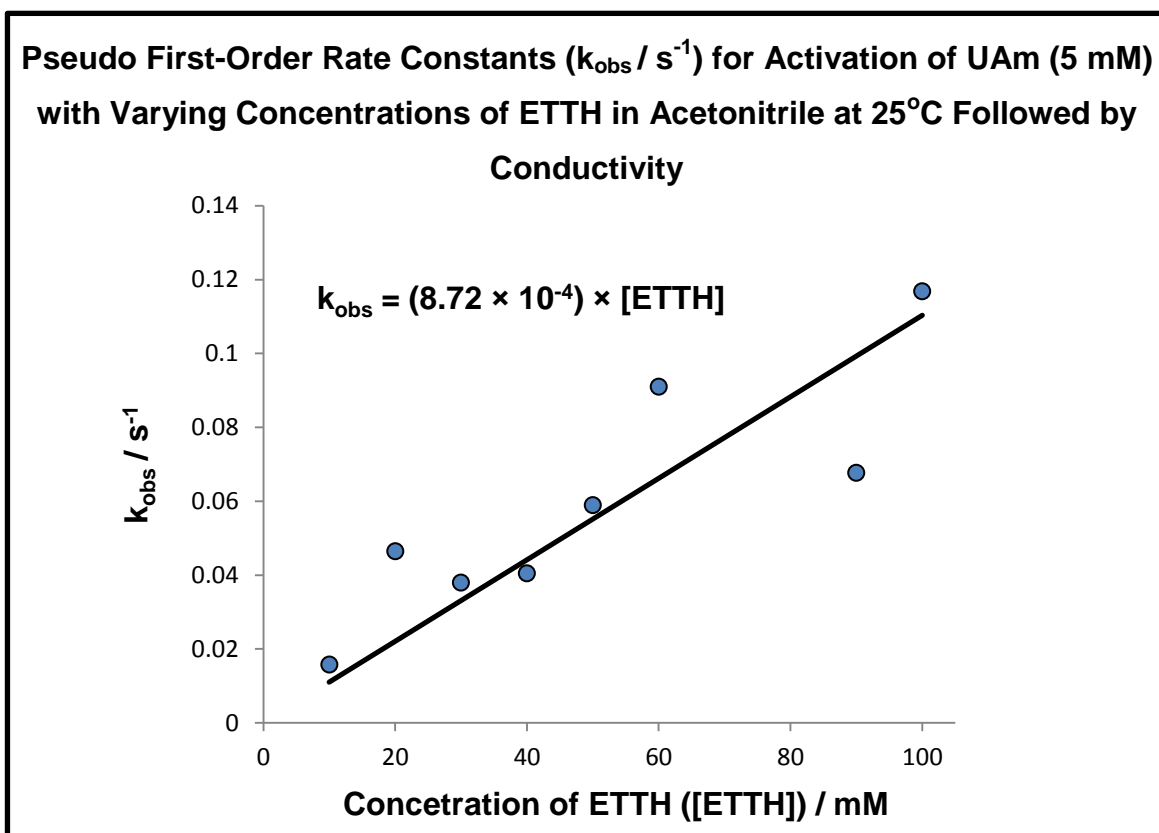
Figure 62: Pseudo first-order rate constants (s⁻¹) for the activation of UAm with various concentration of ETTH as a function of ETTH concentration in acetonitrile at 25ºC followed by conductivity

A plot of the observed pseudo-first order rate constants as a function of the concentration of ETTH (Fig. 62) indicates that the rate of generation of the ionic species during the activation of UAm (and therefore the rate of the reaction) is linearly proportional to the concentration of activator used and the corresponding second order rate constant is 8.72×10^{-4} $s^{-1}M^{-1}$. This signifies a first-order dependence of the rate of activation on the concentration of ETTH.

Acetonitrile is hygroscopic and so absorbs water from the atmosphere. The acetonitrile used in this experiment typically contained 0.4 % w/w (175 mM) H_2O measured by Karl Fischer coulometric titration. Therefore during these reactions there is at least a 3:1 molar excess of water in the reaction which is able to rapidly hydrolyse activated UAm. This hydrolysis reaction generates tetrazolide ions which, as seen previously are able to either engage in ion-pairing with cations present in solution, homo-conjugate with free-tetrazole molecules, or force the acid-base equilibrium (K_1 section 3.5) towards the right thus re-generating free-activator. Therefore it is possible that the observed rate constants are proportional to K_{act} x $k_{hydrolysis}$.

$$k_{obs} = K_{act} \times k_{hyd}$$
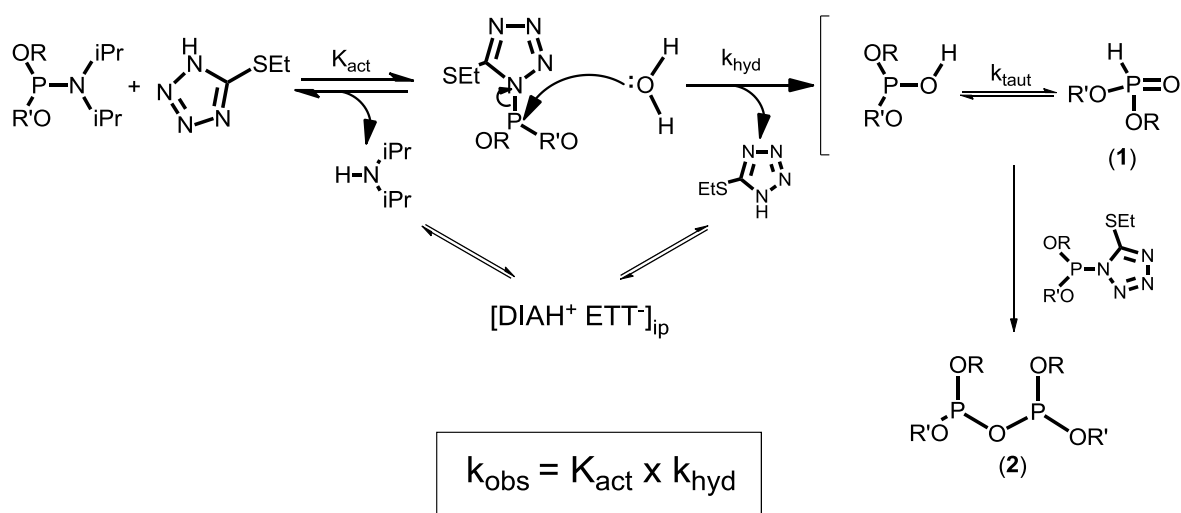
Scheme 33: Mechanism of hydrolysis of activated phosphoramidites.

In order to test this theory, the experiment was repeated, again using Uam (5 mM) with ETTH (50 mM). However in this investigation, varying amounts of methanol were added. Since methanol is a stronger nucleophile than water it was expected that increasing the concentration of methanol should increase the rate of reaction.

Observed Pseudo First-Order Rate Constants (k_{obs} / s^{-1}) of Methanolysis of UAm (5 mM) Using ETTH (50 mM) as an Activator as a Function of Methanol Concentration (mM) in Acetonitrile at 25°C

$$k_{obs} = ((-9.0 \times 10^{-07}) \times [MeOH]) + 0.026$$
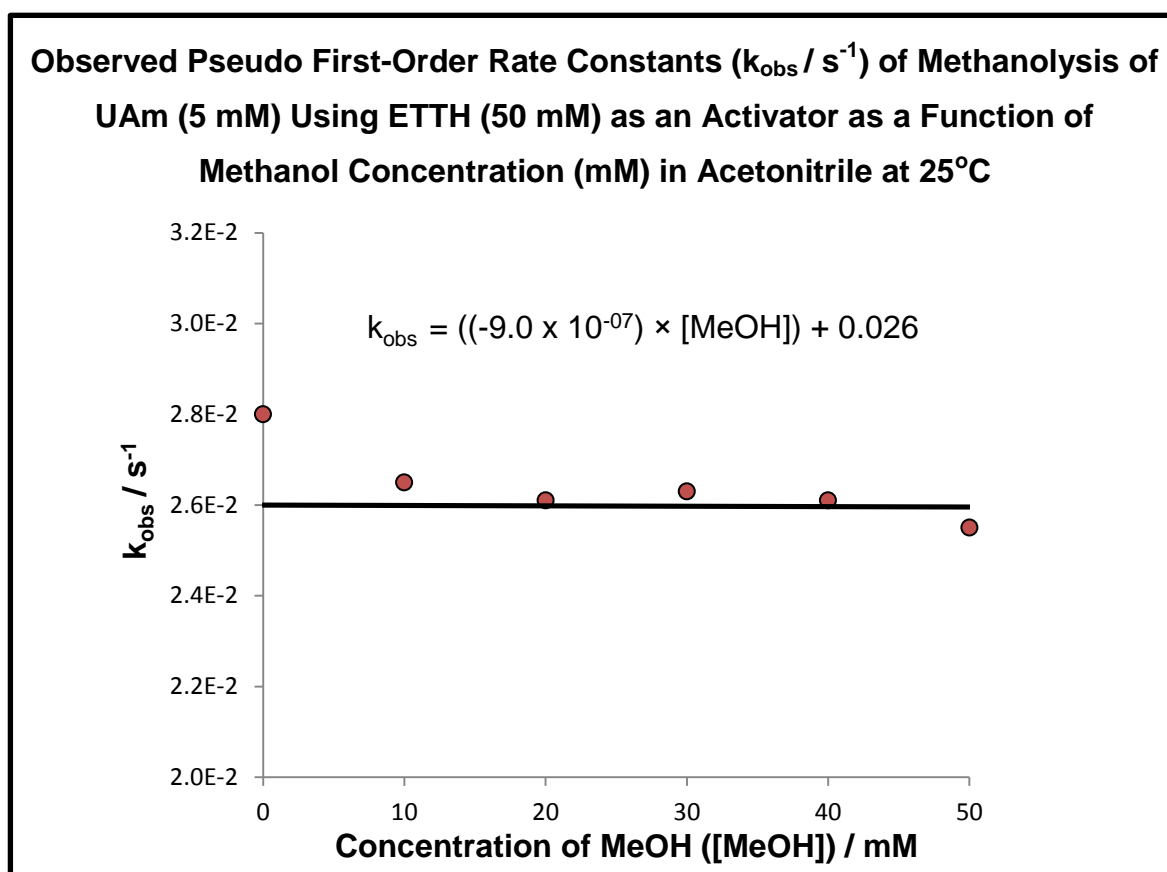
Figure 63: Observed pseudo first-order rate constants (k_{obs}/s^{-1}) for methanolysis of UAm (5 mM) using ETTH (50 mM) as an activator as a function of methanol concentration (mM) in acetonitrile at 25°C

Despite the increased concentration of nucleophiles in solution, the rate of reaction with methanol present was independent of methanol concentration (Fig. 63). Since activated phosphoramidites are known to be highly reactive towards nucleophiles it is likely that the rate of cleavage of the activated phosphoramidite species is much faster than the rate of activation i.e. $k_{hydrolysis} \gg k_{-1\ act}$. This is indicative therefore of a process in which activation of the phosphoramidite with ethylthiotetrazole is the rate limiting step followed by rapid decomposition of the activated species. The rate law for the reaction can be written as:
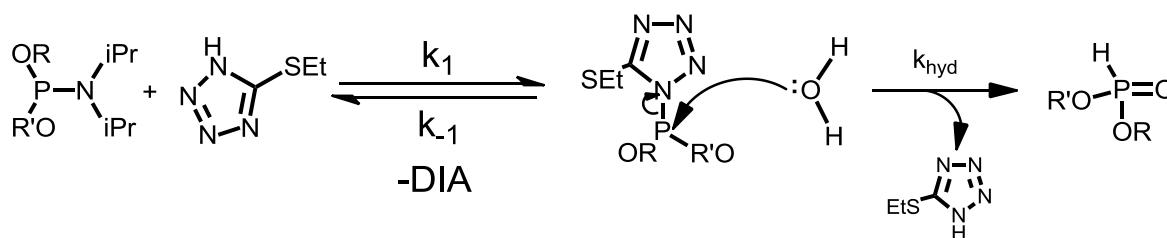
$$Rate_{obs} = \frac{k_1[UAm][ETTH]}{k_{-1}[UAct][DIA]}$$

Scheme 34: Activation and hydrolysis of UAm using ETTH as the activator.

153

5.6 Investigation into the Activation Equilibrium by ^{31}P NMR

The activation of phosphoramidites can be achieved with a number of activators. During activation, an equilibrium is set up, not only between the activator and the amine leaving group (as discussed in previous sections), but also between reactants and products (Scheme 35). This equilibrium is known to be reversible, i.e. adding an excess of the amine leaving group (in this case di-isopropylamine) can push the equilibrium towards the left-hand side[129]. As mentioned previously, the efficacy of the activator is related to its pK_a (in the case of acidic activators) and therefore the position of this equilibrium (K_{act} value) is different for each activator. The activation equilibrium must therefore be investigated using ethylthiotetrazole to assess reversibility.
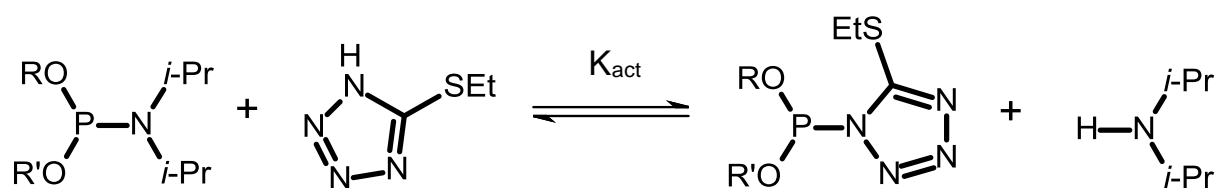
Scheme 35: Equilibrium between un-activated and activated phosphoramidites.

An experiment was set up in which 2'-deoxy-5'-O-DMT-uridine 3'-CE-phosphoramidite (UAm) was titrated using ETTH until full conversion of the starting material to activated species (UAct) was achieved monitored by ^{31}P NMR. To this, di-isopropylamine was added to determine whether the activated species could be converted back to the starting material. The ^{31}P chemical shifts of these species are well known[130]. The structures of the compounds generated during these reactions are shown below:

UAm   UAct   POP   HPhos
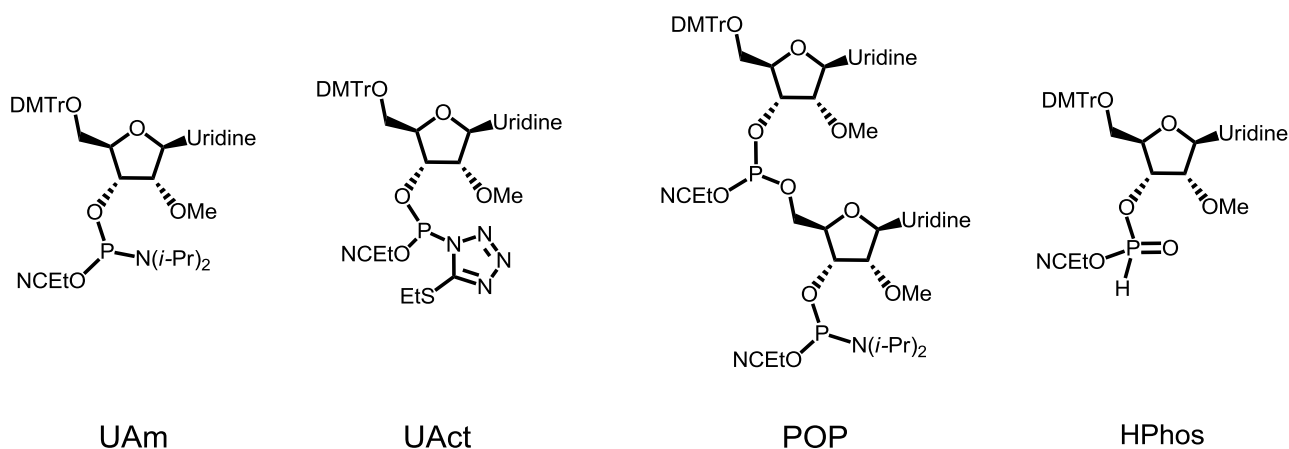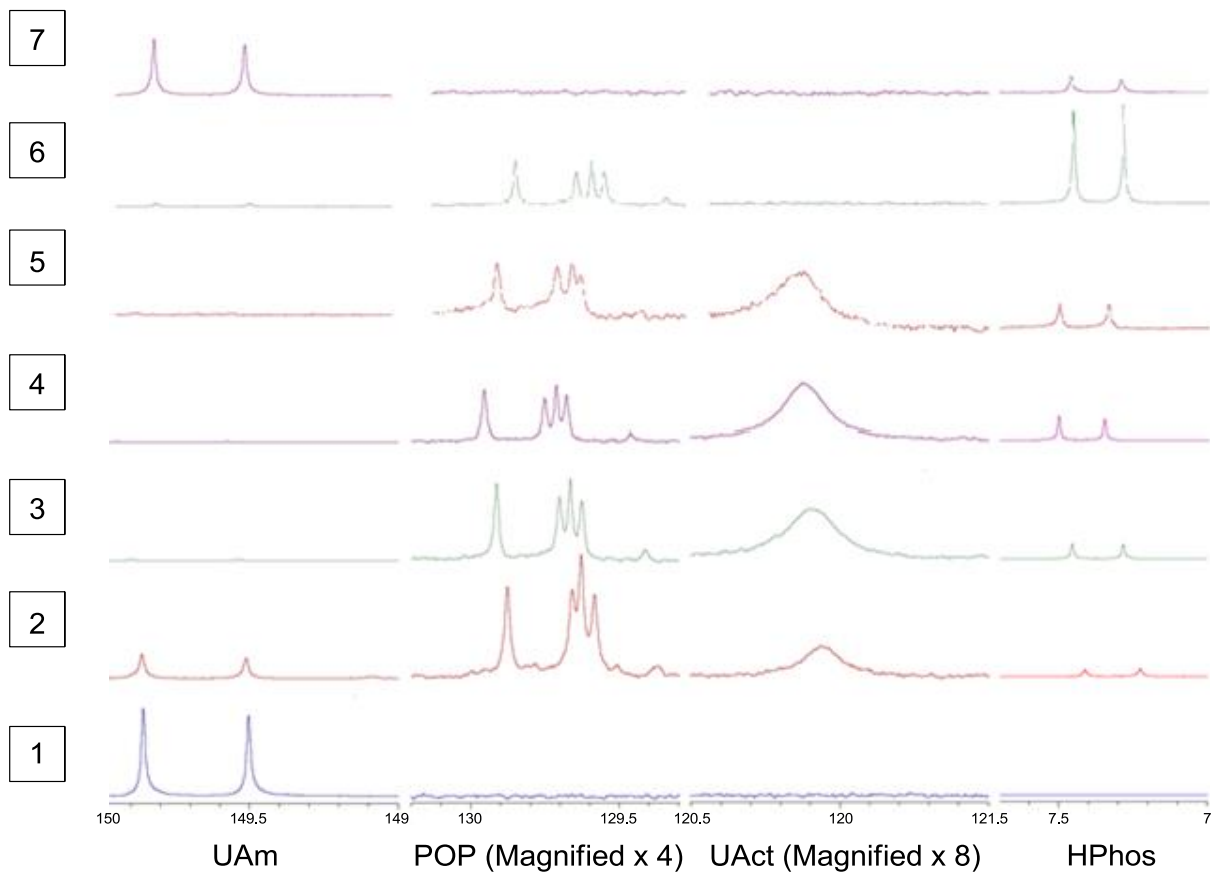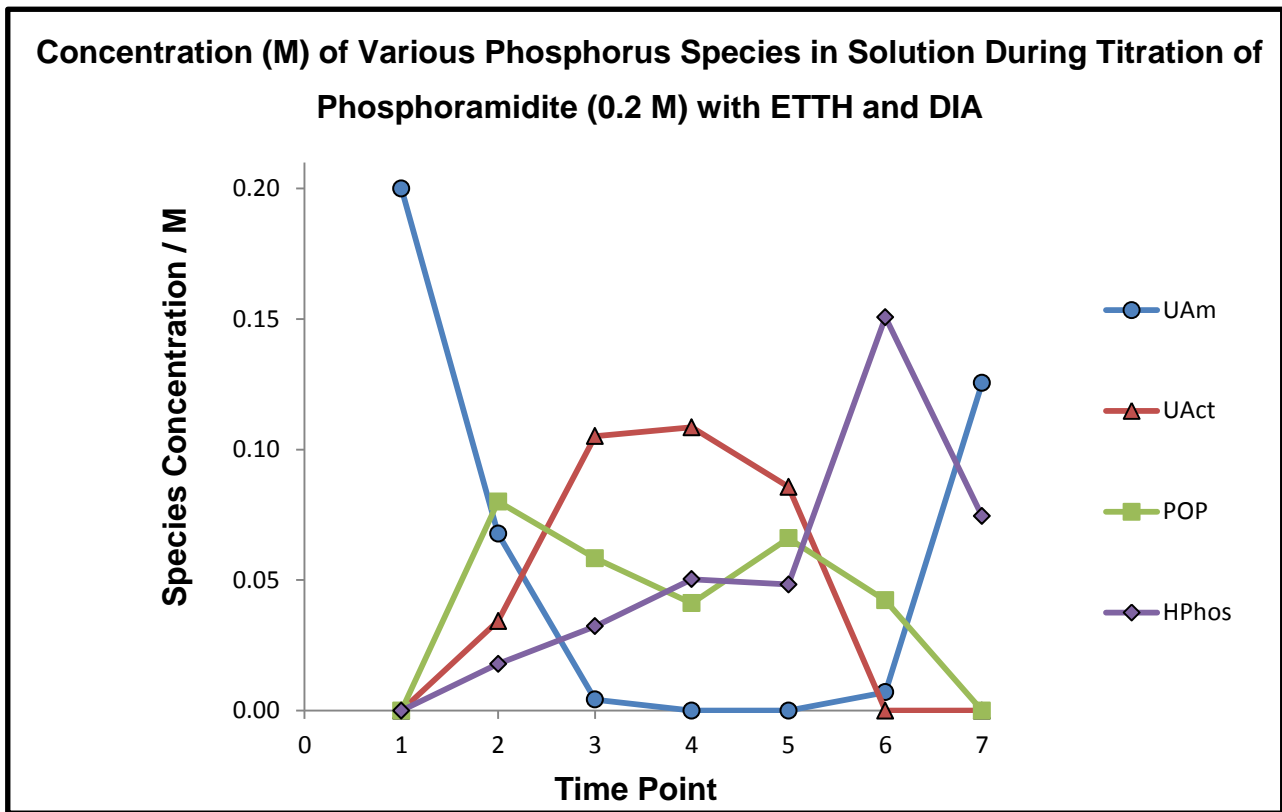
Figure 64: Activation of UAm (0.2 M) using ETT as the activator in acetonitrile. 1: UAm (0.2 M), 2: UAm (0.2 M) + 1eq ETT, 3: UAm (0.2 M) + 2eq ETT, 4: UAm (0.2 M) + 3eq ETT, 5: UAm (0.2 M) + 3eq ETT + 1eq DIA, 6: UAm (0.2 M) + 3eq ETT + 2eq DIA, 7: UAm (0.2 M) + 3eq ETT + 3eq DIA.

The data from these experiments show that the phosphoramidite requires two equivalents of the activator to achieve full conversion to the activated species and this is due to ion-pair formation between the activator and the amine leaving group. The spectra also show that the reaction is indeed reversible: when using excess base the concentration of activated species decreases and the concentration of starting material increases. However, the high reactivity of the activated species means that it is susceptible to nucleophilic attack by any nucleophiles present in the solution, including water, as discussed in the previous section. Thus the spectra also show evidence of the products of hydrolysis of the activated species: H-phosphonate (**1**) and a POP pyrophosphate species (**2**). This hydrolysis distorts the equilibrium somewhat because it not only consumes starting material it also liberates one molecule of activator for each mole of hydrolysed species. (Scheme 36).

$$k_{obs} = K_{act} \times k_{hyd}$$
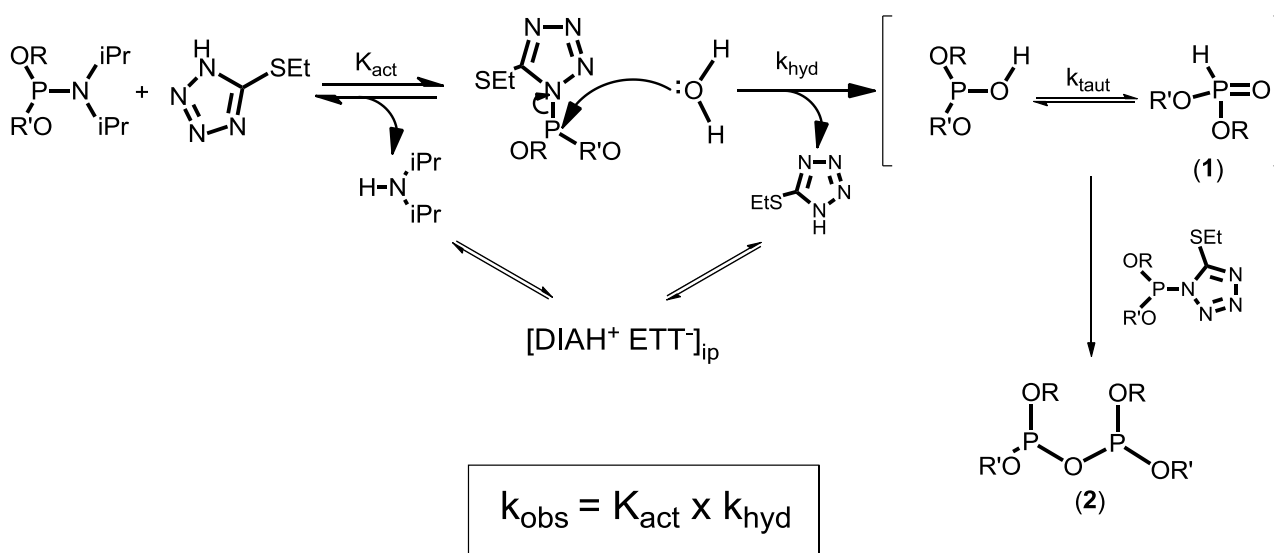
Scheme 36: Mechanism of hydrolysis of activated phosphoramidites

5.7 Investigation of the Kinetics of Activation of di-*tert*-Butyl *N,N*-di-isopropyl phosphoramidite (DBAm) Using Various Tetrazole Activators by ^{31}P NMR

Attempts to follow the kinetics of activation and hydrolysis of a number of phosphoramidites proved difficult since the solvent, and indeed reactants, used in these experiments contained absorbed water which caused full hydrolysis of the activated species within 5 minutes (Scheme 36). This is too fast to follow by conventional ^{31}P NMR since the delay time between starting the experiment and recording spectra is at least 5 minutes. Whilst conductivity allows the determination of reaction rates, it does not allow the quantification of the concentration of individual species (fig. 65). However, since the equilibrium involving activated phosphoramidites and the amine leaving groups is known to be reversible (Fig. 64) a method was devised in which the activation was quenched with excess of a new base at t=*n* s. Adding excess of a different base in this way couples the new base to the activated species, allowing quantification of this species, and also quenches any free activator in solution by reaction with the excess base, preventing further reaction. After the reaction was quenched, a ^{31}P NMR spectrum of the reaction mixture was recorded.
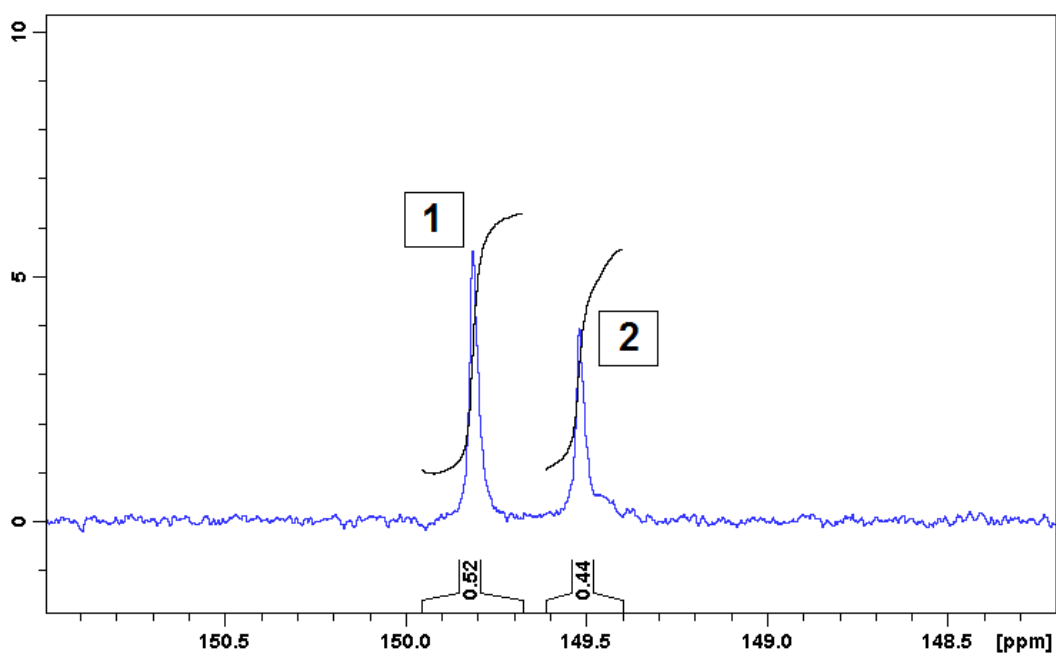
Figure 65: ^{31}P NMR spectrum of activation of DBAm (2.5 mM) using ETTH (5 mM) quenched with diethyl amine (50 eq) at t=30 s in acetonitrile at 25°C. 1: di-tert-butyl N,N-di-isopropyl phosphoramidite; 2: di-tert-butyl N,N-diethyl phosphoramidite

Diethylamine was chosen as the new base, whilst it is basic enough to reverse the activation process, the chemical shift of the N,N-diethyl phosphoramidite is slightly different to that of the N,N-di-isopropyl phosphoramidite. This allows quantification of the concentration of the initial starting material at t= n as the reverse reaction does not re-generate the starting material. Attempts to follow the kinetics of activation by NMR had previously been unsuccessful, and so di-*tert*-butyl N,N-di-isopropyl phosphoramidite (DBAm) was chosen as the phosphoramidite due to its reported low coupling efficiency[131].

Monitoring reaction kinetics in this way allowed the rates of activation of DBAm to be measured using 5 different substituted tetrazole activators (substituted at the 5´ position) (Table 18). Again, these reactions showed first-order kinetics even at low concentrations of activator, due to the regeneration of the activator catalyst with subsequent hydrolysis of the activated species.

Activator	Abbreviation	k_{obs} / s^{-1}	pK$_a$(sol.)
Tetrazole	TetH	1.20×10^{-3}	4.73
Methylthiotetrazole	MTTH	9.32×10^{-3}	3.89
Ethylthiotetrazole	ETTH	8.20×10^{-3}	3.85
4-Fluorophenyltetrazole	(4-F-Ph)TH	5.56×10^{-3}	3.96
Phenyltetrazole	PhTH	4.18×10^{-3}	4.07

Table 18: Pseudo first-order rate constants (k_{obs} / s^{-1}) for reaction of DBAm with various tetrazole activators

In order to quantify and properly compare these results, the pK$_a$(sol.) of these activators were determined in a solvent mixture of 10% v/v DMSO in water (Table 18). This solvent composition was chosen as some of the activators were highly insoluble in water and so needed the DMSO co-solvent before any experiments could be performed. Addition of 10% DMSO was not expected to alter the ability of the pH probe to measure the pH. The pK$_a$(sol.)s of the activators were determined by pH titration with NaOH in 10% DMSO in H$_2$O in a similar way to that used to measure the pK$_a$(H$_2$O) of ETTH. Using these data, a Brønsted plot (Fig. 66) was constructed in order to determine the dependence of the rate of activation on the pK$_a$ of the activator.
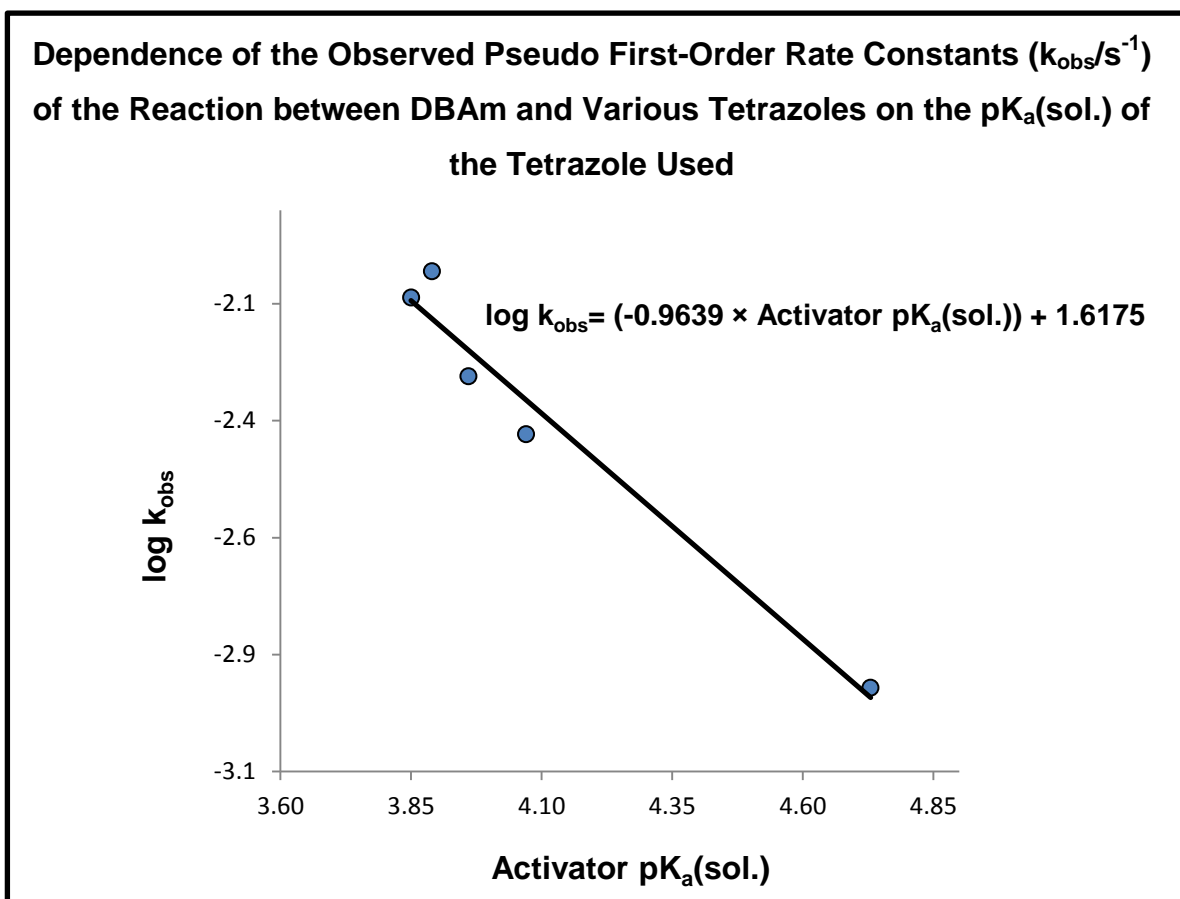
Figure 66: Brønsted plot showing the dependence of the observed rate constants of reaction of DBAm with various tetrazoles on the $pK_a(sol.)$ of the tetrazole.

Although the Brønsted plot covers only a narrow range of pK_a it clearly indicates activity increase with increased acidity of the activator. Correlation of the $pK_a(s)$ of the activators with the observed rate constants shows a linear correlation. The fact that the observed α-value is approximately equal to 1 indicates that activation of phosphoramidites proceeds via specific acid catalysis involving a rapid pre-equilibrium in which a proton has been completely transferred to from the protonated reactant in the transition state. It can be said, therefore, that activation proceeds via a two-step process: step 1- proton transfer to the phosphoramidite amine group followed by a nucleophilic attack by the conjugate base of the activator at the phosphorus centre (Scheme 37).

$$\text{Rate} = k_1 k_2 \text{ [DBAm] [TetH]}$$
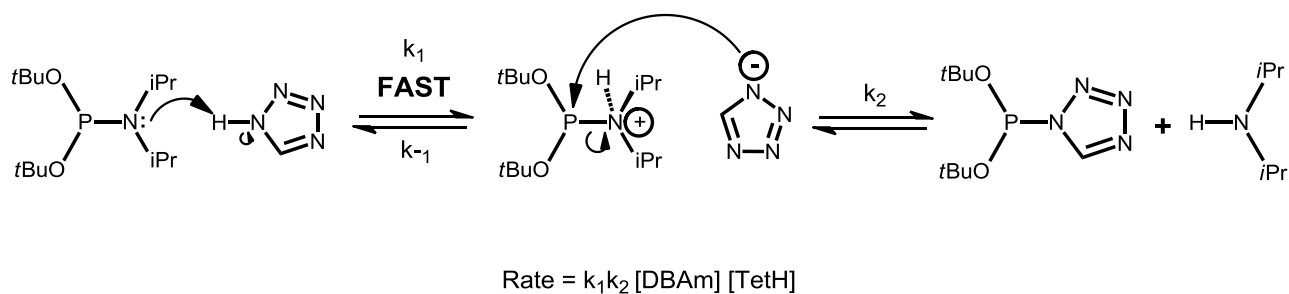
Scheme 37: Rate equation for activation of DBAm with ETTH

It is likely that the pK$_a$s in acetonitrile would be linearly related to those in 10% DMSO-water similar to the linear correlation observed in figure 58 showing the correlation between the pK$_a$(ACN) and the pK$_a$(H$_2$O) for various heterocyclic nitrogen acids. It is reasonable, therefore, to assume that the Brønsted coefficient based on pK$_a$s in acetonitrile would be similarly high and approximately 1, suggesting that in the transition state the tetrazole is fully deprotonated and bears a full negative charge compatible with a a rapid pre-equilibrium and rate-limiting attack by the tetrazolide ion on the N-protected phosphoramidite (step k$_2$, Scheme 37).

6. Conclusions and Further Work

6.1 Ageing PADS

PADS degrades in basic acetonitrile solution to yield acyl polysulfides which are the active sulfurizing reagents. The generation of these species is responsible for the observed increase in rate of sulfur transfer from aged PADS solutions compared with 'fresh' or non-aged solutions.

This process is initiated by an E1cB mechanism in which the methylene protons are removed by the base to form a semi-stable carbanion. This process is reversible as demonstrated by H/D exchange. The carbanion formed by the proton abstraction degrades to form a ketene intermediate and a disulfide anion. The ketene intermediate can be trapped via an intramolecular [2+2]-cycloaddition reaction upon addition of an allyl group in the σ position of the phenyl ring in PADS. The disulfide anions generated from the degradation of the carbanion subsequently react with other unreacted PADS and polysulfide molecules to form species with extended sulfur chains.
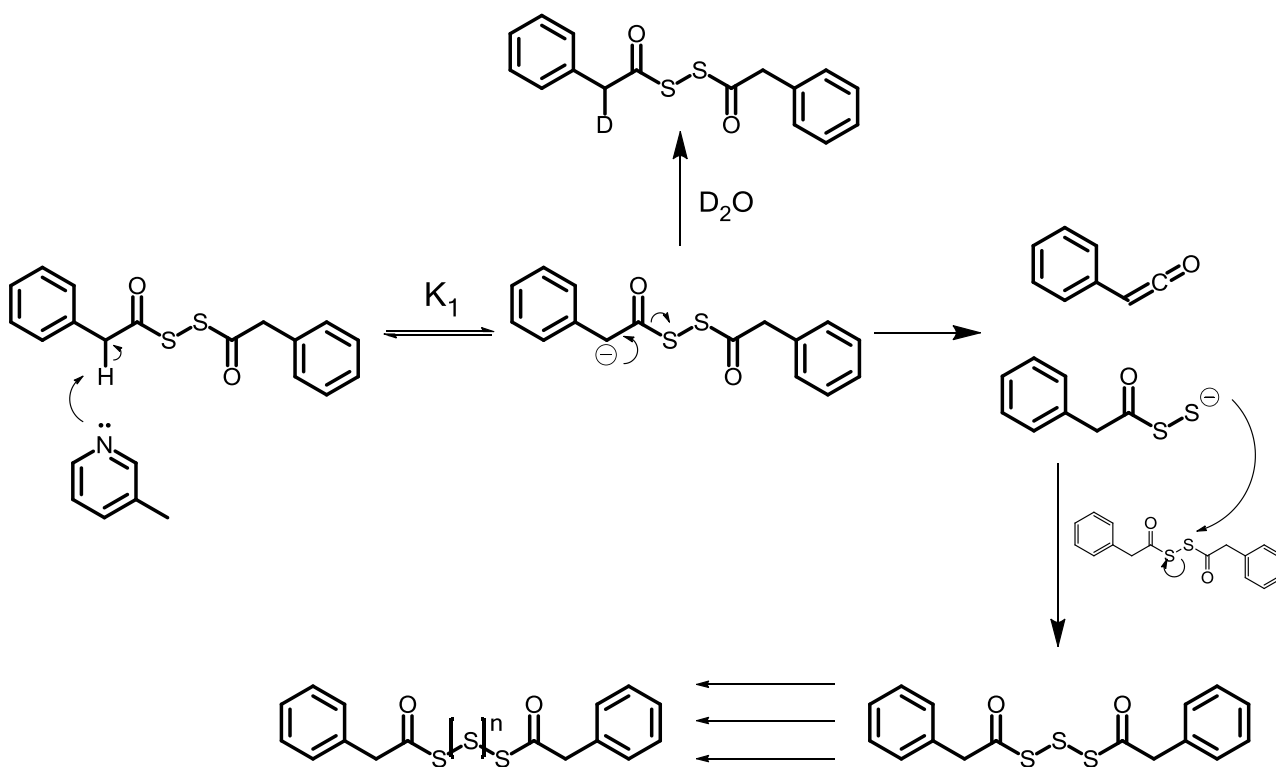
Ageing of PADS is first-order with respect to PADS and the pyridine base used. The rate of decomposition of PADS can be slowed by using a less basic pyridineor, conversely, the rate can be increased using a stronger base. Similarly, the rates of decomposition of PADS and deuterium exchange are increased when electron withdrawing substituents are added to the PADS phenyl ring. Removal of the methylene protons in PADS prevents any decomposition of the PADS molecule.

The solvent dependence of this process and the fact that the reaction occurs in the presence of the radical trap butylated hydroxy toluene indicates that this is an ionic process and does not involve the generation of radicals.

Further work on this area could include further preparative HPLC on aged PADS solutions in order to obtain a suitable sample size, allowing more physical and spectroscopic data on the polysulfides to be obtained. This would also allow more kinetic measurements of the sulfur transfer reactions with the isolated species to be recorded. Conversely, the phenylacetyl polysulfide molecules could also be synthesised and isolated. Similarly, PADS molecules could be synthesised in which the methylene protons are exchanged for deuterium in order to assess the effect of the isotopes on the kinetics of ageing.

During this work, the reaction kinetics have been followed solely by HPLC and NMR. Monitoring the ageing process by infra-red spectroscopy via a react-IR method would allow the concentration of the ketene intermediate to be followed in order to observe this species in a non-invasive way (i.e. without trapping).

6.2 Sulfurisation of Phosphites using Fresh and Aged PADS

Ageing PADS solutions in basic acetonitrile increases the rate of sulfurisation. The reason for the increase in reactivity of aged PADS solutions is due to the presence of polysulfides. This difference in reactivity is demonstrated by the kinetic behaviour and the dependencies of the rate of these solutions on the concentrations of the reactant components. The sulfurisation reaction with both fresh and aged PADS is first-order with respect to each reagent: phosphite, PADS and base at low concentrations however with aged PADS the reaction rate becomes independent of base at higher concentrations. First and foremost, this indicates that the pyridine base used in the reaction is intimately involved in the mechanism of sulfurisation, a point previously overlooked in the literature. Brönsted β_{nuc} values for the base dependence of the reactions of fresh and aged PADS on the pK_a of the pyridine used are +0.43 and +0.26 respectively indicating positive charge transfer to the pyridine nitrogen before or during the rate-limiting step of the reaction.

Brönsted β_{nuc} value for varying the substituent on the alkyl phosphite used in reactions of fresh PADS is +0.51 which is indicative of a build-up of positive charge on the phosphite, i.e. nucleophilic attack by the phosphite on the disulfide bond to yield a phosphonium ion intermediate.

Removing the methylene protons from the PADS molecule decreases the rate of sulfurisation, indicating that the rate limiting step of sulfurisation is the breakdown of the phosphonium intermediate since removing the protons from this position forces an alternate decomposition mechanism.

Breakdown of the mono-sulfide phosphonium generated by reaction with fresh PADS proceeds via an E1cB-type elimination involving cleavage of the C-S bond, similar to that seen in the initiation of PADS decomposition by pyridines in chapter 3. This is supported by the Hammett plot of various phenyl substituted PADS molecules in which it was seen that electron withdrawing substituents increase the rate of reaction. Breakdown of the polysulfide phosphonium intermediate generated by reaction with aged PADS proceeds via a nucleophilic attack of the pyridine base to break the weaker S-S bond. This more facile pathway results in a faster rate of reaction with aged PADS.
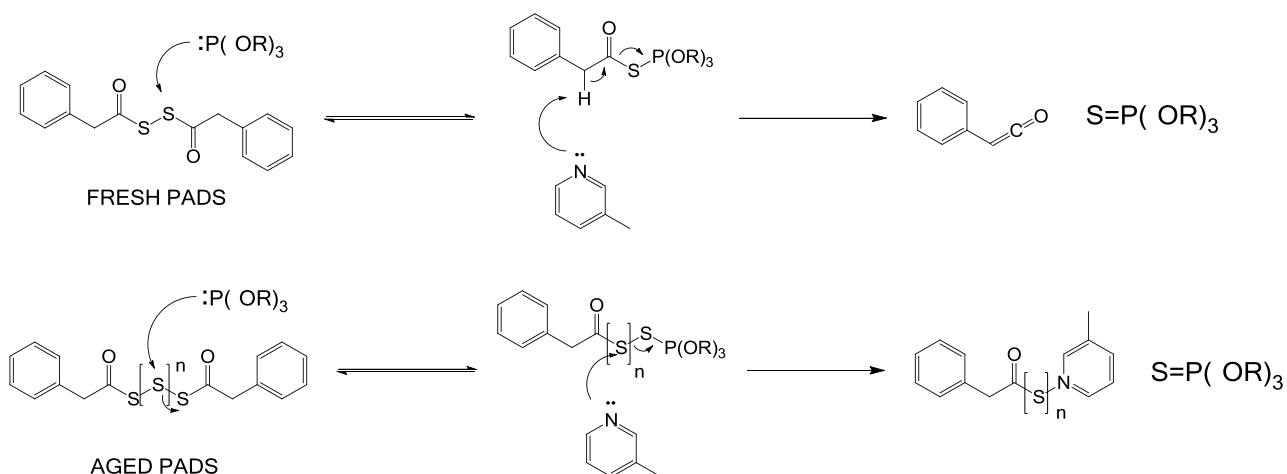
The solvent dependence of these reactions and the fact that the reactions still proceed in the presence of the radical trap butylated hydroxyl toluene indicates that this is an ionic process and does not involve the generation of radicals.

In order to further this work experiments could be done in which the methylene protons in the PADS molecules are replaced by deuterium molecules in order to assess the kinetic isotope effects of PADS degradation and distinguish between a base-catalysed process (fresh PADS) and a nucleophile-catalysed process (aged PADS). Similarly, reactions using the *o*-allyl analogue of PADS and σ-allyl polysulfides could be used in sulfurisation experiments in order to detect the presence of the cycloaddition products, again distinguishing between the two pathways.

6.3 Coupling and Activation

Ethylthiotetrazole (ETTH) has been shown to be an efficient activator of phosphoramidites for use in coupling reactions in oligonucleotide synthesis. The equilibrium between unreacted tetrazole and di-isopropylamine means that the activator cannot fully act catalytically. It is shown here that the tetrazolide and ammonium ions generated in this acid-base equilibrium are strongly ion paired and are therefore effectively removed from the reaction.

Initial conductivity work has shown that the activation of phosphoramidites by ETTH is first order with respect to activator and to amidite. It is also shown here that the rate limiting step of the alcoholysis of phosphoramidites is the activation by ETTH and that the nucleophilic substitution is rapid.

Further work must be carried out in order to fully understand the acid-base equilibrium between ETTH, $DIAH^+$ and the homo-conjugate species. This includes full mass balance equations to assess the extent of homo-conjugation as well as experiments to determine the specific ionic conductivities of the ETT^- and $DIAH^+$ ions. In this work structure-activity relationships of the activation of phosphoramidites have been constructed varying tetrazole substituents. However, more information about the transition state of the activation could be gleaned by varying the phosphoramidite leaving group, for example, by modifying the amine pK_a. This will allow a value of β_{nuc} L.G. to be deduced, providing information about the state of the bond between the phosphorus and both the amine and tetrazole in the transition state.

7. References

1   Berg, J. M., L., Tymoczko, J. & Stryer, L. *Biochemistry*. 5th ed., (W. H. Freeman and Co., 2003).
2   Devlin, T. M. *Textbook of Biochemistry: With Clinical Correlations*. 6th ed., (John Wiley & Sons Inc., 2006).
3   Kvaerno, L. & Wengel, J. *Chem. Commun.*1419-24 (2001).
4   Voet, D. V., Voet, J. G. & Pratt, C. W. *Fundamentals of Biochemistry: Life at the Molecular Level*. 2nd ed., (John Wiley & Sons Inc., 2006).
5   Uhlmann, E. & Peyman, A. *Chem. Rev.* **90** (1990).
6   Wang, S. & Kool, E. T. *Biochemistry* **34**, 4125-4132 (1995).
7   Zamecnik, P. C. & Stephenson, M. L. *Proc. Natl. Acad. Sci. U.S.A.* **75**, 285-288 (1978).
8   Boado, R. J., Tsukamoto, H. & M., Padridge, W. M. *J. Pharm. Sci.* **87**, 1308-15 (1998).
9   Kennewell, P. *Curr. Opin. Mol. Ther.* **5** (1), 76-80 (2003).
10   Aershot, A. V. *Antiviral Res.* **71**, 307-16 (2006).
11   Lu, Q. L., Rabinowitz, A., Yin, H., Alter, J., Bou-Gharios, G., & Partridge, T. *Mol. Ther.* **11**, 306-306 (2005).
12   Hélène, C. Montenay-Garestier, T., Saison, T., Takasugi, M., Toulmé, J. J., Asseline, U., Lancelot, G., Maurizot, J. C., Toulmé, F. & Thuong, N. T. *Biochimie* **67**, 777-783 (1985).
13   Lebedeva, I. & Stein, C.; *Annu. Rev. Pharmacol.* **41**, 403-419 (2001).
14   Ts'O, P. O. P., Miller, P. S., Aurelian, L., Murakami, A., Agris, C., Blake, K. R., Lin, S. B., Lee, B. L. & Smith, C. C. *Ann. N.Y. Acad. Sci.* **507**, 220 (1988).
15   Le Doan, T., Perrouault, L., Praseuth, D., Habhoub, N., Decout, J. L., Thuong, N. T., Lhomme, J. & Hélène, C. *Nucleic Acids Res.* **15**, 7749-7760 (1987).
16   Uhlmann, E. & Peyman, A. *Chem. Rev.* **90**, 543-584 (1990).
17   Juliano, R. L., Ming, Nakagawa, X. & Nakagawa, O. *Acc. Chem. Res.* **45**, 1067-1076 (2012).
18   Juliano, R. L., Ming, X and Nakagawa, O. *Acc. Chem. Res* **45**, 1067-1076 (2011).
19   Wilton, S. D., Fall, A. M., Harding, P. L., McClorey, G., Coleman, C. & Fletcher, S. *Mol. Ther.* **15**, 1288-1296 (2007).
20   Moulton, H. M. & Moulton, J. D. *Biochim. Biophys. Acta* **1798**, 2296-2303 (2010).
21   Van Deutekom, J. C. Janson, A. A., Ginjaar, I. B., Frankhuizen, W. S., Aartsma-Rus, A., Bremmer-Bout, M., Den Dunnen, J. T., Koop, K., Van der Kooi, A. J., Goemans, N. M. & De Kimpe, S. J. *New Engl. J. Med.* **357**, 2677-2686 (2007).
22   Aartsma-Rus, A., Van Deutekom, J. C., Fokkema, I. F., Van Ommen, G. J. B. & Den Dunnen, J. T. *Muscle & nerve* **34**, 135-144 (2006).
23   Strachan, T. & Read, A. *Human Molecular Genetics*. 3rd ed.,(Wiley, Oxford, 1999).
24   Monio, B. P., Lesnik, E. A., Gonzalez, C., Lima, W. F., McGee, D., Guinosso, C. J., Kawasaki, A. M., Cook, P. D. & Freier, S. M. *J. Biol. Chem.***268**, 14514-14522 (1993).
25   Clark, R. E. *Leukemia lymphoma* **19**, 189-195 (1995).
26   Leonetti, J. P., Degols, G. & Lebleu, B. *Bioconjugate Chem.* **1**, 149-153 (1990).
27   Loke, S., Stein, C. A., Zhang, X. H., Mori, K., Nakanishi, M., Subasinghe, C., Cohen, J. S. & Neckers, L. M. *Proc.Nat. Acad.Sci.* **86**, 3474-3478 (1989).
28   Wang, L., Chen, S., Xu, T., Taghizadeh, K., Wishnok, J. S., Zhou, X., You, D., Deng, Z. and Dedon, P. C. *Nat. Chem. Biol.* **3**, 709-710 (2007).
29   Richard, J. P. & Frey, P. A. *J.Am.Chem. Soc.* **100**, 7757-7758 (1978).
30   Eckstien, F. *Angew. Chem. Int. Ed. Engl.* **22**, 423-439 (1983).
31   Suska, A., Grajkowski, A., Wilk, A., Uznanski, B., Blaszczyk, J., Wieczorek, M. & Stec, W. J. *Pure Appl. Chem.* **65**, 707-707 (1993).
32   Stec, W. J. & Wilk, A. *Angew. Chem. Int. Ed. Engl.***33**, 709-722 (1994).
33   Guga, P. & Koziołkiewicz, M. *Chem. Biodiv.* **8**, 1642-1681 (2011).

34   Stec, W. J., Grajkowski, A., Koziolkiewicz, M. & Uznanski, B. *Nucleic Acids Res.* **19**, 5883-5888 (1991).

35   De Mesmaeker, A., Altmann, K.-H., Waldner, A. & Wendeborn, S. *Curr. opin. Struc. Biol.* **5**, 343-355 (1995).

36   Marshall, W. & Caruthers, M. *Science* **259**, 1564-1564 (1993).

37   Frey, P. A. & Sammons, R. D. *Science* **228**, 541-545 (1985).

38   Iversen, P. L., Mata, J., Tracewell, W. G. & Zon, G. *Antisense Res.Dev.* **4**, 43-52 (1994).

39   De Clercq, E., Eckstein, F., Sternbach, H. & Merigan, T. C. *Virology* **42**, 421-428 (1970).

40   Nielsen, J., Brill, W. K. D. & Caruthers, M. H. *Tetrahedron Lett.* **29**, 2911-2914 (1988).

41   Jayaraman, K., McParland, K., Miller, P. & Ts'o, P. O. P. *P. Nat. Acad. Sci.* **78**, 1537-1541 (1981).

42   Akhtar, S. B., S., Wickstrom, E, Juliano, R. L. *Nucl. Acids Res.* **19**, 5543-5550 (1991).

43   Quartin, R. S. & Wetmur, J. G. *Biochemistry* **28**, 1040-1047 (1989).

44   Lin, S. B., Blake, K. R., Miller, P. S. & Ts'o, P. O. P. *Biochemistry* **28**, 1054-1061 (1989).

45   Miller, P. Y., J., Yano, E., Carroll, C., Jayaraman, K. & Ts'O, P. O. P. *Biochemistry* **18**, 5134-5143 (1979).

46   Agrawal, S. & Goodchild, J. *Tetrahedron Lett.* **28**, 3539-3542 (1987).

47   Stec, W. J., Zon, G., Egan, W., Byrd, R.A., Phillips, L.R. & Gallo, K.A.*J. Org. Chem.* **50**, 3908-3913 (1985).

48   Froehler, B., Ng, P. & Matteucci, M. *Nucleic Acids Res.* **16**, 4831-4839 (1988).

49   Letsinger, R. L. & Heavner, G. A. *Tetrahedron Lett.* **16**, 147-150 (1975).

50   Jäger, A., Levy, M. J. & Hecht, S. M. *Biochemistry* **27**, 7237–7246 (1988).

51   Sood, A., Shaw, B. R. & Spielvogel, B. F. *J. Am. Chem. Soc.* **112**, 9000-9001 (1990).

52   Sproat, B. S., Beijer, B., Rider, P. & Neuner, P. *Nucleic Acids Res.* **15**, 4837-4848 (1987).

53   Morr, M., Ernst, L. & Grotjahn, L. *Z.Naturforsch. B.* **38**, 1665-1668 (1983).

54   Sproat, B. S., Beijer, B. & Rider, P. *Nucleic Acids Res.* **15**, 6181-6196 (1987).

55   Hata, T., Yamamoto, I. & Sekine, M. *Chem. Lett.* **5**, 601-604 (1976).

56   Ogilvie, K. & Cormier, J. *Tetrahedron Lett.* **26**, 4159-4162 (1985).

57   Jones, D. & Tittensor, J. *J. Chem. Soc. D.: Chem. Commun.*, 1240a-1240a (1969).

58   Marcus-Sekura, C., Woerner, A. M., Shinozuka, K., Zon, G. & Quinnan, G. V. *Nucleic Acids Res.* **15**, 5749-5763 (1987).

59   Qiu, J., El-Sagheer, A. H. & Brown, T. *Chem. Commun.* **49**, 6959-6961 (2013).

60   Monia, B. P., Lesnik, E. A., Gonzalez, C., Lima, W. F., McGee, D., Guinosso, C. J., Kawasaki, A. M., Cook, P. D. & Freier, S. M.*J. Biol. Chem.* **268**, 14514-14522 (1993).

61   De Mesmaeker, A., Haener, R., Martin, P. & Moser, H. E. *Accounts Chem. Res.* **28**, 366-374 (1995).

62   Bellon, L., Morvan, F., Barascut, J. L. & Imbach, J. L. *Biochem. Biophys. Res. Co.* **184**, 797-803 (1992).

63   Sagi, J., Szemzõ, A., Szécsi, J. & Ötvös, L. *Nucleic Acids Res.* **18**, 2133-2140 (1990).

64   Sanghvi, Y. S. & Cook, P. D. *Carbohydrate Modifications in Antisense Research.* Vol. 580 (ACS Publications, 1994).

65   Jones, R. J., Lin, K. Y., Milligan, J. F., Wadwani, S. & Matteucci, M. D. *J. Org. Chem.* **58**, 2983-2991 (1993).

66   Gryaznov, S. & Schultz, R. G. *Tetrahedron Lett.* **35**, 2489-2492 (1994).

67   Saenger, W. *Principles of nucleic acid structure*. Vol. 7 (Springer-Verlag New York, 1984).

68   Khorana, H. G. *Federation Proc.* **19**, 931-941 (1960).

69   Shibahara, S., Mukai, S., Nishihara, T., Inoue, H., Ohtsuka, E. & Morisawa, H., *Nucleic Acids Res.* **15**, 4403-4415 (1987).

70   Matteucci, M. D. & Caruthers, M. *J. Am. Chem. Soc.* **103**, 3185-3191 (1981).

71   Froehler, B. & Matteucci, M. *Tetrahedron Lett.* **27**, 469-472 (1986).

72   Froehler, B. C. *Tetrahedron Lett.* **27**, 5575-5578 (1986).

73   Hall, R., Todd, A. & Webb, R. *J. Chem. Soc. (Resumed)*, 3291-3296 (1957).

74   Froehler, B. C., Ng, P. G. & Matteucci, M. D. *Nucleic Acids Res.* **14**, 5399-5407 (1986).

75   Reese, C. B. *Tetrahedron* **58**, 8893-8920 (2002).

76   Beaucage, S. & Caruthers, M. *Tetrahedron Lett.* **22**, 1859-1862 (1981).

77   Dahl, B. H., Nielsen, J. & Dahl, O. *Nucleic Acids Res.* **15**, 1729-1743 (1987).

78   Nurminen, E. J., Mattinen, J. K. & Lonnberg, H. *J. Chem. Soc., Perkin Trans.* **2**, 2159-2165 (2001).

79   Berner, S., Mūhlegger, K. & Seliger, H. *Nucleic Acids Res.* **17**, 853-864 (1989).

80   Hayakawa, Y., Iwase, T., Nurminen, E. J., Tsukamoto, M. & Kataoka, M. *Tetrahedron* **61**, 2203-2209 (2005).

81   Nurminen, E. J., Mattinen, J. K. & Lönnberg, H. *J. Chem. Soc., Perkin Trans.* **2**, 1621-1628 (1998).

82   Knaap, T. A. V. D. & Bickelhaupt, F. *Phosphorus Sulfur* **21**, 227-236 (1984).

83   Nurminen, E. J., Mattinen, J. K. & Lönnberg, H. *J. Chem. Soc., Perkin Trans.* **2**, 2238-2240 (2000).

84   Korkin, A. *Russ. Chem. Rev.* **61**, 473 (1992).

85   Dąbkowski, W., Tworowska, I., Michalski, J. & Cramer, F. *Tetrahedron Lett.* **41**, 7535-7539 (2000).

86   Nurminen, E. J., Mattinen, J. K. & Lönnberg, H. *J. Chem. Soc., Perkin Trans.* **2**, 2159-2165 (2001).

87   Sproat, B., Colonna, F., Mullah, B., Tsou, D., Andrus, A., Hampel, A. & Vinayak, R. *Nucleos. Nucleot. Nucl.* **14**, 255-273 (1995).

88   Wu, X. & Pitsch, S. *Nucleic Acids Res.* **26**, 4315-4323 (1998).

89   Froehler, B. & Matteucci, M. *Tetrahedron Lett.* **24**, 3171-3174 (1983).

90   Welz, R. & Müller, S. *Tetrahedron Lett.* **43**, 795-797 (2002).

91   Connolly, B. A., Potter, B. V., Eckstein, F., Pingoud, A. & Grotjahn, L. *Biochemistry* **23**, 3443-3453 (1984).

92   Iyer, R. P., Egan, W., Regan, J. B. & Beaucage, S. L. *J. Am. Chem. Soc.* **112**, 1253-1254 (1990).

93   Hanusek, J., Russell, M. A., Laws, A. P., Jansa, P., Atherton, J. H., Fettes, K. & Page, M. I. *Org. Biomol. Chem.* **5**, 478-484 (2007).

94   Zhang, Z., Nichols, A., Tang, J. X., Han, Y. & Tang, J. Y. *Tetrahedron Lett.* **40**, 2095-2098 (1999).

95   Xu, Q., Barany, G., Hammer, R. P. & Musier-Forsyth, K. *Nucleic Acids Res.* **24**, 3643-3644 (1996).

96   Krotz, A. H., Gorman, D., Mataruse, P., Foster, C., Godbout, J. D., Coffin, C. C. & Scozzari, A. N.*Org. Proc. Res. Dev.* **8**, 852-858 (2004).

97   Cheruvallath, Z. S., Carty, R. L., Moore, M. N., Capaldi, D. C., Krotz, A. H., Wheeler, P. D., Turney, B. J., Craig, S. R., Gaus, H. J., Scozzari, A. N. & Cole, D. L.*Org. Proc. Res. Dev.* **4**, 199-204 (2000).

98   Efimov, V. A., Kalinkina, A. L., Chakhmakhcheva, O. G., Hill, T. S. & Jayaraman, K. *Nucleic Acids Res.* **23**, 4029-4033 (1995).

99   Iyer, R. P., Egan, W., Regan, J. B. & Beaucage, S. L. *J. Am. Chem. Soc.* **112**, 1253-1254 (1990).

100   Oae, S. & Doi, J. *Organic Sulfur Chemistry*. Vol. 1 (CRC Press, 1991).

101   Steudel, R. Properties of sulfur-sulfur bonds. *Angew. Chem. Int. Ed. Engl.* **14**, 655-664 (1975).

102   Epplequist, C. H. D., K. Reinhart. *Introduction to Organic Chemistry. 3rd ed.* (1982).

103   Houk, J. & Whitesides, G. M. *J. Am. Chem. Soc.* **109**, 6825-6836 (1987).

104   Belen'kii, L. The Chemistry of Organic Compounds of Sulfur. *General Aspects* (1988).

105   Koval, I. V. *Russ. Chem. Rev.* **63**, 735-750 (1994).

106   Wiewiorowski, T. K. & Touro, F. J. *J. Phys. Chem.* **70**, 234-238 (1966).

107   Pickering, T. L., Saunders, K. & Tobolsky, A. V. *J. Am. Chem. Soc.* **89**, 2364-2367 (1967).

108   Sierzchala, A. B., Dellinger, D. J., Mokler, V. R. & Timar, Z. Use Of Thioacetic Acid Derivatives In The Sulfurization Of Oligonucleotides With Phenylacetyl Disulfide. US 2010/0331533 A1 (2009).

109   Vu, H. & Hirschbein, B. L. *Tetrahedron Lett.* **32**, 3005-3008 (1991).

110   Kamyshny, A., Goifman, A., Gun, J., Rizkov, D. & Lev, O. *Environmental Science & Technology* **38**, 6633-6644 (2004).

111   Cox, B. G. *Acids and Bases: Solvent Effects on Acid-Base Strength.* (OUP Oxford, 2013).

112   Roelen, H., Kamer, P., Van den Elst, H., Van der Marel, G. & Van Boom, J. *Recl. Trav. Chim. Pay. B.* **110**, 325-331 (1991).

113   Black, H. S. *Front. Biosci.* **7**, 1044-1055 (2002).

114   Scotson, J. L., Andrews, B. I., Laws, A. P. & Page, M. I. *Org. Biomol. Chem.* **14**, 8301-8308 (2016).

115   Bakshi, M. S. *J. Chem. Soc., Faraday Trans.* **89**, 3049-3054 (1993).

116   Walling, C. & Rabinowitz, R. *J. Am. Chem. Soc.* **81**, 1243-1249 (1959).

117   Stratakis, M., Rabalakos, C. & Sofikiti, *Tetrahedron Lett.* **44**, 349-351 (2003).

118   Hammett, L. P. *J. Am. Chem. Soc.* **59**, 96-103 (1937).

119   Pearson, R. G. & Williams, F. V. *J. Am. Chem. Soc.* **76**, 258-260 (1954).

120   Johnson, S. *Adv. Phys. Org. Chem.* **5**, 237-330 (1967).

121   Bunton, C. & Fendler, J. *J. Org. Chem.* **31**, 2307-2312 (1966).

122   Serjeant, E. P. & Dempsey, B. *Ionisation constants of organic acids in aqueous solution.* Vol. 23 (Pergamon, 1979).

123   Harpp, D. N., Ash, D. K. & Smith, R. A. *J. Org. Chem.* **45**, 5155-5160 (1980).

124   Deacon, T., Farrar, C. R., Sikkel, B. J. & Williams, A. *J. Am. Chem. Soc.* **100**, 2525-2534 (1978).

125   Nag, S. & Datta, D. *Indian J. Chem.* **46**, 1263-1265 (2007).

126   Gearey, W. J. *Coord. Chem. Rev.* **7**, 81 (1971).

127   Zielińska, J., Makowski, M., Maj, K., Liwo, A. & Chmurzyński, L. *Anal. Chim. Acta* **401**, 317-321 (1999).

128   Huyskens, P., Platteborze, K. & Zeegers-Huyskens, T. *J. Mol. Struct.* **436**, 91-102 (1997).

129   Russell, M. A. *Kinetics and Mechanisms of Steps in Anti-Sense Oligonucleotide Synthesis*, University of Huddersfield, (2007).

130   Russell, M. A., Laws, A. P., Atherton, J. H. & Page, M. I. *Org. & Biomol. Chem.* **6**, 3270-3275 (2008).

131   Scheuer-Larsen, C., Dahl, B. M., Wengel, J. & Dahl, O. *Tetrahedron Lett.* **39**, 8361-8364 (1998).

132   Shelton, R. S., Rider, T. H. *J. Am. Chem. Soc.* **58**, 1282-4 (1936).

Appendix 1: X-Ray Crystal Structure Data

X-Ray Crystal Structure Information for Bis-benzoyl Disulfide
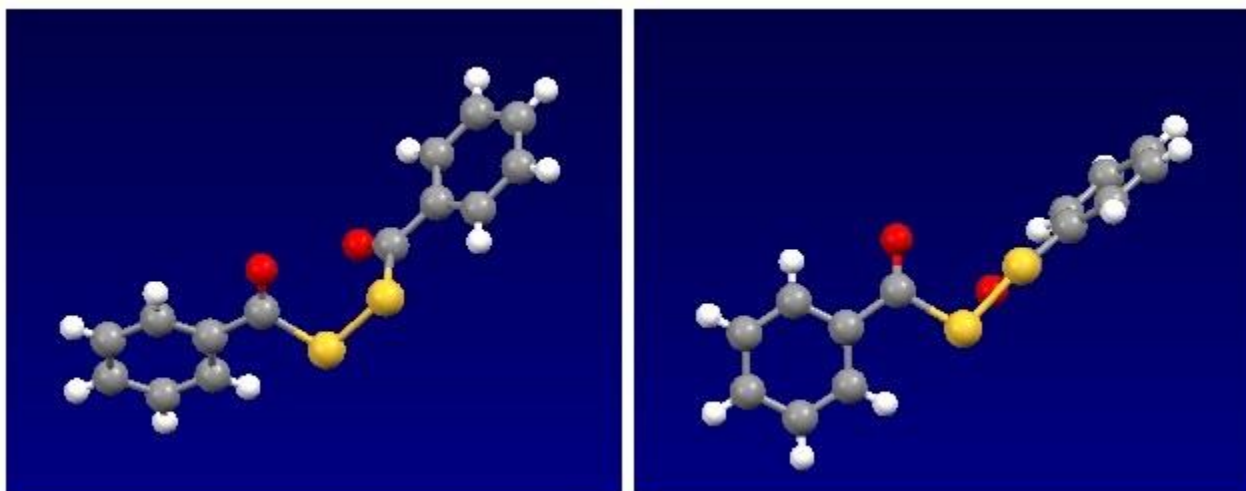
Chemical Formula	$C_{14}H_{10}O_2S_2$
Formula Mass	274.34
Crystal System	Monoclinic
a/Å	12.2493(3)
b/Å	12.0214(3)
c/Å	8.9707(2)
α/°	90
β/°	107.4043(11)
γ/°	90
Unit cell volume/Å^3	1260.49(5)
Temperature/K	150(2)
Space group	P 21/c
No. of formula units per unit cell, Z	4
R_{int}	0.0599
Final R1 values	0.0645

Appendix 2: Publications from this Work

Phosphorothioate anti-sense oligonucleotides: the kinetics and mechanism of the generation of the sulfurising agent from phenylacetyl disulfide (PADS)†

James L. Scotson,[a] Benjamin I. Andrews,[b] Andrew P. Laws[a] and Michael I. Page*[a]

The synthesis of phosphorothioate oligonucleotides is often accomplished in the pharmaceutical industry by the sulfurisation of the nucleotide–phosphite using phenylacetyl disulfide (PADS) which has an optimal combination of properties. This is best achieved by an initial 'ageing' of PADS for 48 h in acetonitrile with 3-picoline to generate polysulfides. The initial base-catalysed degradation of PADS occurs by an E1cB-type elimination to generate a ketene and acyldisulfide anion. Proton abstraction to reversibly generate a carbanion is demonstrated by H/D exchange, the rate of which is greatly increased by electron-withdrawing substituents in the aromatic ring of PADS. The ketene can be trapped intra-molecularly by an *o*-allyl group. The disulfide anion generated subsequently attacks unreacted PADS on sulfur to give polysulfides, the active sulfurising agent. The rate of degradation of PADS is decreased by less basic substituted pyridines and is only first order in PADS indicating that the rate-limiting step is formation of the disulfide anion from the carbanion.

Introduction

Synthetic oligonucleotides have been used in many different ways for several decades,[1] such as therapeutic agents and in diagnostics. An anti-sense oligonucleotide (ASO) is usually a single-stranded deoxy-ribonucleotide (usually 15–35 base pairs in length) which is complementary to a target mRNA. Complex dimer formation between the ASO and the target mRNA through normal Watson–Crick base pairing can lead to inhibition of translation and so prevent synthesis of an unwanted target protein. The formation of the ASO–mRNA hetero-duplex often activates RNase H endonuclease activity which then catalyses the hydrolysis of the mRNA leaving the ASO intact.[2] The first approved anti-sense oligonucleotide was Vitravene (formiversen, for treating the blinding viral condition cytomegalovirus induced retinitis afflicting some of those infected with HIV[3]), which was followed by numerous clinical trials of other oligonucleotides[4] and, more recently, Kynamro (mipomersen) to treat genetically inherited high cholesterol levels.[5] Other mechanisms of action of ASOs include 'exon-skipping' where, instead of binding to mRNA, the ASO binds to longer pre-mRNA chains sterically blocking an unwanted mutation and its surrounding sequence preventing the exon, containing the mutation, being spliced into the mRNA. Antisense-mediated exon skipping is a promising therapeutic for neuromuscular diseases,[6] although trials for drisapersen to treat Duchenne Muscular Dystrophy have recently been stopped. ASOs are also useful as valuable genetic diagnostic tools, for example, HyBeacon probes are single-stranded oligonucleotides with one or more internal bases labelled with a fluorescent dye so that when duplex formation occurs with its target sequence there is an increase in fluorescence.[7]

However, the use of phosphodiester anti-sense oligonucleotides is limited because they are rapidly hydrolysed by intracellular endonucleases and exonucleases.[8] Consequently, ASOs have been modified to decrease their susceptibility to nuclease cleavage and to increase their uptake into cells, binding efficiency, bio-stability and potency.[9] Examples of these modifications are the inclusion of phosphorothioate backbones (**1**)[10] and changes to the 2′ position of the ribose sugar (*e.g.* 2′-*O*-methoxyethyl) or the sugar-phosphate (*e.g.* morpholino and locked nucleic acid, (*S*)-constrained-2′-*O*-ethyl – bicyclic constrained riboses).[11] These changes do not disrupt H-bonding between the nucleobases.

[a]*Department of Chemistry, University of Huddersfield, Queensgate, Huddersfield HD1 3DH, UK. E-mail: m.i.page@hud.ac.uk*
[b]*GSK Medicines Research Centre, Gunnels Wood Road, Stevenage, Hertfordshire, SG1 2NY, UK*
†Electronic supplementary information (ESI) available: Detailed kinetic data. See DOI: 10.1039/c6ob01531j

This journal is © The Royal Society of Chemistry 2016

Org. Biomol. Chem., 2016, **14**, 8301–8308 | 8301
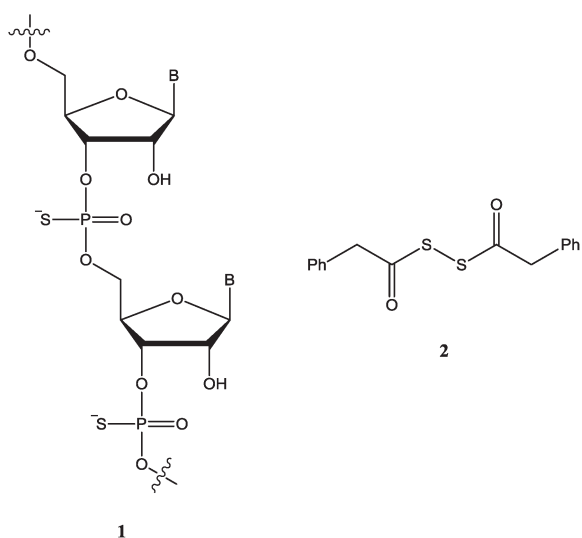
Phosphorothioates (**1**) are the most widely investigated oligonucleotides because of their relative nuclease stability and ease of synthesis and a naturally occurring phosphorothioate has even been found in bacterial DNA.[12] The replacement of one of the phosphate non-bridging oxygens by sulfur introduces chirality at phosphorus and it is only the (*S*)-P phosphorothioate diastereomer that is nuclease resistant.[13] However, phosphorothioate oligonucleotides can reduce the affinity of the ASO for its mRNA target as shown by the melting temperature of the ASO–mRNA hetero-duplex which is decreased by approximately 0.5 °C per nucleotide.[14] Conversely, the introduction of the hydrophobic sulfur increases cell uptake compared with the wild-type phosphodiester. Phosphorothioate oligonucleotides remain highly water soluble, still bind well to mRNA and activate RNase H making them the most common modification of ASOs undergoing clinical trials.

The synthesis of phosphorothioate oligonucleotides is often accomplished by the sulfurisation of the nucleotide–phosphite through reaction of the corresponding P(III) analogue, usually attached to a solid support, with an organic sulfurising agent which is present in an organic solvent. As with all the steps involved in the synthesis of oligonucleotide based phosphorthioates, the sulfurisation step of the synthesis should be rapid, have a near quantitative yield and give a maximal P=S to P=O ratio. The sulfurisation of phosphorus(III) compounds has been achieved with a number of reagents such as: phenylacetyl disulfide (PADS) (**2**),[15] 3*H*-1,2-benzodithiol-3-one-1,1-dioxide (Beaucage reagent),[16] tetraethylthiuram disulfide (TETD),[17] dibenzoyl tetrasulfide,[18] bis-(*O,O*-diisopropoxyphosphinothioyl) disulfide (S-tetra),[19] benzyltriethylammonium tetrathiomolybdate (BTTM),[20] bis-(*p*-toluenesulfonyl) disulfide,[21] 3-ethoxy-1,2,4-dithiazoline-5-one (EDITH) and 1,2,4-dithiazolidine-3,5-dione (DTSNH),[22] bis(ethoxythiocarbonyl) tetrasulfide,[23] 3-methyl-1,2,4-dithiazolin-5-one (MEDITH)[24] and 3-amino-1,2,4-dithiazole-5-thione (ADTT, xanthane hydride).[25]

Although PADS (**2**) has an optimal combination of properties and is often used as the sulfurising reagent in the pharmaceutical industry,[26,27] there have been very few mechanistic studies of the sulfurisation reactions of phosphorus(III) analogues using PADS. In particular, PADS must be 'aged' in a basic acetonitrile solution to obtain optimal sulfurisation activity[28] and the reasons for this are not understood. Herein we report the results of our kinetic and mechanistic studies which identify the actual sulfurising agent and suggest an unexpected pathway for its generation. Elsewhere we describe the kinetics and mechanism of the sulfurisation step of substituted triphenyl phosphites and trialkyl phosphites using PADS.[29]

Results and discussion

It is known that a freshly made solution of PADS (**2**) is not an optimal sulfurising agent.[26] Solutions of PADS usually consist of 50% v/v 3-picoline in acetonitrile or other bases such as pyridine or collidine but their efficiency improves greatly upon 'ageing' for about 2 days.[26] PADS degrades completely over this period of time as shown by HPLC, ^{1}H NMR and MS and the colour of the solution changes dramatically from pale yellow through green/blue to brown/black over about 5 days. The pseudo first-order rate constants for the sulfurisation of 0.05 M triphenyl phosphite in acetonitrile by 0.5 M PADS with 1.0 M 3-picoline increase with the length of 'ageing' (Fig. 1), such that PADS 'aged' for 48 h is 13-fold more active than a freshly prepared solution of PADS. It is apparent therefore that the degradation product(s) of PADS are more efficient sulfurising agents, but their identity is not known.

The exponential rate of degradation of 3.3 M PADS (**2**) in acetonitrile 25 °C was followed by HPLC and the associated first-order rate constants depend on the concentration of 3-picoline (Fig. 2). This increase in rate is unlikely to be a consequence of a change in the dielectric constant of the solution as, for example, PADS is stable in a solution of acetonitrile/
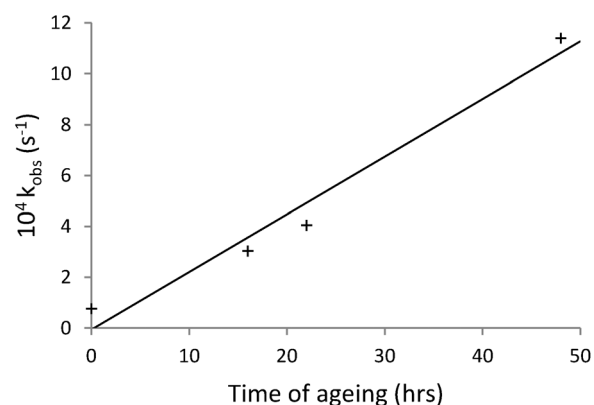
Fig. 1 The pseudo first-order rate constants for the sulfurisation of triphenyl phosphite (0.05 M) to (PhO)$_3$P=S by (0.5 M) PADS (**2**) as a function of the time that PADS has been 'aged' in acetonitrile with (1.0 M) 3-picoline at 25 °C.
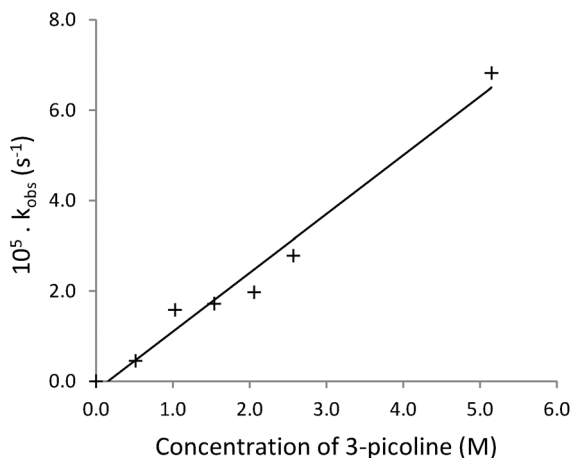
Fig. 2 The dependence of the pseudo first-order rate constants for the decomposition of PADS (2) in acetonitrile on the concentration of 3-picoline at 25 °C.

philes than the corresponding thiolate.[31] The formation of phenylacetyl disulfide anion (5) could result from either nucleophilic attack on PADS or a general-base catalysed elimination reaction of PADS by the picoline base. It is likely that there is an equilibrium set up between the diacylpolysulfides and acylpolysulfide anions and sulfur.[32]

3 n = 1   4 n = 3

5   6
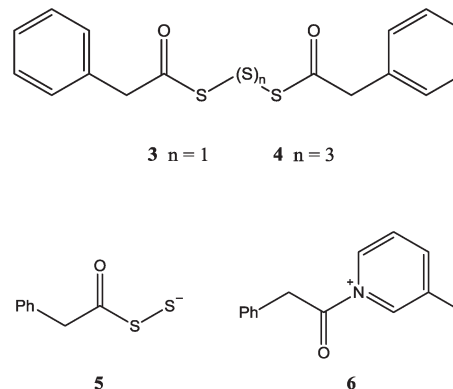
Nucleophilic attack on PADS (2) by picoline would generate an acyl-picolinium ion intermediate (6) but no direct experimental evidence for this could be found nor could its presence be inferred from trapping experiments with a variety of nucleophiles. However, the general-base catalysed formation of the disulfide anion by an E1cB – type mechanism (Scheme 1) is indicated by both D-exchange and trapping of the ketene intermediate.

The rate of H/D exchange was measured by ^{1}H NMR using a solution of 0.17 M PADS (2) in d_3-acetonitrile containing various concentrations of 3-picoline and 0.6 M D_2O at 25 °C. The CH_2 singlet at δ 4.15 ppm disappeared with a first-order decay generating a triplet for CHD at δ 4.13 ppm which reached a maximum intensity followed by its disappearance to give CD_2. The pseudo first-order rate constants for D-exchange showed a first-order dependence on the concentration of 3-picoline (Fig. 3) which gives a second-order rate constant $k_{pic} = 5.37 \times 10^{-3}$ M^{-1} s^{-1}.

The mechanism of D-exchange presumably occurs through the formation of the intermediate carbanion. The relatively low dielectric constant of the solvent may mean that the ionization of this carbon acid may give rise to ion-pairs in

dimethylsulfoxide 90/10% v/v over 24 h. Furthermore, the rate of degradation of PADS in acetonitrile increases with the basicity of the pyridine base. The slope of the dependence of the observed pseudo first-order rate constants for the decomposition of PADS (2) (Fig. 2) gives the associated second-order rate constant. These rate constants for the 'ageing' of PADS by substituted pyridines (Table 1) generate a Brønsted β-value of 0.37 based on the estimated pK_a in acetonitrile.[30] This is compatible with the pyridine acting as either a base or as a nucleophile with little charge development on the basic nitrogen. The rate of degradation of PADS in acetonitrile is faster with a more basic amine, e.g. with 1.0 M triethylamine it is complete within 5 min.

The products of the 'ageing' of PADS are a mixture of diacylpolysulfides and acylpolysulfide anions. HPLC-mass spectroscopy data performed on aged PADS solutions showed the presence of m/z values corresponding to a variety of diacylpolysulfides, in particular the tri-sulfide (3) at m/z = 357 (Na$^+$ adduct) and the penta-sulfide (4) at m/z = 437 (K$^+$ adduct). After several days elemental sulfur crystallised from the solution. The diphenylacetyl polysulfides are presumably formed from nucleophilic attack of the disulfide anion on PADS at sulfur. It is known that disulfide anions are better nucleo-

Table 1 The second-order rate constants for the decomposition of PADS (2) in acetonitrile (ACN) as a function of the basicity of substituted pyridines in ACN at 25 °C

Pyridine substituent	pK_a (ACN) conjugate acid	k_{cat} (M^{-1} s^{-1})
4-MeO	14.73	7.76×10^{-6}
3-Me	13.70	3.34×10^{-6}
H	12.60	1.63×10^{-6}
3-MeO	12.45	3.79×10^{-7}
4-CN	8.50	3.76×10^{-8}
2,6-DiMe	14.72	4.44×10^{-6}
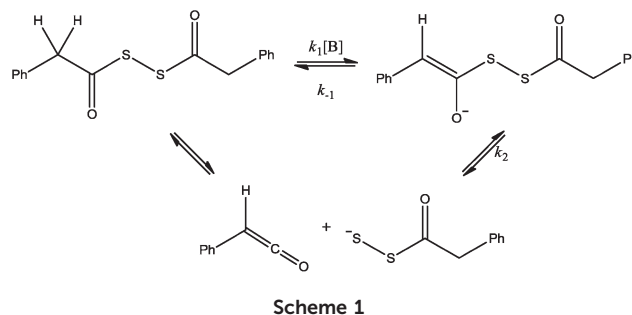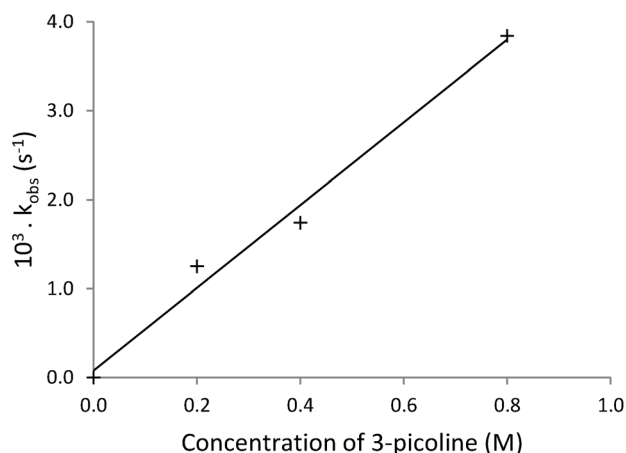
Scheme 1

Fig. 3 The dependence of the pseudo observed first-order rate constants for the H/D – exchange of PADS on the concentration of 3-picoline in acetonitrile at 25 °C.
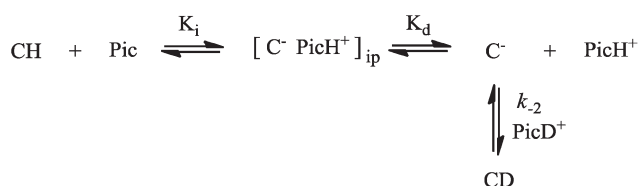
Scheme 2

equilibrium with the dissociated species (Scheme 2), where the product $K_i K_d$ corresponds to the normal ionization constant K_a. However, it is unlikely that exchange can occur from the ion-pair and so if isotopic exchange occurs with the dissociated carbanion, then the rate of protonation of the carbanion k_{-2} can be assumed to be diffusion-controlled,[33] which, based on a viscosity of 0.35 cP for acetonitrile can be assumed to be ~10^{10} M^{-1} s^{-1}. The pK_a value for PADS in acetonitrile/water (90/10% v/v) can then be calculated to be 26.0 by using this estimated diffusion-controlled rate constant, the measured rate of D-exchange and the pK_a of 13.7 for 3-picoline in acetonitrile.[34] There are no pK_a data for thioesters in acetonitrile but that for ethyl thioacetate in water is 21 (ref. 35) and, based on substituent and solvent effects,[30] that for ethyl thiophenylacetate PhCH$_2$COSEt in acetonitrile is ~31, so the estimated value of 26.0 for PADS is reasonable given the additional electron-withdrawing SSCOCH$_2$Ph residue.

The rate of degradation of PADS (**2**) is *ca.* 500-fold slower than the rate of D-exchange under the same conditions, indicating that carbanion formation is relevant to the formation of the degradation products of PADS. Indeed, removing the dissociable protons in PADS by α,α-dimethylation prevents the degradation of the tetramethyl derivative (**7**) which remains unchanged after 1 week in acetonitrile with 5 equivalents of picoline at 25 °C. Similarly, bis-benzoyl disulfide is stable in acetonitrile with 5 equivalents of picoline at 25 °C for 1 week,

confirming the elimination mechanism for the degradation of PADS (**2**).
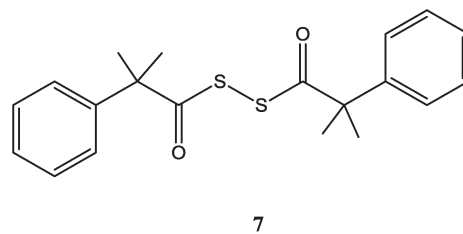
7

The proposed mechanism for the degradation of PADS (Scheme 1) involves the generation of the ketene intermediate. The reaction of *o*-allyl PADS (**8**) in 50% v/v acetonitrile/3-picoline yields the bicyclic ketone (**9**) identified by MS and ^{1}H NMR, consistent with trapping the intermediate ketene by a [2 + 2] cycloaddition. With PADS itself, the ketene forms the 3-hydroxycyclobutenone dimer, (**10**) and the pyran-4-one trimer (**11**) as observed with the base-catalysed reaction of phenylacetyl chloride.[36]
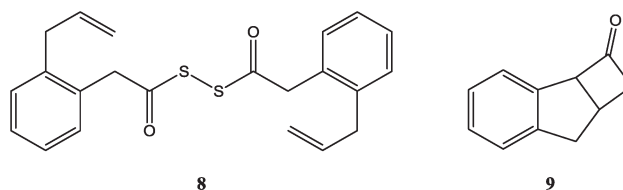
8   **9**
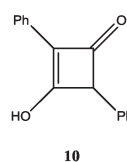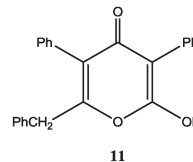
10   **11**

The relative effect of substituents in the aromatic ring of PADS (**2**) on the rate constants for H/D-exchange and the degradation process are shown in Table 2.

All of the above observations suggest that a polar mechanism is taking place, which is also supported by the rate of degradation of PADS (**2**) being unaffected by light or dark or the addition of the radical scavenger 2,6-di-*tert*-butyl-4-methylphenol (BHT).

In summary, the degradation of PADS (**2**) in acetonitrile catalysed by pyridine bases involves reversible carbanion formation, which expels acyl disulfide anion to generate a ketene

Table 2 The dependence of the second-order rate constants for H/D-exchange and for the degradation of substituted PADS (**2**) in acetonitrile at 25 °C

PADS substituent	σ	k_{ex} (M^{-1} s^{-1})
4-MeO	−0.27	1.38×10^{-3}
H	0	5.16×10^{-3}
4-Cl	0.23	2.20×10^{-2}
4-CN	0.66	1.09×10^{-1}

8304 | *Org. Biomol. Chem.*, 2016, **14**, 8301–8308

This journal is © The Royal Society of Chemistry 2016
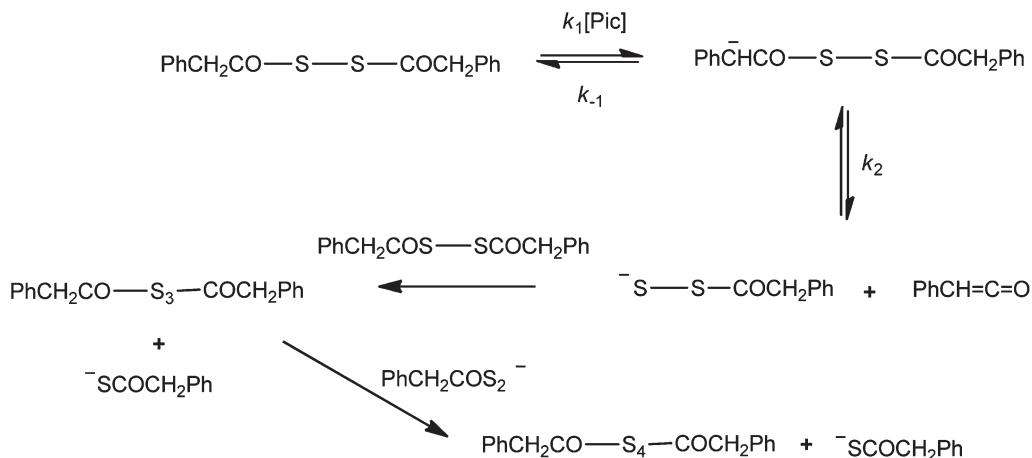
Scheme 3

intermediate. The disulfide anion then attacks unreacted PADS at sulfur to give polysulfides (Scheme 3). Other possibilities are feasible, including polysulfide anion attack on PADS (**2**) and diacylated polysulfides. It is interesting that the rate of degradation is only first order in PADS (**2**) indicating that the rate-limiting step is k_2 formation of the disulfide anion from the carbanion, rather than its subsequent reaction with a second mole of PADS.

Conclusion

The activation of PADS by its 'ageing' for 48 h in acetonitrile with 3-picoline involves the generation of polysulfides which are the actual nucleotide–phosphite sulfurising agents. The initial base-catalysed degradation of PADS occurs by an E1cB-type elimination to generate a ketene and acyldisulfide anion. Carbanion formation from PADS is reversible, demonstrated by H/D exchange, the mechanism of which occurs by base catalysis and is greatly increased by electron-withdrawing substituents in the aromatic ring of PADS. The ketene can be trapped intramolecularly by an *o*-allyl group. The disulfide anion generated subsequently attacks unreacted PADS on sulfur to give polysulfides, the active sulfurising agent. The rate of degradation of PADS is decreased by less basic substituted pyridines and is only first order in PADS indicating that the rate-limiting step is formation of the disulfide anion from the carbanion.

Experimental

NMR experiments were performed using a 400 MHz Bruker Avance DP X400 NMR spectrometer. HPLC traces were acquired using a Shimadzu SIL 50AH instrument with a Luna 5μ C18 4.67 × 250 mm column. The gradient used for kinetic measurements was 30–95% acetonitrile in water over 10 minutes followed by isocratic elution for a further 10 minutes.

H/D exchange of PADS

To a solution of phenylacetyl disulfide in deuterated acetonitrile (0.2 M, 400 μl) and D_2O (50 μl) was added 3-picoline (15.5 μl, 16.2 mg, 0.17 mmol). The ^1H NMR of this mixture was run every 2 minutes until exchange was complete.

General degradation kinetics of PADS

A solution of PADS (1000 ppm, 3.3 mM) in HPLC-grade acetonitrile containing the appropriate concentration of 3-picoline was divided between 2 HPLC vials and chromatograms were taken every 30 minutes for 48 hours.

General sulfurisation kinetics with 'aged' PADS

A solution of PADS (1 M) 50/50 v/v acetonitrile/3-picoline was left to age for 48 hours. At $T = n$ h a 1 ml sample of this was removed and quenched with dilute hydrochloric acid (10 ml, 2 M) to remove the picoline as the protonated pyridinium ion. This was then washed with DCM (2 × 10 ml) the combined organic layers dried and the solvent removed under vacuum. The resulting oil was then made up to 1 ml using deuterated acetonitrile. To an NMR tube containing triphenyl phosphite in deuterated acetonitrile (0.1 M, 200 μL) and 3-picoline in deuterated acetonitrile (2 M, 200 μL) was added 'aged' PADS solution (200 μL, 1 M) and ^{31}P NMR spectra recorded every 90 seconds.

Trapping the ketene intermediate

A mixture of 2,2′-allyl-2,2′-phenylacetyl disulfide (330 mg, 0.852 mmol) and 3-picoline (165.6 μl, 1.7 mmol) in acetonitrile (10 ml) was refluxed for 2 h. The reaction was followed by HPLC and was complete after 2 h. The mass spec and NMR analysis showed evidence of the product 7,7a-dihydro-1*H*-cyclobuta[*a*]inden-2(2aH)-one as described below.

Synthesis

Methyl 2′-iodo-2-phenylacetate. 2′-Iodo-phenylacetic acid (5.01 g, 19.1 mmol) and H_2SO_4 (98%, 1.25 ml) were dissolved

in methanol (7.5 ml). The reaction mixture was stirred for 2.5 h at 65 °C, then diluted with 250 ml dichloromethane (DCM), extracted with water (2 × 100 ml) and brine (50 ml). The organic solution was dried over MgSO$_4$, and gravity filtered. DCM was removed under vacuum to give a pale yellow oil (4.88 g, 92.6% yield). HPLC retention time 5.397 min; ^{1}H NMR (CDCl$_3$, 400 MHz) δ 3.69 (s, 3H, CH$_3$), 3.79 (s, 2H, CH$_2$), 6.92–6.96 (m, 1H, ArH), 7.22–7.32 (m, 2H, ArH), 7.83 (d, 1H, J 7.91 Hz, ArH) ppm; ^{13}C NMR (CDCl$_3$, 100 MHz) δ 46.12 (CH$_3$), 52.22 (CH$_2$), 101.07 (CI), 128.48 (CH), 128.94 (CH), 130.68 (CH), 137.72 (Cq), 139.54 (CH), 170.95 (CO) ppm; IR (film) 1732.81 cm^{-1}.

Methyl 2′-allyl-2-phenylacetate.[37] Methyl 2′-iodo 2-phenyl-acetate (3.0 g, 10.9 mmol), CsF (6.6 g, 43.6 mmol), and Pd(PPh$_3$)$_4$ (0.63 g, 0.55 mmol) were dissolved in THF (250 ml), stirred for 30 min at room temperature. A solution of allylboronic acid pinacol ester (3.3 ml, 21.8 mmol) in THF (50 mL) was added and then heated under reflux for 24 h. The reaction mixture was diluted with petroleum ether (bpt. 60–80 °C, 300 mL), extracted with water (2 × 200 ml) and the combined aqueous layers washed with petroleum ether (bpt 60–80 °C, 100 ml). The combined organic layers were washed with water (100 mL), brine (100 mL), dried over MgSO$_4$. The solvent was removed under vacuum to give an orange oil product (2.5 g) which was purified using a Biotage SP4 chromatography system fitted with a Biotage Snap 10 column eluting with a gradient of 0–25% ethyl acetate in hexane over 15 column volumes to give the product ester as a yellow oil (1.6 g, 77.2% yield). HPLC retention time 5.630 min; ^{1}H NMR (CDCl$_3$, 400 MHz) δ 3.39 (dt, 2H, J 6.29 Hz, CH$_2$), 3.61 (s, 2H, CH$_2$), 3.65 (s, 3H, CH$_3$), 4.94–5.06 (m, 2H, CH$_2$), 5.87–5.97 (m, 1H, CH), 7.14–7.23 (m, 4H, ArH) ppm; ^{13}C NMR (CDCl$_3$, 100 MHz) δ 37.35 (CH$_2$), 38.45 (CH$_2$), 51.94 (CH$_3$), 115.96 (CH$_2$), 126.65 (CH), 127.55 (CH), 129.91 (CH), 130.65 (CH), 132.66 (Cq), 136.57 (CH$_2$), 138.35 (Cq), 171.95 (CO) ppm; IR (film) 1734.52 cm^{-1}.

2′-Allyl 2-phenylacetic acid. To methyl-2′-allyl 2-phenylacetate (1.7 g, 8.9 mmol) in THF (20 ml) was added an aqueous lithium hydroxide solution (0.4 M, 20 ml) and the solution stirred at room temperature for 3 h after which the mixture was diluted with water (40 ml) and extracted with DCM (2 × 20 ml). The pH of the aqueous layer was reduced to pH 1 with HCl, extracted with DCM (2 × 20 ml), dried over MgSO$_4$ and the solvent removed under vacuum giving the brown oil product (1.7 g, 9.7 mmol, 82.9% yield). HPLC retention time 4.634 min; ^{1}H NMR (CDCl$_3$, 400 MHz) δ 3.38 (dt, 2H, J 6.37 Hz, CH$_2$), 3.65 (s, 2H, CH$_2$), 4.94–5.06 (m, 2H, CH$_2$), 5.86–5.96 (m, 1H, CH), 7.14–7.23 (m, 4H, ArH), 10.76 (broad, s, 1H, OH) ppm; ^{13}C NMR (CDCl$_3$, 100 MHz) δ 37.5 (CH$_2$), 38.45 (CH$_2$), 116.22 (CH$_2$), 126.79 (CH), 127.96 (CH), 130.08 (CH), 130.88 (CH), 132.05 (Cq), 136.52 (CH), 138.55 (Cq), 178.41 (CO) ppm; IR (film) 1702.49 cm^{-1}.

2′,2′-Diallyl 2,2-phenylacetyl disulfide (8).[38] Sodium hydrosulfide (798 mg, 14.25 mmol) was dissolved in ethanol (5 ml) and chilled over ice. The flask was fitted with an exhaust line allowing any gasses generated to be scrubbed by sodium hypo-

chlorite in a well-ventilated fume hood. In a separate flask, to 2′-allyl 2-phenylacetic acid (1.0 g, 5.7 mmol) dissolved in DCM (10 ml) was added Ghosez reagent (1.04 g, 1.03 ml, 8.5 mmol) then stirred at room temperature for 30 min and the solvent removed under vacuum to yield an orange oil. This oil was added to the ethanolic sodium hydrosulfide solution which instantly turned yellow and the precipitate of sodium chloride removed under vacuum filtration and washed with ice cold ethanol (1.5 ml). To the solution, stirred over ice, iodine was slowly added until the colour of the suspension changed from white to pale brown (approximately 1 g, 7.8 mmol). The resulting mixture was diluted with DCM (10 ml), washed twice with saturated sodium thiosulfate solution (2 × 15 ml) and the organic layer concentrated under vacuum to yield the brown oil product which was purified using a Biotage SP4 chromatography system fitted with a Biotage Snap 10 column eluting with 25% ethyl acetate in hexane (R_f = 0.41) to give the product as a clear oil (384 mg, 1 mmol, 14.1% yield). HPLC retention time 7.6 min; ^{1}H NMR (CDCl$_3$, 400 MHz) δ 3.41 (d, 4H, J = 6.3 Hz, CH$_2$), 4.00 (s, 4H, CH$_2$), 4.96–5.60 (m, 4H, CH$_2$), 5.88–5.98 (m, 2H, CH), 7.17–7.30 (m, 8H, ArH) ppm; ^{13}C NMR (CDCl$_3$, 100 MHz) δ 37.51 (CH$_2$), 46.68 (CH$_2$), 116.63 (CH$_2$), 126.95 (CH), 128.58 (CH), 130.22 (CH), 130.88 (Cq), 131.53 (CH), 136.12 (CH), 139.07 (Cq), 191.81 (CO) ppm.

7,7a-Dihydro-1H-cyclobuta[a]inden-2(2aH)-one (9). A mixture of 2′-allyl 2-phenylacetylchloride (100 mg, 0.514 mmol) and 1-chloro-N,N,2-trimethyl-1-propenylamine (74.7 μl, 0.56 mmol) in DCM (10 ml) was stirred for 30 min at room temperature, triethylamine (78 μl, 0.56 mmol) in DCM (4 ml) was added and refluxed for 2 h. The reaction mixture was cooled and extracted with 2 M hydrochloric acid (20 ml) to remove the 3-picoline. The crude bright orange oil product mixture was purified using a Gilson prep. HPLC system equipped with a phenomenex luna C18, 5μ 250 × 20 mm column. The mobile phase consisted of a gradient of 50–100% acetonitrile (0.05% TFA) in water (0.05% TFA) over 15 minutes then isocratic elution at 50% acetonitrile (0.05% TFA) in water (0.05% TFA) for a further 3 minutes. The product eluted at 7.5 min. All fractions were combined and the solvent removed under vacuum to give the product as a white, crystalline solid (24 mg, 41.8% yield). HPLC retention time 4.775 min; ^{1}H NMR (d$_3$ACN, 400 MHz) δ 2 2.75–2.87 (m, 1H, CH$_2$), 3.05 (d, 1H, J 16.73, CH$_2$), 3.11–3.18 (m, 1H, CH), 3.30–3.42 (m, 1H, CH$_2$), 3.38–3.45 (m, 1H, CH$_2$), 4.71 (broad, s, 1H), 7.23–7.36 (m, 4H, ArH); ^{13}C NMR (ACN-d^3, 100 MHz) δ 26.18 (CH), 38.82 (CH$_2$), 52.32 (CH$_2$), 71.81 (CH), 124.45 (CH), 125.50 (CH), 126.82 (CH), 127.52 (CH), 137.6 (Cq), 143.38 (Cq), 206.13 (CO), IR (film) 1771.39 cm^{-1}.

2,2,2′,2′-Tetramethyl 2,2′-phenylacetyl disulfide (7). Sodium hydrosulfide (4.2 g, 75 mmol) was dissolved in ethanol (30 ml) and chilled over ice. The flask was fitted with an exhaust line allowing any gasses generated to be scrubbed by sodium hypochlorite in a well-ventilated fume hood. In a separate flask, to 2-phenylisobutyric acid (5 g, 30 mmol) dissolved in DCM (20 ml) was added Ghosez reagent (6.16 g, 5.6 ml, 45 mmol) then stirred at room temperature for 30 min and

8306 | *Org. Biomol. Chem.,* 2016, **14**, 8301–8308

This journal is © The Royal Society of Chemistry 2016

the solvent removed under vacuum to yield an orange oil. This oil was added to the ethanolic sodium hydrosulfide solution which instantly turned yellow and the precipitate of sodium chloride removed under vacuum filtration and washed with ice cold ethanol (1.5 ml). To the solution, stirred over ice, iodine (2 g, 15.6 mmol) was slowly added. The resulting precipitate was collected by vacuum filtration and washed with ice-cold ethanol (5 ml) and water (10 ml) to give a waxy yellow solid (2.2 g, 5.9 mmol, 39.3% yield). HPLC retention time 7.6 min; ^{1}H NMR (CDCl$_3$, 400 MHz) δ 1.68 (s, 12H), 7.34 (m, 10H) ppm; ^{13}C NMR (CDCl$_3$, 100 MHz) δ 26.82, 54.21, 127.27, 127.86, 128.61, 142.14, 199.39 ppm. HRMS (m/z): [M + NH$_4$]$^+$ for C$_{20}$H$_{22}$O$_2$S$_2$, calculated 390.0782, measured 390.0788; IR: 1707.3 cm^{-1} (film).

2,2′-(4-Chlorophenyl)acetyl disulfide. As above using sodium hydrosulfide (1.6 g, 29.25 mmol) in ethanol; (15 ml) 4-chlorophenylacetic acid (2 g, 11.7 mmol) in DCM (20 ml); Ghosez reagent (1.72 g, 1.57 ml, 12.9 mmol); iodine (0.5 g, 3.9 mmol) to give product (1.5 g, 4.1 mmol, 70.1% yield). HPLC retention time 7.3 min; ^{1}H NMR (CDCl$_3$, 400 MHz) δ 3.94 (s, 4H, CH$_2$), 7.22 and 7.32 (2d, 8H, J 8.53 Hz, ArH) ppm; ^{13}C NMR (CDCl$_3$, 100 MHz) δ 48.37 (CH$_2$), 129.12 (CH), 130.48 (Cq), 131.06 (CH), 134.12 (Cq), 190.83 (CO) ppm. HRMS (m/z): [M + NH$_4$]$^+$ for C$_{16}$H$_{12}$Cl$_2$O$_2$S$_2$, calculated 387.9994, measured 388.0000; IR: 1720.2 cm^{-1} (film).

2,2′-(4-Cyanophenyl)acetyl disulfide. As above using sodium hydrosulfide (2.4 g, 43 mmol) in ethanol (20 ml); 4-cyanophenylacetic acid (2.753 g, 17.1 mmol) in DCM (20 ml); Ghosez reagent (3.432 g, 3.120 ml, 25.7 mmol); iodine (0.5 g, 3.9 mmol) to give the product as a oragne/yellow solid (1.6 g, 4.6 mmol, 53.8% yield). HPLC retention time 6.0 min; ^{1}H NMR (CDCl$_3$, 400 MHz) δ 4.08 (s, 4H), 7.41 and 7.64 (2d, 8H, J 8.23 Hz, ArH) ppm; ^{13}C NMR (CDCl$_3$, 100 MHz) δ 48.82 (CH$_2$), 112.06 (CN), 118.41 (Cq), 130.47 (CH), 132.65 (CH), 137.28 (Cq), 189.76 (CO) ppm. HRMS (m/z): [M + NH$_4$]$^+$ for C$_{18}$H$_{12}$N$_2$O$_2$S$_2$, calculated 352.0340, measured 352.0352; IR: 1715.6 cm^{-1} (film).

2,2′-(4-Methoxyphenyl)acetyl disulfide. As above using sodium hydrosulfide (4.26 g, 75.3 mmol) in ethanol (20 ml); 4-methoxyphenylacetic acid (5 g, 30.1 mmol) in DCM (20 ml); Ghosez reagent (8.03 g, 7.96 ml, 60.2 mmol); iodine (1 g, 7.8 mmol) to give product (1.19 g, 3.28 mmol, 10.9% yield). ^{1}H NMR (CDCl$_3$, 400 MHz) δ 3.79 (s, 6H, CH$_3$), 3.92 (s, 4H, CH$_2$), 6.89 and 7.16 (2d, 8H, J 8.15 Hz, ArH) ppm; ^{13}C NMR (CDCl$_3$, 100 MHz) δ 48.6 (CH$_3$), 55.2 (CH$_2$), 114.7 (CH), 124.5 (Cq), 131.1 (CH), 159.5 (Cq), 192.5 (CO) ppm; HRMS (m/z): [M + NH$_4$]$^+$ for C$_{18}$H$_{18}$O$_4$S$_2$, calculated 362.0647, measured 362.0634.

Bis-benzoyl disulfide.[39] To sodium sulfide (1.84 g, 23.6 mmol) in water (12 ml) and heated to 50 °C was added tetra-N-butylammonium bromide (380 mg, 1.18 mmol) then stirred for 30 minutes. In a separate flask, (fitted with an exhaust line allowing any gasses generated to be scrubbed by sodium hypochlorite in a well-ventilated fume hood) benzoyl chloride (2 ml, 1.65 g, 11.8 mmol) in toluene (12 ml). This was

chilled in an ice bath. After 30 minutes the sodium sulfide solution was cooled to room temperature and slowly added to the rapidly stirring, chilled benzoyl chloride solution under a nitrogen atmosphere creating a biphasic reaction mixture. This was stirred for 24 hours at room temperature. The organic and aqueous layers were separated, the aqueous layer washed with 2 × 5 ml portions of toluene and the organic layers combined. The toluene was then removed under vacuum giving the product as white crystals (738 mg, 45.7% yield) from which a single crystal X-ray diffraction pattern was resolved. The aqueous layer contains residual Na$_2$S which will generate H$_2$S if exposed to acid and was disposed of carefully. ^{1}H NMR (CDCl$_3$, 400 MHz) δ 7.43 (t, 4H, ArH), 7.57 (t, 2H, ArH), 7.89 (d, 4H, ArH) ppm; ^{13}C NMR (CDCl$_3$, 100 MHz) δ 127.91 (CH), 128.79 (CH), 134.02 (CH), 136.61 (Cq), 190.37 (CO) ppm.

Acknowledgements

Notes and references

1 P. C. Zamecnik and M. L. Stephenson, *Proc. Natl. Acad. Sci. U. S. A.*, 1978, **75**, 285.

2 R. S. Geary, D. Norris, R. Yu and C. F. Bennett, *Adv. Drug Delivery Rev.*, 2015, **87**, 46; S. T. Crooke, T. Vickers, W. F. Lima and H. Wu, Mechanisms of antisense drug action, an introduction, in *Antisense Drug Technology: Principles, Strategies, and Applications*, ed. S. T. Crooke, CRC Press, Boca Raton, 2nd edn, 2007, pp. 3–46; C. F. Bennett and E. E. Swayze, *Annu. Rev. Pharmacol. Toxicol.*, 2010, **50**, 259; H. Wu, W. F. Lima, H. Zhang, A. Fan, H. Sun and S. T. Crooke, *J. Biol. Chem.*, 2004, **279**, 181.

3 R. M. Orr, *Curr. Opin. Mol. Ther.*, 2001, **3**, 288; B. Roehr, *J. Int. Assoc. Physicians AIDS Care*, 1998, **4**, 14.

4 S. Agrawal and E. R. Kandimalla, *Mol. Med. Today*, 2000, **6**, 72.

5 D. A. Bell, A. J. Hooper and J. R. Burnett, *Expert Opin. Inves. Drugs*, 2011, **20**, 265.

6 A. Goyenvalle, J. Wright, A. Babbs, V. Wilkins, L. Garcia and K. E. Davies, *Mol. Ther.*, 2012, **20**, 1212.

7 D. J. French, D. G. McDowell, P. Debenham, N. Gale and T. Brown, *Methods Mol. Biol.*, 2008, **429**, 17.

8 P. S. Eder, R. J. DeVine, J. M. Dagle and J. A. Walder, *Antisense Res. Dev.*, 1991, **1**, 141–151.

9 B. Nawrot and K. Sipa, *Curr. Top. Med. Chem.*, 2006, **6**, 913; E. L. Chernolovskaya and M. A. Zenkova, *Curr. Opin. Mol. Ther.*, 2010, **12**, 158; S. P. Walton, M. Wu, J. A. Gredell and C. Chan, *FEBS J.*, 2010, **277**, 4806; M. R. Laresa, J. J. Rossia and D. L. Ouellet, *Trends Biotechnol.*, 2010, **28**, 570; P. Guga, *Curr. Top. Med. Chem.*, 2007, 7, 695.

This journal is © The Royal Society of Chemistry 2016

Org. Biomol. Chem., 2016, **14**, 8301–8308 | 8307

10 F. Eckstein, *Antisense Nucleic Acids Drug Dev.*, 2000, **10**, 117.

11 J. H. P. Chan, S. Lim and W. S. F. Wong, *Clin. Exp. Pharmacol. Physiol.*, 2006, **33**, 533; T. Yamamoto, M. Nakatani, K. Narukawa and S. Obika, *Future Med. Chem.*, 2011, **3**, 339; N. M. Bell and J. Micklefield, *ChemBioChem*, 2009, **10**, 2691.

12 L. Wang, S. Chen, T. Xu, K. Taghizadeh, J. S. Wishnok, X. Zhou, D. You, Z. Deng and P. C. Dedon, *Nat. Chem. Biol.*, 2007, **3**, 709.

13 P. Guga and M. Koziołkiewiczb, *Chem. Biodiversity*, 2011, **8**, 1642.

14 S. T. Crooke, *Methods Enzymol.*, 2000, **313**, 3; C. A. Stein and Y. C. Cheng, *Science*, 1993, **261**, 1004.

15 P. C. J. Kamer, H. C. P. F. Roelen, H. van den Elst, G. A. van der Marel and J. H. van Boom, *Tetrahedron Lett.*, 1989, **30**, 6757–6760.

16 R. P. Iyer, L. R. Phillips, W. Egan, J. B. Regan and S. L. Beaucage, *J. Org. Chem.*, 1990, **55**, 4693–4699.

17 H. Vu and B. L. Hirschbein, *Tetrahedron Lett.*, 1991, **32**, 3005–3008.

18 M. V. Rao, C. B. Reese and Z. Zhao, *Tetrahedron Lett.*, 1992, **33**, 4839–4842.

19 W. J. Stec, B. Uznanski and A. Wilk, *Tetrahedron Lett.*, 1993, **33**, 5317–5320.

20 M. V. Rao and K. Macfarlane, *Tetrahedron Lett.*, 1994, **35**, 6741–6744.

21 V. A. Efimov, A. L. Kalinkina, O. G. Chakhmakhcheva, T. S. Hill and K. Jayaraman, *Nucleic Acids Res.*, 1995, **23**, 4029–4033.

22 Q. Xu, K. Musier-Forsyth, R. P. Hammer and G. Barany, *Nucleic Acids Res.*, 1996, **24**, 1602–1607.

23 Z. Zhang, A. Nichols, M. Alsbeti, J. X. Tang and J.-Y. Tang, *Tetrahedron Lett.*, 1998, **39**, 2467–2470.

24 Z. Zhang, A. Nichols, J. X. Tang, Y. Han and J.-Y. Tang, *Tetrahedron Lett.*, 1999, **40**, 2095–2098.

25 J.-Y. Tang, Z. Han, J. X. Tang and Z. Zhang, *Org. Process Res. Dev.*, 2000, **4**, 194–198.

26 A. H. Krotz, D. Gorman, P. Mataruse, C. Foster, J. D. Godbout, C. C. Coffin and A. N. Scozzari, *Org. Process Res. Dev.*, 2004, **8**, 852–858.

27 Z. S. Cheruvallath, R. L. Carty, M. N. Moore, D. C. Capaldi, A. H. Krotz, P. D. Wheeler, B. J. Turney, S. R. Craig, H. J. Gaus, A. N. Scozzari, D. L. Cole and V. T. Ravikumar, *Org. Process Res. Dev.*, 2000, **4**, 199–204.

28 A. H. Krotz, D. Gorman, P. Mataruse, C. Foster, J. D. Godbout, C. C. Coffin and A. N. Scozzari, *Org. Process Res. Dev.*, 2004, **8**, 852–858.

29 J. Scotson, B. I. Andrews, A. P. Laws and M. I. Page, in preparation.

30 B. G. Cox, *'Acids and Bases, solvent effects on acid–base strength'*, Oxford UP, Oxford, 2013.

31 M. Benaïchouche, G. Bosser, J. Paris and V. Plichon, *J. Chem. Soc., Perkin Trans. 2*, 1990, 1421.

32 J. Robert, M. Anouti and J. Paris, *J. Chem. Soc., Perkin Trans. 2*, 1997, 473–478.

33 P. Ji, N. T. Powles, J. H. Atherton and M. I. Page, *Org. Lett.*, 2011, **13**, 6118–6121.

34 I. Kaljurand, A. Kutt, L. Soovali, V. Maemets, I. Leito and I. A. Koppel, *J. Org. Chem.*, 2005, **70**, 1019.

35 T. L. Amyes and J. P. Richard, *J. Am. Chem. Soc.*, 1992, **114**, 10297.

36 D. G. Farnum, J. R. Johnson, R. E. Hess, T. B. Marshall and B. Webster, *J. Am. Chem. Soc.*, 1965, **87**, 5191–5197.

37 S. Kotha, M. Behera and V. R. Shah, *Synlett*, 2005, 1877–1880.

38 C. D. Dittmer, *Encyclopedia of Reagents for Organic Synthesis*, John Wiley & Sons, Chichester, 2001.

39 Z. S. Cheruvallath, R. L. Carty, M. N. Moore, D. C. Capaldi, A. H. Krotz, P. D. Wheeler, B. J. Turney, S. R. Craig, H. J. Gaus, A. N. Scozzari, D. L. Cole and V. T. Ravikumar, *Org. Process Res. Dev.*, 2000, **4**, 199–204.

8308 | *Org. Biomol. Chem.*, 2016, **14**, 8301–8308

This journal is © The Royal Society of Chemistry 2016

PAPER

Phosphorothioate anti-sense oligonucleotides: the kinetics and mechanism of the sulfurisation of phosphites by phenylacetyl disulfide (PADS)†

James L. Scotson,[a] Benjamin I. Andrews,[b] Andrew P. Laws[a] and Michael I. Page*[a]

In the pharmaceutical industry the sulfurisation of nucleotide-phosphites to produce more biologically stable thiophosphates is often achieved using 'aged' solutions of phenylacetyl disulfide (PADS) which consist of a mixture of polysulfides that are more efficient sulfur transfer reagents. However, both 'fresh' and 'aged' solutions of PADS are capable of the sulfurisation of phosphites. The rates of both processes in acetonitrile are first order in sulfurising agent, phosphite and a pyridine base, although with 'aged' PADS the rate becomes independent of base at high concentrations. The Brönsted β values for sulfurisation using 'fresh' and 'aged' PADS with substituted pyridines are 0.43 and 0.26, respectively. With 'fresh' PADS the Brönsted $\beta_{nuc} = 0.51$ for substituted trialkyl phosphites is consistent with a mechanism involving nucleophilic attack of the phosphite on the PADS disulfide bond to reversibly generate a phosphonium intermediate, the rate-limiting breakdown of which occurs by a base catalysed elimination process, confirmed by replacing the ionisable hydrogens in PADS with methyl groups. The comparable polysulfide phosphonium ion intermediate seen with 'aged' PADS presents a more facile pathway for product formation involving S–S bond fission as opposed to C–S bond fission.

Introduction

Anti-sense oligonucleotides (ASOs)[1] are usually single-stranded deoxy-ribonucleotides of 15–35 bases which bind to a specific section of mRNA to form a dimer that may then inhibit translation and therefore prevent synthesis of an unwanted target protein. ASOs are promising therapeutics[2] but the incorporation of a native phosphodiester link means they are rapidly hydrolysed by intracellular endonucleases and exonucleases.[3] To overcome this problem ASOs have been modified to decrease their susceptibility to nuclease catalysed hydrolysis and improve their pharmacokinetics.[4] One of the most common examples of these changes is the introduction of a phosphorothioate backbone (**1**)[5] to give derivatives which are poor substrates for enzyme catalysed hydrolysis and yet do not disrupt binding between the nucleobases.[6] The introduction

of the relatively hydrophobic sulfur also increases cell uptake compared with the native P=O phosphodiester whilst still maintaining good water solubility as a polarisable anion. Although the replacement of one of the phosphate non-bridging oxygens by sulfur makes the phosphorus chiral, it is only the (*S*)-P phosphorothioate diastereomer that is nuclease resistant.[7]

The successful large scale synthesis of oligonucleotides with phosphorothioate links requires the sulfurisation step to have a near quantitative yield, to be rapid and give a maximal P=S to P=O ratio. Sulfurisation of the protected nucleotide-phosphite (**2**), attached to a solid support, is often carried out with the sulfurising agent present in an organic solvent. Although there are a number of reagents available[8,9] phenyl-acetyl disulfide (PADS) (**3**) is commonly used in the pharmaceutical industry.[10–12] This reagent is unusual in that it is best 'aged' in a basic acetonitrile solution to obtain optimal sulfurisation activity,[13] often using 3-picoline as the base. We have recently shown that this is due to the formation of diacyl polysulfides (**4**) by an unusual elimination E1cB mechanism.[14] Although both 'fresh' and 'aged' PADS convert phosphite esters to the corresponding thiophosphate, 'ageing' improves the rate and efficiency of sulfurisation. Herein we address the

[a]*Department of Chemistry, University of Huddersfield, Queensgate, Huddersfield HD1 3DH, UK. E-mail: m.i.page@hud.ac.uk*
[b]*GSK Medicines Research Centre, Gunnels Wood Road, Stevenage, Hertfordshire, SG1 2NY, UK*
†Electronic supplementary information (ESI) available: Detailed kinetic data. See DOI: 10.1039/c6ob02108e

10840 | *Org. Biomol. Chem.*, 2016, **14**, 10840–10847

This journal is © The Royal Society of Chemistry 2016

reasons for this difference and report the kinetics and mechanism of both sulfurisation reactions.

Fig. 1   Pseudo first-order rate constants (k_{obs}) at 25 °C as a function of the concentration of 3-picoline for the sulfurisation of 0.10 M triphenyl phosphite by 1.0 M PADS.
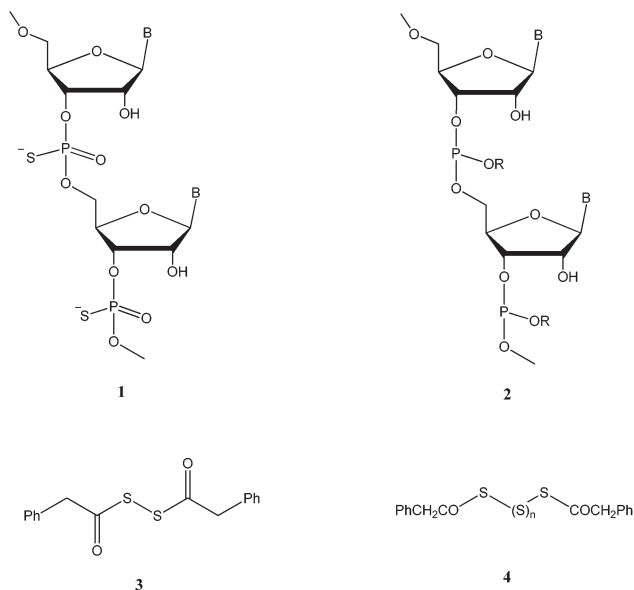
Results and discussion

Sulfurisation by 'fresh' PADS

Although a freshly made solution of PADS (**3**) is not an optimal sulfurising agent[13] it is still capable of converting phosphite triesters to the corresponding thiophosphate (Scheme 1). For example, a solution of 1.0 M PADS (**3**) and 2.0 M 3-picoline in acetonitrile sulfurises 0.1 M triphenyl phosphite to triphenyl thiophosphate at 25 °C with a half-life of ~15 min. The kinetics of this process were determined by following the reaction by ^{31}P NMR from which the rate law was found to be first order in each reagent (eqn (1)). With excess PADS and 3-picoline there is an exponential decrease in phosphite concentration from which the observed pseudo first-order rate constants were found to increase with increasing concentration of catalytic base, 3-picoline (Fig. 1) giving a second-order rate constant $k_{cat} = 4.13 \times 10^{-4}$ M^{-1} s^{-1} at 25 °C. Similarly the observed pseudo first-order rate constants increase with the concentration of PADS.

$$\text{Rate} = k[\text{PADS}][\text{picoline}][(\text{RO})_3\text{P}] \qquad (1)$$

Solutions of PADS in acetonitrile with 3-picoline slowly degrade to give polysulfides.[14] However, when using 'fresh' solutions of PADS for the sulfurisation of phosphites, the active sulfurising reagent must be the intact diacyl disulfide (**3**) as the rate of sulfurisation of phosphite esters by 'fresh'

PADS are two orders of magnitude faster than the rate of degradation of PADS under similar conditions.
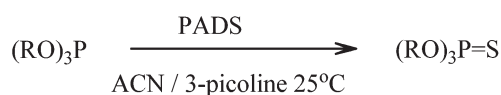
The sulfurisation process is likely to occur by an ionic mechanism as indicated by the dependency of the rate on a base, substituent effects in all three reagents and on the polarity of the solvent. For example, the relative rates of sulfurisation of triphenyl phosphite in toluene, chloroform, acetonitrile and DMSO are 1 : 4 : 86 : 230, respectively, and these ratios remain similar for the sulfurisation of substituted triaryl phosphites.

The mechanism of the reaction was investigated by determining the effect of substituents in the three reagents – the phosphite, the sulfurising agent and the catalytic base on the rates of sulfurisation. Trialkyl phosphites undergo sulfurisation extremely rapidly in acetonitrile making kinetic investigations difficult, but the reactions are measurable in chloroform (Table 1). Electron-withdrawing substituents in trialkyl-phosphites (RO)$_3$P decrease the rate of sulfurisation and there is a Brönsted-type linear dependence of the observed pseudo first-order rate constants (k_{obs}) on the pK_a of the corresponding alcohol in water generating an apparent $\beta_{nuc} = 0.51$ (Fig. 2) indicative of positive charge development on phosphorus in the transition state and compatible with the phosphite acting

$$(\text{RO})_3\text{P} \xrightarrow[\text{ACN / 3-picoline 25°C}]{\text{PADS}} (\text{RO})_3\text{P}=\text{S}$$

Scheme 1

Table 1 The observed pseudo first-order rate constants (k_{obs}) for the sulfurisation of substituted trialkyl and triphenyl phosphites (0.10 M) by 'fresh' PADS (1.0 M) and 3-picoline (2.0 M), in CDCl$_3$ at 25 °C

(RO)$_3$P R substituent	pK_a ROH (H$_2$O)	k_{obs} (s^{-1})
Ethyl	16.0	1.43×10^{-2}
Methyl	15.54	5.10×10^{-3}
2-Chloroethyl	14.31	5.60×10^{-4}
2,2,2-Trifluoroethyl	12.43	1.98×10^{-4}
4-Methoxyphenyl	10.20	3.51×10^{-5}
4-Methylphenyl	10.19	6.55×10^{-5}
Phenyl	9.95	3.28×10^{-5}
4-Fluorophenyl	9.95	2.66×10^{-5}
4-Chlorophenyl	9.38	7.88×10^{-5}
3-Chlorophenyl	9.02	4.62×10^{-5}

Fig. 2 Dependence of the observed pseudo first-order rate constant (k_{obs}) for the sulfurisation of substituted trialkyl phosphites (RO)$_3$P by PADS with 3-picoline in chloroform at 25 °C on the pK_a of the corresponding alcohol (ROH) in water.

Fig. 3 Dependence of the observed pseudo first-order rate constant (k_{obs}) for the sulfurisation of triphenyl phosphite (0.10 M) by aryl substituted PADS (1.0 M) with 3-picoline (2.0 M) in acetonitrile at 25 °C on the Hammett σ-value of the aryl substituent.

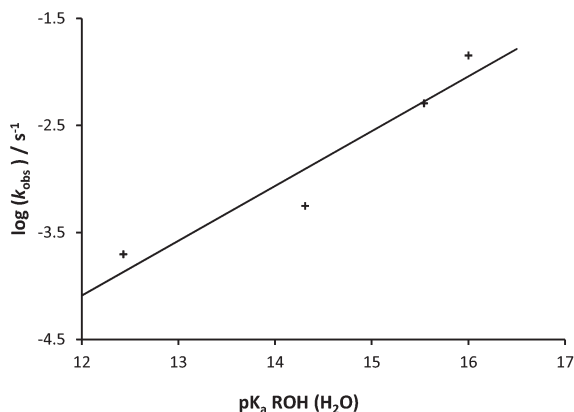Table 2 The observed pseudo first-order rate constants (k_{obs}) for the sulfurisation of triphenyl phosphites (0.10 M) by 'fresh' aryl-substituted PADS (1.0 M) and 3-picoline (2.0 M), in acetonitrile at 25 °C

Ar substituent in $(ArCH_2COS)_2$	k_{obs} (s^{-1})	Hammett σ substituent
4-MeO	2.56×10^{-4}	-0.27
H	7.70×10^{-4}	0
4-F	1.07×10^{-3}	0.06
4-Cl	4.01×10^{-3}	0.23
3-Cl	4.67×10^{-3}	0.37
4-CN	6.27×10^{-3}	0.66

Table 3 The observed pseudo first-order rate constants (k_{obs}) for the sulfurisation of triphenyl phosphite (0.10 M) by 'fresh' PADS (1.0 M) and the pK_a of the catalysing base, substituted pyridines (2.0 M), in acetonitrile at 25 °C

Pyridine substituent	pK_a (ACN)	k_{obs} (s^{-1})
4-CN	8.50	7.26×10^{-6}
3-CN	8.00	7.38×10^{-6}
3-Cl	9.77	2.27×10^{-5}
3-MeO	12.45	4.92×10^{-4}
H	12.60	2.96×10^{-4}
3-Me	13.70	8.81×10^{-4}
4-MeO	14.73	7.15×10^{-3}
2,6 diMe	14.70	8.75×10^{-4}

as a nucleophile in the sulfurising reaction. Trialkyl phosphites have a high thiophilicity and their S-nucleophilicity is greater than that of sulfides.[15] There is little or no dependence of the rates of sulfurisation of triaryl phosphites on the aryl substituent (Table 1).

On the other hand, electron-withdrawing substituents in the aromatic rings of PADS (3) increase the rate of sulfurisation of triphenyl phosphite (0.10 M) with 3-picoline (2.0 M) in acetonitrile (Table 2). However, there is a non-linear dependence on the Hammett σ-values probably suggesting a change in rate-limiting step (Fig. 3). For the 4-methoxy to the 4-chlorosubstituted PADS the Hammett ρ-value is 2.34 indicative of significant generation of negative charge near the PADS residue in the transition state.

The rates of sulfurisation of triphenyl phosphite by 'fresh' PADS (3) in acetonitrile also increase with the basicity of substituted pyridines. A Brönsted-type plot of the dependence of the observed pseudo first-order rate constants at 25 °C on the pK_a of the conjugate acid of substituted pyridines in acetonitrile (Table 3) generates a slope β = 0.43 (Fig. 4), compatible with positive charge development on the pyridine nitrogen in the transition state.

In order to distinguish between the role of the catalytic pyridines acting as general bases or as nucleophiles, sulfurisation was investigated with hindered bases and sulfurising agent.

Fig. 4 Dependence of the observed pseudo first-order rate constants (k_{obs}) for the sulfurisation of triphenyl phosphite by 'fresh' PADS on the pK_a of substituted pyridines in acetonitrile at 25 °C.

For example, the observed first-order rate constant for the sulfurisation of triphenyl phosphite in acetonitrile with PADS using sterically hindered 2,6-lutidine as the base is 3-fold greater than that for pyridine which is similar to the ratios seen for proton abstraction from carbon acids.[16] Whereas for pyridine acting as a nucleophilic catalyst such as in the hydro-

10842 | Org. Biomol. Chem., 2016, 14, 10840–10847

This journal is © The Royal Society of Chemistry 2016

lysis of acetic anhydride[17] and acetyl fluoride,[18] through the intermediate formation of the acetyl pyridinium ion, 2,6-lutidine is an ineffective catalyst despite its higher basicity.[3,4] The sulfurising reaction with 'fresh' PADS therefore appears to involve the pyridine acting as a base abstracting a proton from the benzyl methylene in an elimination step. Such a role can be prevented by replacing these ionisable hydrogens and indeed the rate of sulfurisation of triphenyl phosphite with 2,2,2′,2′-tetramethyl PADS (5) and 3-picoline in acetonitrile is an order of magnitude slower than with PADS (3) under the same conditions. With the sterically hindered 2,6-lutidine as the base and (5) there is no observable sulfurisation of triphenyl phosphite indicating that the mechanism of sulfurisation with tetramethyl PADS (5) and 3-picoline occurs by nucleophilic catalysis in contrast to the general base catalysed reaction of PADS (3) itself.

Finally, removing the methylenes of PADS to give dibenzoyl disulfide (DBDS) (6) generates a sulfurising agent which is 20-fold less effective than PADS under the same reaction conditions ($k^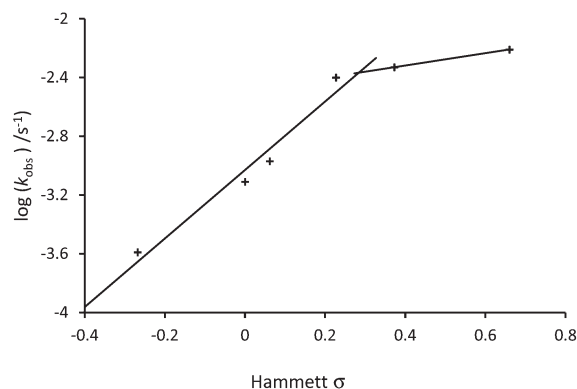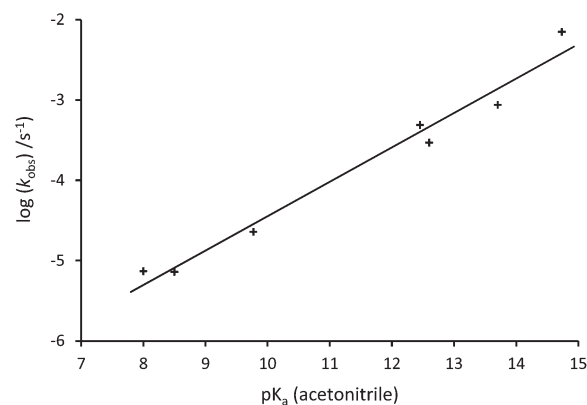{DBDS} = 3.82 \times 10^{-5}$ s^{-1}, $k^{PADS} = 7.70 \times 10^{-4}$ s^{-1}). The dependence of the observed pseudo first-order rate constants (k_{obs}) for the sulfurisation of triphenyl phosphite by dibenzoyl disulfides (6) with substituted pyridines in acetonitrile at 25 °C on the pK_a of the conjugate acid of substituted pyridines in acetonitrile generates a $\beta = 0.16$ compared with $\beta = 0.43$ with 'fresh' PADS. The different β-values are consistent with different roles of the base in the sulfurisation reactions using dibenzoyl disulfides (5) and 'fresh' PADS (3).
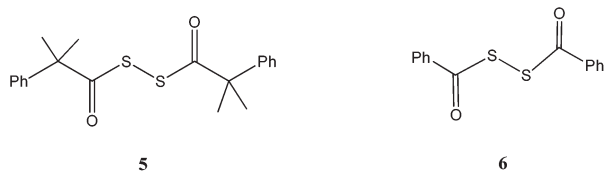

These observations are compatible with sulfurisation using 'fresh' PADS (3) occurring with the phosphite acting as a nucleophile and the pyridine acting as a general base suggesting the mechanism outlined in Scheme 2. Cleavage of the S–S bond in disulfides by nucleophiles is well established[19]

and, in this case, initial nucleophilic attack of the phosphite on sulfur of the diacylsulfide generates an intermediate phosphonium ion and thioacetate anion in a reversible step; in acetonitrile these two species probably exist as an ion-pair. Rate-limiting breakdown of the phosphonium ion occurs by an elimination step involving proton abstraction by the pyridine base to give the product thiophosphate. This step is similar to that which we have suggested for the 'ageing' of PADS by trapping the ketene and D-exchange of the methylene hydrogens. In acetonitrile, the pK_a of the thioacid is ~20 and that for 3-picoline 13.7 [20] so favouring formation of the neutral species (Scheme 2). Rate-limiting breakdown of the phosphonium ion is compatible with the LFER observations reported here which indicate that in the transition state the phosphorus and the catalytic pyridine base nitrogen are both relatively positively charged, whilst there is relative negative charge development transmitted to the aryl ring of PADS. There may be a change in rate-limiting step with electron-withdrawing substituents in the aryl ring of PADS due to the increased acidity of the methylene hydrogens facilitating proton abstraction causing the first step to become rate-limiting.

Sulfurisation by 'aged' PADS

A freshly made solution of PADS (3) is not an optimal sulfurising agent[11] and a solution 'aged' for about 2 days in 50% v/v 3-picoline in acetonitrile improves their efficiency. For example, the pseudo first-order rate constants for the sulfurisation of 0.05 M triphenyl phosphite in acetonitrile by 0.5 M PADS with 1.0 M 3-picoline increase with the length of 'ageing' (Fig. 5), such that PADS 'aged' for 48 h is more than an order of magnitude more active than a freshly prepared solution of PADS. We have shown that PADS degrades completely over this period of time due to its degradation to phenylacetyl polysulfides. Given that the molar concentration of the polysulfides is less than that derived from PADS they are thus much more efficient sulfurising agents.

The general procedure for preparing 'aged' PADS was to dissolve (3) (3 M) in acetonitrile with 3-picoline (5 M) maintained at 25 °C for 48 h. This was then quenched with excess aqueous
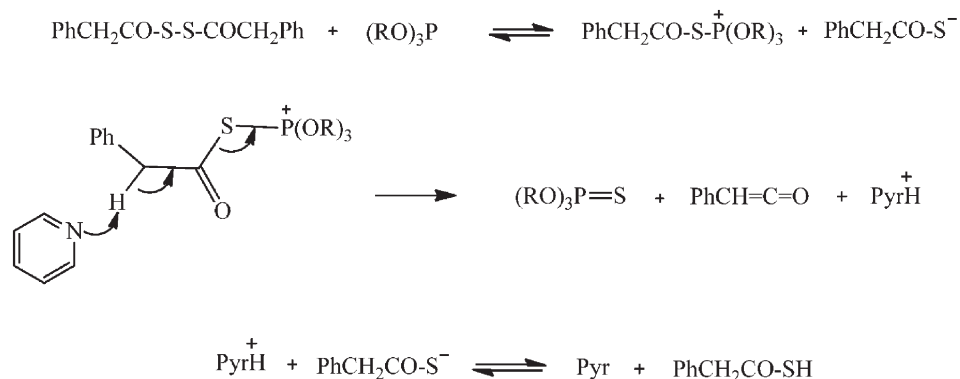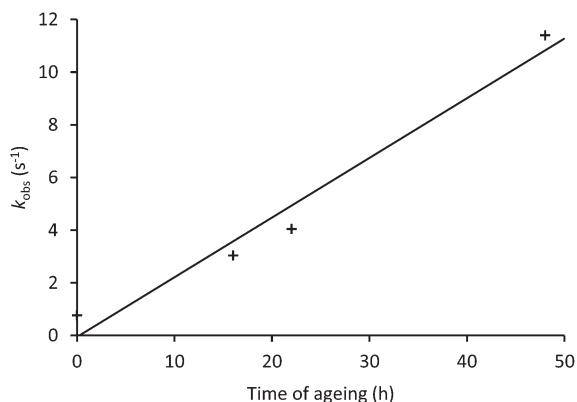

Scheme 2

Fig. 5 The pseudo first-order rate constants for the sulfurisation of triphenyl phosphite (0.05 M) to (PhO)$_3$P=S by (0.5 M) PADS (**3**) as a function of the time that PADS has been 'aged' in acetonitrile with (1.0 M) 3-picoline at 25 °C.

hydrochloric acid (2 M) to remove excess 3-picoline and the mixture extracted using dichloromethane, which was then dried and removed under vacuum. The resultant yellow oil was then made up to the same volume as the original solution generating a solution with the same nominal concentration as the original PADS solution. A crude estimate of the total concentrations of the phenylacetyl polysulfides generated from the standard solution of PADS is 1.45 M based on HPLC data assuming similar extinction coefficients for all species.

The kinetics of the sulfurisation reactions of phosphites were determined by following the reaction by ^{31}P NMR usually with excess PADS and 3-picoline so there is an exponential decrease in phosphite concentration from which the observed first order constants could be obtained. The rate law using 'aged' PADS is first order in each reagent at low base concentrations, similar to that seen with 'fresh' PADS (eqn (1)). However, there is a non-linear dependence on base concentration (Fig. 6) indicative of a change in rate-limiting step with
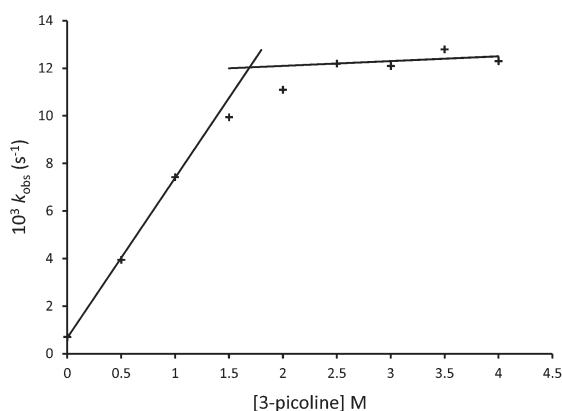
increasing concentration and therefore a stepwise reaction mechanism. In the region where there is a first-order dependence on 3-picoline concentration, the corresponding second-order rate constant $k_{cat} = 6.72 \times 10^{-3}$ M^{-1} s^{-1} at 25 °C which is 16 fold greater than that using 'fresh' PADS for which $k_{cat} = 4.13 \times 10^{-4}$ M^{-1} s^{-1} However, the second-order rate constant for 'aged' PADS is based on the nominal concentration of PADS before it is degraded to a mixture of lower molar concentration of polysulfides and so the true constant is much higher than this.
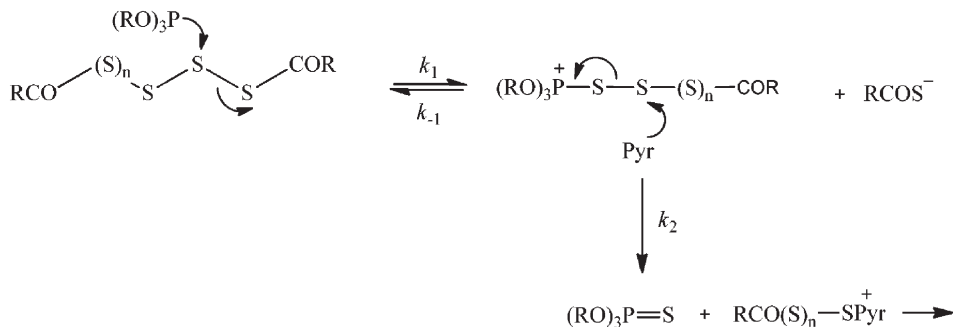
The rates of sulfurisation of triphenyl phosphite by 'aged' PADS (**4**) in acetonitrile have a smaller dependency on the basicity of the catalytic base. A Brönsted-type plot of the dependence of the observed pseudo first-order rate constants at 25 °C on the pK_a of the conjugate acid of substituted pyridines in acetonitrile (Table 4) generates a slope $\beta = 0.26$ compared with $\beta = 0.43$ using 'fresh' PADS. This indicates a transition state with less positive charge development on the pyridine nitrogen for 'aged' PADS. One of the consequences of the smaller dependency of the rate of sulfurisation on the basicity of the pyridine catalyst using 'aged' PADS is that the rates of sulfurisation with 4-methoxypyridine using 'aged' and 'fresh' PADS are similar, based on the same starting concentration of PADS.

If the mechanism of sulfurisation using 'aged' PADS involved nucleophilic attack by trialkyl phosphite on the sulfur adjacent to the acyl group of diacyl polysulfides (**4**), as occurs with 'fresh' PADS (Scheme 2), this would eliminate a sulfide anion compared with the better leaving group thiocarboxylate anion using 'fresh' PADS. Therefore this seems an unlikely process to explain the greater reactivity of 'aged' PADS as the pre-equilibrium constant K_1 would be reduced and the rate constant for the reverse step k_{-1} increased because of the greater nucleophilicity of sulfide anion compared with thioacetate ion.

It is proposed that the sulfurisation reaction with 'aged' PADS occurs with initial nucleophilic attack by trialkyl phosphite on a central sulfur of diacyl polysulfides (**4**) to liberate a thioacetate anion in a pre-equilibrium step similar to that suggested for 'fresh' PADS (Scheme 2). Nucleophilic attack by phosphite on the polysulfide (**4**) reversibly generates a phosphonium ion (Scheme 3) and both the magnitude of the rate

Fig. 6 The dependence of the observed pseudo first-order rate constants for the sulfurisation of triphenyl phosphite (0.10 M) to (PhO)$_3$P=S by (1.0 M) PADS (**3**) that has been 'aged' for 48 h in acetonitrile and 3-picoline (5.0 M) on the concentration of 3-picoline at 25 °C.

Table 4 The observed pseudo first-order rate constants (k_{obs}) for the sulfurisation of triphenyl phosphite (0.10 M) by 'aged' PADS (1.0 M) and the pK_a of the catalysing base, substituted pyridines (2.0 M), in acetonitrile at 25 °C

Pyridine substituent	pK_a (ACN)	k_{obs} (s^{-1})
4-CN	8.50	3.92×10^{-4}
3-CN	8.00	4.09×10^{-4}
3-Cl	9.77	8.75×10^{-4}
3-MeO	12.45	4.78×10^{-3}
H	12.60	9.88×10^{-3}
3-Me	13.70	1.14×10^{-2}
4-MeO	14.73	1.28×10^{-2}

10844 | *Org. Biomol. Chem.*, 2016, **14**, 10840–10847

This journal is © The Royal Society of Chemistry 2016

Scheme 3

$(k_1$ and $k_{-1})$ and equilibrium constants (K_1) for this process are similar to those for the comparable step using 'fresh' PADS (**3**). However, the pyridine base now acts as a nucleophile in the sulfurisation reaction with 'aged' PADS compared with its role as a base using 'fresh' PADS (Scheme 2).

However, the polysulfide phosphonium ion intermediate presents a more facile pathway for product formation involving S–S bond fission as opposed to C–S bond fission. The bond dissociation energy is 226 kJ mol^{-1} for the former compared with 272 kJ mol^{-1} for the latter and the force constant for S–S stretch (440 N m^{-1})[21] is significantly smaller leading to facile bond cleavage, especially in polysulfides.[22] There are many examples of S–S bond cleavage as a result of nucleophilic attack by nitrogen nucleophiles.[19,23] The relatively small value for the Brönsted β_{nuc} = 0.26 for catalysis by substituted pyridines is also compatible with a facile process for the second step k_2 and the change in rate-limiting step[24] with increasing picoline concentration (Fig. 6) occurs when $k_2[\text{pic}] \gg k_{-1}$.

Conclusion

Although an 'aged' solution of phenylacetyl disulfide (PADS), consisting of polysulfides, is a more efficient sulfur transfer reagent than 'fresh' PADS to convert trialkylphosphites to the corresponding thiophosphate 'fresh' PADS is still an effective sulfurising reagent. The differences in reactivity of the two solutions are reflected in their kinetic behaviour and the dependencies of their respective rates on variables such as substituent effects and concentration of the catalysing pyridine base. The rates of both processes in acetonitrile are first order in sulfurising agent, phosphite and a pyridine base. However, with an 'aged' solution of PADS the rate becomes independent of base at high concentrations. The Brönsted β values for sulfurisation using 'fresh' and 'aged' PADS with substituted pyridines are different, 0.43 and 0.26, respectively. With 'fresh' PADS the Brönsted β_{nuc} = 0.51 for substituted trialkyl phosphites is consistent with a mechanism involving nucleophilic attack of the phosphite on the PADS disulfide bond to reversibly generate a phosphonium intermediate. Replacing the ionisable hydrogens in PADS with methyl groups significantly reduces the rate of sulfurisation indicating that the rate-limit-

ing breakdown of the phosphonium ion intermediate occurs by a base catalysed elimination process. The comparable polysulfide phosphonium ion intermediate seen with 'aged' PADS allows a more facile pathway for product formation involving S–S bond fission as opposed to C–S bond fission.

Experimental

General sulfurisation kinetics with 'aged' PADS

A solution of PADS (1 M) 50/50 v/v acetonitrile/3-picoline was left to 'age' for 48 h. At $T = n$ h a 1 ml sample of this was removed and quenched with dilute hydrochloric acid (10 ml, 2 M) to remove the picoline. This was then washed with dichloromethane (DCM) (2 × 10 ml), dried over magnesium sulfate and the solvent removed under vacuum. The resulting oil was then made up to 1 ml using deuterated acetonitrile. To an NMR tube containing triphenyl phosphite in deuterated acetonitrile (0.1 M, 200 μl) and 3-picoline in deuterated acetonitrile (2 M, 200 μl) was added 'aged' PADS solution (200 μl, 1 M) and ^{31}P NMR spectrum recorded every 90 s.

Synthesis

The syntheses of the various arylacetyl disulfides have been previously reported.[14]

Tris-(4-methoxyphenyl)phosphite. To a solution of 4-methoxyphenol (9.77 g, 78.7 mmol) and pyridine (8.10 ml, 7.92 g, 100 mmol) in diethyl ether (80 ml) phosphorus trichloride (1.74 ml, 2.74 g, 20.0 mmol) was added dropwise at room temperature under a nitrogen atmosphere and stirred for 1.5 h. When the reaction was complete, the reaction mixture was quenched with water (100 ml) and the organic phase then washed with water (50 ml) and brine (50 ml), dried over magnesium sulfate and the solvent removed under vacuum. The crude mixture was purified by silica gel column chromatography using chloroform as the eluent to give the product as a colourless oil (4.87 g, 4.03 ml, 12.2 mmol, 61% yield). ^{1}H NMR (CDCl$_3$, 400 MHz) δ 3.78 (s, 9H, CH$_3$), 6.87 (d, 6H, J 9.23 Hz, ArH), 7.11 (d, 6H, J 9.23 Hz, ArH) ppm; ^{13}C NMR (CDCl$_3$, 100 MHz) δ 55.6 (CH$_3$), 114.7 (CH), 121.7 (CH), 145.1 (Cq), 156.3 (Cq) ppm; ^{31}P NMR (CDCl$_3$, 400 MHz), δ 128.9 ppm,

This journal is © The Royal Society of Chemistry 2016

Org. Biomol. Chem., 2016, **14**, 10840–10847 | **10845**

HRMS (m/z): $[M + H]^+$ for $C_{21}H_{21}O_6P$ calculated 401.1149, observed 401.1150

Tris-(3-chlorophenyl)phosphite. As above using 3-chlorophenol (14.04 g, 112.8 mmol) and pyridine (10.78 ml, 10.58 g, 141 mmol) in diethyl ether (120 ml), phosphorus trichloride (4.0 ml, 3.87 g, 28.2 mmol). The crude mixture was purified by silica gel column chromatography using chloroform as the eluent to give the product as a pale yellow oil (9.1 g, 6.8 ml, 22 mmol, 78% yield). ^{1}H NMR (CDCl$_3$, 400 MHz) δ 7.01–7.29 (m, 12H, ArH) ppm; ^{13}C NMR (CDCl$_3$, 100 MHz) δ 118.8 (d, J_{C-P} 7.49 Hz, CH), 121.2 (d, J_{C-P} 6.55 Hz, CH), 124.9 (CH), 130.6 (CH), 135.1 (Cq), 151.8 (Cq) ppm; ^{31}P NMR (CDCl$_3$, 400 MHz), δ 126.5 ppm, HRMS (m/z): $[M + H]^+$ for $C_{18}H_{12}O_3Cl_3P$, calculated 412.9662, observed 412.9672.

Tris-(4-chlorophenyl)phosphite. As above using 4-chlorophenol (10.3 g, 80 mmol) and pyridine (8.10 ml, 7.92 g, 100 mmol) in diethyl ether (80 ml), phosphorus trichloride (1.74 ml, 2.74 g, 20.0 mmol). The crude mixture was purified by silica gel column chromatography using chloroform as the eluent to give the product as a white solid (5.06 g, 12.2 mmol, 61% yield). ^{1}H NMR (CDCl$_3$, 400 MHz) δ 7.06 (d, J 8.93 Hz, 6H, ArH), 7.30 (d, J 8.96 Hz, 6H, ArH) ppm; ^{13}C NMR (CDCl$_3$, 100 MHz) δ 121.9 (d, J_{C-P} 6.6 Hz, Cq), 129.9 (CH), 149.8 (d, J_{C-P} 2.8 Hz, Cq) ppm; ^{31}P NMR (CDCl$_3$, 400 MHz), δ 126.8 ppm, HRMS (m/z): $[M + H]^+$ for $C_{18}H_{12}O_3Cl_3P$, calculated 412.9662, observed 412.9665.

Tris-(4-fluorophenyl)phosphite. To a solution of 4-fluorophenol (4.41 g, 39.3 mmol) and triethylamine (5.6 ml, 4.06 g, 40 mmol) in diethyl ether (40 ml) was added dropwise phosphorus trichloride (0.87 ml, 1.37 g, 10.0 mmol) then stirred at room temperature under nitrogen atmosphere for 24 h. The solid precipitate from the reaction was removed by vacuum filtration and washed with diethyl ether (2 × 10 ml). The solvent from the filtrate was removed under vacuum and the crude product purified by silica gel column chromatography eluting with chloroform to give the product as a white solid (4.77 g, 13.1 mmol, 71% yield). ^{1}H NMR (CDCl$_3$, 400 MHz) δ 7.01–7.13 (m, 12H, ArH) ppm; ^{13}C NMR (CDCl$_3$, 100 MHz) 116.4 (d, J_{C-F} 23 Hz, CH), 122.0 (t, J_{C-F} 7.4 Hz, J_{C-P} 7.3 Hz, CH), 147.2 (d, J_{C-F} 2.9 Hz, J_{C-P} 3.0 Hz, Cq), 159.5 (d, J_{C-F} 243 Hz, CF) ppm; ^{31}P NMR (CDCl$_3$, 400 MHz) δ 127.5 (127.8) ppm, HRMS (m/z): $[M + H]^+$ for $C_{18}H_{12}O_3F_3P$, calculated 365.0549, observed 365.0550.

Acknowledgements

Notes and references

1 P. C. Zamecnik and M. L. Stephenson, *Proc. Natl. Acad. Sci. U. S. A.*, 1978, **75**, 285.

2 R. M. Orr, *Curr. Opin. Mol. Ther.*, 2001, **3**, 288; B. Roehr, *J. Int. Assoc. Physicians AIDS Care*, 1998, **4**, 14; S. Agrawal and E. R. Kandimalla, *Mol. Med. Today*, 2000, **6**, 72; D. A. Bell, A. J. Hooper and J. R. Burnett, *Expert Opin. Invest. Drugs*, 2011, **20**, 265; A. Goyenvalle, J. Wright, A. Babbs, V. Wilkins, L. Garcia and K. E. Davies, *Mol. Ther.*, 2012, **20**, 1212.

3 P. S. Eder, R. J. DeVine, J. M. Dagle and J. A. Walder, *Antisense Res. Dev.*, 1991, **1**, 141–151.

4 B. Nawrot and K. Sipa, *Curr. Top. Med. Chem.*, 2006, **6**, 913; E. L. Chernolovskaya and M. A. Zenkova, *Curr. Opin. Mol. Ther.*, 2010, **12**, 158; S. P. Walton, M. Wu, J. A. Gredell and C. Chan, *FEBS J.*, 2010, **277**, 4806; M. R. Laresa, J. J. Rossia and D. L. Ouellet, *Trends Biotechnol.*, 2010, **28**, 570; P. Guga, *Curr. Top. Med. Chem.*, 2007, 7, 695.

5 F. Eckstein, *Antisense Nucleic Acids Drug Dev.*, 2000, **10**, 117.

6 S. T. Crooke, *Methods Enzymol.*, 2000, **313**, 3; C. A. Stein and Y. C. Cheng, *Science*, 1993, **261**, 1004.

7 P. Guga and M. Koziołkiewiczb, *Chem. Biodiversity*, 2011, **8**, 1642.

8 R. P. Iyer, L. R. Phillips, W. Egan, J. B. Regan and S. L. Beaucage, *J. Org. Chem.*, 1990, **55**, 4693–4699; H. Vu and B. L. Hirschbein, *Tetrahedron Lett.*, 1991, **32**, 3005–3008; M. V. Rao, C. B. Reese and Z. Zhao, *Tetrahedron Lett.*, 1992, **33**, 4839–4842.

9 W. J. Stec, B. Uznanski and A. Wilk, *Tetrahedron Lett.*, 1993, **33**, 5317–5320; M. V. Rao and K. Macfarlane, *Tetrahedron Lett.*, 1994, **35**, 6741–6744; V. A. Efimov, A. L. Kalinkina, O. G. Chakhmakhcheva, T. S. Hill and K. Jayaraman, *Nucleic Acids Res.*, 1995, **23**, 4029–4033; Z. Zhang, A. Nichols, J. X. Tang, Y. Han and J.-Y. Tang, *Tetrahedron Lett.*, 1999, **40**, 2095–2098; J.-Y. Tang, Z. Han, J. X. Tang and Z. Zhang, *Org. Process Res. Dev.*, 2000, **4**, 194–198.

10 P. C. J. Kamer, H. C. P. F. Roelen, H. van den Elst, G. A. van der Marel and J. H. van Boom, *Tetrahedron Lett.*, 1989, **30**, 6757–6760.

11 A. H. Krotz, D. Gorman, P. Mataruse, C. Foster, J. D. Godbout, C. C. Coffin and A. N. Scozzari, *Org. Process Res. Dev.*, 2004, **8**, 852–858.

12 Z. S. Cheruvallath, R. L. Carty, M. N. Moore, D. C. Capaldi, A. H. Krotz, P. D. Wheeler, B. J. Turney, S. R. Craig, H. J. Gaus, A. N. Scozzari, D. L. Cole and V. T. Ravikumar, *Org. Process Res. Dev.*, 2000, **4**, 199–204.

13 A. H. Krotz, D. Gorman, P. Mataruse, C. Foster, J. D. Godbout, C. C. Coffin and A. N. Scozzari, *Org. Process Res. Dev.*, 2004, **8**, 852–858.

14 J. Scotson, B. I. Andrews, A. P. Laws and M. I. Page, *Org. Biomol. Chem.*, 2016, **14**, 8301–8308.

15 D. R. Hogg, in *Comprehensive Organic Chemistry*, ed. D. Barton and W. D. Ollis, Pergamon, Oxford, 1979, vol. 5, p. 445.

16 R. G. Pearson and F. V. Williams, *J. Am. Chem. Soc.*, 1953, **75**, 3073; R. G. Pearson and F. V. Williams, *J. Am. Chem. Soc.*, 1954, **76**, 258; E. S. Lewis and J. D. Allen, *J. Am. Chem. Soc.*, 1964, **86**, 2022; J. P. Calmon, M. Calmon and V. Gold, *J. Chem. Soc. B*, 1969, 659.

17 A. R. Butler and V. Gold, *J. Chem. Soc.*, 1961, 4362.

10846 | *Org. Biomol. Chem.*, 2016, **14**, 10840–10847

This journal is © The Royal Society of Chemistry 2016

18 C. A. Bunton and J. H. Fendler, *J. Am. Chem. Soc.*, 1966, **31**, 2307.

19 I. V. Koval, *Russ. Chem. Rev.*, 1994, **63**, 735–750.

20 B. Cox, *Acids and Bases, solvent effects on acid-base strength*, Oxford UP, Oxford, 2013.

21 K. B. Wiberg and A. Shruke, *Spectrochim. Acta, Part A*, 1973, **29**, 583.

22 R. Steudal, *Angew. Chem., Int. Ed. Eng.*, 1975, **14**, 655–720.

23 S. Oae, Y. Tsuchida, K. Tsujihara and N. Furukawa, *Bull. Chem. Soc. Jpn.*, 1972, **45**, 2856; N. N. Mel'nikov, B. A. Kashkin and N. A. Torgasheva, *Zh. Obshch. Khim.*, 1972, **45**, 2856.

24 M. I. Page and A. Williams, in *Organic and Bio-Organic Mechanisms*, Longmans, 1997, p. 26.